Université de Valenciennes et du Hainaut-Cambrésis

Thèse de doctorat

Pour obtenir le grade de Docteur de l'Université de

VALENCIENNES ET DU HAINAUT-CAMBRESIS

Spécialité : GENIE MECANIQUE

Présentée par Hai Quan DO le 11/12/2015

Version finale

Ecole doctorale :

Sciences Pour l'Ingénieur (SPI)

Equipes de recherche, Laboratoires :

Laboratoire d'Automatique, de Mécanique et d'Informatique Industrielles et Humaines (LAMIH)

Modèles réduit et propagation d'incertitude pour les problèmes de contact frottant et d'instabilité vibratoire

JURY

Président du jury

— Chevallier Gaël, Professeur, Université de Franche-Comté

Rapporteurs

— Berger Sébastien, Professeur, INSA Centre Val de Loire
— Hanss Michael, Professeur, Université de Stuttgart

Examinateurs

— Chevallier Gaël, Professeur, Université de Franche-Comté
— Zahrouni Hamid, Professeur, Université de Lorraine-Metz

Co-encadrant : Massa Franck, Maître de Conférences, Université de Valenciennes

Directeur de thèse : Tison Thierry, Professeur , Université de Valenciennes

Résumé

Afin d'améliorer la qualité des produits et tendre vers des conceptions fiables et robustes, la simulation numérique joue de nos jours un rôle clé dans de nombreux secteurs de l'ingénierie. Malgré l'utilisation de modèles de plus en plus complexes et réalistes, les corrélations entre les mesures expérimentales et les simulations déterministes ne s'avèrent pas toujours évidentes, en particulier, si le phénomène observé est de nature fugace. Afin de prendre en compte les variations possibles de comportement, des techniques de tirages multiples comme les plans d'expériences, les analyses de sensibilité ou les approches non déterministes peuvent être exploitées. Cependant, ces simulations avancées conduisent inévitablement à des temps de calcul prohibitifs qui ne sont pas en adéquation avec des phases de conception de plus en plus courtes.

L'objectif de cette thèse est d'explorer de nouvelles stratégies de résolution pour les problèmes mécaniques, où la non-linéarité de contact frottant et des variations sur les paramètres du modèle numérique sont considérés en même temps. Pour y parvenir, nous avons, dans un premier temps, étudié l'intégration de contrôleurs, basés sur la logique floue, pour résoudre un problème de contact frottant. L'idée proposée est de transformer le problème non linéaire en un ensemble de problèmes linéaires de tailles réduites que l'on peut réanalyser grâce des développements homotopiques et des techniques de projection. Dans un second temps, nous avons étendu la démarche proposée au cas des problèmes de vibrations induites par le frottement comme le crissement.

Mots Clés

Contact frottant - Instabilité - Crissement - Incertitudes - Perturbations - Logique floue - Ensemble flou - Réanalyse - Développement homotopique

Abstract

To improve the quality of products and tend to reliable and robust designs, numerical simulations have nowadays taken a key role in many engineering domains. In spite of more complex and realistic numerical models, the correlation between a deterministic simulation and experimentations are not obvious, especially if the observed phenomenon have a fugitive nature. To take into account possible evolutions of behaviour, multiple samplings techniques such as designs of experiments, sensitivity analyses or non-deterministic approaches are currently performed. Nevertheless, these advanced simulations necessarily generate prohibitive computational times, which are not compatible with more and more shorter design steps.

The aim of this work is to explore new numerical ways to solve mechanical problems including both the contact nonlinearity, the friction and several variability on model parameters. To achieve this objective, the integration of Fuzzy Logic Controllers has been first studied in the case of static frictional contact problems. The proposed idea is to decompose the non linear problem in a set of reduced linear problems. These last ones can be reanalyzed thanks to homotopy developments and projection techniques as a function of introduced perturbations. Second, the proposed strategy has been extended to the case of friction induced vibrations problems such as squeal.

Keywords

Frictional contact - Instability - Squeal - Uncertainty - Perturbations - Fuzzy Logic - Fuzzy sets - Reanalysis - Homotopy development

Contents

Introduction **8**

1 Uncertainty in design step: towards reliable and robust design 9

2 Aims of proposed research 10

3 Organization of report 10

1 Uncertainty, reduced model techniques and friction induced vibration: a state of the art **13**

1 Non-deterministic approaches in mechanical engineering 14

1.1 Some definitions 14

1.2 Uncertainty modelisation 15

1.3 Uncertainty propagation 15

1.4 Uncertain data management 19

2 Reduced model techniques 21

2.1 Surrogate models 21

2.2 Reanalysis techniques 22

2.3 Integration in uncertain context 23

3 Friction induced vibrations 24

3.1 Noises and squeal phenomenon 24

3.2 Fugitive nature of squeal 26

3.3 Non-linearity of contact 29

4 Reduced models and uncertainty propagation for frictional contact and stability problems 30

2 Finite element analysis of frictionless contact problems using fuzzy control approach **33**

1 Introduction 34

2 2D Frictionless contact problem in a finite element context 35

2.1 Continuous formulation . . . 35
2.2 Finite element discretization and numerical methods . . . 36
3 Fuzzy Logic Controller for Contact method . . . 38
3.1 Fuzzy Logic Controller and normal contact management . . . 38
3.2 Definition of the reduced contact problem . . . 42
3.3 Design of fuzzy controller and contact solving . . . 43
4 Numerical applications for frictionless contact problem . . . 45
4.1 Elastic beam on beam problem . . . 46
4.2 Elastic beam on rigid segment problem . . . 51
4.3 Two semicircular structures in contact . . . 53
5 Conclusion . . . 56

3 Using fuzzy logic control approach and model reduction for solving frictional contact problems 57
1 Introduction . . . 58
2 2D frictional contact problems in a finite element context . . . 58
2.1 Frictional contact problems . . . 58
2.2 Finite element static contact problem . . . 60
3 Fuzzy Logic Controller for frictional Contact method . . . 61
3.1 Extension to frictional contact management . . . 61
3.2 Definition of the reduced contact problem . . . 63
4 Numerical applications for frictional contact problems . . . 63
4.1 2D elastic slab on rigid plate . . . 64
4.2 Design of controllers . . . 65
4.3 Resolution of the full contact problem with the FL2C method . . . 66
4.4 Resolution of reduced contact problem through eigenvector integration . . . 68
4.5 Resolution of reduced contact problem using static modes integration . . . 71
4.6 Influence of controller fuzzy laws . . . 74
4.7 Solutions for fuzzy controller integration . . . 76
4.8 Discussion about computational time . . . 78
5 Conclusion . . . 79

4 Reanalysis of perturbed frictional contact problems 80
1 Introduction . . . 81
2 Perturbations in a static finite element contact problem . . . 82

2.1 Nominal problem . . . 82
2.2 Fuzzy Logic Controller for Contact method . . . 83
2.3 Modified problem and reduction techniques . . . 84
3 Reanalysis of the modified projection matrix . . . 85
3.1 Homotopy perturbation and series development . . . 85
3.2 Reanalysis of modified static modes . . . 85
4 Proposed HPP-FL2C method . . . 87
5 Numerical applications for frictional contact problem with perturbations . . . 88
5.1 Description of the numerical model . . . 89
5.2 Nominal contact problem validation . . . 90
5.3 Nominal reduced contact problem validation . . . 92
5.4 Modification of the friction coefficient . . . 93
5.5 Validation of HPP method for projection matrix reanalysis . . . 94
5.6 Perturbed reduced contact problem . . . 95
5.7 Parametric analysis by DOE . . . 98
6 Conclusion . . . 99

5 A global strategy for the stability analysis of friction induced vibration problem with parameter variations 101
1 Introduction . . . 102
2 Stability analysis for friction-induced vibrations problems . . . 103
2.1 Nominal description . . . 103
2.2 Modified configuration and perturbation integration . . . 105
3 Reanalysis of modified stability analysis . . . 107
3.1 Main steps of the CHOC strategy . . . 107
3.2 Reanalysis of the equilibrium position . . . 109
3.3 Reanalysis of modified eigenmodes . . . 110
3.4 Calculation of the modified complex eigendata . . . 112
4 Application to simplified brake system stability analysis . . . 113
4.1 Numerical model description . . . 113
4.2 Nominal coalescence graph . . . 114
4.3 Perturbed coalescence graph . . . 118
4.4 Effects of input parameter modifications . . . 121
5 Conclusion . . . 122

6 Uncertain friction induced vibration study: coupling of fuzzy logic, fuzzy sets and interval theories **124**

1 Introduction . . . 125

2 Uncertainty management . . . 125

2.1 Fuzzy sets theory . . . 125

2.2 Interval discretization . . . 126

3 Proposed strategy for calculating fuzzy membership function . . . 127

3.1 Uncertainty propagation by optimization . . . 127

3.2 Integration of reanalysis techniques . . . 129

4 Numerical Applications for friction induced vibration problem with fuzzy data . . . 131

4.1 System description . . . 131

4.2 Deterministic results . . . 132

4.3 Definition of fuzzy input parameters . . . 133

4.4 Validation of fuzzy contact loads . . . 133

4.5 Validation of fuzzy equilibrium position . . . 135

4.6 Validation of fuzzy complex frequencies . . . 135

4.7 Effects of fuzzy input data on instability . . . 136

5 Conclusion . . . 137

Conclusion and perspectives **139**

A Mac-Neal Component Modal Synthesis method **145**

Bibliography **147**

Introduction

Contents

1	**Uncertainty in design step: towards reliable and robust design**	**9**
2	**Aims of proposed research**	**10**
3	**Organization of report**	**10**

1 Uncertainty in design step: towards reliable and robust design

The competition in industries constantly increases through improving the quality of products and reducing the cost of their products. To achieve these drastic objectives, numerical simulations have taken a key role in many engineering domains such as automotive, aeronautics and nuclear. Considering for example Finite Element Method (FEM) [Zienkiewicz and Taylor, 2002], Smoothed-Particle Hydrodynamics (SPH) techniques [Gingold and Monaghan, 1977] or more recently isogeometric analyses [Hughes et al., 2005], it is nowadays possible to easily test different materials, different designs, new processes and simulate the related physic mechanisms without systematically performing experimental tests. Numerical simulations have the advantage of being compatible with economic challenges such as reactivity and anticipation and they are becoming cheaper than experiments on 1 : 1 ratio models. Recent years, evolving computational resources contribute to the increasingly frequent use of more complex numerical models including more components of mechanical systems, more geometrical details and nonlinearities (geometry, material and contact). On the other hand, as the size of some FEM models can currently reach several tens of millions of degrees of freedom, CPU time associated to complex simulations remains constant.

In spite of the advanced tools, the correlation between a deterministic simulation and experimentations are not obvious in many case studies. The resulting gaps can be significant, especially if the studied phenomenon have a fugitive or chaos nature. Indeed, during the manufacturing of mechanical structures, it is not uncommon to observe some uncertainties resulting in product variability either on material properties (Young modulus, strain-stress law), on geometric characteristics (gaps, fillets and small geometries) and on interface and boundary conditions. These observed variability necessarily affect the static and dynamic behaviours of structures and more generally the component life and the global efficiency of the system. To significantly characterize experimental behaviour, it is so necessary to consider a family of components rather than only one specimen that can generate significant financial costs. Numerically, to take into account these uncertainties and tend to reliable and robust designs, a current industrial trend involves making multiple numerical simulations by performing sensitivity analyses, designs of experiments [Fisher, 1935, Kleijnen, 2010, Taguchi et al., 2005] non-deterministic studies [Shinozuka, 1972, Moore, 1966, Ben-Haim and Elishakoff, 1990, Zadeh, 1978] or even reliable and robust optimizations [Goldberg, 1989, Kennedy and Eberhart, 1995]. The idea is to simulate the evolution of mechanical responses as a function of input parameter variations and to detect failures and performance reductions of products. Once again, it is obvious to imagine the same computational limitations than in the deterministic case. Currently, several researches are

performed in that sense in order to develop efficient, precise and less time consuming numerical advanced methods.

2 Aims of proposed research

In LAMIH's mechanical team, the recent works [Tison et al., 2014, Renault et al., 2014] have highlighted the contribution of uncertainty to improve numerical and experimental correlation in the case of squeal instabilities for several industrial automotive systems. Indeed, the authors have first showed the limitations of deterministic simulations to predict squeal phenomenon with efficiency. Secondly, it has been shown that several classes of uncertainties, mainly the geometric topology of pads, material properties, damping and friction, play a key role and their integration in simulation is essential to tend to robust designs. The results have been presented in term of families of unstable modes and based on a robustness criterion. For the uncertainty propagation step, Latin Hypercube Samplings (LHS) coupling to Abaqus frequency stability simulations are currently used leading to significant CPU times. In an industrial context, this kind of calculations are necessarily performed during several weekends and distributed on different servers.

Nevertheless, to go farther to this way and to integrate these results in an optimization scheme, it is necessary to revisit the numerical strategy and propose less time consuming alternatives methods. The frequency stability analysis, used to predict squeal, relies on three steps namely a non linear static frictional contact problem, a creation of coupling matrices and a complex eigenvalue problem. As the equilibrium position takes a considerable importance in this study, the thesis proposal is to study frictional contact problems in a multiple sampling context. The first objective is thus to develop a reanalysis method for the static frictional contact problem and to study the integration of the automation control approaches for the solving. Moreover, to decrease the computational time, it is necessary to develop reduced order models at different steps of the proposed strategy. Thus, the second objective is to define a reduced contact problem and a reduced complex eigenvalue problem. Finally, an introduction of fuzzy sets formalism in friction induced vibration analysis is investigated and problematics of uncertainty propagation are discussed.

3 Organization of report

This report contains six chapters:

In chapter 1, a bibliographic review about the main topics, investigated in PhD works, is

supplied. First, a discussion is proposed concerning the introduction of uncertainty in numerical simulations. After recalling some general definitions, the modelisation, propagation and management aspects are detailed considering different theories and methods. Second, we focus the state of the art on reduced model techniques by taking into account both surrogate models and reanalysis techniques coupled to projection techniques. Their integration in advanced mechanical applications is presented too. Next, we summarize experimental and numerical, already published, works for friction induced vibrations problems and more precisely squeal phenomenon. Contact phenomena, which plays a key role in this kind of applications, is underlined. Finally, an assessment of recent developments about reduced models and uncertainty propagation for frictional contact and stability problems is proposed.

Chapter 2 entitled "Finite element analysis of frictionless contact problems using fuzzy control approach " describes a new numerical method to solve a mechanical frictionless contact problem. The proposed method has been developed to be compatible within a context of multiple sampling (such as parametric analysis or design of experiments). The proposal relies on a control based method currently used in automation domain. A Fuzzy Logic Controller (FLC) is designed to link the normal gaps identified between the bodies and the normal contact pressures applied at the interface. The initial nonlinear problem can be decomposed into a set of reduced linear problems. Some 2D numerical applications will highlight the strengths of the proposed method called Fuzzy Logic Controller for Contact (FL2C).

The aim of the chapter 3 named "Using Fuzzy Logic control approach and model reduction for solving nonlinear frictional contact problem" is to expand the previously proposed FL2C method for solving mechanical frictional contact problems. A second FLC is added to take into account the tangential gaps in the case of sticking conditions. Moreover, a model reduction for each component in contact is performed to decrease the size of the global finite element problem and consequently, the computational time of numerical simulations. A complete numerical application is proposed to assess the efficiency of the proposal in terms of precision, robustness and computational time.

Chapter 4 "Reanalysis of perturbed frictional contact problems" shows how homotopy perturbation techniques and projection can be integrated in control-based approach to reanalyze the perturbed frictional contact problems. Thus, the perturbed non linear problem is decomposed into perturbed linear problems dedicated to each component in contact. Each solution of perturbed linear problems is approximated. A numerical application is performed to verify the efficiency and the robustness of the proposed method. Finally, a design of experiments is proposed to quantify the effects of input perturbations on output mechanical data.

Chapter 5 "A global strategy for the stability analysis of friction induced vibration problem with parameter variations" discusses on the definition of reduced order model for stability prob-

lem in the case of friction induced vibrations. The stability analysis of a mechanical system relies on several coupling steps, namely a non linear static analysis followed by linear and complex eigenvalue problems. We thus propose a numerical strategy to perform more rapidly multiple complex eigenvalue analyses. This strategy couples three methods namely, Fuzzy Logic Controllers to manage frictional contact problem, homotopy developments and projection techniques to reanalyse the projection matrices and Component Mode Synthesis to calculate the modified eigensolutions. First, a numerical application is proposed to validate the different steps of the strategy. Secondly, the effects of input variability on squeal phenomenon are investigated to highlight the necessity to take into account uncertainty in finite element simulations.

Chapter 6 entitled "Uncertain friction induced vibration study: coupling of fuzzy logic, fuzzy sets and interval theories" presents a complete method to carry out a fuzzy study of a friction induced vibration system and to analyze the effects of uncertainty on the output data of a stability problem. The fuzzy problem will be decomposed by interval problems and interval output solutions are calculated by optimization. Each output data of the stability problem is reanalyzed by integrating FL2C method for static step while homotopy development and projection techniques are used for the modal step. The results obtained with the proposed strategy are compared with those given by Zadeh's extension principle reference.

Finally, conclusions and some perspectives of these different works will be provided to finish the PhD report.

Chapter 1

Uncertainty, reduced model techniques and friction induced vibration: a state of the art

Contents

1 Non-deterministic approaches in mechanical engineering 14

1.1 Some definitions 14

1.2 Uncertainty modelisation 15

1.3 Uncertainty propagation 15

1.4 Uncertain data management 19

2 Reduced model techniques 21

2.1 Surrogate models 21

2.2 Reanalysis techniques 22

2.3 Integration in uncertain context 23

3 Friction induced vibrations 24

3.1 Noises and squeal phenomenon 24

3.2 Fugitive nature of squeal 26

3.3 Non-linearity of contact 29

4 Reduced models and uncertainty propagation for frictional contact and stability problems 30

1 Non-deterministic approaches in mechanical engineering

1.1 Some definitions

The notion of uncertainty makes reference to many qualification criteria such as uncertain, variable, vague, imprecise, poor, incomplete depending on the employed models. Several authors have tried to propose some definitions and classifications to facilitate the comprehension of these ambiguous terminologies. Oberkampf et al [Oberkampf et al., 1999] defines the term variability as variation which is inherent to the modelled physical system or the environment under consideration where as uncertainty is a potential deficiency in any phase or activity of the modelling process that is due to lack of knowledge. In agreement with this previous description, two major classes of uncertainties [Moens and Vandepitte, 2005] are currently adopted. The first class is called irreducible uncertainties and refers to the fact that even when all information on a particular property is available, the quantity cannot be deterministically determined. On the contrary, the second class is called reducible because uncertainty can be reduced or even eliminated if a sufficient amount of information is collected. Reducible uncertainty is usually due to missed information or subjective notions and is also assimilated to ignorance.

As described by Bouchon-Meunier [Bouchon-Meunier, 1994], three cases of uncertainty can be identified namely definition, modelisation and measurement. This definition is naturally true in mechanical engineering. When different specimens or structures are analyzed, variations of geometrical and material characteristic parameters are classically observed. Indeed, during the manufacturing and the use of structure, the sources of errors can be numerous [Alvin et al., 1998] and so the parameter uncertainties are inevitable. Moreover, the quantification of the quality of numerical model remains tricky and is dependent of several assumptions, formulation used, chosen discretization or algorithms. These model uncertainties, difficult to take into account, represent the insufficiency of the numerical model to describe the reality of the observed phenomena. Finally, the experimental uncertainties are present during measurement campaigns. Even if rigorous protocols are followed, it is difficult to maintain unchanged variations of temperature, boundary conditions and level of excitations for example. Whatever the nature of uncertainty, their integration in simulation requires in a first time a phase of modelisation described in the next part.

1.2 Uncertainty modelisation

Many non-deterministic approaches have been introduced to model the different kind of uncertainties previously mentioned. In mechanical engineering, the more prevalent theories are the probabilistic theory, the interval theory, and the fuzzy set theory. Among these theories, the probabilistic theory [Metropolis and Ulam, 1949] is provided as a reference to model the uncertainties. Uncertainty is described either by random variables or by random fields if spatial variation of the model properties is concerned. Construction of the associated probability distributions requires a statistical study of measured data from specific tests. This particular phase of uncertainty quantification is primordial to introduce realistic variations. When few experimental data are available from some observations of the system, these experimental data can be used to identify an optimal prior stochastic model of uncertainties using the maximum likelihood method. In mechanical engineering, Gaussian, log-normal and uniform laws are preferred in most applications. In interval theory [Moore, 1966] , the uncertain data are represented by intervals of variation. The inferior and superior bounds represent the minimal and maximal observed data and each value has the same confidence degree. Fuzzy set theory, introduced by Zadeh [Zadeh, 1978], can be seen as an extension of the classical set theory and a generalisation of the interval theory. Fuzzy set introduces a degree of membership, represented by the membership function. This membership function describes the grade of membership for each element in the domain defined by the fuzzy set. The concept allows thus membership values between zero and one. Different forms of membership functions can be chosen, depending on the kind of imperfection considered. Triangular membership functions are the simplest and common choice to represent imprecisely known quantities. Indeed, one can fix a membership degree of 1 to the classical used value while membership values of 0 are affected to an estimate of the bounds of this value. However, with additional information, other membership functions can be chosen (p-shape, trapezoidal ....) to model the perception and the expert judgment of the user.

1.3 Uncertainty propagation

As soon as the data have been correctly modelled with one of the available theories, the next challenge is to propagate the uncertainty presented on input parameter to the output mechanical solutions. Depending on the encountered problem (static, modal, dynamic ...), studied parameters (dimensions, geometry, materials or boundary conditions) or the configuration of models, the task is more or less complex. It directly depends on the natural evolutions (linear, quadratic, monotonic or nonlinear) of solutions (displacements, eigenvalue, eigenvector...) in terms of uncertain parameters. This step is clearly essential but relatively complex whatever the theory. Indeed,

the propagation methods must be precise concerning the quantification of extreme evolutions and values and perform in a compatible time with design step. Two major axes have generally been chosen considering intrusive or non-intrusive propagation methods. With intrusive approaches, the uncertain parameters are replaced in the governing equations by appropriate expansions or approximations. To implement this category of approach in a classical simulation code, it is necessary to rewrite a large part of the software. On the contrary, the main objective of non-intrusive methods is to obtain the perturbed output quantities without making any modifications to the deterministic software. This second approach treats the deterministic code as a black-box and approximates the unknown coefficients with formulas based on deterministic code evaluations. The strategy for the selection of samples in the design space and their number depend on the chosen non-intrusive technique. Several alternative, intrusive or non-intrusive, propagation methods have been developed in order to overcome inconveniences of reference intensive samplings methods. They are presented in the case of probability and fuzzy sets modelisation in the next two subsections.

Probabilistic approach

In probabilistic approach, Monte Carlo Simulations (MCS) [Metropolis and Ulam, 1949], represent the numerical reference method to propagate uncertainty. This method is based on random sampling of input parameters and on deterministic calculations associated with each combination of generated parameters [Schueller, 1997, Schueller, 2001]. Simple to implement, this method presents guarantee in terms of convergence but can be proved prohibitive when the number of uncertain parameters increase or the deterministic method itself is time consuming. Many improvements have been proposed to reduce this drawback, such as the parallelization [Johnson et al., 1997, Papadrakakis and Kotsopulos, 1999, Johnson et al., 2003], the sampling technique [Helton and Davis, 2003, Cambier et al., 2002] or the used of meta-model [Gayton et al., 2003, Lew et al., 2006] which will be discussed in the next subsection.

If a classification is considered as a function of uncertainty nature, two main categories can be built namely parametric and non-parametric methods. The parametric methods [Sudret, 2007] are the most popular and allow to take into account uncertainties on the parameters of the model. Amongst numerous proposals, the first methods were based on Taylor series expansion or perturbation techniques [Benfratello and Muscolino, 1998, Chakraborty and Dey, 1998, Nieuwenhof and Coyette, 2002, Falsone and Ferro, 2005] with the aim to substitute the equations of numerical model and the random functions by the mathematic developments to quantify the first statistical moments (mean, variance) of output solutions [Sudret, 2007].

These methods are dependent on the validity of Taylor series expansion and can only be applied for linear static and dynamic problems [Handa and Andersson, 1981, Liu et al., 1986, Shinozuka and Yamazaki, 1988] with low output dispersions around the nominal values as shown by Ghanem and Spanos [Ghanem and Spanos, 1991]. These last years, the authors were particularly interested in methods relying on polynomial chaos expansion developed by Wiener [Wiener, 1938]. The first works in mechanical engineering are due to Ghanem and Spanos [Ghanem and Spanos, 1991] who have combined Wiener-Hermite developments with finite element method to model and propagate uncertainty in mechanical structure. A more general extension, called generalized polynomial chaos, was proposed by Xiu et al. [Xiu and Karniadakis, 2002]. The method is based on the correspondence between the probability density functions of certain random variables and the weight functions of orthogonal polynomials of the Askey scheme. The polynomial chaos method allows the stochastic contribution of a random variables and the deterministic contribution to be dissociated. The random part is then decomposed on a basis of orthogonal polynomials (for example Hermite polynomials for Gaussian variable, Legendre for uniform variable). Intrusive and non-intrusive methods have been successively applied to calculate stochastic modes useful to uncertainty propagation. The intrusive method is based on the Galerkin projection to expand the uncertain model on the polynomial chaos basis as a linear system of deterministic coupled equations [Ghanem and Spanos, 1991, Babuska et al., 2004]. Nevertheless, this way is limited to a low number of random parameters and mainly applied to the case of linear problems to avoid the significant difficulties of implementation for non-linear problems. The second way, non-intrusive, relies on either regression methods or spectral projection methods. The first category calculates the stochastic modes by minimizing the gap between random function and its approximation on the polynomial chaos basis. On the contrary, the Non-Intrusive Spectral Projection (NISP) methods [Nechak et al., 2012] project the solution of problem on the basis of chaos. The initial problem is transformed into a calculation of integrals [Crestaux et al., 2009] by the collocation approach for example [Babuska et al., 2007, Loeven et al., 2007]. To avoid some limitations encountered in the case of large numbers of random variables or large range of variations, several alternatives have been proposed such as sparse generalized polynomial chaos [Ganapathysubramanian and Zabaras, 2007, Xiu and Hesthaven, 2005, Blatman and Sudret, 2008], multi-element generalized polynomial chaos [Wan and Karniadakis, 2005], Wiener-Haar chaos [Maître et al., 2004] or Wiener-Fourier chaos [Millman et al., 2005].

As the parametric probabilistic approach are not sufficient to take modeling errors and modeling uncertainties into account, a second category, called the non-parametric methods [Soize, 2000] has been developed and are based on the use of a reduced-order model and the random ma-

trix theory. The random matrix theory [Mehta, 1991] is used to construct the prior probability distribution of the random matrices modeling the uncertain operators of the mean computational model. On the same way, the non-parametric method consists in constructing directly the stochastic modeling of the operators of the mean computational model. In practice, the generalized matrices issued from the nominal finite element model of the structure are replaced by random matrices. The uncertainties are introduced directly on global matrices of the model by using a dispersion parameter and its prior probability distribution. The dispersion parameter is estimated according to the Maximum Entropy Principle [Jaynes, 1957] for which the constraints are defined by the available information [Soize, 2005a, Soize, 2005b]. Many works have been published in order to validate the non-parametric probabilistic approach with experimental results [Chebli and Soize, 2004, Chen et al., 2006] and to extend the applicability of the theory to different areas in structural mechanics [Capiez-Lernout and Soize, 2004]. Recently, an improvement of the non-parametric approach, called the generalized probabilistic approach of uncertainties, has been proposed [Soize, 2010] and allows the prior stochastic model of each type of uncertainties (uncertainty on the parameters of the model and modeling errors) to be separately constructed. Other developments are dedicated to quantify the role of each kind of uncertainty (parametric and non-parametric) and to integrate them simultaneously in uncertain applications.

Interval and fuzzy sets approach

The numerical developments proposed in interval and fuzzy set theory are very close and can be explained together since a fuzzy problem can be decomposed into a set of interval problems [Massa et al., 2006, Massa et al., 2008b, Massa et al., 2015a]. The reference method used to solve problems described by the fuzzy formalism is based on Zadeh's Extension Principle [Zadeh, 1975a, Zadeh, 1975b, Zadeh, 1975c], which extends general operations for real numbers to the corresponding operations for fuzzy numbers. The extension principle states that the degree of membership of one combination is equal to the smallest degree of membership of the independent parameters of this combination. In the case of multiple occurrences of a solution, the final membership degree is equal to the maximum membership degree of the different solutions. In practice, fuzzy numbers can be discretized either according to the support (membership value equal to 0) or, more conveniently, according to the membership function. Formally, implementation of the method leads to a combinatorial process which can be compared to MCS in the sense that it presents the same drawback in terms of computational time. In a similar way as with the probabilistic theory, many researches have been performed to propose alternatives considering successively interval arithmetic [Moore, 1966], perturbation

or series expansion [Qiu and Elishakoff, 1998, Lallemand et al., 1999] and specific samplings or designs of experiments [Hanss, 2002, Hanss, 2003, Donders et al., 2005, Hanss and Turrin, 2010, Haag et al., 2010]. However, these methods have rapidly shown some limitations such as the overestimation of the output set with interval arithmetic or a bad approximation of non-linear problems with perturbation techniques. The best results have been obtained using either sensibility analyses or optimization algorithms. The first works have been initiated by McWilliam [McWilliam, 2001] and relied on monotonic evolutions of response surfaces. Bounds of solutions are determined with bounds of the intervals associated to each parameter. More recently, an interesting solution has been proposed by transforming interval problems as a min-max optimization problem to limit computational time of the uncertainty propagation step and thus to be compatible with an industrial context [Massa et al., 2009a]. Indeed, this approach relies on iterative search for global optima (local gradient algorithm) in a search space, the size of which is gradually increasing when the degree of membership is decreasing [Massa et al., 2006, Massa et al., 2008b, Degrauwe et al., 2009]. For the crisp values, the output quantities and their first sensitivities are determined for each fuzzy parameter. The signs of the first-order sensitivities indicate the functional dependence of the response function and define the combinations of discrete fuzzy parameter values for the following level of degree of membership, which then can supply the minimum and maximum variations. For each α-cut level, the first derivatives of the output quantities are evaluated for the combinations of discrete fuzzy parameter values determined at the previous level. The comparison of the signs of the derivatives with those obtained at the previous level indicates the search path. In this context, the uncertainty propagation have already been studied in different linear problems such as static [Massa et al., 2006], modal [Massa et al., 2008b], frequency responses [Massa et al., 2009b, Ruffin-Mourier, 2008] and transient [Rao et al., 2010]. Moreover, to control the computational time, the proposed methods have been coupled with different approximations or reanalyses to limit the number of calls of finite element calculations.

1.4 Uncertain data management

After having calculated the non-deterministic solutions, it is possible to integrate them either on sensitivity analyses, to identify the most sensitive parameters or in optimization process, to study and improve the reliability and the robustness of the design.

The aim of sensitivity analysis [Saltelli et al., 2000, Zhang and Pandey, 2014, Cao et al., 2013] is to quantify the influence of each uncertain input parameter of a model. In this context, a global sensitivity is considered rather than a local deterministic sensitivity based on the com-

putation of gradients of the response with respect to input parameters around a specific value. First, the aim is to take into account both the input interactions and the information for all the possible ranges of variation of the uncertain parameters with the aim to estimate their influence [Gauger et al., 2008]. Secondly, the idea is to avoid the drawback linked to the choice of a reference point where local gradients are generally calculated. In non-probabilistic context, a state-of-the-art of available methods is proposed [Saltelli et al., 2000]. Regression-based methods or variance-based methods are mainly considered to measure the effects of inputs on outputs. In the case of variance methods, generally called ANalysis Of VAriance (ANOVA), the variances of the output are decomposed as a sum of contributions of each input variable.

Next, the reliability analysis [Ditlevsen and Madsen, 1996, Melchers, 1999, Lemaire, 2005] consists in computing the probability of failure of the system which can be described by a failure criterion. This mathematic criterion is directly linked to uncertain input parameters and mechanical output responses and is represented by a limit state function which separates safe and failure domain. The probability of failure is defined as the integral of the failure domain of the joint probability function of random vector and cannot be computed analytically. It is necessary to use numerical methods such as MCS or approximation methods such as First Order Reliability Method (FORM) or Second Order Reliability Method (SORM) [Kiureghian et al., 1987] to evaluate the joint probability function. With the two last methods, the idea is to approximate the probability of failure and to limit the computational time compared to MCS. In current industrial applications, the objective is to optimize the system and to guaranty that 95%, even 99%, of the samplings stay in the safe domain. The recent developments are focussed on the integration of efficient approximation to define a more suitable approximated probabilistic problem.

Finally, the robustness analysis traduces the ability of the optimum to be insensitive with respect to the input uncertainty. The aim is to guarantee in operation, low modifications of the proposed design behaviour. Robustness measures can be directly incorporates in the objective functions of non-probabilistic approaches of the non-deterministic optimization problem. For example, Kelesoglu [Kelesoglu, 2007] has proposed a method for fuzzy multi-objective optimization of space trusses, and Ramík [Ramík, 2007] has developed a class of fuzzy optimization problems with an objective function depending on fuzzy parameters. Massa et al [Massa et al., 2011a] have proposed a robust fuzzy optimization of a lower wall of micro satellite. The aim was to minimize the mass of the component while maximizing the robustness of the design parameters. In probabilistic theory, the robustness problem can be seen as a minimization problem of the variance of output data. Shah et al [Shah et al., 2015] have proposed a robust and computationally efficient optimization algorithm for air foil design under mixed uncertainty. The algorithm exploits stochastic expansions derived from the Non-Intrusive Polynomial Chaos techniques. Li et

al [Li et al., 2015] proposed a multi-objective robust optimization procedure mixing both random and interval variables in crashworthiness design of a foam filled column.

These advanced developments require very expensive computational times, which must be reduced, or at least maintained, using mathematical approximation as an alternative to the evaluation of large systems of equations (due to the finite element discretization for example).

The next section gives an overview of the main developments concerning the reduced model techniques.

2 Reduced model techniques

Although the modelisation of input data and the considered theories (probability, fuzzy and interval) are different, the underlying developments (Taylor series, projection) or algorithms (designs of experiments, optimizations), the main encountered problems (order of truncation, number of degrees of freedom and number of uncertain parameters) and scientific locks (precision, modularity, CPU time) are finally quite similar. Indeed, the proposed methods must be able to propagate uncertainty with a targeted level of precision while preserving a computational time compatible with the design step. Currently, for large industrial model, a solution can be considered as interesting if the entire calculations can be performed in less than one weekend. With the exception of parallel calculations (several cores or parallel algorithms) mathematical approximations are currently integrated in the solving scheme to achieve this objective. The aim is to predict the behaviours of studied solutions as a function of perturbed inputs. The computational time is thus reduced compared to traditional numerical methods. Reduced models can be separated in two classes developed in the two next subsections.

2.1 Surrogate models

The surrogate models or metamodels such as Proper Generalized Decomposition (PGD) [Ryckelynck, 2005, David et al., 2012, Chinesta et al., 2010, Nouy, 2010, Ladevèze and Chamoin, 2011], Proper Orthogonal Decomposition (POD) [Ryckelynck, 2005, Yvonnet et al., 2007, David et al., 2012], kriging [Kaymaz, 2005, Wang et al., 2013, Wei et al., 2004, Sakata et al., 2003], Radial Basis Functions (RBF) [Baxter, 1992], neural networks [Haykin, 1999] allow to build functions alternative to classical numerical simulations from only a set of specific samples of a Design Of Experiments (DOE). The general idea is to approximate a higher dimension system by another one of much lower dimension. PGD [Chinesta et al., 2010, Chinesta et al., 2011] is a technique where a separated representation of

the variables is introduced. It belongs to the family of Reduced-Order Modeling techniques, along with the ROM-POD method [Lieu et al., 2006] and the reduced-basis element method [Maday and Ronquist, 2002]. This method has been introduced by Ladevèze [Ladevèze, 1999] and called radial approximation in the Large Time INcrement (LATIN) method framework. On the contrary to POD, the PGD construction of the representation takes into account the nature of the problem directly. In the case of POD, an optimal basis is built considering proper orthogonal modes extracted from a correlation matrix, composed of different snapshots of numerical simulations or experiments. Surrogate modeling with different predictors such as the Response Surface Method (RSM) [Myers et al., 2009], neural networks [Haykin, 1999] and Kriging [Sacks et al., 1989, Forrester et al., 2008, Jones et al., 1998] have been introduced in several applications of structural dynamics. More precisely, Kriging is a statistical surrogate model that can be used to approximate the input-output function on its input space based starting from a small initial DOE. The Kriging model is a Gaussian process composed of an optional regression model estimated from available data and a random process associated to an error.

The main problem, lied to surrogate model, is to identify the necessary number of samples to build surrogate models with accuracy. Indeed, if too few samples are achieved, the prediction capability of resulting approximated models would be insufficient. On the contrary, ill-conditioning and expensive cost of additional computations can be observed with large samples.

2.2 Reanalysis techniques

With reanalysis techniques, specific developments are performed thanks to the mechanical problem (static, modal, dynamic) in consideration. The main idea is to perform only one nominal calculation and to re-utilize previous results to evaluate the perturbed solutions. In this case, perturbed data and matrices are built and integrated in perturbations techniques such as homotopy coupled or not with projection. Different numerical reanalysis techniques have already been developed in the literature such as the Taylor series expansion [Massa et al., 2004], perturbation and series development [Sliva et al., 2010, Rong et al., 2003, He, 1999], Combined Approximation (CA) [Kirsch and Bogomolni, 2004, Kirsch et al., 2006, Kirsch and Bogomolni, 2007], Padé approximants [Damil et al., 1999, Massa et al., 2008b, Yang et al., 2001, Duigou et al., 2003], projection on reduced basis [Balmès, 1996b, Corus et al., 2006, Bouazzouni et al., 1997, Boyaval et al., 2009, Nouy, 2010] and component mode synthesis [Masson et al., 2006, Balmès, 1996a, Guedri et al., 2006]. The main problem of these approaches is the intrusive character as they required an adaptation of the equations for each studied problem.

2.3 Integration in uncertain context

Surrogate models have largely been integrated in uncertainty propagation methods. For example, the Bayesian approach to incorporate global information and the fuzzy set approach to simplify the model and to take into account local uncertainties are combined [Bandemer and Gebhardt, 2000] for prediction of fields through the usual kriging technique. Wang et al [Wang et al., 2013] employed kriging method in global sensitivity analysis to study the effect of both epistemic and aleatory uncertainties. Li et al [Li et al., 2014] used kriging-based solution of second-level limit state function to regional sensitivity analysis of aleatory and epistemic uncertainties on failure probability. Bi et al [Bi et al., 2013] combined radial basis function to create a low-order model and hierarchical cluster analysis to give an accurate validation outcome with acceptable calculation cost. The procedure integrating parameter selection, uncertainty propagation, uncertainty quantification, parameter calibration, and model assessment is thus suitable for FE-models of a satellite. In electric domain, Arya et al [Arya et al., 2006] had determinate the probabilistic risk of voltage collapse, accounting uncertainties in system parameters, using radial basis function. Nobari et al [Nobari et al., 2015b] proposed a kriging-based surrogate model of a brake system constructed in order to reproduce the outputs of the large-scale finite element model. They overcome the issue of computational workloads in order to quantify the resulting squeal instability from different uncertain input variables. Chowdhury and Adhikari [Chowdhury and Adhikari, 2012] used correlated function expansion based meta-modelling approach for fuzzy parametric uncertainty analysis of linear dynamical systems. Louf and Champaney [Louf and Champaney, 2013] used a surrogate model based on the PGD method to obtain a quick estimate of the response of a structure whose material parameters are considered to be uncertain. Moller et al [Moller et al., 2008] employed the response surface method based on neural networks to improve numerical efficiency with structural collapse simulation under uncertainty.

For reanalysis techniques, Lallemand et al [Lallemand et al., 1999] utilized Neumann series expansion to treat eigenvalue problems including fuzzy parameters. Massa et al [Massa et al., 2006, Massa et al., 2008b] integrated Taylor series development and Padé approximations in fuzzy static and modal problems. Qiu and Elishakoff [Qiu and Elishakoff, 1998] propagated uncertainty with combination of the perturbation technique and interval mathematics to determine the region of static response surface. Chen et al [Chen et al., 2014] employed first-order Taylor series to study the exterior acoustic field prediction with interval and random variables. Pradlwarter et al [Pradlwarter et al., 2002] solved random eigenvalue problems for large systems using component mode synthesis, based on subspace iteration scheme, in which converged eigenvectors from previous calculations was used in the simulation loop as starting vectors of the current calculation.

Tran et al [Tran et al., 2010] used a robust component mode synthesis, in which the basis was enriched by residual response vectors, for stochastic damped vibroacoustics including uncertainty related to viscoelastic and poro-viscoelastic materials. Park [Park, 2008] introduced component-level analysis for constructing parametric reduced-order models which can be applied only to one component (and a single parametric variability). Hong et al [Hong et al., 2011] proposed the multiple-component parametric reduced-order models, based on component mode synthesis, for predicting the vibration response of complex structures with parametric variability in multiple components, in which the modified component matrix was described by the Taylor series development. Massa et al [Massa et al., 2015b] combined the homotopy perturbation and projection technique to reanalyze perturbed eigensolutions with uncertainty modelled by fuzzy numbers.

3 Friction induced vibrations

3.1 Noises and squeal phenomenon

Beside the pleasant noises as violin's sound, there is a lot of unpleasant noise in the current life such as the noise of ground-wheel contact in aviation [Asensio et al., 2007, Spalart et al., 2010], rail-wheel contact in railway engineering [Montenegro et al., 2015, Ramalho, 2015, Lyu et al., 2015], brake squeal in automotive [Oberst and Lai, 2011, Esgandari and Olatunbosun, 2015] or hip endoprosthesis squeaking noise [Ouenzerfi et al., 2015, Fan et al., 2011]. Indeed, vibrations are responsible for a large number of acoustical nuisances. In brake noise context for example, Akay [Akay, 2002] made a classification that contains two categories presented in figure 1.1, namely the forced vibrations (obtained from 10 Hz to 1 kHz) and self-sustained vibrations at higher frequency (1 kHz to several tens of kilohertz).

Brake noises frequently cited in the literature are groaning (frequencies under 100 Hz), moaning (100-500 Hz) and squealing (1-16 kHz). Low frequency noises involved mainly rigid body movements of the brake systems whereas high frequency noises are rather associated with eigenmodes of the structure. For the sake of respect of environmental criteria about acoustic pollution and customer's satisfaction, these noises are a major preoccupation of manufacturers and scientist communities.

Squeal and more generally friction-induced vibrations problems have largely been studied in the literature and the main works, performed before 2000, have been summarized in review papers proposed [Kinkaid et al., 2003, Ouyang et al., 2005]. Several experimental setups have been developed to understand conditions of apparition of noise. Beam-on-beam

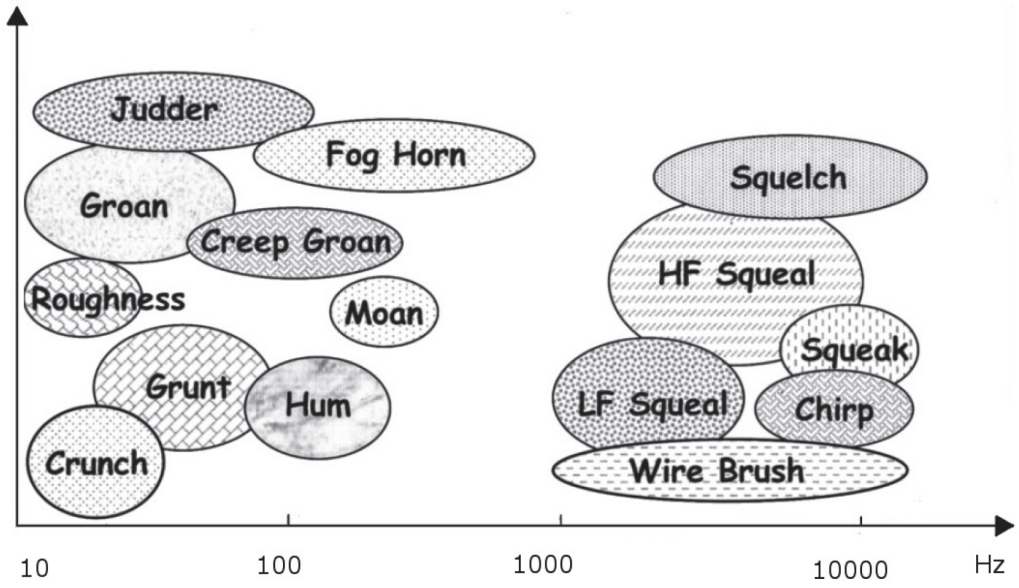


Figure 1.1 – Brake noises classification [Akay, 2002]

[Meziane et al., 2010], pin-on-disc [Butlin and Woodhouse, 2011, Butlin and Woodhouse, 2013], beam-on-disk [Massi et al., 2006, Akay et al., 2009] or tribometer [Meziane et al., 2007] tests rig was successively considered. For many years, a decreasing coefficient of friction with increasing sliding velocity was the only explanation of brake squeal triggering. Thereafter, engineers and researchers suggested that structural mechanisms may also be root causes of friction induced vibration. Today, many theories and models are available in the literature. All these models, coming from various domains, aim to explain the root causes of friction related dynamic instabilities and to predict the conditions under which oscillation may occur. One of the most famous theories is the stick-slip. Observations of the oscillation of the system reveal the existence of two distinct phases. The first phase presents no relative motion of the sliding bodies and is known as sticking. The second phase shows the relative motion of the bodies in contact and is known as sliding. Moving back and forth between these two states leads to stick-slip oscillation. Linck [Linck, 2005] identified thus the instabilities of sliding-separation, sticking-sliding-separation and sticking-sliding by dynamic friction coefficient. Otherwise, in the sprag-slip theory, vibrations are caused by multiple degrees-of-freedom interactions. The sprag situation leads to component buckling. After the components have been sufficiently deformed, they come loose and return to the original contact situation. Spragging in an elastic system can lead to sprag-slip limit cycles. This structural mechanism highlights the fact that friction induced vibration can be predicted without a decreasing coefficient of friction. Finally, most articles consider brake squeal to be vibration caused by mode coupling phenomena. When instability appears, a coupling between

frequencies of different component of the studied system is observed. Considering this problem in the Lyapunov's sense, squeal can be analyzed through the appearance of negative damping which leads to exponentially growing responses of the system and then an unstable state.

To numerically study squeal phenomenon, two kinds of methods are generally considered. First, the frequency way consists in performing a Complex Eigenvalue Analysis (CEA), in which system of equations are linearized around a stationary state determined from a non-linear static contact analysis. For each obtained complex eigenvalues, the real part represents the damping or growth rates whereas the imaginary part indicates the instable mode frequencies. However, CEA allows all possible unstable frequencies to be found but does not indicate which frequency is truly unstable in operation. Besides, the response level of the system during instability is not known. CEA studies [AbuBakar and Ouyang, 2006] have been investigated to detect brake squeal in relation to different physical parameters [Fritz et al., 2007]. Secondly, the transient way relies on a nonlinear dynamic analysis where the time evolutions of mechanical solutions are evaluated (e.g., velocities, loads, contact node status) [Massi et al., 2007, Meziane, 2007, Vermot Des Roches, 2011]. This analysis allows to determine the level of amplitude for accelerations or acoustic pressures. Massi et al [Massi et al., 2007] proposed performing both stability and transient non-linear simulations to reproduce squeal phenomena and to propose numerical and experimental correlations. Sinou [Sinou, 2010] focused on non-linear transient vibrations to illustrate the limitations of a local stability analysis based on an equilibrium position. Soobbarayen et al [Soobbarayen et al., 2013, Soobbarayen et al., 2014] have proposed a characterization of brake squeal from the calculation of sound pressures associated to the non-linear vibrations. In spite of appropriate computing facility, a CEA however requires several hours of calculation for a complete brake system, whereas a transient analysis costs several days and can be unreachable for full industrial systems.

3.2 Fugitive nature of squeal

Experimental and numerical investigations have allowed to highlight the main significant parameters and associated ranges of interest for squeal appearance. Indeed, the suitable external conditions for screeching of braking system are low speed braking (near to 3 km/h) [Liu et al., 2007] and a moderate level of braking pressure (20 and 30 bars) [Cazier, 2012]. For a pressure between 0 and 10 bars and a velocity of 10 km/h, the occurrence of a squeal is twice more important [Cazier, 2012]. Next, friction coefficient has been largely studied. Feng [Feng, 1998] highlighted the influence of friction effects on the contact behaviors with the observation of sticking, sliding and detachment zones. The number and status of contacts vary

clearly with different friction coefficient [Meziane, 2007, Feng, 1998]. Several authors observed that a reduction of effective friction coefficient (defined as the ratio of tangential load by normal load) allows the appearance of squeal to decrease [Fieldhouse et al., 2010, Liu et al., 2007]. The most significant range for squeal is observed between 0.4 and 0.5 as shown by Cazier [Cazier, 2012]. This parameter is link to experimental space parameters such as hygrometry [Blau and McLaughlin, 2003, El-Tayeb and Liew, 2008, El-Tayeb and Liew, 2009] or temperature [Júnior et al., 2008]. The latter influences the values of effective friction coefficient, Young's modulus and damping [Júnior et al., 2008]. Moreover, complementary investigations have been performed to quantify uncertainty related to material properties mainly for linings of pads which can be composed by up to twenty constituents [Kolluri et al., 2011, Hinrichs et al., 2011]. Linck [Linck, 2005] proved that variations on external parameters such as friction coefficient, imposed velocity, applied pressure or Young's modulus may cause different regimes of instabilities developed at the interface, namely sticking-sliding, sticking-sliding-detachment, sliding-detachment. Finally, Renaud et al. [Renaud et al., 2012] have highlighted the key role of brake pads component by observing the piston pad motion before and during squeal phenomenon.

In spite of these serious researches to understand the squeal phenomenon and the mechanism of appearance, it is always difficult to predict and eliminate squeal. Indeed, brake squeal is a highly fugitive phenomenon whose operational conditions are difficult to reproduce. Cazier [Cazier, 2012] have highlighted that the behaviour of two brake systems of a same car was clearly different. One can observe the emergence of unstable frequencies only for one of the systems or frequency shifts between the two brakes (Fig 1.2).

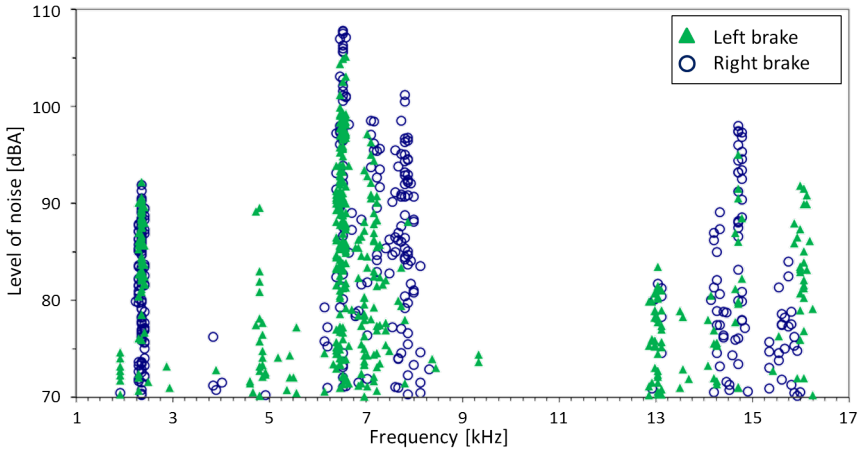


Figure 1.2 – Noise level of squeal occurrence for the left and right brake system [Cazier, 2002]

Moreover, one of the root causes of this fugitive nature is due to the evolution and nature of the contacting surfaces under sliding conditions [Guangxiong et al., 2002]. This evolution has

been studied in static condition [Heussaff et al., 2012] using Fujifilm pressure-sensitive films between the pads and the disc. Observations of pressure distributions on pads coming from different braking programs revealed a high variability. The topography of the contact surface is not perfectly smooth [Heussaff et al., 2012] and indentation measurements have shown contact stiffness heterogeneities [Magnier et al., 2014].

Considering these recent publications, the topography parameters seems to be the most significant parameter in squeal simulations (Fig 1.3)

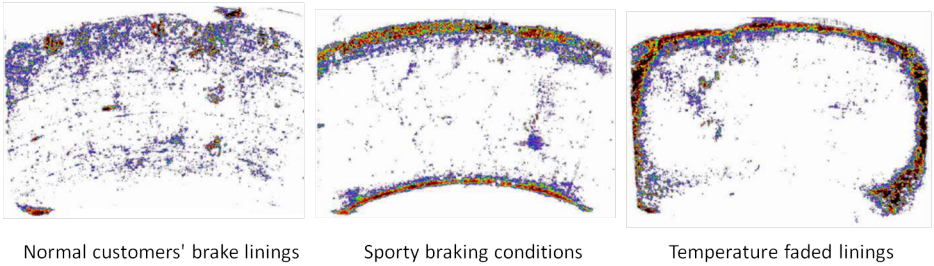


Figure 1.3 – Pressure distribution from different braking conditions [Heussaff et al, 2012]

Although frequency stability computations can supply important information about the behavior of a nonlinear system, the validity range is unknown and clearly depends on the stationary state. The static equilibrium position is directly related to the description of the contact surface. Thus, a modification of the contact surface can introduce a new distribution of normal pressure, and subsequently a new state of stiffness matrix asymmetry. Hetzler and Willner [Hetzler and Willner, 2012] presented the evolution of stability behavior as a function of the shape of pressure contact, for example, a half cosine-shaped pressure distribution. Research on the contact pressure distribution between discs and pads of brake systems has been carried out by a great number of scientists and engineers. The study of this parameter is becoming obvious and essential to brake research in order to predict the wear behavior of pads and discs, and thus, their topographic evolutions according to appropriate parameters (such as pressure, sliding velocity or time, for the most cited in the literature). Most of the authors who investigated wear mechanisms [AbuBakar and Ouyang, 2008, Soderberg and Andersson, 2009] either developed their own frictional law or integrated existing or modified models adapted from empirical equations into their computations. Thus, the contact area and the useful parameterization are the key elements of the general strategy.

3.3 Non-linearity of contact

Contact phenomena play a very important role in engineering structure. These last years, advances about the computational power have matched to the increasing of the size and the complexity of numerical models. Numerical simulations of mechanical engineering applications are nowadays clearly more predictive but integrate now some strong numerical difficulties such as mechanical frictional contacts. Although such phenomena have been studied for many years [Laursen, 2003, Wriggers, 2006], these nonlinearities are difficult to take into account and always represent a major challenge to the scientific community [Yastrebov, 2013, Kudawoo, 2013, Bussetta et al., 2012]. This is especially true when friction is considered.

In practice, the solving of a finite element simulation with contact nonlinearities can be seen as an optimization problem, subjected or not to optimization constraints, integrated in several solving loops dedicated to contact pairs management. To solve contact problems, formulations called variational inequality are largely present in literature [Cocu et al., 1996, Dilintas et al., 1988, Renouf and Alart, 2005] and can be seen as a minimization problem under constraints, generally solved with conjugate gradient techniques. Also, other formulations can be classified into linear or non-linear complementarity problems [Klarbring, 1986, Klarbring and Bjoourkman, 1992] in the mathematical optimization theory. The solving is performed with specific algorithms such as Lemke's algorithm, but turns out to be very intrusive within the frame of the finite element implementation. Finally, the last category is linked to formulations without constraints such as the bipotential method proposed by DeSaxcé and Feng [Saxcé and Feng, 1998] or Augmented Lagrangian approaches [Cocu et al., 1996, Dilintas et al., 1988, Curnier and Alart, 1988, Alart and Curnier, 1991, Bussetta et al., 2012] which are the most widespread formulations.

To overcome the difficulty relative to the non-differentiability of contact laws (contact/no contact, sticking/sliding), regularization methods relying on penalty functions or Lagrange multipliers are currently considered to transform contact inequations to a set of equations. These techniques allow to build a system of linear equations compatible with classical numerical methods such as the well-known Newton Raphson algorithm. Indeed, with penalization method [Perić and Owen, 1992], the contact loads are proportional to the displacements considering penalty coefficients for normal and sticking cases. During the solving, this method authorizes a slight penetration of bodies in contact. In practice, the penalty method does not require additional variables in the problem and, thus, is simple to implement. Nevertheless, the choice of penalty parameter is a major drawback of this technique. A low value of this coefficient leads to large values of penetration that are not physically acceptable while large values lead to ill-conditioned stiffness matrices. In addition, many contact laws depending on material and

interface characteristics have already been developed to model interface phenomena for frictional contact problem and to study local behaviours (stick-slip, dynamic friction coefficient). On the contrary, the Lagrangian Multiplier method [Chaudhary and Bathe, 1986] does not allow any penetration of each body and the contact conditions are fully verified. This method requires the introduction of additional unknowns, namely the Lagrange multipliers homogeneous to contact loads. Therefore, the problematics of conditioning can be frequently encountered as previously. To overcome this problem, the use of augmented Lagrange formalism, which couples the two previous approaches, has been developed and standardized as the reference method. Moreover, the contact pair management is the main barrier to achieve a fast and accurate solving of the problem. Indeed, the most used spatial discretization method is the Point-Surface method [Ponthot, 1997, Marceau, 2001, Goulet, 2004, Feng, 1991, Mouatassim, 1989], for which the contact is calculated between every point of one surface and the other ones. This method presents some limitations in term of representativity and regularity of the solution due to the discretization. To improve the reliability of results, other alternatives such as Surface-Surface method or mortar element method [Yang et al., 2005, Puso and Laursen, 2004a, Puso and Laursen, 2004b] have been developed more recently. Thus, no universal method is available to solve with precision and robustness all kinds of contact problems.

Moreover, characterizing the contact zone remains a significant scientific lock because parameters such as the friction coefficient, material properties or geometric characteristics at the contact interface are not precisely known [Heussaff et al., 2012]. This statement clearly justifies the use of parametric analyses or the introduction of uncertainty in this class of simulations, as exposed in the next section.

4 Reduced models and uncertainty propagation for frictional contact and stability problems

With the aim to propose less time consuming methods for solving a non linear contact problem, one can cite the work of Damil et al [Damil et al., 1999] about the use of asymptotic numerical method to solve contact problems. The idea is to replace the classical Newton-Raphson algorithm by homotopy developments [Abichou et al., 2002]. To perform implicit transient non-linear simulations, Vermot Des Roches [Vermot Des Roches, 2011] has suggested a fixed jacobian matrix within a modified Newton-Raphson algorithm. Balajewicz et al [Balajewicz et al., 2015] have recently introduced a projection-based model reduction approach for studying static and dynamic contact problems. The authors used a singular value decomposition method and a specific matrix

factorization method to build with efficiency the primal and dual reduced-order bases respectively dedicated to displacements and contact loads. Giacoma et al [Giacoma et al., 2015] have proposed an efficient a priori model reduction strategy for frictional contact problems. To solve the contact problem in a finite element context, a hybrid LATIN-PGD formulation [Ladevèze et al., 2010] has been investigated.

In this nonlinear context, significant modifications of behaviour can be observed even if the input variations level is low [Ragot, 2007]. Many studies have highlighted the sensitivity of contact parameters and dynamic properties of systems according to input parameters such as material properties, geometric characteristics or interface conditions [Ibrahim, 1994a, Ibrahim, 1994b, Shin et al., 2002, Shin et al., 2002, Hoffmann and Gaul, 2003, Sinou et al., 2004, Sinou et al., 2006a, Sinou et al., 2006b]. In the case of friction induced vibrations problems under uncertainty, Gauger et al [Gauger et al., 2006] used fuzzy formalism to model respectively the influence of uncertain friction and Young modulus on the modal behavior of a beam/disc model and an industrial brake model. Culla and Massi [Culla and Massi, 2009] employed MCS and substructured model for investigating contact instability under the influence of uncertainties, which leads to the occurrence of squeal noise. Chentouf et al [Chentouf et al., 2011] take uncertainties into account to predict the modification of behaviors and to reduce the numerical costs using a robust reduction basis. For each modified system, the robust reduction basis is reanalyzed based on nominal normal modes of Craig-Bampton's components. Considering a polynomial chaos approach, Nechak et al [Nechak et al., 2013] takes the influence of uncertain friction coefficient into account on a dry friction system to predict stable and instable behaviors. In the same way, Sarrouy et al [Sarrouy et al., 2013b] have determined both uncertain eigenvalues and stochastic limit cycles of a self-excited non-linear system. They have also computed stochastic complex eigenvalues of a simplified brake system with uncertain friction coefficient [Sarrouy et al., 2013a]. Fazio et al [Fazio et al., 2015] have studied a friction induced vibration problem through the stability analysis of an industrial brake system. A reduction technique is proposed to create Super-Element to reduce number of nodes in contact, which consequently reduce computational time. Recently, the statistics of complex eigenvalues have been studied with the application to friction induced vibration problems. The second-order perturbation method is retained to propagate uncertainty of input parameters [Nobari et al., 2015a]. Finally, Nobari et al [Nobari et al., 2015b] predict squeal instability of uncertain brake systems through the construction of kriging surrogate model.

Many of the researches cited above rely on the underlying assumption that a sufficient number of observations can reproduce different unstable behaviour of the studied system. From previous simulations and experiments [Renault et al., 2014, Tison et al., 2014] we have observed that pa-

rameters, particularly the topography of contact surfaces, may lead to very different behaviour than the nominal model. Thus, we propose here to develop a strategy which takes variability into account to speed up the calculation without modifying the sequence of the complex eigenvalue analysis. In other words, each step of the simulation is conserved. In that sense, a new method to address contact non linearity in the context of multiple samplings is proposed. The method relies on the use of automation control technique and is presented in the next chapter.

Chapter 2

Finite element analysis of frictionless contact problems using fuzzy control approach

Contents

1 Introduction 34

2 2D Frictionless contact problem in a finite element context 35

2.1 Continuous formulation 35

2.2 Finite element discretization and numerical methods 36

3 Fuzzy Logic Controller for Contact method 38

3.1 Fuzzy Logic Controller and normal contact management 38

3.2 Definition of the reduced contact problem 42

3.3 Design of fuzzy controller and contact solving 43

4 Numerical applications for frictionless contact problem 45

4.1 Elastic beam on beam problem 46

4.2 Elastic beam on rigid segment problem 51

4.3 Two semicircular structures in contact 53

5 Conclusion 56

1 Introduction

The bibliography study have highlighted that the number of papers about reduced order models, uncertainty propagation is increasing these last years and in particularly for the friction induced vibrations and squeal analyses [Nobari et al., 2015a, Nobari et al., 2015b, Fazio et al., 2015, Sarrouy et al., 2013b]. Indeed, the authors have as objective to build alternative strategy to calculate the stability data with reduced computational costs or quantify the possible evolution of behaviour. The sensitivity analyses have clearly shown that the equilibrium position and so the contact problem plays a key role in a friction induced vibrations problems, where the mode coupling assumption is considered. Moreover, the recent works of Tison et al [Tison et al., 2014] have shown that the surface topography is clearly one of the most significant parameters, even the most influential. A consequence is that the unstable modes spectrum can be drastically modified. Taking into account different evolutions of parameters in design step generate multiples samplings and so important computational time. Nevertheless, only few papers directly discussed of alternative strategy (surrogate model, reanalysis or uncertainty propagation) for nonlinear contact problems in a multiple sampling context.

Thus, we propose in this chapter to study the contact problem in a context of multiple samplings and develop an alternative method for the numerical solving. The aim is to calculate the output solutions with reduced computational time and without losing precision. Only the frictionless case is investigated in a finite element context. We proposed to study the possibility of using a Fuzzy Logic Control approach to manage contact problem.

This chapter is decomposed into 4 sections: continuous and variational contact problem formulations and the associated finite element discretization are recalled in Section 2. A new method, named Fuzzy Logic Controller for Contact (FL2C) method, which relies on the design and implementation of a fuzzy logic controller to link the normal gap and contact load, is described in Section 3. To assess the efficiency of the proposed method, three numerical applications for contact problems are presented in Section 4. The results are compared with those obtained using industrial code Abaqus. Conclusions and remarks are provided in Section 5.

2 2D Frictionless contact problem in a finite element context

2.1 Continuous formulation

Let us consider an elastic solid Ω, defined using isotropic linear constitutive law, in contact with fixed rigid body Ω_R through interface Γ_C in Fig 2.1. The boundary of Ω, denoted by Γ, is subjected to prescribed pressure Γ_d on Γ_F, prescribed displacement field $\mathbf{U}_d$ on Γ_U and body force $\mathbf{f}_v$ on Γ. The $\vec{\mathbf{n}}$ and $\mathbf{p}_n$ variables designate the unit normal vector pointing outward from Γ and the contact pressure respectively. The deformations are considered to be infinitesimal relative to the initial configuration.

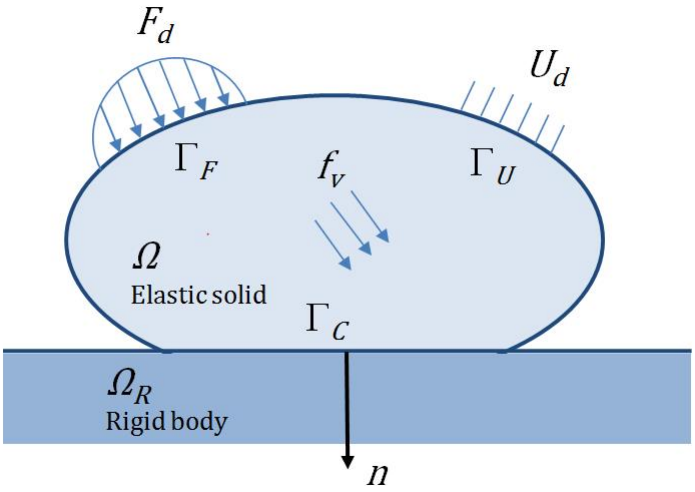


Figure 2.1 – Description of contact problem

The problem involves calculating displacement field $\mathbf{u}$ and the Cauchy stress tensor $\sigma(\mathbf{u})$. The equations that govern the static motion for Ω are:

$$div\sigma(\mathbf{u}) + \mathbf{f}_v = 0 \quad \text{in} \quad \Omega \tag{2.1}$$

$$\sigma(\mathbf{u}) = \mathbf{D} : \epsilon(\mathbf{u}) \quad \text{in} \quad \Omega \tag{2.2}$$

$$\sigma(\mathbf{u})\mathbf{n} = \mathbf{F}_d \quad \text{on} \quad \Gamma_F \tag{2.3}$$

$$\mathbf{u} = \mathbf{U}_d \quad \text{on} \quad \Gamma_U \tag{2.4}$$

where $\mathbf{D}$ and ϵ are Hooke's tensor and the linearized Eulerian-Lagrangian strain tensor respectively.

Managing contact between two solids requires the definition of normal gap variable $\mathbf{g}_n$ as the shortest distance between the solids along normal vector $\vec{\mathbf{n}}$. Penetration between solids is detected as soon as the gap value is negative. In this case, a normal reaction is defined between master to slave components to avoid interpenetration. Fig 2.2-a summarizes the contact data limited to one contact pair defined by a slave node, noted C, and a master segment, noted AB. Vector $\vec{\mathbf{n}}$ is the outgoing normal of the master segment, and normal clearance $\mathbf{d}$ is written as the distance between slave node C and its projection P in AB.

Therefore, Signorini conditions in Fig 2.2-b state:

$$\begin{cases} \mathbf{g}_n \geq 0 \\ \mathbf{p}_n \geq 0 \\ \mathbf{g}_n \mathbf{p}_n \geq 0 \end{cases} \tag{2.5}$$

where $\mathbf{p}_n$ is the normal contact pressure applied on the surface of solids in contact. Eq 2.5 represents two contact states, i.e., either an open contact state for a strictly positive gap and contact pressure equal to 0 or a closed contact state with a null gap and strictly positive pressure.

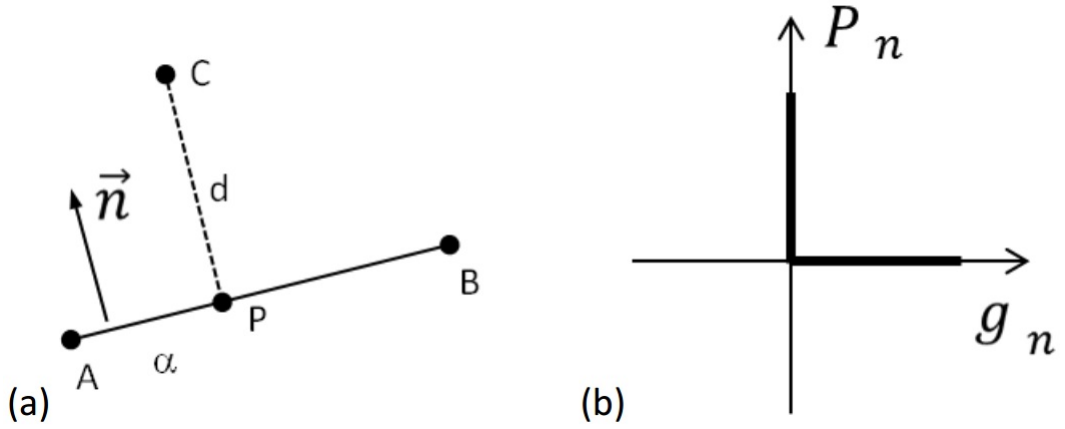


Figure 2.2 – (a) Definition of the normal contact problem (b) Signorini's contact pressure law

2.2 Finite element discretization and numerical methods

The formulation of the mechanics of a continuous medium, called strong formulation, cannot be analytically solved for complex systems. A variational form, qualified as weak formulation and directly stemming from the virtual work principle ([Duvaut and Lions, 1976] and [Oden and Martins, 1985]), is necessary first. The studied problem is defined by two integral equations derived from the virtual work principle and the weak formulation of Signorini's uni-

lateral contact conditions. Next, the Ritz-Galerkin method is used to perform finite element discretization [Zienkiewicz and Taylor, 1994] for these equations. Subsequently, the equilibrium equation in Eq 2.1 is written as follows:

$$\mathbf{KU} + \mathbf{F}_c(\mathbf{U}) \quad = \quad \mathbf{F} \tag{2.6}$$

where $\mathbf{K}, \mathbf{U}, \mathbf{F}$ and $\mathbf{F}_c(\mathbf{U})$ respectively designates the stiffness matrix, the nodal displacement vector, the external load vector and the non-linear contact loads, which are dependent upon the displacement of all solid bodies in contact.

The constraints of contact management become:

$$\mathbf{GU} \quad \leq \quad 0 \tag{2.7}$$

where $\mathbf{G}$ is the global matrix of the displacement conditions that ensure non-penetration and the contact law of the bodies in contact with each other.

To solve this kind of non-linear problem, iterative methods, such as the Newton-Raphson method, are usually used in industrial code coupled with regularization methods such as a penalty method, the Lagrange multiplier procedure or a hybrid method, like the augmented Lagrangian method. The Newton-Raphson method involves calculating a series of incremental corrections to obtain a targeted solution to a problem from a previous equilibrium state. Incremental corrections $\Delta\mathbf{U}_i$ at the i^{th} iteration are calculated using the following equation:

$$\mathbf{K}_T(\mathbf{U}_i)\Delta\mathbf{U}_i \quad = \quad \mathbf{R}(\mathbf{U}_i) \tag{2.8}$$

$$\mathbf{U}_{i+1} \quad = \quad \mathbf{U}_i + \Delta\mathbf{U}_i \tag{2.9}$$

where $\mathbf{R}(\mathbf{U}_i)$ and $\mathbf{K}_T(\mathbf{U}_i)$ are respectively the residual of the static equation calculated for $\mathbf{U}_i$ and the tangent stiffness matrix corresponding to the first order development of vector $\mathbf{R}$ through current displacements.

Resolving a contact problem is not a small task, numerically speaking, and generates a wide range of resolution methods. For example, Aggoune et al [Aggoune et al., 2004] presented an alternative method using a high-order prediction correction algorithm based on the asymptotic numerical method and a perturbation technique. DeSaxcé and Feng [Saxcé and Feng, 1998] developed the so-called bipotential method to take into account Signorini and Coulomb laws in a single formalism.

In a multiple sampling context, the aforementioned traditional methods are not appropriate because intermediary calculation steps cannot be used for different input parameter values. It is

necessary to re-build the tangent stiffness matrix for each calculation, and doing so will increase the already long computational times. Therefore, Vermot des Roches [Vermot Des Roches, 2011] has suggested using a fixed jacobian matrix within a modified Newton-Raphson algorithm adapted for studying contact vibrations. This strategy avoids repeating jacobian matrix factorizations and keeps the left member of the Eq 2.8 unchanged for the different iterations. This enables computational time to be substantially disminished.

3 Fuzzy Logic Controller for Contact method

3.1 Fuzzy Logic Controller and normal contact management

The pioneering research [Mamdani, 1974, Mamdani and Assilian, 1975] on fuzzy control was motivated by Zadeh's seminal papers on the linguistic approach and system analysis according to fuzzy set theory. Fuzzy set theory was introduced by Zadeh [Zadeh, 1965] as an extension or generalization of classic set theory. In Zadeh's theory, the membership degree, which varies between 0 and 1, is attributed to the different values of non-deterministic parameters. In this context, a fuzzy number is then defined using a membership function that can take different forms, depending on the kind of imperfection considered. Without information about the data to be modeled, triangular membership functions are the simplest and most common choice. However, with additional information, best-suited membership functions can be chosen (e.g., π-shape, trapezoidal) to model a user's perception. Fig 2.3 presents triangular and trapezoidal membership functions.

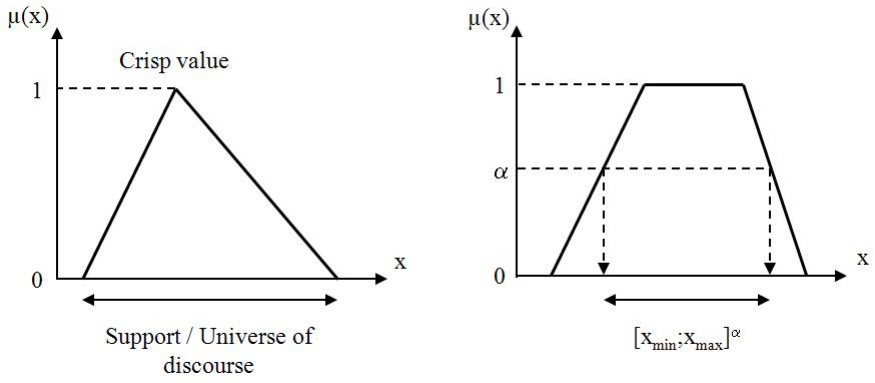


Figure 2.3 – (a) Triangular membership function (b) Trapezoidal membership function

The advantage of fuzzy sets is being able to mathematically model linguistic concepts based on expert knowledge. This approach permits modeling of imprecise, vague or ill-defined parameters and may be suitable for modeling imprecise parameters that are only known by

their bounds. Massa has already represented imprecision in this way in mechanical engineering to successfully study a variety of non-deterministic problems, for example, in dynamic analyses [Massa et al., 2008b], optimization [Massa et al., 2009a] and experimental processes [Massa et al., 2009b].

Fuzzy logic [Zadeh, 1975a, Zadeh, 1975b, Zadeh, 1975c] is a multi-valued logic derived from fuzzy set theory to deal with reasoning that is approximate rather than precise. In contrast with binary sets, in which the membership value of a variable in the set is either 0 or 1, the membership value of a variable can be between 0 and 1. This concept is based on the fact that a Boolean variable is ill adapted to represent common phenomena. Fig 2.4-a shows the basic configuration of a Fuzzy Logic Controller (FLC), which includes four principal components: a fuzzification interface, a knowledge base, decision-making logic and a defuzzification interface. The fuzzy model relies on both scientific observations and operator experience.

In engineering, Liao, Tanyildizi [Liao, 1996, Tanyildizi, 2009] and Khabbaz et al. [Khabbaz et al., 2009] recently considered fuzzy sets and fuzzy logic to select or predict material properties for mechanical designs. Hayajneh et al [Hayajneh et al., 2006] has implemented a fuzzy logic controller to move the overhead crane along a desired path while ensuring that the payload is swing free at the end of the motion. Yapici et al [Yapici et al., 2009] has developed a model based on the use of a fuzzy logic classifier to predict the values of moduli elasticity and rupture. Kohn-Rich and Flashner [Kohn-Rich and Flashner, 2003] has employed a robust control design approach for tracking the control of mechanical systems, whereas Bingul and Karahan [Bingul and Karahan, 2011] has controlled robot dynamics by optimizing fuzzy controller parameters. More recently, Mabrouk et al [Mabrouk et al., 2013] proposed to design a fuzzy controller to study the modeled behavior of an electrodynamic levitation device using a finite volume method.

Since fuzzy logic is effective for linking multiple inputs to an output in a non-linear domain, we propose to design and implement a fuzzy logic controller for linking the normal gap and contact load. In this work, the FLC is designed by considering the following observation: "If a load is applied on a node of the finite element model following a specific direction, then this node will move in this direction". This statement can then be used to reduce the gap between components.

The initial problem is broken down into a set of rules, in the form "IF variable IS property, THEN action" that define the desired system output response for the input conditions of a given system. The number and complexity of the rules depends on the number of input parameters to be managed and the number of fuzzy variables associated with each parameter. The fuzzifier converts a crisp value into degrees of membership by applying the corresponding membership functions. The α-cut levels associated with each membership function for input variables are determined. First, the deterministic inputs are received by the logical system for each input

variable. Second, the intersections between these values and the different membership functions are used to define the α-cut levels, which are used in turn in the inference mechanism. If no intersection is found with membership functions, the α-cut level associated to these membership functions is set as 0.

Fig 2.4 shows the configuration of a FLC that includes four principal steps.

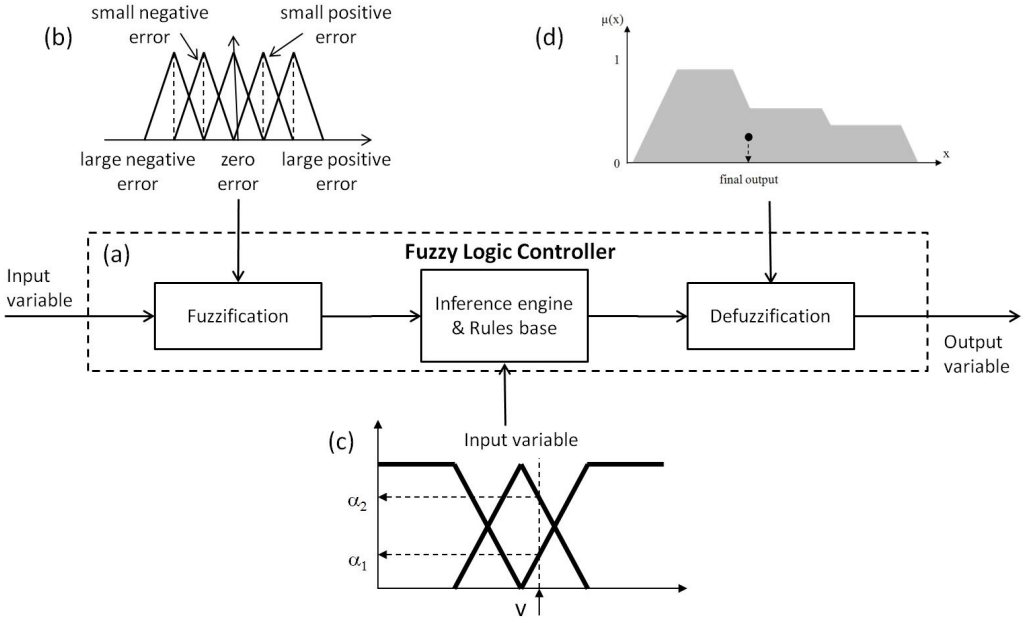


Figure 2.4 – (a) Basic FLC configuration (b) membership functions associated with linguistic adjectives (c) inference mechanism step (d) defuzzification step using the center-of-gravity method

The description of these steps is here adapted to the contact problem:

- Definition of knowledge base (Step 1): Normal gaps g_n^k and g_n^{k+1} calculated for two consecutive iterations are defined as input variables, whereas the γ-coefficient associated with the increment of normal loads ΔF_n is considered as an output variable. Taking into account two successive states of normal gaps improves the convergence of the proposed method. Each input variable is modeled using five fuzzy linguistic terms in Fig 2.5, respectively "Negative Large (NL)", "Negative Small (NS)", "Null (N)", "Positive Small (PS)" and "Positive Large (PL)" for each input variable.

  For output variables in Fig 2.6, five linguistic qualifiers are used as well, namely "Near to Zero (NZ)", "Small (S)", "Medium (M)", "Large (L)" and "Near to One (NO)". The initial problem is broken down into a set of rules in the form "IF variable IS property, THEN action" that define the desired system output response for the input conditions of a given system.

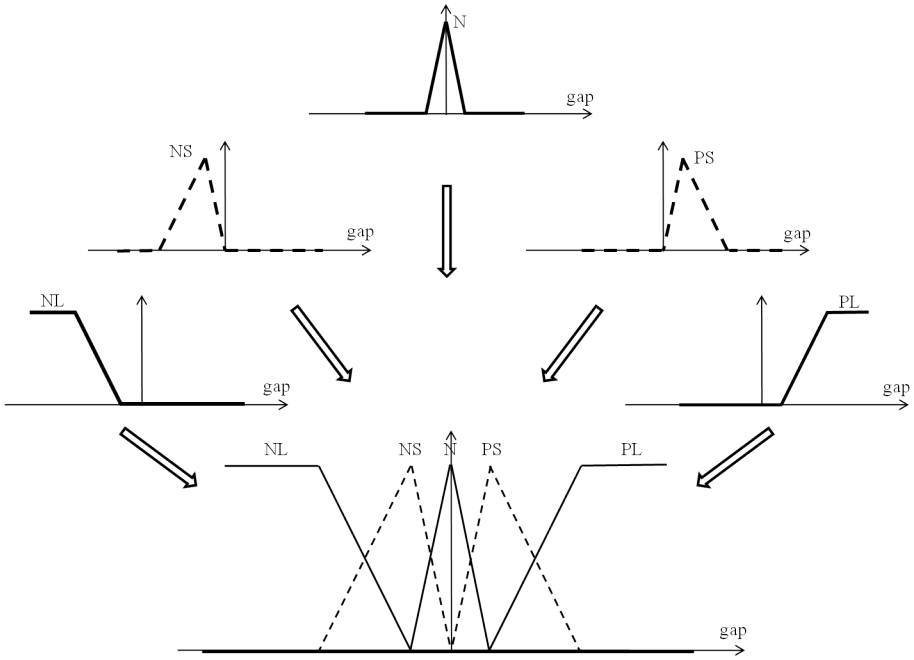


Figure 2.5 – Definition of FLC laws for gap

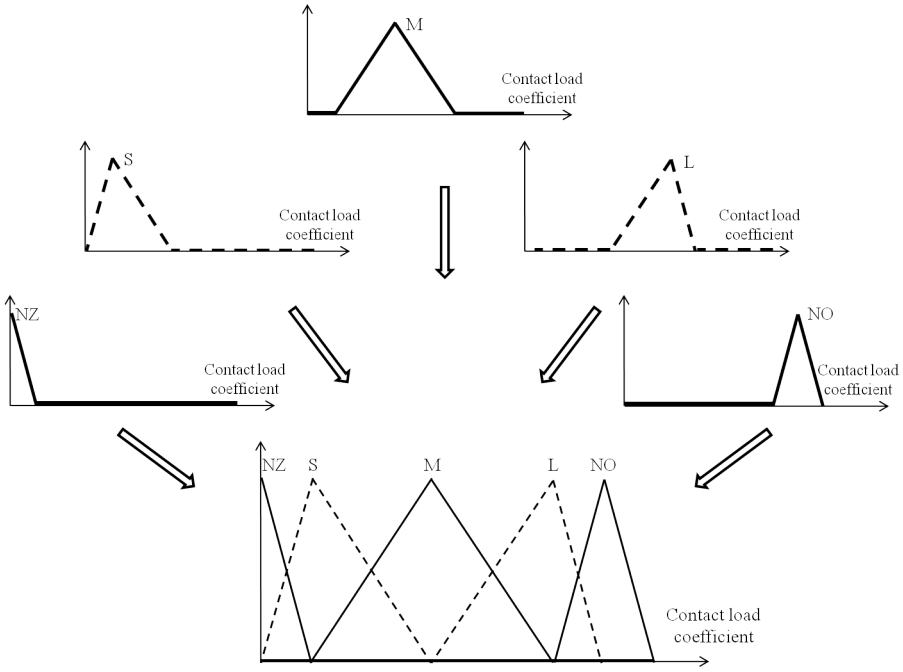


Figure 2.6 – Definition of FLC laws for contact loads

- Fuzzification step (Step 2): The fuzzifier converts a crisp value of gaps into degrees of membership by applying the corresponding membership functions. The α-cut levels associated with each membership function for input variables are determined. Firstly, the

deterministic inputs are received by the logical system for each input variable. Secondly, the intersections between these values and the different membership functions are used to define the α-cut levels, which are used in turn in the inference mechanism. If no intersection is found with membership functions, the α-cut level associated with these membership functions is set to 0.

- Decision-making logic (Step 3): The inference mechanism transfers the α-cut levels for each gap membership function associated with an output contact load variable using the rules. For each rule, the inputs are combined logically using the AND operator to produce output response values by taking into account the α-cut levels obtained in the second step. The final output level is calculated by using the max-min method. Executing the rules in the rule base generates multiple shapes that represent the modified membership functions.
- Defuzzification step (Step 4): A defuzzification step is necessary to obtain the deterministic value. Defuzzification is the transformation of this set of percentages into a single deterministic value. Here, the center-of-gravity method is used to find the centroid of the shape obtained by superimposing the shapes resulting from applying the rules. The output of the defuzzifier is the value of coefficient γ associated with normal loads.

Thus, fuzzy logic allows us to link numerical and quantitative representation to symbolic and qualitative representation using fuzzy set theory.

3.2 Definition of the reduced contact problem

The main idea of the FL2C method is to consider the normal contact problem as a regulation/control problem that solves the nonlinear problem iteratively as a linear problem set. Thus, normal gap $\mathbf{g}_n$ is controlled at each iteration and is reduced to the tolerance value. The contact load is only considered an external load, such as:

$$\mathbf{K}\mathbf{U}^{i+1} = \mathbf{F}_{ext} + \mathbf{F}_n^{i+1} \tag{2.10}$$

where $\mathbf{F}_n^{i+1}$ represents the contact load at the i^{th} iteration.

We suggest keeping an uncoupled stiffness matrix while solving the contact problem in order to limit the number of factorizations. In the proposed strategy, Eq 2.6. is reorganized by considering the contact load only as an external load. The stiffness matrix of the bodies in contact remains thus unchanged while solving the problem. The nonlinear problem is solved iteratively as a linear problem set by using the finite element method for specific contact load values, which are calculated using a FLC (see section 3.3). The idea is to consider the determination of contact loads as a regulation problem, and to refrain from considering regularization techniques and

tangent matrices in the proposed resolution.

Moreover, a **T**-based projection is considered to reduce the size of the system. For example:

$$\mathbf{U}^{i+1} = \mathbf{T}\mathbf{q}^{i+1} \tag{2.11}$$

$$\mathbf{T}^T\mathbf{K}\mathbf{T}\mathbf{q}^{i+1} = \mathbf{T}^T\mathbf{F}_{ext} + \mathbf{T}^T\mathbf{F}_n^{i+1} \tag{2.12}$$

In the present case, the projection basis is built with a concatenation of the first eigenvectors given by each component taken separately from the entire system. The modal bases are then completely independent from the contact problem. Only boundary conditions associated to each component are taken into account. Variable $\mathbf{q}^{i+1}$ of Eq 2.12 represents the modal coordinates vector. This makes it possible to replace the linear system solution with standard mathematical operations and reduce the computational time.

3.3 Design of fuzzy controller and contact solving

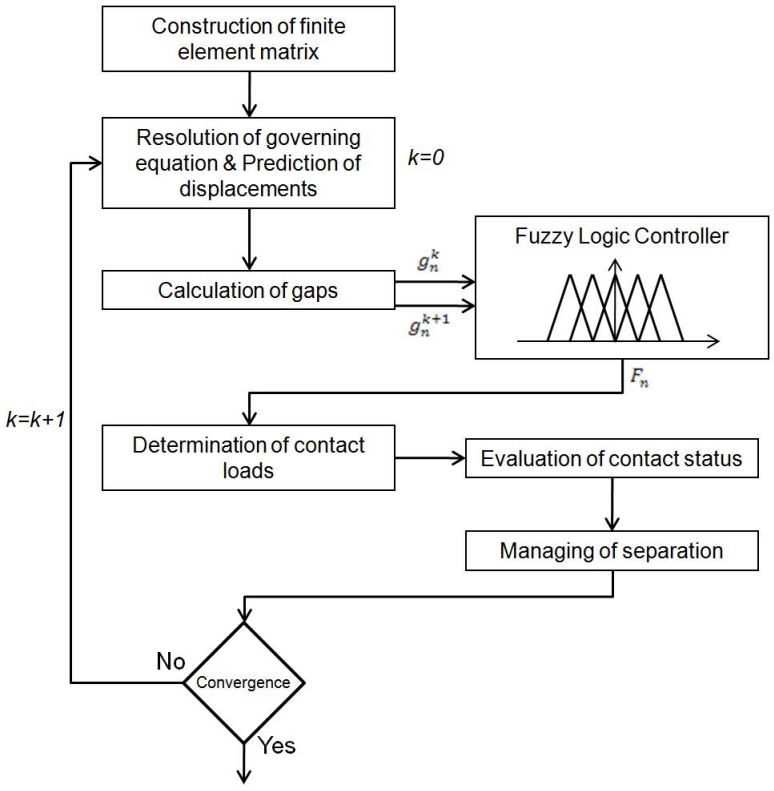


Figure 2.7 – Computational procedure for the FL2C method

The FL2C method, integrates the controller into a static computational procedure described

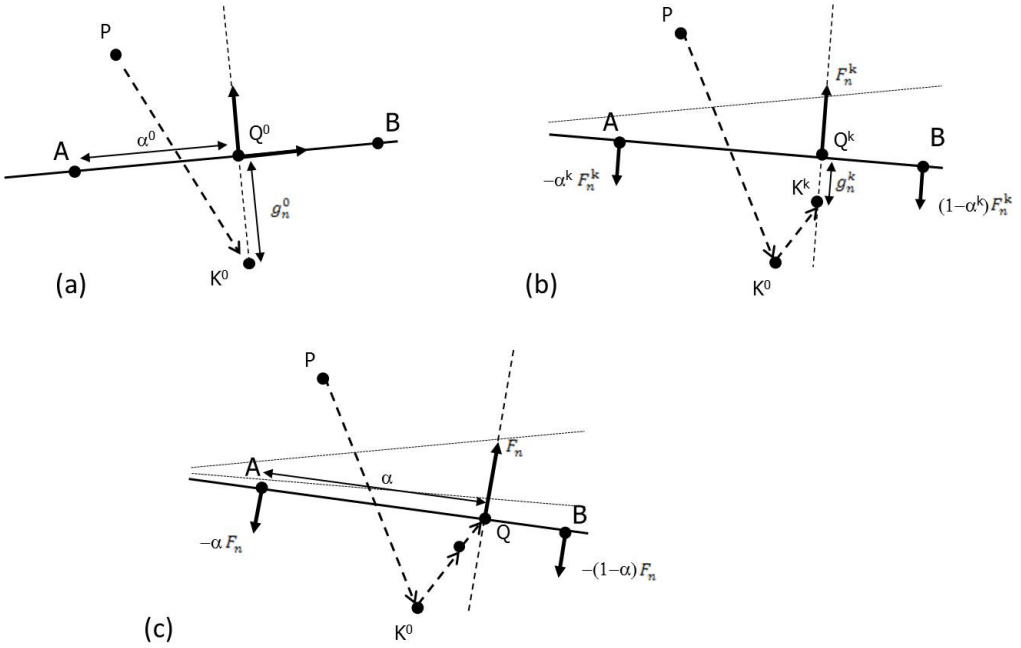


Figure 2.8 – Contact problem (a) before correction, (b) after k iterations (c) after determination of static equilibrium

in Fig 2.7. The first step is to build the finite element matrices of the different bodies. The second step uses Eq 2.12 to predict the body displacements without contact loads to calculate. In step 3, the initial normal gaps between bodies, respectively denoted as $\mathbf{g}_n^0$ are calculated. Fig 2.8-a shows the local base $(\vec{\mathbf{n}}, \vec{\mathbf{t}})$, which is defined for each master element. Using the controller, the penetration between the bodies Fig 2.8-b is iteratively reduced to reach the static equilibrium position Fig 2.8-c. Step 4 determines the loads by considering the Signorini model. The non-penetration and non-compression conditions are verified for each slave node. If the normal load becomes negative, a relaxation phase is considered.

The FLC is defined by considering, as the input variable, the normal gaps $\mathbf{g}_n^k$ and $\mathbf{g}_n^{k+1}$ calculated for two consecutive iterations, and, as output variable, the γ-coefficient associated with the increment of normal loads $\Delta\mathbf{F}_n$, as described in Eqs 2.13 & 2.14.

$$\mathbf{F}_n^{k+1} = \mathbf{F}_n^k + \Delta\mathbf{F}_n^{k+1} \tag{2.13}$$

$$\Delta\mathbf{F}_n^{k+1} = \gamma\Delta\mathbf{F}_n^k \tag{2.14}$$

The fuzzy if-then rules for gap control are given in Table 2.1. The total number of rules is then set as 25.

Table 2.1 – Fuzzy logic rule base

		Gap $\mathbf{g}_n^{k+1}$				
		NL	**NS**	**N**	**PS**	**PL**
	NL	NO	NO	L	L	M
	NS	L	M	M	M	S
Gap $\mathbf{g}_n^k$	**N**	NZ	S	M	S	NZ
	PS	S	M	M	M	L
	PL	M	L	L	NO	NO

4 Numerical applications for frictionless contact problem

For the three cases studied, five linguistic terms, namely "Negative Large (NL)", "Negative Small (NS)", "Null (N)", "Positive Small (PS)" and "Positive Large (PL)" are considered for each input variable in Fig 2.9 whereas five linguistic qualifiers are used for output variables "Near to Zero (NZ)", "Small (S)", "Medium (M)", "Large (L)" and "Near to One (NO)" in Fig 2.10.

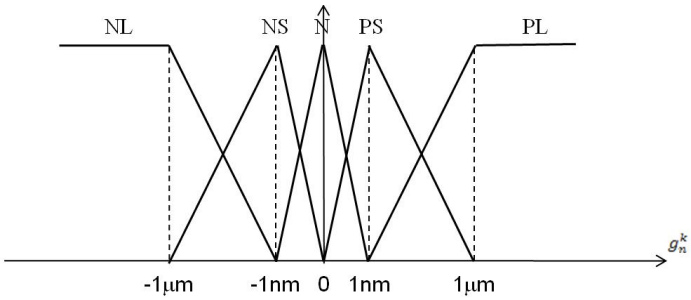


Figure 2.9 – Membership functions associated to normal gap variables

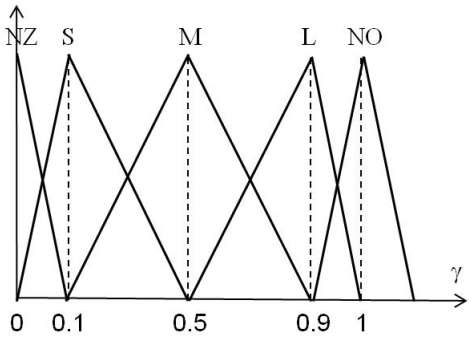


Figure 2.10 – Membership functions associated with normal load increments

The FL2C method has been implemented in Matlab. However the following subsections present three tests cases with increasing difficulty. The first test case considers two elastic beams involving a one node contact problem. With the second test case, the problem of multi-contacts is addressed considering an elastic beam in contact with a rigid curved surface. The third test case addresses the case of multi-contact and large relative displacements between the two curved shape elastic media. In all cases, solutions of FL2C are compared with those calculated with Abaqus software.

4.1 Elastic beam on beam problem

Description of the model

The contact problem is composed of two horizontal elastic beams P(1) and P(2) in Fig 2.11, modeled using quadrinodal plane finite elements. Boundary conditions are such that the beams are completely fixed in translation at their extremities. The initial vertical gap between the two beams is initially imposed as $1.10^{-8}m$. The geometric characteristics and material properties of beams are presented in Table 2.2. In this non-linear static problem, an external load F, the amplitude of which will be considered between 10000 N and 100000 N, is applied to beam P(1). P(2) is chosen to be the master structure while P(1) is the slave one.

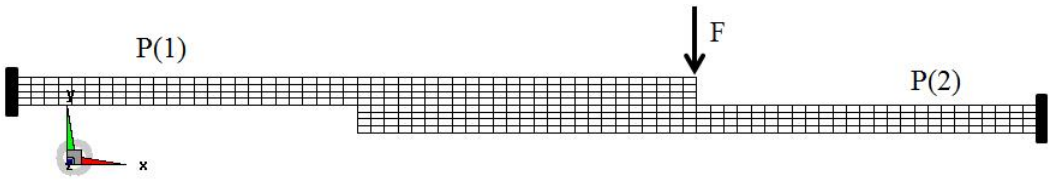


Figure 2.11 – 2D finite element beam-on-beam model

Table 2.2 – Geometric characteristics and material properties of beams of P(1) and P(2)

	Length [m]	Width [m]	Young modulus [GPa]	Poisson's ratio	Density [kg/m^3]
Beams P(1) / P(2)	0.2	0.008	210	0.3	7900

The eigensolutions, which are useful in building the basis of the projection, are calculated up to 25 kHz for the two identical beams. The eigenfrequencies are summarized in Table 2.3.

Table 2.3 – Eigenfrequencies of beams P(1) and P(2)

	1	2	3	4	5	6	7	8	9
Frequencies [Hz]	174.8	1087.1	3007.7	5796.6	6449.5	9387.7	13693	18625	24094

Validation of the results of FL2C method

Fig 2.12 presents the normal gap obtained, at the end of the computational procedure, by the FL2C method for ten values of the external load. The results, in the order of $10^{-10}m$, highlight that the proposed method is compatible with different load values without modifying the universe of membership functions and the FLC rules.

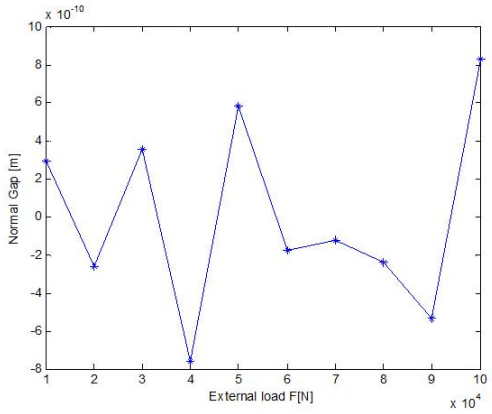


Figure 2.12 – Normal gap evolution as a function of external load amplitude

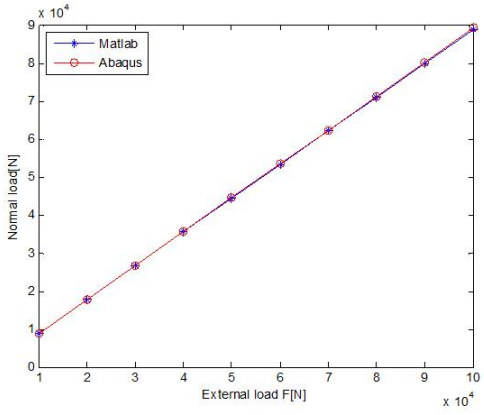


Figure 2.13 – Normal contact load evolution as a function of external load amplitude

Figs 2.13 & 2.14 show that the results obtained in term of normal load and contact surface displacements are equivalent to those supplied by the Abaqus software (Augmented Lagrangian

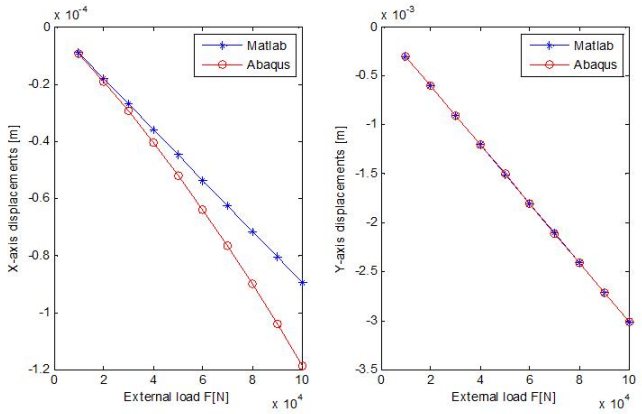


Figure 2.14 – Slave node displacement evolution as a function of external load amplitude (a) x-axis displacements (b) y-axis displacements.

contact algorithm) for the entire external load range. The maximal error for the normal load is inferior to 1%, while the maximal differences for the displacements following the X-axis and Y-axis respectively are in the order of $10^{-4}m$ and $10^{-6}m$. Moreover, at the end of calculation, the maximum residue in term of load and displacement, respectively equal to $10^{-5}N$ and $10^{-11}m$, confirms the good accuracy of the proposed FL2C method.

Robustness of the FL2C method

In this section, the robustness of the FL2C method is evaluated thanks to the definition of the controller variables and the size of the projection basis.

To test the robustness of the proposed method and observe the influence of defining the controller variables, the crisp values of the output variable membership functions previously noted S, M and L in Fig 2.9 are modified. The intervals of variation are respectively [0.05 ; 0.2] for S, [0.4 ; 0.6] for M and [0.8 ; 0.95] for L. Calculations are performed considering 16 values taken from each interval. The external load is set at 50000 N. The evolution of normal load variation and iteration numbers are represented respectively on Fig 2.15 and Fig 2.16 as a function of the three fuzzy number crisp values. The maximum variation does not exceed $3.10^{-3}N$. In comparison with the contact load $(4,449.10^4N)$, the small variation shows that the choice of crisp values only weakly influences the precision of the contact solutions as long as the value range is compatible with the study. Naturally, if we deviate from these values, the algorithm naturally diverges. The choice of crisp value directly affects iteration number (between 22 and 35 iterations, depending on crisp values) and consequently, the convergence rate. More research on tuning of crisp values using optimization algorithms [Bingul and Karahan, 2011] would complete this work.

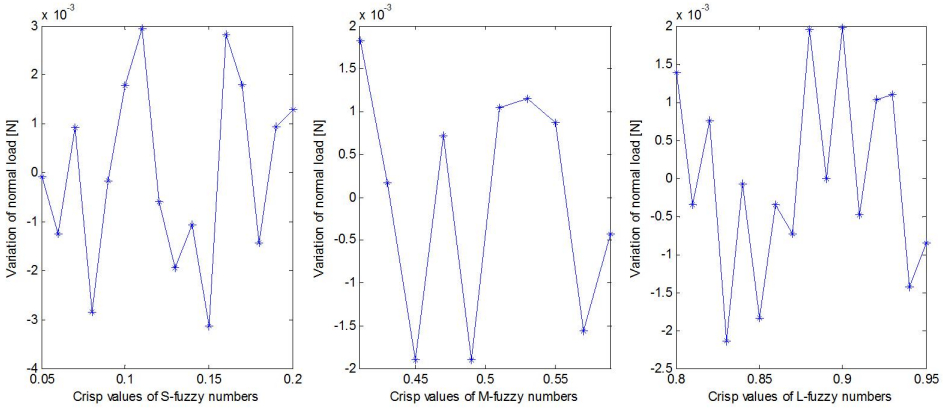


Figure 2.15 – Normal load variation as a function of S, L and M fuzzy number crisp values

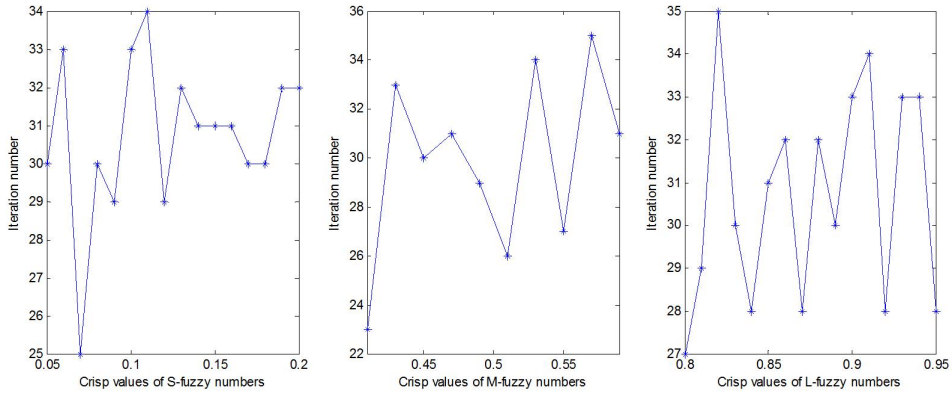


Figure 2.16 – Iteration number as a function of S, L and M-fuzzy number crisp values

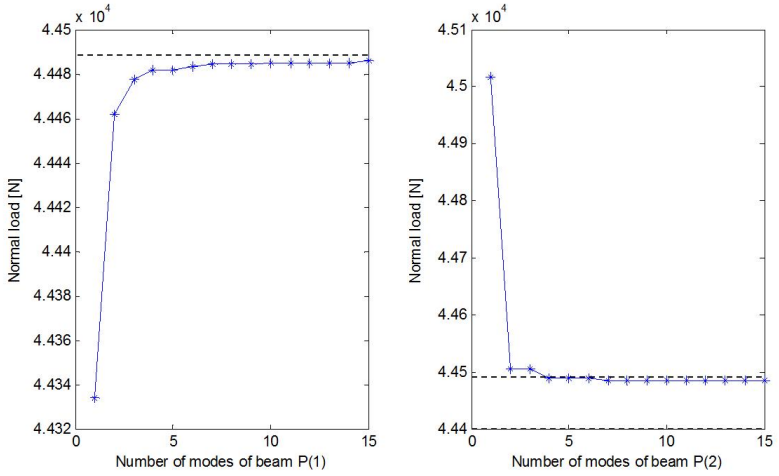


Figure 2.17 – Convergence of normal loads as a function of selected modes for beam P(1) and P(2)

To evaluate the precision of the results as a function of selected projection basis, we propose to modify the number of modes retained for each component in contact. As the normal gap is near to $10^{-11}m$ whatever the number of modes selected for each beam, we focus only on normal loads in Fig 2.17.

The evolution of number of modes is considered separately. When beam P(1) is concerned, the number of modes of beam P(2) is fixed to 15. The contrary holds for the other case. Fig 2.17 highlights that the projection does not really degrade the precision of the contact load as long as the number of modes is sufficient. For this problem, the solutions converge to the case without projection near to $4,449.10^4N$ (marked by a dotted line) as soon as more than 5 modes are retained whatever the beam. This result can be explained by the kinematics of the beams which are properly represented by the first modes of cantilever beams. As a complement of this assertion, more than 99% of the threshold contact load is obtained with only the first mode which shape corresponds to the bending of a cantilever beam.

Efficiency of FL2C method

To estimate the efficiency of the FL2C method in terms of computational time, the size of the finite element model is increased. The number of degrees of freedom (dof) is defined as 500 to 25000 per beam. To achieve these values, the beams are divided in 50 elements (respectively 400 elements) along the length and 4 elements (respectively 38 elements) along the height.

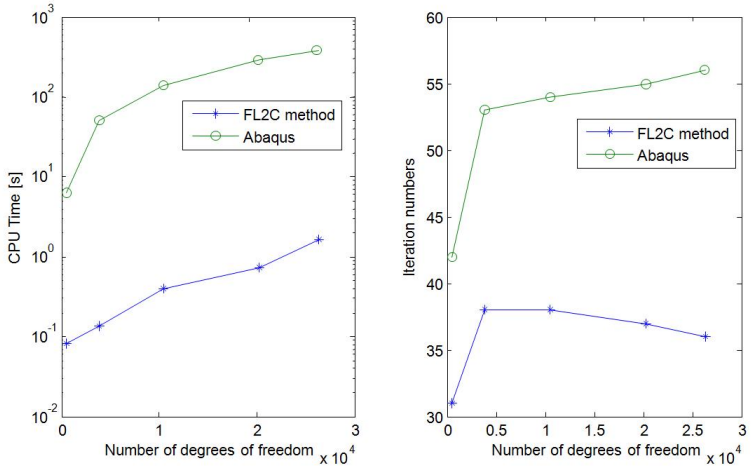


Figure 2.18 – Computational time (a) and iteration number (b) evolution as a function of finite element model size

The evolution of computational time in Fig 2.18-a follows a classical tend as it increase with the increasing number of dof. Nevertheless, in this case, the FL2C method is more efficient than

Abaqus regardless of finite element mesh size. Computational time can be reduced by a factor 100 for the finer mesh. To assure convergence for the finer mesh on the Abaqus software, the variable associated with the load increment was decreased, which explains the long CPU time.

Fig 2.18-b highlights that the number of iterations for FL2C method is inferior to Abaqus too. If large models are managed with FL2C method, the number of iterations is globally stable and even decreases but without significant effect (38 iterations to 36 iterations). Nevertheless, even if the number of iteration is stable or decreases for larger FE models, the associated CPU increases because the size of vectors or matrices to manage increases too.

In conclusion, for this first study, the obtained results encourage us to pursue a problem involving multiple contact pairs in the next section.

4.2 Elastic beam on rigid segment problem

Description of the model

The contact problem comprises an elastic cantilever beam, identical to the one used in the first example, subjected to external load F and in contact with a rigid curved surface in Fig 2.19. This example is inspired by Aggoune et al [Aggoune et al., 2004].

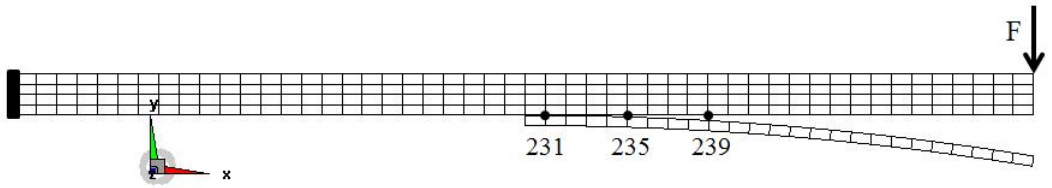


Figure 2.19 – Contact between an elastic beam and a rigid curved segment

Boundary conditions are such that the beam is completely fixed in translation at its left extremity. The initial vertical gap between the two components is first set as $1.10^{-8}m$ on the left side of the curved surface. To change the number of contact pairs and the position of the contacts, external vertical load F, with increasing intensity from 1000 N to 20000 N, is applied to the right side of the beam. The master and slave structures are respectively the curved surface and the beam.

Validation of the results of the FL2C method

The sum of normal loads at interface obtained with the FL2C method and Abaqus for the entire external load range is presented in Fig 2.20. The obtained results are very interesting

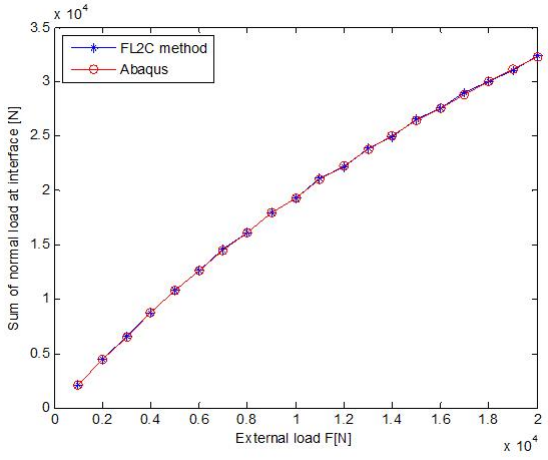


Figure 2.20 – Evolution of the sum of normal loads as a function of external load amplitude

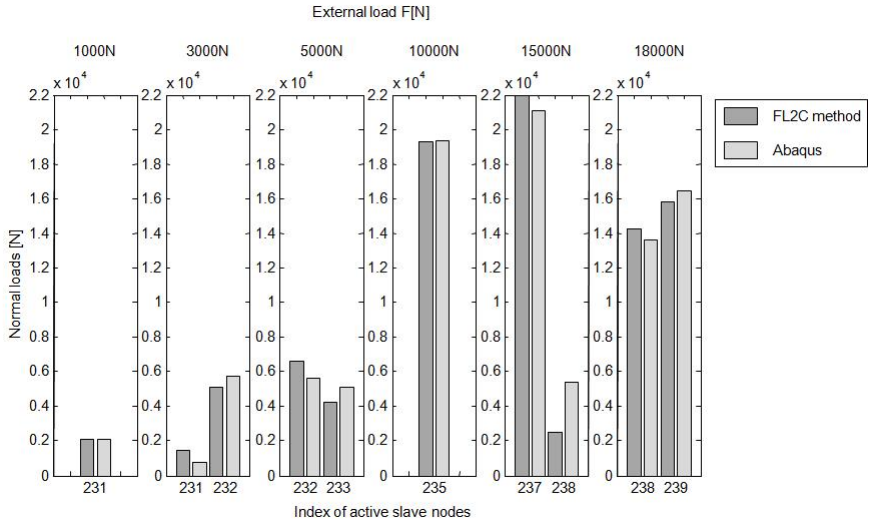


Figure 2.21 – Evolution of normal loads and index of active slave nodes as a function of external load amplitude

because the maximal error is less than 0.5%. As in the previous test case, the final normal gap as a function of the external load does not follow a particular tends. The mean normal gap is close to $1.10^{-8}m$ with a minimal gap equal to $1.10^{-10}m$ and a maximal gap equal to $2.10^{-6}m$.

In a way to show more precisely the precision of the FL2C method according to the evolution of contact, Fig 2.21 presents the normal load values for six specific external loads (1000 N, 3000 N, 5000 N, 10000 N, 15000 N, 18000 N). The successive active slave nodes (located in Fig 2.19) are also reported. The results are compatible with those obtained using Abaqus in terms of load distribution between the different active slave nodes. The maximal error for normal loads is less

than 15%. The maximum residue in term of load and displacement at the end of calculation is respectively equal to $10^{-6}N$ and $10^{-11}m$ that confirms the good accuracy of the proposed FL2C method.

As previously, the FL2C method is more efficient than Abaqus in term of computational time. For example, computational time can be reduced by a factor 20 for the present mesh.

To confirm the previous results, the last test case deals with a multi-contact problem with curved shape elastic structures.

4.3 Two semicircular structures in contact

Description of the model

The last example, represented in Fig 2.22, is inspired from an example of Feng [Feng, 1998] and simulates the contact between two deformable semicircular rings. The geometrical and material characteristics of the two identical rings are reported in Table 2.4. The initial position of the center of the upper ring is fixed to 120 mm left and 160 mm up from the center of the lower ring.

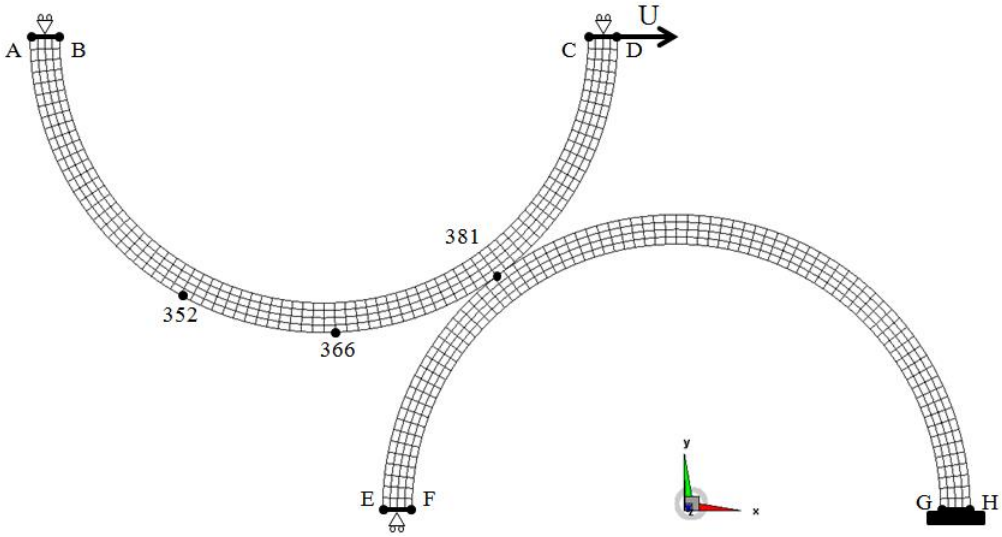


Figure 2.22 – Contact between two deformable semicircular rings

Table 2.4 – Geometric characteristics and material properties ofthe two semicircular rings

	Outer radius [mm]	Inner radius [mm]	Young modulus [MPa]	Poisson's ratio	Density [g/mm^3]
Semicircular rings	100	90	210000	0.3	7.8 10^{-6}

Imposed displacements, defined between 0 and 240 mm, are successively applied on the nodes of the segment CD of the upper ring. Nodes of segment GH are clamped while nodes of segments AB, CD and EF are simply supported along Y axis. The finite element discretization includes 320 quadrinodal plane stress elements and 405 nodes per ring corresponding to 4 divisions of the radius and 80 sectors. At the end of the simulation the rings are no longer in contact, the upper ring being to the right of the lower ring. The upper ring is chosen to be the slave structure and the lower ring, the master one. The potential contact zones of the two rings correspond to the outer radius. The dimension being in millimeter, the normal gap threshold is in this case fixed to $1.10^{-3}mm$ but lower values does not cause any convergence problem.

This test is interesting as it involves important modifications of the active contact zones and important change of the orientations of the contact zones consecutive to large deformation of the rings.

Validation of the FL2C method

Firstly, we interest on horizontal displacements of two nodes indexed B on upper ring and node F on lower ring in Fig 2.22. Fig 2.23 presents a comparison of obtained results between FL2C method and Abaqus for different values of imposed displacements. The global evolution of displacements along x-axis for these two nodes is very near between FL2C and Abaqus. The maximum errors, observed for intermediary imposed displacements (near to 150 mm), are equal to 12%. On the contrary, for lowest and highest imposed displacements, the detected errors, of the order of 2%, are much lower.

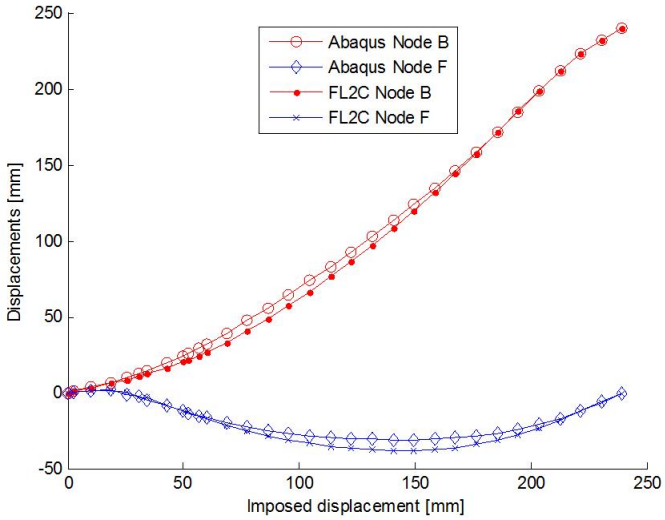


Figure 2.23 – Evolution of horizontal displacements as a function of imposed displacements

Secondly, Fig 2.24 presents the evolution of the normal contact loads for eight contact slave nodes. Each slave node can be active for different imposed displacements and multi-contacts are observed. As previously, the obtained results are really comparable to those obtained with Abaqus. Globally, the mean error in term of normal contact loads for the entire simulation is inferior to 17% that represents the same order of errors as the previous application presented in Section 4.2. Locally, most important errors on contact loads are detected for example for the node 378 in Fig 2.24. This slave node is active at the beginning of the simulation for low imposed displacements where results in term of displacements are very good. Thus, the observed error on contact loads between FL2C and Abaqus has no significant effect on the global kinematic behavior. This phenomenon can be explained by slight differences in terms of contact quantities such as localization matrices and local normal vectors. However, the maximum residue in term of load and displacement, respectively equal to $10^{-7}N$ and $10^{-11}m$, highlights the good accuracy of the proposed FL2C method.

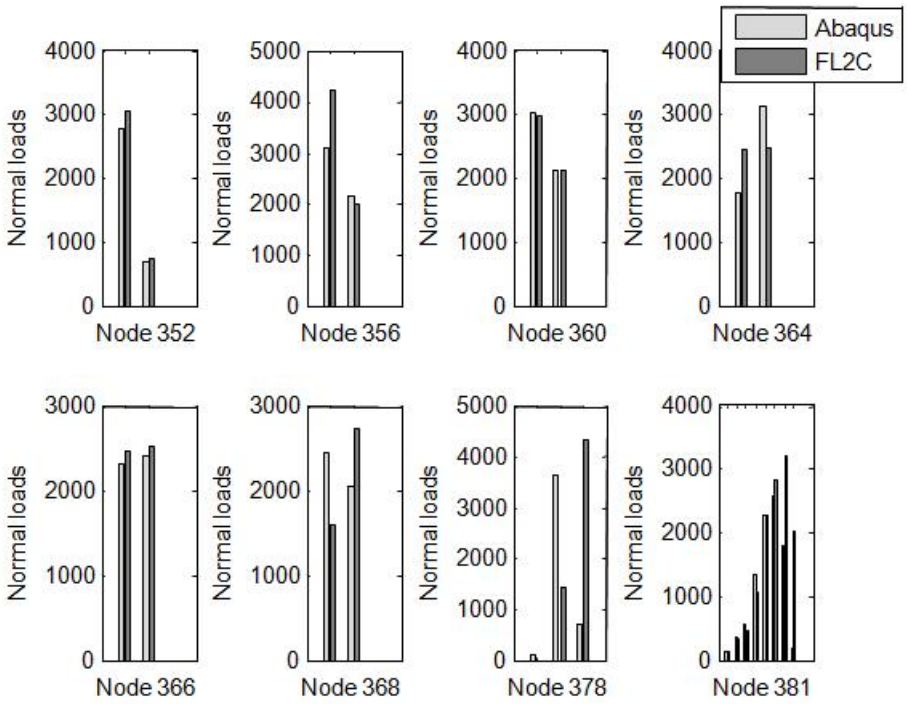


Figure 2.24 – Evolution of normal contact loads for different contact slave nodes

We can note that an implementation of the constraint Aster method [Abbas, 2013] in Matlab supplies exactly the same results as FL2C method. In that case, all secondary quantities involved in the calculation of contact loads are computed in the same way but this cannot be realized with Abaqus. For the present mesh, computational time is reduced of a factor 10.

These three numerical applications highlight that the FL2C method is a viable way to solve a contact problem. More generally, the use of a controller, deterministic or otherwise, and automation techniques, such as robust control, provides an interesting alternative to consider, especially within a multiple sampling context. The different tests show also that as soon as the controller is designed, it is possible to calculate mechanical solutions for different input parameter values (external loads or imposed displacements).

5 Conclusion

This chapter has highlighted that it is possible to replace classical iterative methods, such as the Newton-Raphson method, by a Fuzzy Logic Control approach to manage frictionless contact problem. Indeed, the proposed approach FL2C relies in the design of a FLC and the fuzzy logic theory. This theory is an effective way for linking multiple inputs to an output in a non-linear domain and so for linking the normal gap to normal contact load. The FLC is integrated into a contact loop where the current states (contact/no contact) of nodes are managed. Thus, the nonlinear contact problem is solved considering a series of linear contact problem. The FL2C method does not require the definition of a tangent or coupling matrix as classically. The solving can be performed without considering an explicit coupling between the components in contact and it is possible to build a projection matrix for each component, managed independently. This matrix is built with the eigenmodes of each component that allows to reduce the computational time of the solving.

Next, we have investigated numerical 2D applications and presented interesting results in terms of precision and computational time through results supplied by industrial code Abaqus. We have shown that it is possible to reduce the size of the contact problem considering the modal bases of each component in contact. Moreover, the FLC is robust enough to calculate output solutions for different contact problem simulations without the need to modify the definition of contact variable membership functions. To manage more complex problems, future developments investigated in chapter 3 will be expanded on friction-dependent problems.

Chapter 3

Using fuzzy logic control approach and model reduction for solving frictional contact problems

Contents

1 Introduction 58

2 2D frictional contact problems in a finite element context 58

2.1 Frictional contact problems 58

2.2 Finite element static contact problem 60

3 Fuzzy Logic Controller for frictional Contact method 61

3.1 Extension to frictional contact management 61

3.2 Definition of the reduced contact problem 63

4 Numerical applications for frictional contact problems 63

4.1 2D elastic slab on rigid plate 64

4.2 Design of controllers 65

4.3 Resolution of the full contact problem with the FL2C method 66

4.4 Resolution of reduced contact problem through eigenvector integration . 68

4.5 Resolution of reduced contact problem using static modes integration . 71

4.6 Influence of controller fuzzy laws 74

4.7 Solutions for fuzzy controller integration 76

4.8 Discussion about computational time 78

5 Conclusion 79

1 Introduction

The previous chapter has highlighted the possibility to replace classical iterative solving methods by a Fuzzy Logic control approach in the case of frictionless case with interesting results in terms of precision and computational time. The FLC can be designed only one time and so used for different samplings where the input parameters of finite element matrices are modified. Now, with the aim to investigate friction induced vibrations problem, it is necessary to take into account the frictional effect in the solving and calculate the associated static equilibrium position. The frictional contact problem adds a new nonlinearity to be managed due to Coulomb's law.

In this chapter, we propose to extend the FL2C method to the case of friction. The new way, which consists in designing the FLC to link gaps and contact loads, is kept. To achieve this objective, a new controller is added and dedicated to the frictional sticking case. A large part of this chapter is associated to the integration of these two controllers of the solving scheme and the management of the different frictional state (sticking or sliding). Moreover, a projection matrix is defined by integrating static modes to capture local deformation at the contact interface. Considering eigenmodes as in a frictionless contact problem will be shown to be insufficient.

Thus, Section 2 reiterates the main data useful to study a 2D frictional contact problem in a finite element context. Section 3 describes the proposed method, named the FL2C method, which is based on the decomposition of the nonlinear problem into a set of linear problems and the design and implementation of fuzzy logic controllers into a contact scheme. To assess the efficiency of the proposed method, a complete numerical application is presented in Section 4. The results are compared in terms of precision, robustness and computational time with those obtained by a numerical reference method for different friction coefficient values to consider different frictional states. A discussion is proposed on the resolution of the full and reduced contact problem, the definition of projection matrix and static modes, the influence of controller variable definitions and the implementation of controllers in the contact solving process. Conclusions and remarks are provided in Section 5.

2 2D frictional contact problems in a finite element context

2.1 Frictional contact problems

The contact and friction representations used in this paper rely on the well-known Signorini-Coulomb law.

The normal contact contribution has already been described by Eq. 2.5 and Fig. 2.2 in chapter 2. Now, Coulomb's law conditions, which are associated with friction, are defined as follows:

$$\begin{cases} \|\vec{\mathbf{f}}_t\| \leq \mu \|\vec{\mathbf{f}}_n\| \\ \|\vec{\mathbf{f}}_t\| < \mu \|\vec{\mathbf{f}}_n\| \Leftrightarrow v_g = 0 \quad \text{(sticking condition)} \\ \|\vec{\mathbf{f}}_t\| = \mu \|\vec{\mathbf{f}}_n\| \Leftrightarrow \vec{\mathbf{f}}_t = -\mu \|\vec{\mathbf{f}}_n\| \dfrac{\vec{v}_g}{\|\vec{v}_g\|} \quad \text{(sliding condition)} \end{cases} \tag{3.1}$$

where $\vec{\mathbf{f}}_n$ and $\vec{\mathbf{f}}_t$ are respectively the normal and tangential contact load vectors, μ the friction coefficient and $\vec{v}_g$ the sliding velocity vector. As previously mentioned, two states are distinguished as a function of the existence of movements between solids in close contact. The sticking state corresponds to the case without sliding velocity. A tangential reaction is defined in the tangent plane orthogonal to the normal vector $\vec{\mathbf{n}}$. This value is always inferior to a threshold defined through normal load value and the friction coefficient. For a sliding state, the friction load is considered proportional to the normal load through the introduction of a friction coefficient. In this case, a sliding velocity can be observed. This inequality concept is traditionally described by Coulomb's cone in Fig 3.1-a & Coulomb's law in 3.1-b.

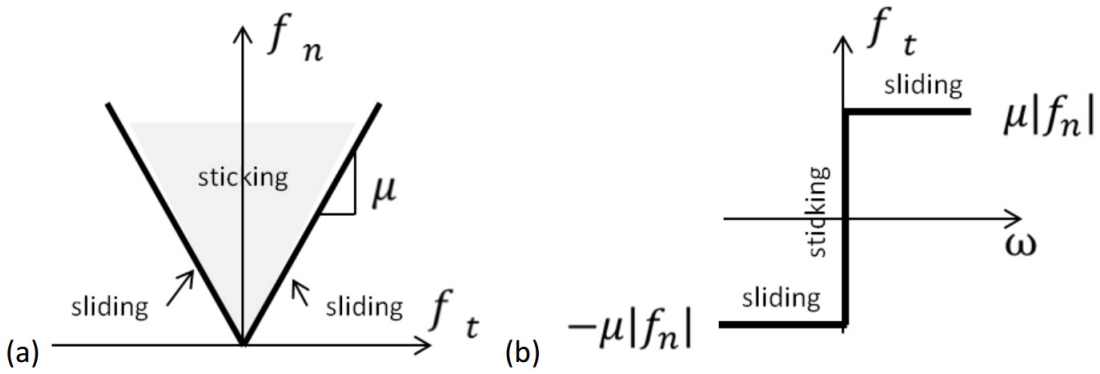


Figure 3.1 – (a) Representation of Coulomb's cone (b) Coulomb's law

Thus, normal and tangential loads (or pressures) are directly defined from displacements of solids in contact and some unknowns are used to determine the equilibrium state of a mechanical problem.

2.2 Finite element static contact problem

In a finite element context, the equilibrium equation, which governs the static problem, is written as follows:

$$\mathbf{KU} + \mathbf{F}_c(\mathbf{U}) = \mathbf{F}_{ext} \tag{3.2}$$

where $\mathbf{K}, \mathbf{U}, \mathbf{F}_{ext}$ and $\mathbf{F}_c(\mathbf{U})$ respectively designate the stiffness matrix, the nodal displacement vector, the external load vector and non-linear contact loads. This problem is nonlinear because the contact loads depend directly on the displacement of all bodies in contact.

Normal close contact constraints can be expressed as follows:

$$\mathbf{P}_n\mathbf{U} = \mathbf{d}_n \tag{3.3}$$

where $\mathbf{d}_n$ is an initial normal gap and $\mathbf{P}_n$ is a normal contact matrix that couples the displacements of each contact pair to ensure non-penetration, such as:

$$\mathbf{P}_n = \begin{bmatrix} \vec{\mathbf{n}} & -(1-\alpha)\vec{\mathbf{n}} & -\alpha\vec{\mathbf{n}} \end{bmatrix} \tag{3.4}$$

The concept of contact matrix is extended to the tangent plane: friction matrix $\mathbf{P}_t$ is defined following the same rules using tangential vector $\vec{\mathbf{t}}$:

$$\mathbf{P}_t = \begin{bmatrix} \vec{\mathbf{t}} & -(1-\alpha)\vec{\mathbf{t}} & -\alpha\vec{\mathbf{t}} \end{bmatrix} \tag{3.5}$$

To manage sticking and sliding conditions, subparts of friction matrix $\mathbf{P}_t$, respectively noted $\mathbf{P}_a$ and $\mathbf{P}_g$, will be considered. The tangential contact constraints in a sticking state can be summarized in the same manner:

$$\mathbf{P}_a\mathbf{U} = 0 \tag{3.6}$$

To solve this non-linear problem, iterative methods, used in frictionless contact problem can be used too. Indeed, Newton-Raphson method, are usually used in industrial code coupled with regularization methods such as a penalty method, the Lagrange multiplier procedure or a hybrid method, like the augmented Lagrangian method.

This method requires the definition of a tangent matrix, which must be regularly updated to ensure the convergence of the algorithm. Indeed, the matrix explicitly creates a coupling between the different components in contact to guarantee the Signorini's and Coulomb's conditions. In

proposed FL2C method, the first objective is to avoid any coupling of the matrices of components in contact by integrating a regulation of contact loads treated as external loads. Second, we propose to exploit this uncoupling to integrate a projection matrix in a way to reduce the size and consequently the computational time of the simulated problem.

3 Fuzzy Logic Controller for frictional Contact method

In this section, we propose to extend the FL2C method, proposed in chapter 2, to the frictional case by designing a new Fuzzy Logic Controller. Finally, to control computation time, a reduced contact problem is proposed by considering a projection matrix.

3.1 Extension to frictional contact management

For frictional conditions, a tangential contact load is added to Eq 3.7:

$$\mathbf{K}\mathbf{U}^{i+1} = \mathbf{F}_{ext} + \mathbf{F}_n^{i+1} + \mathbf{F}_t^{i+1} \tag{3.7}$$

where $\mathbf{F}_t^{i+1}$ represents the tangential contact load at the i^{th} iteration.

As previously for normal conditions, the tangential contact load $\mathbf{F}_t^{i+1}$ associated with the sticking condition is decomposed as follow:

$$\mathbf{F}_t^{i+1} = \mathbf{F}_t^i + \Delta\mathbf{F}_t^{i+1} \tag{3.8}$$

$$\Delta\mathbf{F}_t^{i+1} = \beta\Delta\mathbf{F}_t^i \tag{3.9}$$

where β is a coefficient associated with the increment of normal loads $\Delta\mathbf{F}_t^i$.

Indeed, to solve a frictional contact problem with FL2C method, shown in Fig 3.2, it is necessary to use two Fuzzy Logic Controllers and so two independent coefficients γ and β associated with the increments of contact loads, respectively for the normal case and the sticking case. Each FLC presents two input variables, namely the two successive gaps, and one output relative to the increment of the contact load.

After building finite element matrices for the different bodies, a prediction step is performed to calculate displacements and initial gaps, denoted $\mathbf{g}_n^0$ and $\mathbf{g}_t^0$, without contact loads. At each iteration, the maximal normal gap and the maximal tangential gap are identified considering the contact loads, calculated at the previous iteration, and updated contact data (normal and tangential vectors, position of slave nodes in master segment ...). These two maximal gaps are considered as input data of the two controllers, which determines the corresponding γ and β

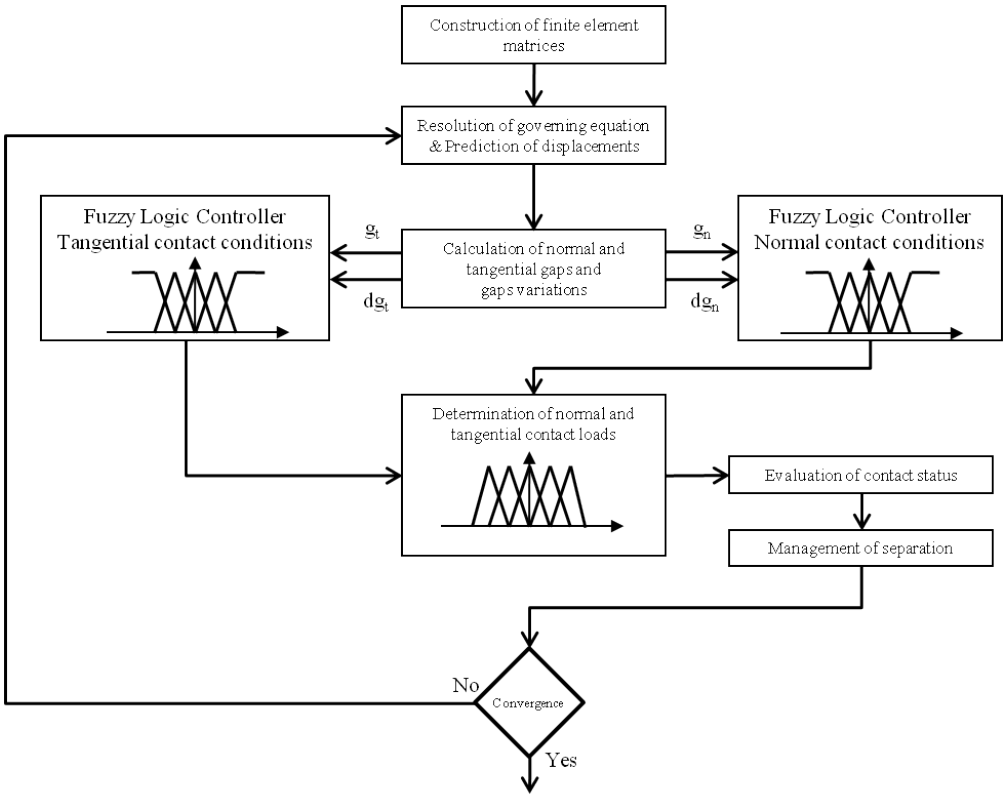


Figure 3.2 – Computational procedure for the FL2C method for the frictional contact problem

coefficients. Next, the current increments of normal and tangential loads are proportionally distributed on each contact pair thanks to related gaps and calculated coefficients. The iterative procedure will be stopped when the normal gaps reach the tolerance values (fixed to $1\mu m$ for the next applications).

At the beginning of the algorithm, all active contact nodes have a sticking status. Using the controllers, the gaps between the bodies are iteratively reduced to reach the static equilibrium position. The normal and tangential contact loads are directly defined as a function of normal and tangential gaps for each iteration. The contact status is evaluated for all nodes by Coulomb's conditions. If the absolute tangential contact loads $\mathbf{F}_t$ are smaller than the absolute $\mu\mathbf{F}_n$, the contacts have sticking status. In contrast, if the absolute tangential contact loads $\mathbf{F}_t$ are bigger than the absolute $\mu\mathbf{F}_n$, the contacts have sliding status and the tangential loads will be replaced by $\mu\mathbf{F}_n$. The management of separation is verified by the sign of normal contact loads (Signorini's condition): the nodes in contact will be removed if the normal contact loads have a negative sign. The removed nodes can be added in contact if the normal contact loads, defined by the normal controllers in the next iteration, have a positive sign. The iterative procedure will be stopped when the normal gaps reach the tolerance values.

3.2 Definition of the reduced contact problem

The FL2C method relies on fuzzy logic controllers to manage the contact problem that does not require regularization techniques and tangent matrices during resolution. The definition of controllers allows for consideration of the contact loads as external loads in the static problem and the stiffness matrix of the bodies in contact remains unchanged at each iteration in Eq 3.10.

Thus, a reduced contact problem can be defined as follows:

$$\left[\mathbf{T}^T\mathbf{K}\mathbf{T}\right]\mathbf{q}^{i+1} = \mathbf{T}^T(\mathbf{F}_{ext} + \mathbf{F}_n^{i+1} + \mathbf{F}_t^{i+1}) \tag{3.10}$$

$$\mathbf{U}^{i+1} = \mathbf{T}\mathbf{q}^{i+1} \tag{3.11}$$

where $\mathbf{T}$ is a projection matrix and $\mathbf{q}^{i+1}$ represents the reduced coordinates vector.

In chapter 2, the projection basis was built with the n_{mod} first eigenvectors given by each component taken separately from the entire system. Thus, the modal bases are then completely independent from the contact problem and only the boundary conditions associated with each component are taken into account.

Nevertheless, this solution is efficient in the case of global static deformation and without friction. The main condition is that the static deformation of the components in contact can be expressed as a linear combination of eigenvectors. If local deformations are observed at the interface, it is necessary to define the projection matrix using static modes. The modes are calculated by solving linear static problems where an unitary load is successively applied on contact nodes for each main direction. Thus, in 2D, the number of static modes is equal to two times the number of contact (slave and master) nodes n_{ctt}.

$$\mathbf{T} = \begin{bmatrix}\Gamma_1 & \dots \Gamma_{n_{ctt}}\end{bmatrix} \tag{3.12}$$

where Γ_j represents the static modes.

To ensure good approximation, an orthonormalization of the $\mathbf{T}$-matrix is performed. The proposed FL2C method was also implemented in Matlab.

4 Numerical applications for frictional contact problems

To study the efficiency and robustness of the proposed FL2C method, several numerical comparisons are proposed for a 2D elastic slab in contact on a rigid plate. After respectively defining the numerical finite element model and fuzzy rule basis and input/output laws in Sections 4.1 and

4.2, we propose to compare contact normal and tangential load values obtained with the FL2C method to those calculated with Lagrange contact algorithm of Abaqus software by successively considering:

- The resolution of the full contact problem, defined by Eq 3.7 (Section 4.3).
- The definition of matrix projection with elastic slab eigenvectors and the resolution of the reduced contact problem, defined by Eq 3.10 (Section 4.4).
- Definition of matrix projection with elastic slab eigenvectors or static modes and resolution of the reduced contact problem (Section 4.5).
- For each numerical application, different friction coefficient values (defined from 0 to 1) will be taken into account in order to consider both sticking and sliding statuses of slave nodes.

Next, to observe the influence of the controller variable definition and the implementation of controllers in the contact solving process, sensitivity analyses are performed in Sections 4.6 and 4.7. Finally, a discussion of the reduced contact problem and associated computational time gain is proposed in Section 4.8.

4.1 2D elastic slab on rigid plate

The contact problem is composed of a 2D elastic slab in contact on a rigid plate [Feng, 1998]. The elastic component in Fig 3.3 is modeled using quadrilateral plane strain finite elements. Because of symmetry, boundary conditions are such that the slab is fixed in translation along the x-axis on segment BC. The height and half length of the slab (h) are set to $40mm$.

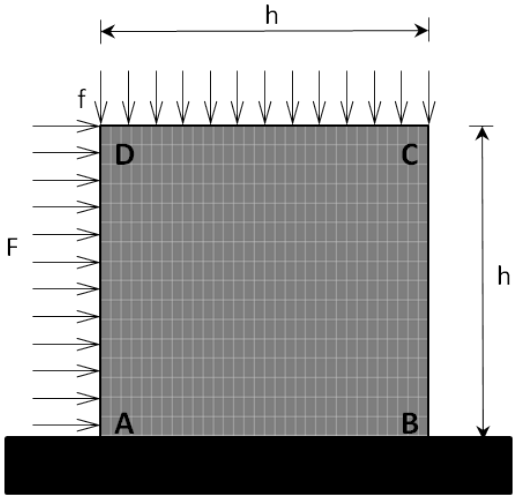


Figure 3.3 – Contact between an elastic slab and a rigid plate

The elastic slab, for which material properties are summarized in Table 3.1, is pressed and pushed (respectively by loads f and F) on the rigid plate. Different friction coefficients (defined between 0 and 1) are managed to create different states (separation, sliding and sticking) in the contact area represented by segment AB. For the first seven subsections, the slab is modeled by 512 quadrilateral elements corresponding to 32 horizontal and 16 vertical subdivisions.

Table 3.1 – Numerical data

Young's modulus (N/m^2)	Poisson's ratio	Load F (N/m^2)	Load f (N/m^2)
$1.3\ 10^{11}$	0.2	$1\ 10^{8}$	$0.5\ 10^{8}$

4.2 Design of controllers

In this study, since the order of magnitude for normal and tangential gaps is about the same, only one set of fuzzy input laws is defined for both normal and tangential gap variables. The crisp values of input laws are respectively established as $-1\mu m, -1pm, 0m, 1pm$ and $1\mu m$. These values are voluntarily low to correspond to observed gaps during prediction and correction contact steps.

Table 3.2 – Fuzzy logic rule base

		Gap g_n^{k+1} or **Gap** g_t^{k+1}				
		NL	**NS**	**N**	**PS**	**PL**
Gap g_n^k	**NL**	NO	NO	L	L	M
	NS	L	M	M	M	S
or	**N**	NZ	S	M	S	NZ
	PS	S	M	M	M	L
Gap g_t^k	**PL**	M	L	L	NO	NO

For output variables, one set of fuzzy output laws is chosen for each output contact load variable. The order of magnitude of the contact load can be different enough, given the nature of equations that link normal and tangential loads. The crisp values of output laws are respectively 0, 0.3, 0.5, 0.79 and 1 for the normal coefficient and 0, 0.3, 0.5, 0.91 and 1 for the tangential one.

The fuzzy "if-then" rules for normal and tangential gap control are summarized in Table 3.2. The total number of rules is then set to 25.

All these data, which are useful to design the normal and tangential fuzzy logic controllers, will be considered for all the following applications.

4.3 Resolution of the full contact problem with the FL2C method

This section is dedicated to comparing the results obtained by the FL2C method and numerical reference and associated with solving of the full contact problem defined by eq 3.7. Fig 3.4-a presents the evolution of the normal mean gap as a function of the friction coefficient obtained with the FL2C method. The obtained values are of an order of magnitude of $10^{-8}m$ regardless of the value of the friction coefficient, which guarantees a good level of convergence for the proposed method. To highlight the precision of the FL2C method, the evolution of normal and tangential loads is drawn in fig 3.5 as a function of segment position AB and for different friction coefficient values. The point A is indexed 1 in the x-axis of fig 3.5 whereas the point B is numbered 33. The results are very interesting because the maximal value is inferior to 1% and is detected for a friction coefficient equal to 0.4 in fig 3.4-b. The observed error is slightly greater for the evaluation of the tangential contact loads than for normal ones.

Table 3.3 shows the evolution of node status for the contact zones by considering FL2C and numerical reference methods. The prediction for the two methods is comparable overall. For $\mu = 0.2$ (32 sliding nodes), $\mu = 0.4$ (30 sliding nodes and 2 sticking nodes), $\mu = 0.6$ (24 sliding nodes, 7 sticking nodes and 1 separate node) and $\mu = 0.8$ (19 sliding nodes, 11 sticking nodes and 2 separate nodes), the results for both methods are identical. The identification of contact status for friction coefficients equaling $\mu = 1.0$ respectively presents only one difference. There are three separate nodes and 16 sliding nodes with the reference method whereas the FL2C method detects only two separate nodes and 17 sliding nodes. This difference is a consequence of a small value (approaching 0) detected for normal and tangential loads.

We have highlighted the efficiency and the robustness of the proposed method for different conditions of friction coefficient values and so different frictional states. Moreover, the obtained results are very close to those obtained in Feng's paper [Feng, 1998] where we extracted the test cases.

Finnaly, this first application shows the ability of the FL2C method to solve a contact problem with precision (normal gap approaching $1nm$). The controllers are designed at the beginning of the application and can be used to solve different data sets (for example a friction coefficient defined between 0 and 1). In the present case, the solution is performed by considering the

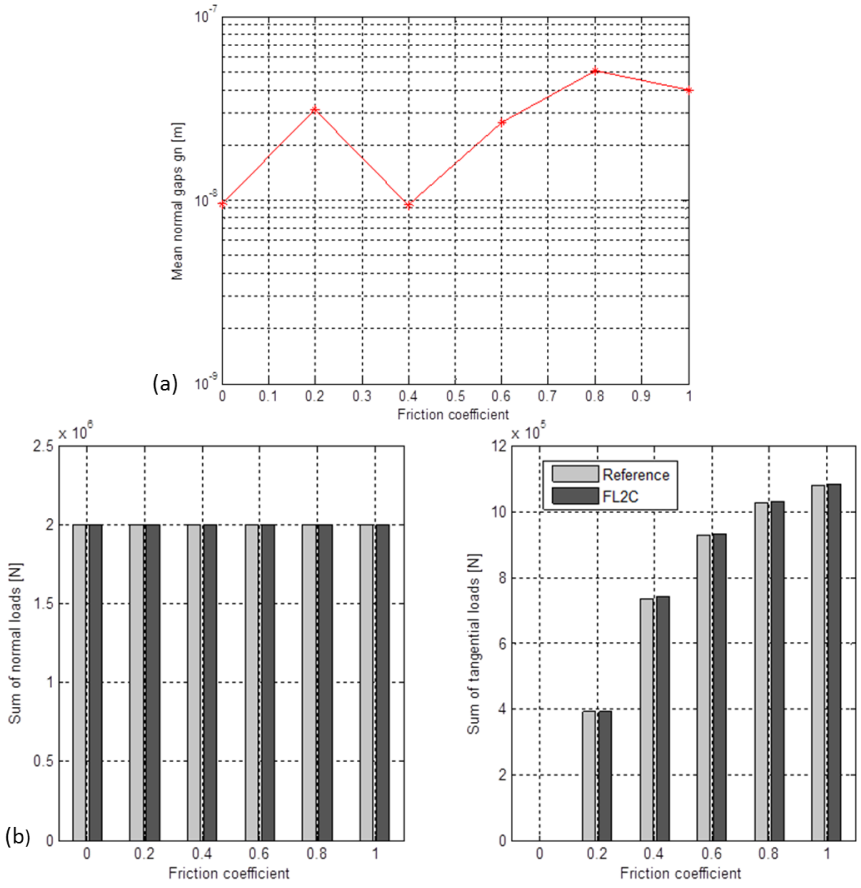


Figure 3.4 – (a) Evolution of normal mean gap for different friction coefficient values (FL2C method) (b) Evolution of mean contact load errors for full contact problem and different friction coefficients

Table 3.3 – Node status for different contact zones

	Reference method			FL2C method		
μ	Separation	Sliding	Sticking	Separation	Sliding	Sticking
0.2	0	32	0	0	32	0
0.4	0	30	2	0	30	2
0.6	1	24	7	1	24	7
0.8	2	19	11	2	19	11
1.0	3	16	13	2	17	13

full contact problem where the static displacements are calculated with the factorization of the stiffness matrix and the resolution of a linear system of equations. Now, we propose to solve the

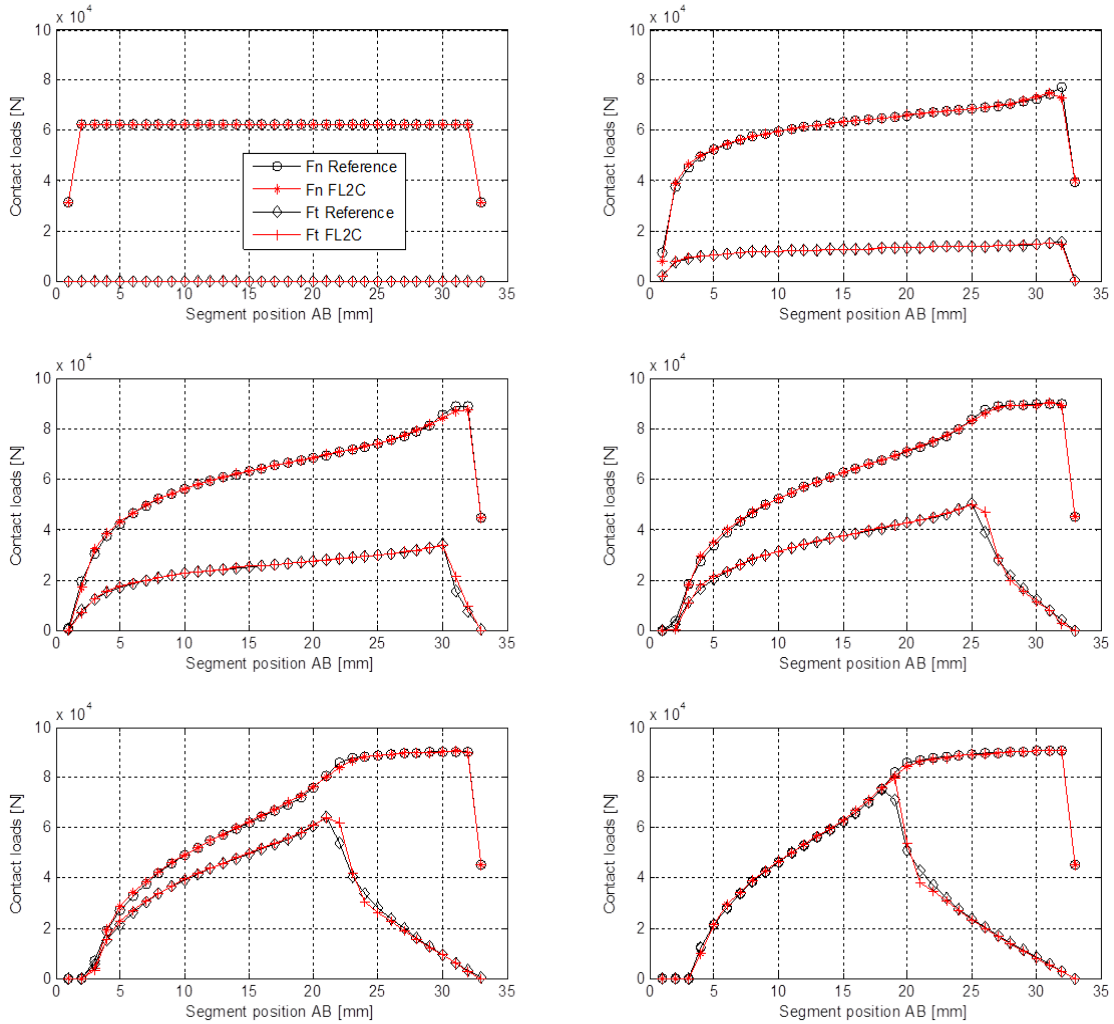


Figure 3.5 – Evolution of normal and tangential contact loads for the full contact problem as a function of segment position AB and for different friction coefficient values (a) $\mu = 0$ (b) $\mu = 0.2$ (c) $\mu = 0.4$ (d) $\mu = 0.6$ (e) $\mu = 0.8$ (f) $\mu = 1$

reduced contact problem in order to improve the computational times.

4.4 Resolution of reduced contact problem through eigenvector integration

In this section, the reduced contact problem is considered with a projection matrix built using the first hundred eigenvectors of the elastic slab. Table 3.4 summarizes a few elastic slab eigenfrequencies inferior to 100 kHz.

The solutions of the reduced contact problem performed with the FL2C method are now compared with the reference solutions. Fig 3.6-a shows first that the reduced problem does not

Table 3.4 – First five elastic slab eigenfrequencies

	1	2	3	4	5
Frequencies [Hz]	30115	45616	74580	80427	94200

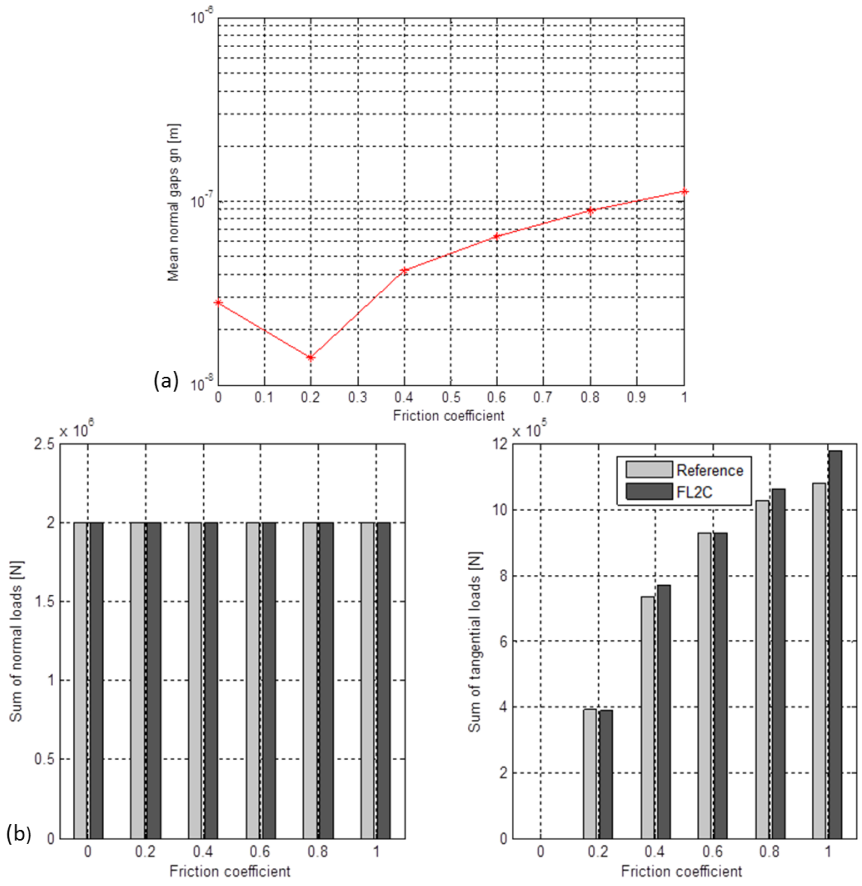


Figure 3.6 – (a) Evolution of normal mean gap for different friction coefficient values (FL2C method) (b) Evolution of average contact load errors for the reduced contact problem (100 eigenmodes) with different friction coefficients

affect the performance of the method in terms of contact gaps. In fact, the values of the average gap for different friction coefficients are of the same order ($10^{-7}m$) as those obtained with the full contact problem. Nevertheless, the errors concerning the evaluation of normal and tangential loads in Fig 3.6-b are consequent. Errors between 10% and 25% mainly can be observed for the tangential loads.

Moreover, in Fig 3.7 we observe some significant oscillations of results calculated with the FL2C method. The global behavior of the contact load evolution is well captured because the results obtained using the FL2C method oscillates around the reference solutions. However,

local errors can be very noteworthy and the friction state modification undetected as for friction coefficients of 0.6 to 1.

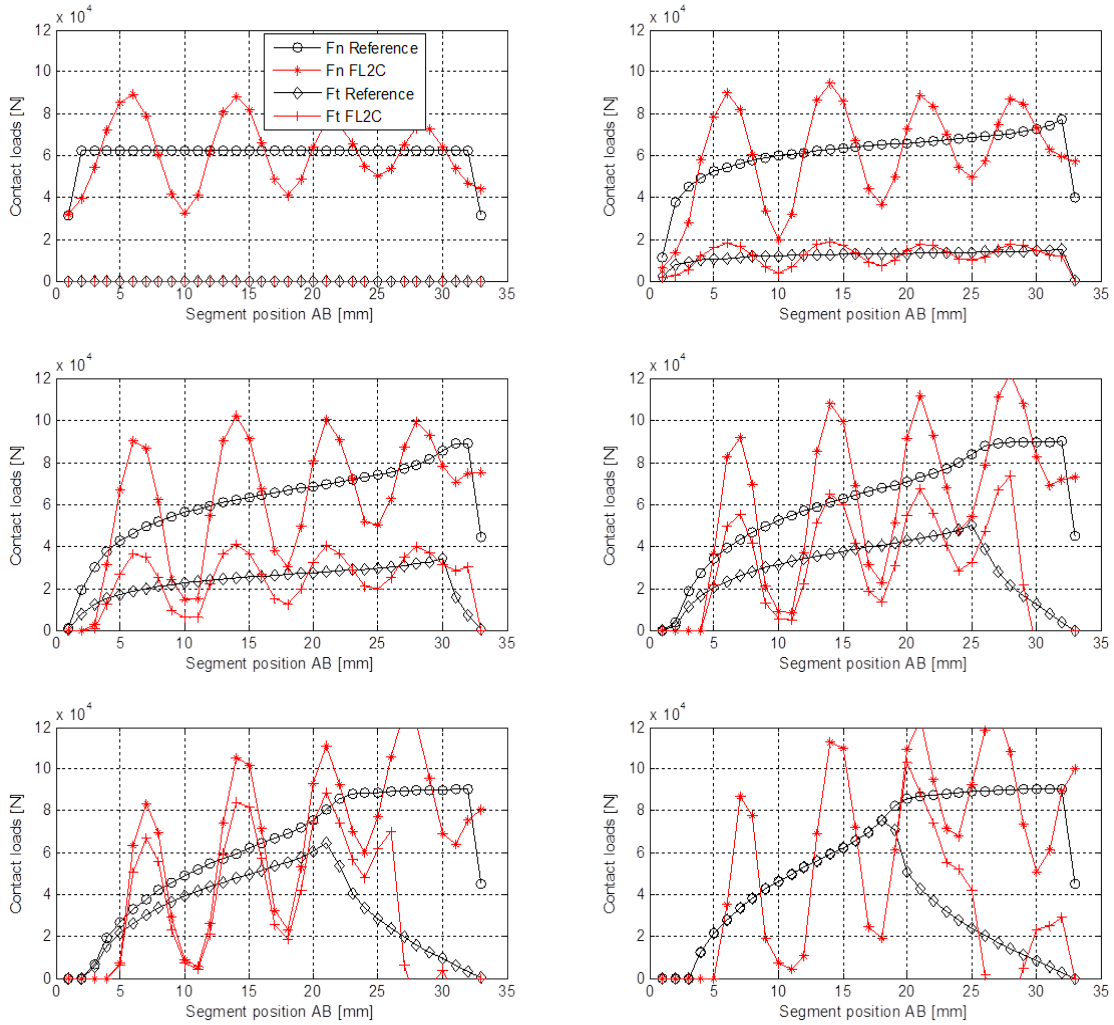


Figure 3.7 – Evolution of normal and tangential contact loads of the reduced contact problem (eigenvectors only) as a function of segment position AB and for different friction coefficient values (a) $\mu = 0.0$ (b) $\mu = 0.2$ (c) $\mu = 0.4$ (d) $\mu = 0.6$ (e) $\mu = 0.8$ (f) $\mu = 1.0$

This second application shows that the FL2C method converges even if a projection matrix is used to reduce the size of the problem. The robustness of the controllers is clearly observed. Nevertheless, the use of a projection matrix composed only of eigenmodes is insufficient to represent the local displacement at the interface. The next section discusses the update of the projection matrix by considering interface static modes.

4.5 Resolution of reduced contact problem using static modes integration

To solve the reduced contact problem, we now propose to consider the static modes calculated at the interface for all nodes in contact.

Figs 3.8-a and 3.8-b. present the evolution of errors concerning the normal and tangential loads as a function of the friction coefficient by respectively adding static modes along the x-axis and along the y-axis in the projection matrix

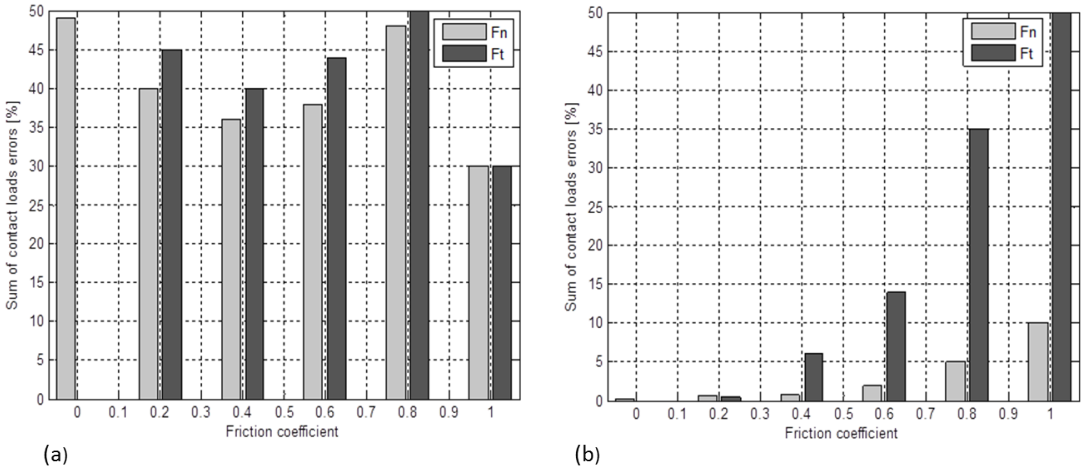


Figure 3.8 – Evolution of average contact load errors of the reduced contact problem for different friction coefficients (a) with static modes along the x-axis (b) with static modes along the y-axis

In fig 3.8-a. the observed errors are in the order of 50% both for normal and tangential loads. Adding x-axis static modes to only ten eigenmodes deteriorates the previous prediction presented in fig 3.8-b. In this case, the global behavior of contact loads is no longer captured. On the contrary, the integration of y-axis static modes in the projection matrix significantly reduces the errors for the normal contact loads (mean error inferior to 10%) as shown in fig 3.8-b. However, the errors for tangential loads remain consequential, i.e., 20% in terms of mean. To drastically reduce contact load errors, it is necessary to add static modes along both the x-axis and y-axis in fig 3.9. In this case, the level of error is inferior to 2% for normal and tangential loads.

The observed errors are very close to those obtained by considering the full contact problem. The behavior of contact loads is completely captured as presented in fig 3.10. No oscillations of contact loads are observed regardless of the value of the friction coefficient.

This third application shows the importance of a projection matrix choice. To precisely approximate contact loads at the interface, it is necessary to consider static modes for local

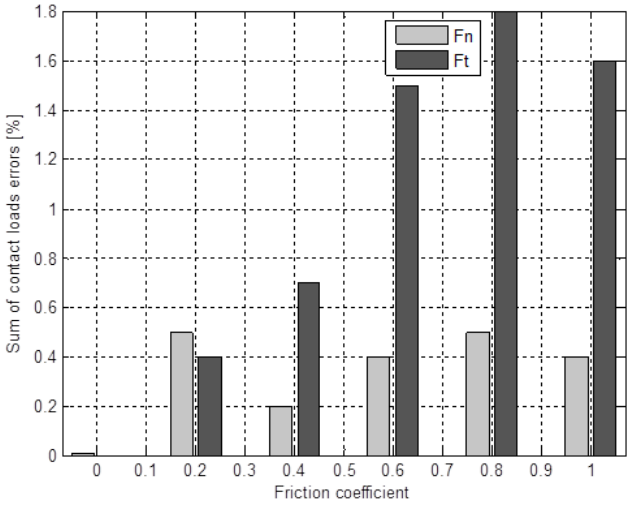


Figure 3.9 – Evolution of average contact load errors for the reduced contact problem (full static modes) for different friction coefficients

behavior.

The last three applications have already shown the interesting robustness of the FL2C method and thus the ability of the controllers to precisely balance the contact problem. The following section focuses on the influence of the control law definition on contact load errors.

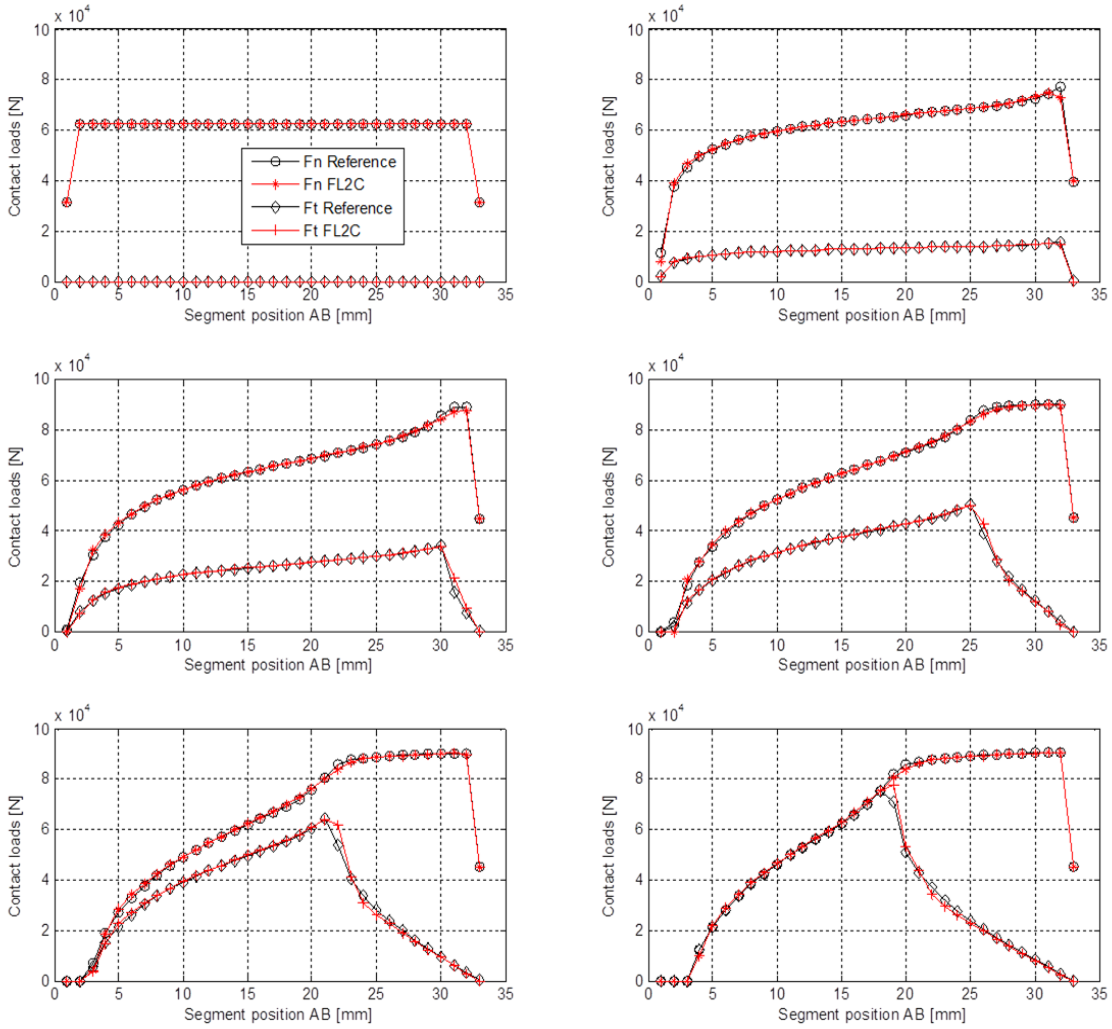


Figure 3.10 – Evolution of normal and tangential contact loads for the reduced contact problem (eigenvectors and static modes) and different values of the friction coefficient (a) $\mu = 0.0$ (b) $\mu = 0.2$ (c) $\mu = 0.4$ (d) $\mu = 0.6$ (e) $\mu = 0.8$ (f) $\mu = 1.0$

4.6 Influence of controller fuzzy laws

To test the robustness of the proposed method and observe the influence of controller variable definition, the crisp values of the output variable membership functions, previously noted as S, M and L in Fig. 1.9, are modified by ±10%. The intervals of variation are respectively for the γ-coefficient [0.27; 0.33] for S, [0.45; 0.55] for M and [0.7; 0.9] for L, and for the β-coefficient [0.27; 0.33] for S, [0.45; 0.55] for M and [0.82; 0.98] for L. Calculations are performed considering five values taken from each interval.

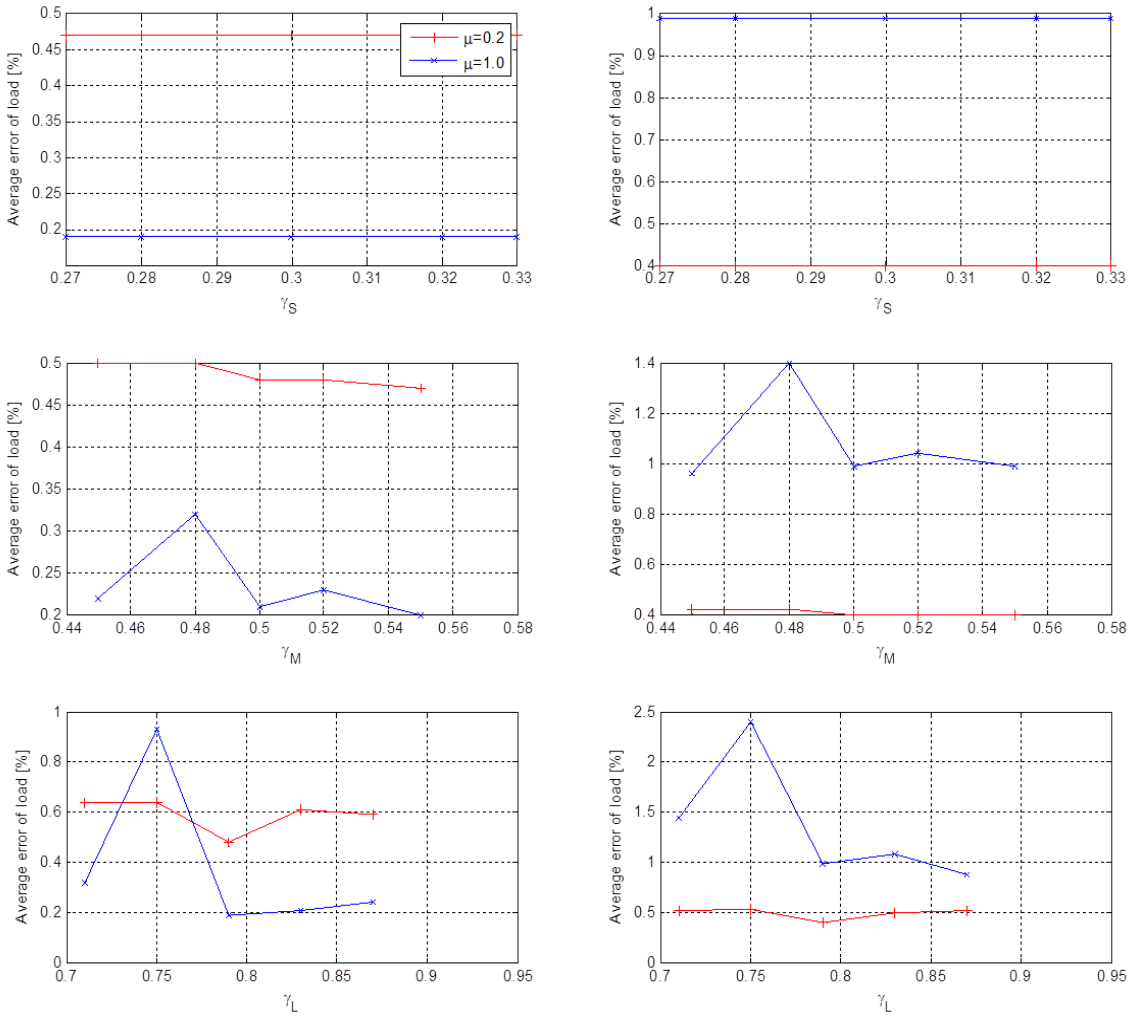


Figure 3.11 – Evolution of mean error of contact load for different γ-coefficient values (a) Normal load as a function of S crisp value (b) Tangential load as a function of S crisp value (c) Normal load as a function of L crisp value (d) Tangential load as a function of L crisp value (e) Normal load as a function of M crisp value (f) Tangential load as a function of M crisp value

Figs 3.11 & 3.12 present the evolution of mean errors of normal and tangential contact loads

between the FL2C method and the numerical reference as a function of different crisp values of fuzzy laws for the γ-coefficient and β-coefficient. Two friction coefficient values are considered, namely $\mu = 0.2$ (mainly sticking conditions) and $\mu = 1.0$ (mainly sliding conditions). The errors of the γ-coefficient variation, observed in fig 3.11, show that the choice of crisp value only weakly influences the precision of the contact solutions as long as the value range is compatible with the study. If we deviate from these values, the algorithm can naturally diverge. The choice of crisp value directly affects iteration number and consequently, the convergence rate.

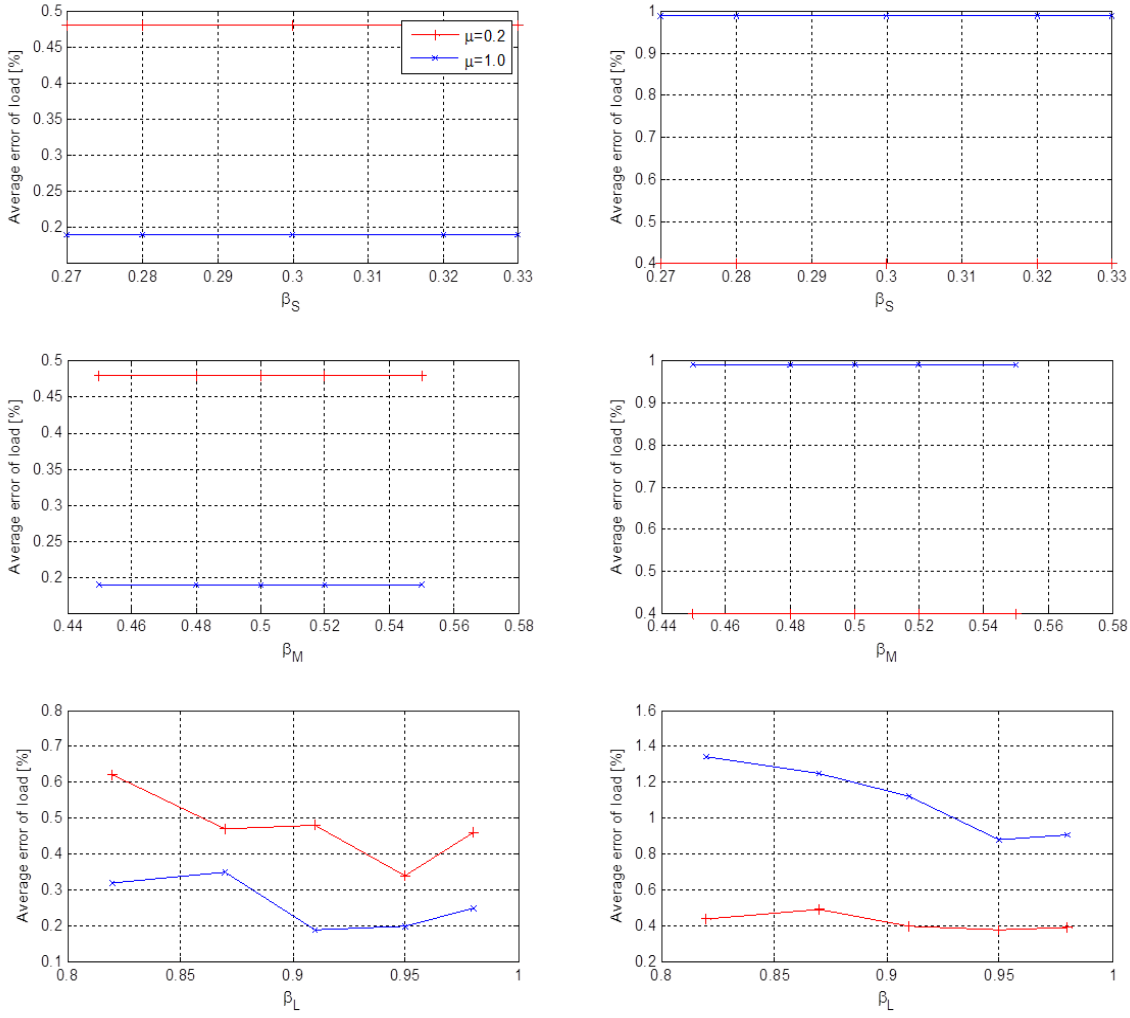


Figure 3.12 – Evolution of mean errors of contact load for different β-coefficient values (a) Normal load as a function of S crisp value (b) Tangential load as a function of S crisp value (c) Normal load as a function of L crisp value (d) Tangential load as a function of L crisp value (e) Normal load as a function of M crisp value (f) Tangential load as a function of M crisp value

For β-coefficient variations, the results in terms of normal load errors are comparable as previously shown fig 3.12. Nevertheless, for the frictional load errors, the effects of variations

are globally comparable as previously shown. Errors can increase up to nearly 2% for L crisp value variations. Thus, the controller design is very important to consider before performing simulations.

This section shows the good controller behavior stability, and more generally of the FL2C method. Controller design is an important step and there must specific focus for the tangential controller since the choice of crisp values for laws can have a greater effect than for the normal controller.

4.7 Solutions for fuzzy controller integration

This section is now associated with the implementation of fuzzy controllers into the contact scheme either in series or in parallel. Indeed, if the controllers are defined in series, we decouple the management of normal and tangential case. First, the normal case is solved to calculate the equilibrium position without friction. Secondly, the tangential case is performed considering as starting point the normal equilibrium position. On the contrary, if the controllers are considered in parallel, we manage both normal and tangential cases. A short discussion about the controller implementation is proposed. Fig 3.13. shows that the normal gap obtained at the end of the two-way calculation is of same order of magnitude as previously mentioned, namely $10^{-8}m$.

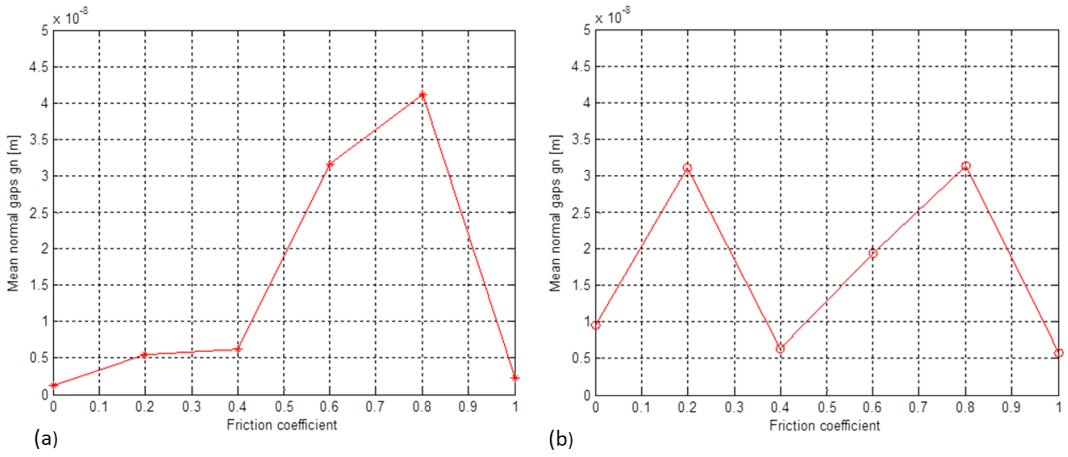


Figure 3.13 – Comparison of mean normal gap as a function of friction coefficient considering two controller implementations (a) use in series of controllers (b) use in parallel controllers

Moreover, the level of normal and tangential load error is almost identical and nearly 2% for both solutions in Fig 3.14. For the tangential load errors, we observe somewhat greater errors when the controllers are used in a series.

However, the controller implementation has a significant effect on the number of iterations

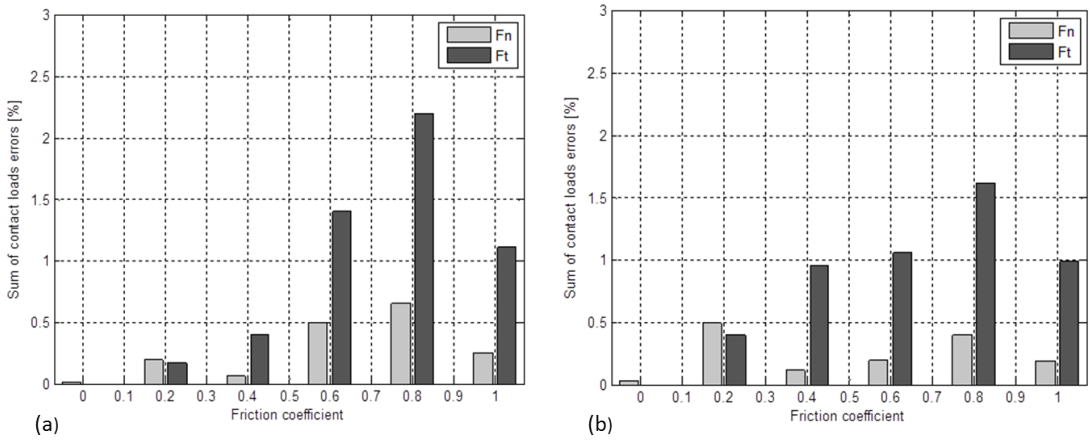


Figure 3.14 – Comparison of normal and tangential errors as a function of controller implementation (a) in series (b) in parallel

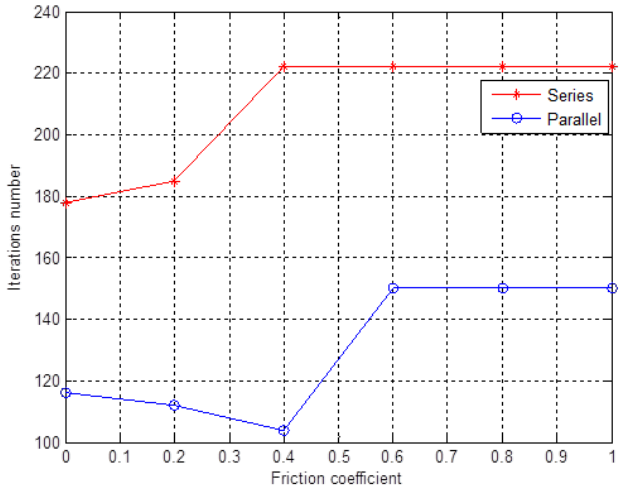


Figure 3.15 – Evolution of iteration number as a function of friction coefficient

necessary to obtain a desired convergence. In Fig 3.15, we observe that the number of iterations is clearly less important when the controllers are used in parallel. For example, the number of iterations is equal to 150 for controllers used in parallel versus 222 for controllers used in series. Moreover, the evolution of iteration number generally increases as a function of friction coefficient.

Before studying the computational time associated with these simulations in the next section, we show in this section that the controller implementation in the contact scheme also has a considerable effect and it is appropriate to consider controllers in parallel to limit the number of iterations.

4.8 Discussion about computational time

To conclude this application, we propose now to study the evolution of computational time and associated iteration number to solve the full contact problem (with the factorization of stiffness matrix and the calculation of displacements by linear system) and of the reduced contact problem (definition of projection matrix with eigenvectors and static modes). For this last application, the number of degrees of freedom is voluntarily increased and established as more than 100,000 elements to consider for a large finite element problem. Firstly, we observe in Fig 3.16-a that the resolution of the reduced contact problem does not have a significant effect on the number of iterations, which is globally constant but clearly higher than that of the application in the previous section. Secondly, a decrease in CPU time is highlighted in Fig 3.16-b.

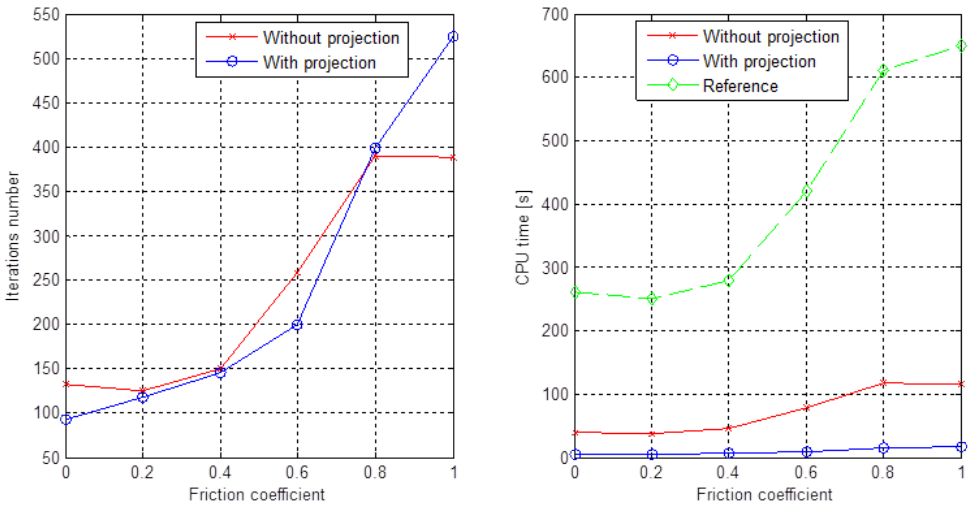


Figure 3.16 – Evolution of computational time and iteration numbers between the full and reduced contact problem and reference for large finite element models

Globally, we observe constant computational times for friction coefficient defined between 0 and 0.4, a high increase of computational time for the interval [0.4-0.8] and finally a new constant evaluation between 0.8 and 1. The computational time associated to the reference is clearly higher for the entire range of friction coefficient value. Moreover, computational gain is approximately equal to a factor of six between the full and reduced contact problem. The size of the reduced contact problem is equal to $2 * n_{ctt}$, with either 200 degrees of freedom for n_{dof} or 102,400 for the full contact problem.

This application shows that the new proposed strategy to study a frictional contact problem is very promising. A reduction of computational time is observed without deteriorating the level of precision regarding the evaluation of contact loads.

5 Conclusion

This chapter has allowed to extend the FL2C method to the case of frictional contact problem. To manage this kind of problem, it is necessary to add a second FLC for sticking state. These two FLC are integrated into to a contact loop where all the modifications of states (no contact, sticking or sliding) are managed for each contact pairs. As previously, the contact loads are considered as external loads and are updated iteratively. The nonlinear contact problem is cut into a series of reduced linear contact problem where no direct coupling is considered for finite element matrices. The projection matrix used for each component in contact is composed of static modes calculated at the contact interface.

To highlight the efficiency of the FL2C method in terms of precision, robustness and computational time, a complete numerical application has been proposed. A discussion is developed regarding the choice of projection matrix for building the reduced contact problem, the integration of the controller into the contact scheme, the choice of crisp value for control laws and the evolution of main contact data as a function of friction coefficient. All the results have been successfully compared with a reference numerical method. We have highlighted that FL2C method decomposes the non linear problem in a set of reduced linear problem, which is directly dependent of modal basis and static modes. Now, we can investigate in the next chapter the reanalysis of frictional contact problem with variable parameters.

Chapter 4

Reanalysis of perturbed frictional contact problems

Contents

1 Introduction 81

2 Perturbations in a static finite element contact problem 82

2.1 Nominal problem 82

2.2 Fuzzy Logic Controller for Contact method 83

2.3 Modified problem and reduction techniques 84

3 Reanalysis of the modified projection matrix 85

3.1 Homotopy perturbation and series development 85

3.2 Reanalysis of modified static modes 85

4 Proposed HPP-FL2C method 87

5 Numerical applications for frictional contact problem with perturbations 88

5.1 Description of the numerical model 89

5.2 Nominal contact problem validation 90

5.3 Nominal reduced contact problem validation 92

5.4 Modification of the friction coefficient 93

5.5 Validation of HPP method for projection matrix reanalysis 94

5.6 Perturbed reduced contact problem 95

5.7 Parametric analysis by DOE 98

6 Conclusion 99

1 Introduction

The two first chapters have allowed to develop a new way for solving a frictional contact problem by considering a Fuzzy Logic control approach. Practically, the normal and tangential (sticking) contact loads are iteratively calculated as a function of observed gaps thanks to two FLCs implemented in parallel. To update the positions of contact nodes at each iteration, reduced linear contact problems are solved. The reduction is performed by static modes of each structure in contact. As highlighted in the state of the art proposed in chapter 1, a current trend is to multiply the number of samplings and used advanced strategies (DOE, sensitivity analyses, non-deterministic analyses or robust optimization) to tend to more robust and reliable designs. In this context of multiple samplings, if perturbations are introduced on input parameters of the problem, the finite element matrices of the problem and so the equilibrium position and the contact data are necessarily modified. To maintain the computational time of these advanced approaches, it is necessary to integrate reduced order or reanalysis techniques [Giacoma et al., 2015].

In this chapter, as the contact problem has been rewritten as a function of static modes, we propose to investigate the reanalysis of these data as a function of the introduced perturbations. Thus, these modified displacements are approximated by considering homotopy perturbation method, which allows to develop the solutions of the nonlinear problem as a series expansion (in the present, the introduced perturbation is seen as a nonlinearity). The method employs a homotopy transform to generate a convergent series solution of mathematical problem. Finally, the obtained high order displacements will be respectively introduced in a projection matrix to reduce the size of each linear problems to be solved and built the contact projection matrix.

Thus, Section 2 summarizes the main equations of a nominal contact problem in a finite element context, the method used to solve the nonlinear problem and the definition of a modified reduced contact problem. In a context of multiple modifications, section 3 presents the reanalysis of the modified projection matrix and more particularly the reanalysis of modified static modes by homotopy perturbation and projection techniques. Section 4 presents the proposed reanalysis method coupling projection and control to solve the modified static frictional contact problem. To verify the efficiency of proposed method, a complete numerical application is presented in Section 5. The results obtained for different classes of perturbations are confronted to those obtained using industrial code Abaqus in terms of precision and computational time. Finally, a Design of Experiments is proposed to quantify the effects of input perturbations on output mechanical data. Conclusions and remarks are provided in Section 6.

2 Perturbations in a static finite element contact problem

2.1 Nominal problem

In a finite element context, the nominal equilibrium equation, which governs the static problem, is written as follows:

$$\mathbf{K}^{(0)}\mathbf{U}^{(0)} + \mathbf{F}_n^{(0)}(\mathbf{U}^{(0)}) + \mathbf{F}_t^{(0)}(\mathbf{U}^{(0)}) \;=\; \mathbf{F}_{ext}^{(0)} \tag{4.1}$$

where the upper script "(0)" defines the nominal or initial configuration and $\mathbf{K}^{(0)}$, $\mathbf{U}^{(0)}$, $\mathbf{F}_{ext}^{(0)}$, $\mathbf{F}_n^{(0)}(\mathbf{U}^{(0)})$ and $\mathbf{F}_t^{(0)}(\mathbf{U}^{(0)})$ respectively represent the nominal stiffness matrix, the nominal nodal displacement vector, the nominal external load vector and the nominal normal and tangential contact loads. The size of the finite element problem is n_{dof}. The problem studied is non-linear because the contact loads $\mathbf{F}_n^{(0)}(\mathbf{U}^{(0)})$ and $\mathbf{F}_t^{(0)}(\mathbf{U}^{(0)})$ depend directly on the unknown displacement $\mathbf{U}^{(0)}$ of all bodies in contact. These two contact load vectors will be assembled by considering the local normal and tangential contact loads detected for each active contact pair of the finite element model.

For the nominal part, the geometrical contact conditions can be expressed by:

$$\mathbf{P}_n^{(0)}\mathbf{U}^{(0)} \;=\; \mathbf{d}_n^{(0)} \tag{4.2}$$

where $\mathbf{d}_n^{(0)}$ is the initial normal gap and $\mathbf{P}_n^{(0)}$ is the normal contact matrix. This equation traduces the non-interpenetration condition described in the well-known contact model of Signorini. Two cases can be encountered for each contact pair, namely a non-contact state with a strictly current positive gap and a contact load equal to 0, or a contact state with a normal gap which tends to zero and a positive contact load. The matrix $\mathbf{P}_n^{(0)}$, which couples the displacements of each contact pair to ensure non-penetration, is thus defined as:

$$\mathbf{P}_n^{(0)} = \begin{bmatrix} \vec{\mathbf{n}}^{(0)} & -(1-\alpha^{(0)})\vec{\mathbf{n}}^{(0)} & -\alpha^{(0)}\vec{\mathbf{n}}^{(0)} \end{bmatrix} \tag{4.3}$$

where $\alpha^{(0)}$ and $\vec{\mathbf{n}}^{(0)}$ are respectively the nominal distance between projection of the slave node on the associated master element (segment or surface) and the first master node and the nominal normal vector.

For the frictional case, Coulomb's law is considered. During a contact state, two cases can be distinguished for each contact pair. First, a sliding state implies that the local frictional contact load is proportional to the normal contact load according to the introduction of a friction

coefficient μ. Secondly, for a sticking state, no sliding velocity is observed and the frictional contact load is always inferior to a threshold defined by the normal contact load value and the friction coefficient.

In a discretization context, a friction matrix $\mathbf{P}_t^{(0)}$ is defined by extension of normal contact matrix to the tangent plane with tangential vector $\vec{\mathbf{t}}^{(0)}$:

$$\mathbf{P}_t^{(0)} = \begin{bmatrix} \vec{\mathbf{t}}^{(0)} & -(1-\alpha^{(0)})\vec{\mathbf{t}}^{(0)} & -\alpha^{(0)}\vec{\mathbf{t}}^{(0)} \end{bmatrix} \tag{4.4}$$

The tangential contact constraints for the sticking state are integrated as follows:

$$\mathbf{P}_a^{(0)}\mathbf{U}^{(0)} = 0 \tag{4.5}$$

where $\mathbf{P}_a^{(0)}$ is the subpart of the friction matrix applied to the nodes in the sticking condition.

To solve the contact problem, the FL2C method is considered. The main steps are recalled in the next section.

2.2 Fuzzy Logic Controller for Contact method

The FL2C method is an iterative method, which decomposes the nonlinear contact problem into a series of linear problems where the contact loads are considered as external loads. Thus, a correction of contact loads and displacements is realized at each step by using Fuzzy Logic Controllers (FLC) to link the observed gaps with contact loads.

The equilibrium Eq 4.1 is rewritten as follows:

$$\mathbf{K}^{(0)}\mathbf{U}^{(0,k+1)} = \mathbf{F}_{ext}^{(0)} + \mathbf{F}_n^{(0,k+1)} + \mathbf{F}_t^{(0,k+1)} \tag{4.6}$$

where $\mathbf{F}_n^{(0,k+1)}$ and $\mathbf{F}_t^{(0,k+1)}$ represent the normal and tangential contact loads at the k^{th} iteration relative to the observed normal and tangential gaps.

Then, each contact load is calculated as follows:

$$\mathbf{F}_n^{(0,k+1)} = \mathbf{F}_n^{(0,k)} + \Delta\mathbf{F}_n^{(0,k+1)} \tag{4.7}$$

$$\Delta\mathbf{F}_n^{(0,k+1)} = \gamma\Delta\mathbf{F}_n^{(0,k)} \tag{4.8}$$

$$\mathbf{F}_t^{(0,k+1)} = \mathbf{F}_t^{(0,k)} + \Delta\mathbf{F}_t^{(0,k+1)} \tag{4.9}$$

$$\Delta\mathbf{F}_t^{(0,k+1)} = \beta\Delta\mathbf{F}_t^{(0,k)} \tag{4.10}$$

where γ and β are respectively normal and tangential coefficients associated with the increment

of normal and tangential loads and determined with FL2C.

2.3 Modified problem and reduction techniques

Let us now consider modifications of material or geometric parameters which are used in the stiffness matrix. These local modifications imply global modifications and a modified contact problem can be defined as:

$$\mathbf{K}^{(m)}\mathbf{U}^{(m)} + \mathbf{F}_n^{(m)}(\mathbf{U}^{(m)}) + \mathbf{F}_t^{(m)}(\mathbf{U}^{(m)}) \quad = \quad \mathbf{F}_{ext}^{(m)} \tag{4.11}$$

where the upper script "(m)" defines the modified configuration and $\mathbf{K}^{(m)}$, $\mathbf{U}^{(m)}$, $\mathbf{F}_{ext}^{(m)}$, $\mathbf{F}_n^{(m)}(\mathbf{U}^{(m)})$ and $\mathbf{F}_t^{(m)}(\mathbf{U}^{(m)})$ represent respectively the modified stiffness matrix, the modified nodal displacement vector, the modified external load vector and the modified normal and tangential contact loads.

The modified geometrical contact conditions can be expressed as follows:

$$\mathbf{P}_n^{(m)}\mathbf{U}^{(m)} = \mathbf{d}_n^{(m)} \tag{4.12}$$

$$\mathbf{P}_a^{(m)}\mathbf{U}^{(m)} = 0 \tag{4.13}$$

where $\mathbf{d}_n^{(m)}$, $\mathbf{P}_n^{(m)}$ and $\mathbf{P}_a^{(m)}$ are respectively the modified normal gap, the modified normal contact matrix and the modified sticking contact matrix.

To reduce problem size and computational time, a modified reduced contact problem can be obtained with the help of a projection matrix, such as:

$$\left[\mathbf{T}^{(m)^T}\mathbf{K}^{(m)}\mathbf{T}^{(m)}\right]\mathbf{q}^{(m)} = \mathbf{T}^{(m)^T}\left(\mathbf{F}_{ext}^{(m)} - \mathbf{F}_n^{(m)}(\mathbf{U}^{(m)}) - \mathbf{F}_t^{(m)}(\mathbf{U}^{(m)})\right) \tag{4.14}$$

$$\mathbf{U}^{(m)} = \mathbf{T}^{(m)}\mathbf{q}^{(m)} \tag{4.15}$$

where $\mathbf{T}^{(m)}$ is a modified projection matrix and $\mathbf{q}^{(m)}$ represents the modified reduced coordinates vector.

The projection basis in Eq 4.16 is composed of static modes of each component in contact. The latter are calculated by solving linear static problem whereas an unitary load is successively applied to contact nodes for each main direction. The number of static modes is noted as n_{sta}.

$$\mathbf{T}^{(m)} = \left[\mathbf{\Gamma}_1^{(m)} \quad \ldots \mathbf{\Gamma}_{n_{sta}}^{(m)}\right] \tag{4.16}$$

To ensure a set of orthonormal linear and an independent set of vectors, an orthonormalization of the projection matrix $\mathbf{T}^{(m)}$ is necessary. It is clear that the projection matrix is related to a specific modified system. A direct evaluation of this matrix can be time consuming and is not recommended but it can be efficiently reanalysed using homotopy perturbation and projection approaches. This is the topic of the next section.

3 Reanalysis of the modified projection matrix

3.1 Homotopy perturbation and series development

This section is dedicated to the reanalysis of the modified projection matrix $\mathbf{T}^{(m)}$ by considering homotopy perturbation and projection techniques.

First, the modified stiffness matrices $\mathbf{K}^{(m)}$ of each component in contact can be decomposed as a function of the nominal stiffness matrices $\mathbf{K}^{(0)}$ and perturbed parts $\Delta\mathbf{K}$, such as:

$$\mathbf{K}^{(m)} = \mathbf{K}^{(0)} + \epsilon\Delta\mathbf{K} \tag{4.17}$$

Secondly, the modified vectors of the modified projection matrix, namely modified static modes $\mathbf{\Gamma}^{(m)}$ can be developed as a series of nominal vectors and different perturbed vectors such as:

$$\mathbf{\Gamma}^{(m)} = \mathbf{\Gamma}^{(0)} + \epsilon^1\mathbf{\Gamma}^{(1)} + \ldots + \epsilon^{n_1}\mathbf{\Gamma}^{(n_1)} \tag{4.18}$$

where n_1 is the order of truncation of the development.

The homotopy perturbation technique allows a non-linear problem to be expressed as a set of linear problems. In the present case, the perturbation included in the problem is seen as the non-linearity and an additional unknown parameter ϵ is introduced to highlight this. Thus, the parameter ϵ is positioned in Eqs 4.18 alongside the perturbation or high order quantities. At the end of the formulation, parameter ϵ will be established to practically evaluate the perturbed solutions. The calculation of modified static modes and modified eigenmodes are detailed in the next subsection.

3.2 Reanalysis of modified static modes

The linear system of equations associated with the modified static modes is defined by Eq 4.19:

$$\mathbf{K}^{(m)}\mathbf{\Gamma}^{(m)} \;=\; \mathbf{F_I} \tag{4.19}$$

Where $\mathbf{F_I}$ is a vector of unitary load.

Introducing Eqs 4.17 and 4.18 into Eq 4.19, one obtains Eq 4.20:

$$\left(\mathbf{K}^{(0)} + \epsilon\Delta\mathbf{K}\right)\left(\mathbf{\Gamma}^{(0)} + \epsilon^1\mathbf{\Gamma}^{(1)} + \ldots + \epsilon^{n_1}\mathbf{\Gamma}^{(n_1)}\right) \;=\; \mathbf{F_I} \tag{4.20}$$

The nominal solution $\mathbf{\Gamma}^{(0)}$ is calculated using a standard algorithm after decomposing the nominal stiffness matrix $\mathbf{K}^{(0)}$.

$$\mathbf{K}^{(0)}\mathbf{\Gamma}^{(0)} \;=\; \mathbf{F_I} \tag{4.21}$$

The perturbed vector $\mathbf{\Gamma}^{(i)}$ is calculated by identifying the different order terms of parameter ϵ

$$\mathbf{K}^{(0)}\mathbf{\Gamma}^{(i)} \;=\; -\Delta\mathbf{K}\mathbf{\Gamma}^{(i-1)} \qquad \text{with} \quad i = 1 \ldots n_1 \tag{4.22}$$

All calculated perturbed vectors $\mathbf{\Gamma}^{(i)}$ depend on the same matrix, $\mathbf{K}^{(0)}$, which will be decomposed only once during the process, whatever the number of perturbed problems.

To ensure the quality of the approximation $\mathbf{\Gamma}^{(m)}$, a projection of the equilibrium in Eq 4.19 onto a subspace spanned by the columns of a rectangular projection basis $\mathbf{T}_\Gamma^{(m)}$ is considered. The projection basis $\mathbf{T}_\Gamma^{(m)}$ is built by using nominal solution $\mathbf{\Gamma}^{(0)}$ of the initial problem and perturbed solution $\mathbf{\Gamma}^{(i)}$, as written in Eq 4.23:

$$\mathbf{T}_\Gamma^{(m)} \;=\; \left[\mathbf{\Gamma}^{(0)}\mathbf{\Gamma}^{(1)} \ldots \mathbf{\Gamma}^{(i)} \ldots \mathbf{\Gamma}^{(n_1)}\right] \tag{4.23}$$

This projection basis, whose size is $[n_{dof}\mathrm{x}(n_{sta}\mathrm{x}(n_1 - 1))]$, is orthonormalized.

The reduced modified static problem is thus defined as follows:

$$\mathbf{T}_\Gamma^{(m)^T}\mathbf{K}^{(m)}\mathbf{T}_\Gamma^{(m)}\mathbf{\Gamma}_R^{(m)} = \mathbf{T}_\Gamma^{(m)^T}\mathbf{F_I} \tag{4.24}$$

$$\mathbf{\Gamma}^{(m)} = \mathbf{T}_\Gamma^{(m)}\mathbf{\Gamma}_R^{(m)} \tag{4.25}$$

Finally, the results $\mathbf{\Gamma}^{(m)}$ of Eq 4.25 are used to update the projection matrix $\mathbf{T}^{(m)}$. The reanalysis method, based on Homotopy Perturbation and Projection, is named HPP method in the rest of the paper. The next section presents the coupling of the reanalysis and the contact methods.

4 Proposed HPP-FL2C method

The proposed method, used to reanalyse a perturbed frictional contact problem, relies on the coupling of the HPP method and on the FL2C method.

To facilitate understanding, a flowchart, summarizing the different steps and the principal equations, is presented in Figure 4.1.

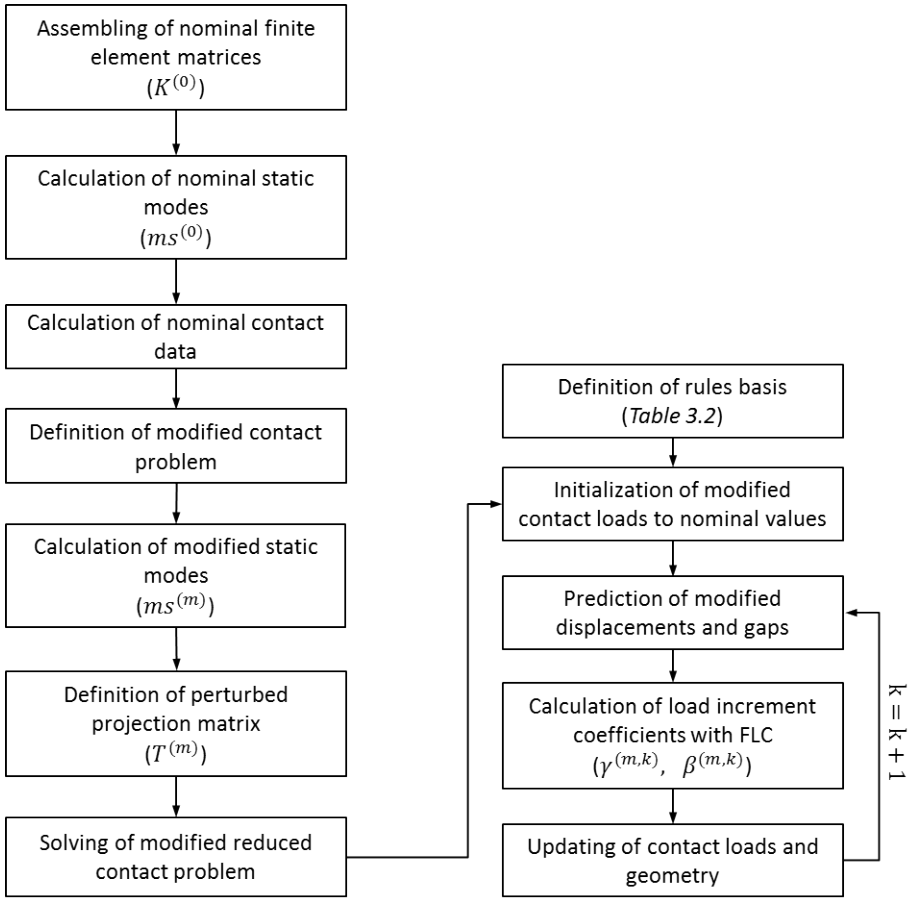


Figure 4.1 – Flowchart of the proposed HPP-FL2C method

First, when the nominal finite element matrices of each structure of the system have been assembled, it is necessary to calculate the nominal static modes of each structure with only their own boundary conditions. These evaluations are performed using classical methods. The nominal solutions of the contact problem can be solved using, for example, the FL2C method. Secondly, for each modified problem, the modified projection matrix is built with a reanalysis method. Thirdly, the reduced modified problem is built by considering a projection of equilibrium equation on the modified projection matrix. Finally, the reduced contact problem is iteratively solved using the

FL2C method.

In summary, to validate the proposed developments step by step, four numerical methods will be considered in the following section dedicated to numerical application, and will be labelled as follows:

— **Abaqus** for calculations performed on Abaqus software (node to surface algorithm and a minimal increment fixed at 1.10^{-5} to guarantee the convergence)
— **Full-FL2C** for calculations performed using the control approach for the contact problem with full finite element matrices size
— **Proj-FL2C** for calculations performed using the control approach for the reduced contact problem
— **HPP-FL2C** for calculations performed using the control approach and reanalysis of the projection matrix

5 Numerical applications for frictional contact problem with perturbations

The aim of this section is to highlight the efficiency and robustness of the proposed method. Thus, the current section studies the management of contact by control, the definition of the reduced contact problem and the reanalysis of the modified projection matrix. Seven subsections are proposed and organized as follows:

— The finite element model, the associated boundary conditions and the studied data are defined in subsection 5.1
— The nominal displacements and contact loads calculated with the Full-FL2C method and Abaqus are compared in subsection 5.2
— The nominal displacements and contact loads calculated with the Full-FL2C and Proj-FL2C methods are presented in subsection 5.3 and followed by a discussion about the size of the projection matrix
— Subsection 5.4 is dedicated to the calculation of mechanical responses as a function of a variation of friction coefficient by using the Proj-FL2C method
— Discussions about the validation of static modes reanalysis by the HPP method are proposed in subsection 5.5 by considering geometric and material perturbations
— Subsection 5.6 presents the reanalyzed results by HPP-FL2C for geometric and material perturbations. A discussion in terms of precision and computational time is proposed

— Parametric analyses are performed in subsection 5.7 to quantify the effects of input variations on output data

5.1 Description of the numerical model

A static frictional contact problem of two 2D semicircular steel rings is considered in Figure 4.2. Each ring is defined by an outer radius of 100 mm and an inner radius of 95 mm. The initial position of the upper ring's center is fixed at 140 mm to the left and 190 mm up from the center of the lower ring. The finite element discretization for each ring includes 640 quadrinodal plane stress elements and 729 nodes per ring, corresponding to 8 divisions of the radius and 80 sectors.

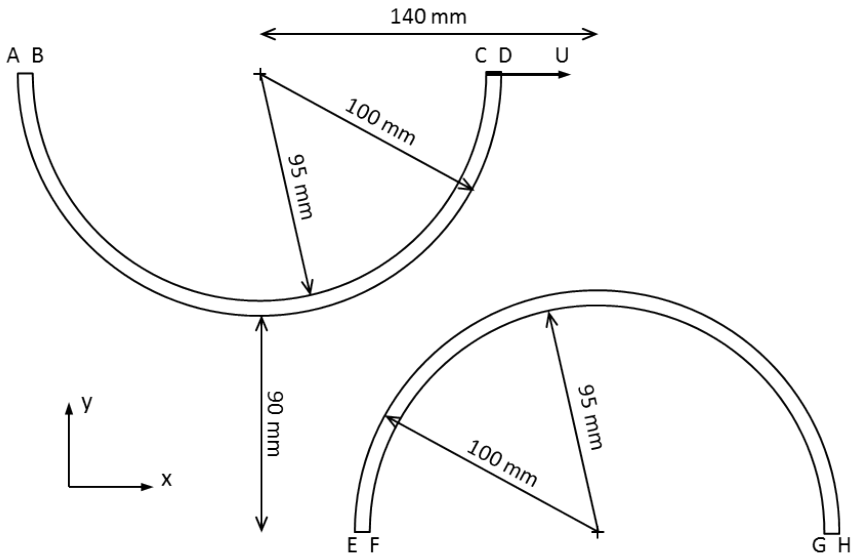


Figure 4.2 – Description of the system studied composed of two elastic rings in contact.

The elastic material properties of the two rings are fixed at 210 GPa for Young's moduli and 0.3 for Poisson's ratios. Fixed boundary conditions are applied to the GH segment along the x and the y-axes, AB, CD and EF segments along the y-axis only. The CD segment is controlled in displacement along the x-axis up to 240 mm. Twenty four steps are performed for this problem, so an horizontal displacement of 10 mm is applied to CD at each step. At the interface, a friction coefficient is set at 0.5. In the following analyses, the evolution of the sum of normal and tangential contact loads as well as the x-axis displacements of nodes A and E will be systematically studied for the different steps.

5.2 Nominal contact problem validation

The nominal results obtained with the Full-FL2C method are compared to those calculated with Abaqus. Figure 4.3 first presents the evolution of the x-axis displacements of nodes A and E.

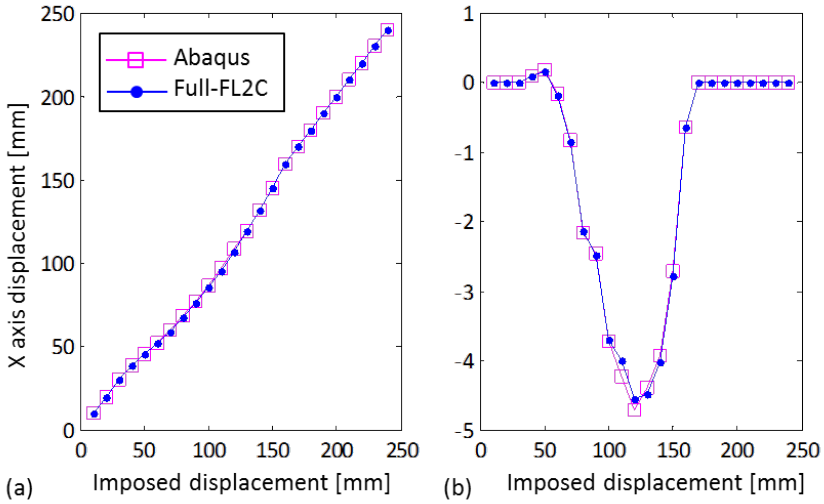


Figure 4.3 – Comparison of x-axis displacement between Abaqus and Full-FL2C. (a) Node A; (b) node E.

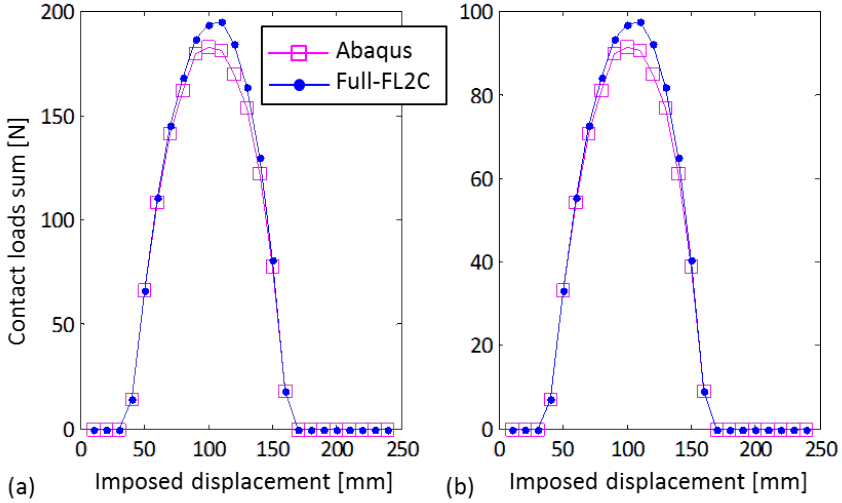


Figure 4.4 – Comparison of the sum of contact loads between Abaqus and Full-FL2C. (a) Surm of normal contact loads; (b) sum of tangential contact loads.

The global evolution of displacements calculated with the Full-FL2C method is very close

to that obtained with Abaqus. The maximum error is inferior to 1.5 percent and is found for node E around an imposed displacement of 110 mm. On the contrary, for lower and higher imposed displacements, errors are much lower as they do not exceed 1 percent. Besides, the maximal difference for the displacement following the x-axis of node A is in the order of $10^{-4}m$ for imposed displacement at 110 mm.

Now, the evolution of the sums of normal and tangential contact loads as a function of imposed displacements in Figure 4.4 is assumed. The results obtained are rather interesting because they are globally close to those given by the Abaqus solutions.

The maximal errors for both normal and tangential loads are inferior to 8 percent and are detected only for imposed displacements around 110 mm and 120 mm. However, these errors have a low effect on the global kinematic behavior concerning the x-axis displacements of nodes A and E previously presented. In the present case, the mean normal gap for the Full-FL2C method after equilibrium is equal to $1\mu m$. These differences are mainly linked to the distribution of contact loads between the two algorithms.

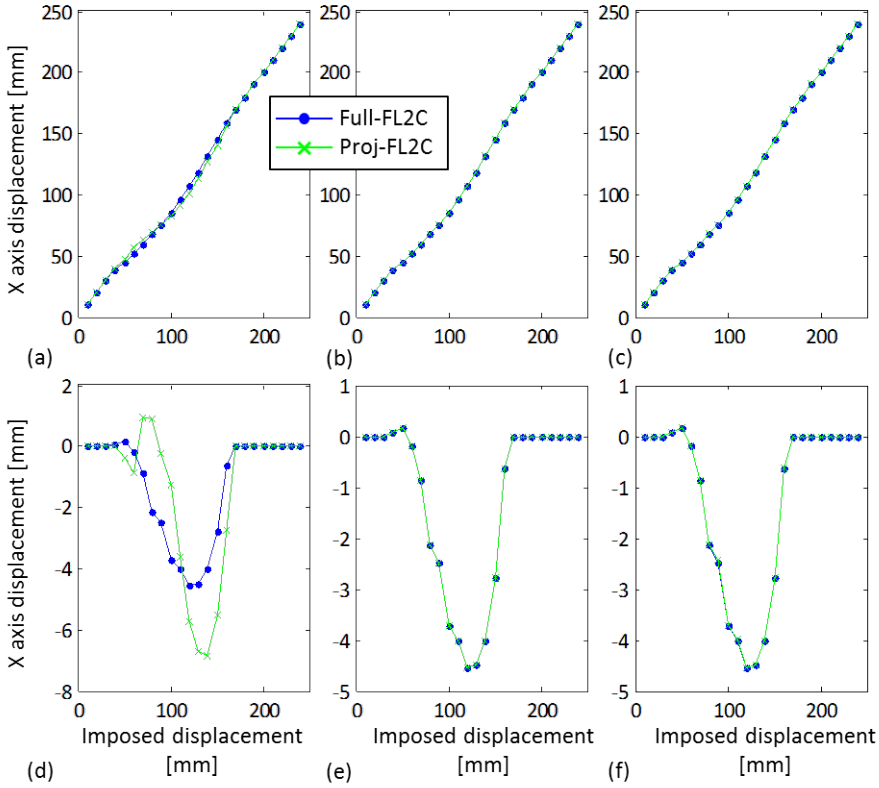


Figure 4.5 – Comparison of x-axis displacement between Full-FL2C and Proj-FL2C for different projection matrices. (a;b;c) Node A; (d;e;f) node E; (a;d) case 1; (b;e) case 2; (c;f) case 3.

5.3 Nominal reduced contact problem validation

This section is dedicated to validation of the nominal reduced problem and the use of a projection matrix to decrease the size of the contact problem and therefore the computational time. A discussion is offered on the number of modal and static modes which must be kept to achieve a good approximation of mechanical output data.

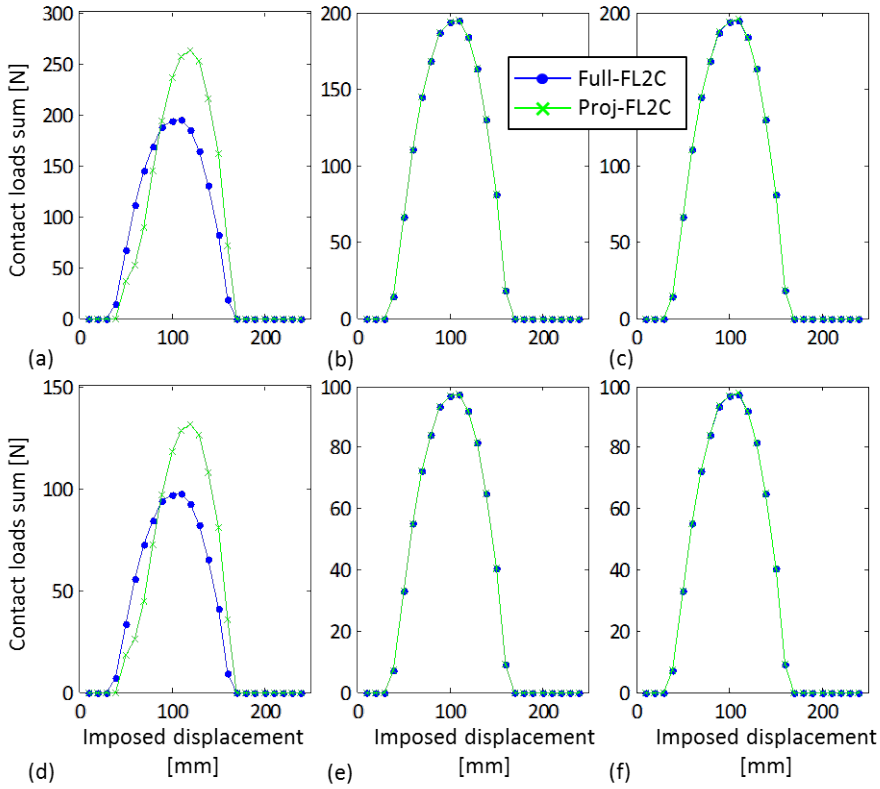


Figure 4.6 – Comparison of the sum of contact loads between Full-FL2C and Proj-FL2C for different projection matrices. (a;b;c) Sum of normal contact loads; (d;e;f) sum oof tangential contact loads;(a;d) case 1; (b;e) case 2; (c;f) case 3.

Figures 4.5 and 4.6 present the evolution of x-axis displacements and the sum of contact loads for Full-FL2C and Proj-FL2C as a function of the number of modes in the projection matrix. Three cases are studied:

— 10 eigenmodes for each elastic ring and no static modes (case 1)

— 10 eigenmodes for each elastic ring and 112 static modes (case 2)

— 112 static modes (case 3)

One can observe that it is necessary to consider the static modes of each ring calculated along both the x-axis and the y-axis at the contact interface. The errors are very close to those obtained

with the Full-FL2C method. The maximal error of contact loads (normal and tangential) is in the order of 10^{-3} percent, while the maximal difference for the x-axis displacement of node A and E is in the order of $10^{-4}mm$. In this case, considering modal basis does not improve the results to any greater degree. On the other hand, a lack of static modes clearly deteriorates the solutions.

5.4 Modification of the friction coefficient

An evolution of the friction coefficient μ, successively equal to 0.4 and 0.6, is now investigated. The results obtained are compared to those calculated with Abaqus to test the robustness of the proposed method.

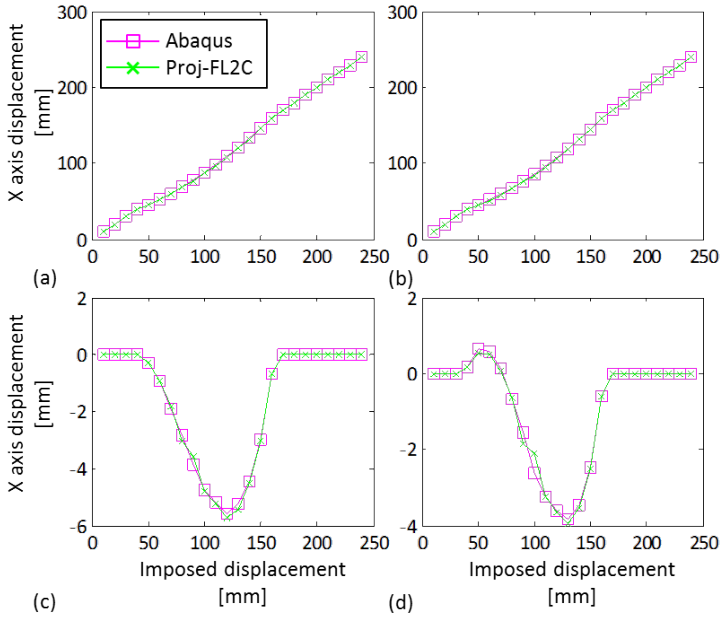


Figure 4.7 – Comparison of x-axis displacement between Abaqus and Proj-FL2C for different friction coefficients. (a;b) Node A; (c;d) node E; (a;c) $\mu = 0.4$; (b;d) $\mu = 0.6$.

In this case, the modification of the system is only due to an external parameter as the friction coefficient does not change the intrinsic characteristics of the structures. As a consequence, the projection matrix remains constant for all calculations. Figures 4.7 and 4.8 present the evolution of x-axis displacements and contact loads for Proj-FL2C and Abaqus by considering a friction coefficient successively equal to 0.4 and 0.6.

The obtained results are of the same quality as for the nominal contact problem exposed in section 5.2. The maximal errors at node E are respectively less than 2 percent in the case of $\mu = 0.4$ and 1.5 percent when $\mu = 0.6$ (compared to 1.5 percent for the nominal case when $\mu = 0.5$). Moreover, the solutions for node A are the same for the two methods. For normal and

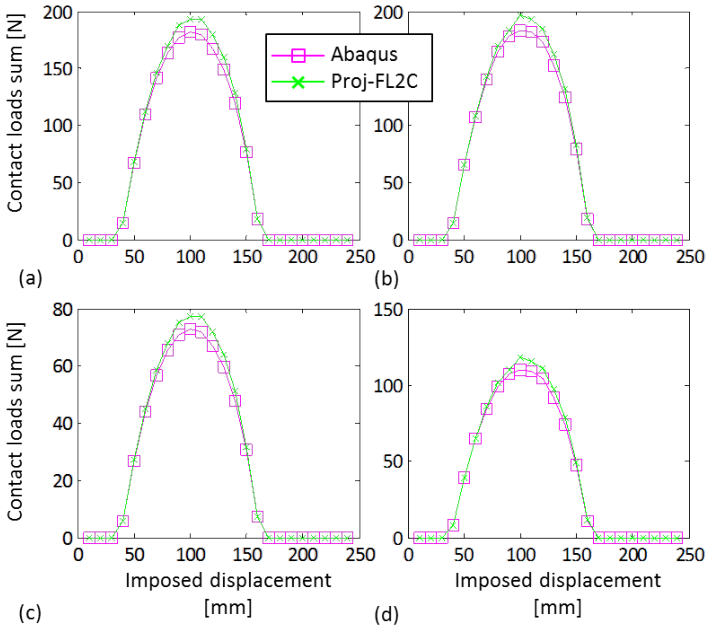


Figure 4.8 – Comparison of the sum of contact loads between Abaqus and Proj-FL2C for different friction coefficients. (a;b) Sum of Normal contact loads; (c;d) sum of tangential contact loads; (a;c) $\mu = 0.4$; (b;d) $\mu = 0.6$.

tangential contact loads, the maximal errors calculated between Proj-FL2C and Abaqus methods are respectively in the order of 7.5 percent and 7 percent in the case of $\mu = 0.4$ and $\mu = 0.6$ (compared to 8 percent for the nominal case when $\mu = 0.5$).

5.5 Validation of HPP method for projection matrix reanalysis

The aim of this section is to highlight the capability of the HPP method to reanalyze the projection matrix used to define the reduced contact problem. Two kinds of perturbation are considered here, namely material perturbation and geometric perturbation. First, material perturbation includes the modification of Young's moduli for each elastic rings. In the present case, Young's moduli are respectively fixed at 215 GPa and 205 GPa for the lower and upper rings. Secondly, the inner radius of the two rings are modified for geometric perturbation. The values of the inner radius are respectively fixed at 96 mm for the lower ring and 94 mm for the upper ring.

Attention is focused on the perturbed static modes due to material and geometric perturbations. In order to compare the reanalyzed and reference mode shapes, the Modal Assurance Criterion (MAC) is used. Figure 4.9 shows the MAC matrix as a function of the order of truncation chosen between 1 and 3. Figure 4.9 presents errors between reference and reanalyzed static

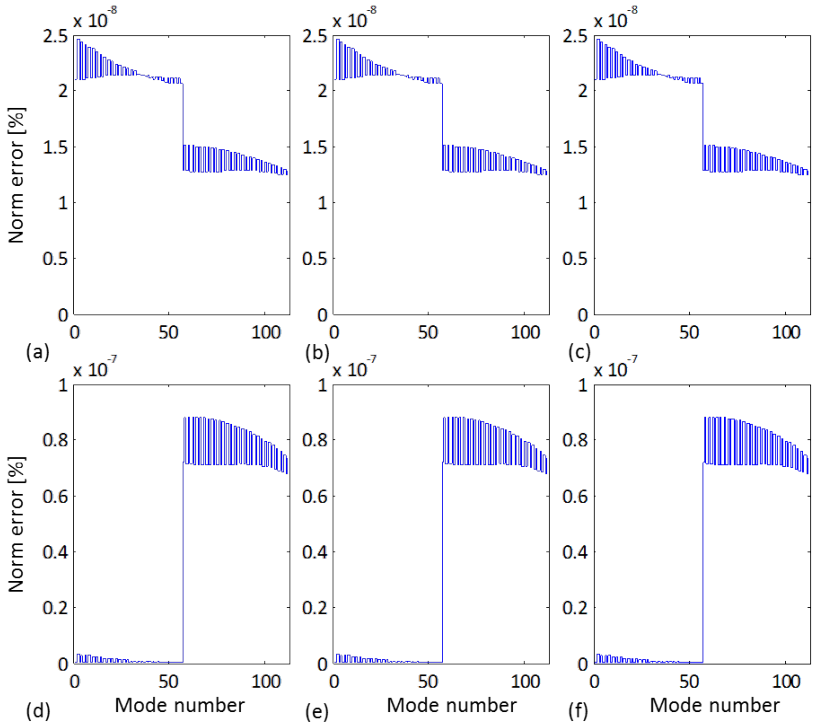


Figure 4.9 – Norm errors between the first 112 reference and reanalyzed static modes. (a;b;c) Material perturbation; (d;e;f) geometric perturbation; (a;d) order 1; (b;e) order 2; (c;f) order 3.

modes for three orders of truncation.

The differences are very small. For material and geometric perturbation respectively, an error of 1.10^{-8} percent and 1.10^{-7} percent can be observed for all the static modes whatever the order of truncation.

Thus, as the errors are globally very small with the first order development, a first order approximation will be considered using the HPP-FL2C method in the next section.

5.6 Perturbed reduced contact problem

In this section, the first order HPP-FL2C method is considered to reanalyze the projection matrix of the perturbed reduced contact problem. The two kinds of perturbations will be tested as previously, namely Young's moduli, respectively equal to 215 GPa and 205 GPa for the lower and upper rings, with an inner radius of 96 mm for the lower ring and 94 mm for the upper ring. The friction coefficient is fixed at its nominal value, namely 0.5.

Figures 4.10 and 4.11 present a comparison of results between Abaqus and HPP-FL2C by considering firstly, the x-axis displacements for node A and E and secondly, the sums of normal

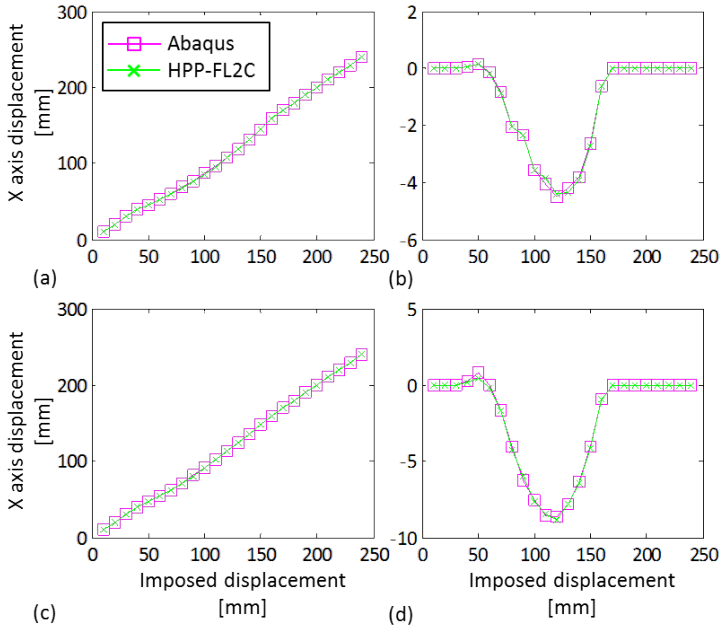


Figure 4.10 – Comparison of x-axis displacements between Abaqus and HPP-FL2C for different categories of perturbations. (a;b) Material perturbation; (c;d) geometric perturbation; (a;c) node A; (b;d) node E.

and tangential contact loads.

The reanalyzed x-axis displacements calculated with the HPP-FL2C method are very close to those obtained with Abaqus, whatever the perturbation. The mean errors are inferior to 1 percent for both nodes A and E. Moreover,the evolution of contact loads is globally well captured. For the totality of the simulation, the rate of error reaches a maximum of 10 percent.

Thus, this study shows the efficiency of the HPP-FL2C method to calculate with precision perturbed mechanical output quantities such as displacements and contact loads. Now, Figure 4.12 presents the evolution of computational time for one reanalysis as a function of the finite element model size. Three methods, namely Abaqus, Full-FL2C and HPP-FL2C, are considered for this comparison. The number of degrees of freedom (dof) of the finite element model is successively fixed at 120, 400, 1400, 5500 and 21000 dofs for each ring.

The computational time for Full-FL2C and HPP-FL2C is always less than Abaqus, regardless of the model size. When the model size increases, the computational gain between Abaqus and HPP-FL2C gradually increases. For the largest model, the computational gain factor between Abaqus and Full-FL2C can reach 75 percent and almost 50 percent between Full-FL2C and HPP-FL2C.

This section highlights the advantage of coupling a reanalysis technique and a control method

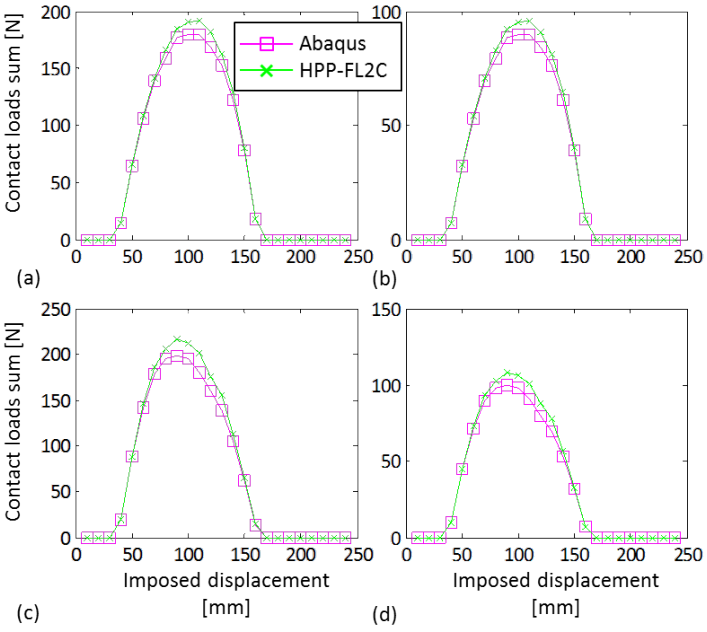


Figure 4.11 – Comparison of contact loads between Abaqus and HPP-FL2C for different categories of perturbations. (a;b) Material perturbation; (c;d) geometric perturbation; (a;c) sum of normal contact loads; (b;d) sum of tangential contact loads.

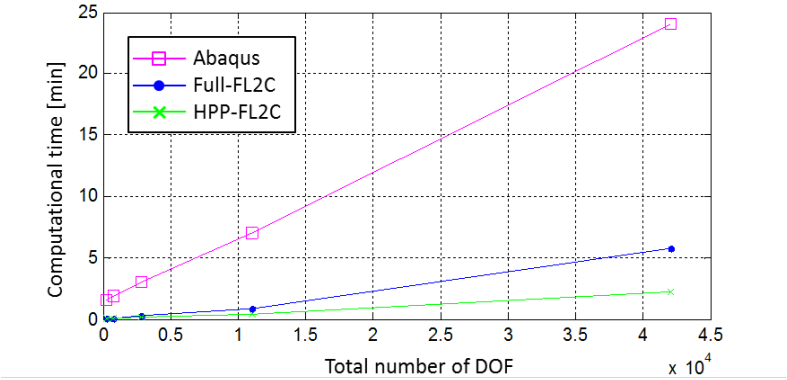


Figure 4.12 – Comparison of computational time of Abaqus, Full-FL2C and HPP-FL2C methods as a function of finite element model size.

to solve a perturbed contact problem.

5.7 Parametric analysis by DOE

Considering the previous observations in terms of precision and computational time to re-analyze a perturbed contact problem, the last test examines the use of the HPP-FL2C method in a DOE. A full factorial DOE considering both an interface parameter (friction coefficient), a material parameter (Young's modulus of each ring) and geometric parameter (inner radius of each ring). The values of each category of parameters can vary respectively between 0.4 to 0.6 (±20 percent), 205 GPa to 215 GPa (±2.4 percent) and 94 mm to 96 mm (±1.05 percent).

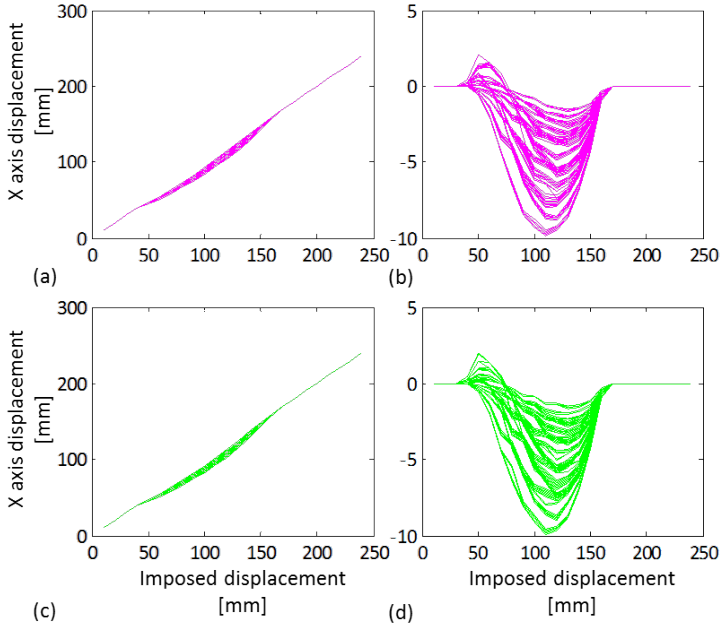


Figure 4.13 – Comparison of DOE results obtained with Abaqus and HPP-FL2C for displacements. (a;b) Abaqus; (c;d) HPP-FL2C; (a;c) x-axis displacement of node A; (b;d) x-axis displacement of node E.

Figures 4.13 and 4.14 present the effects of input perturbations on x-axis displacements and contact loads calculated with the Abaqus and HPP-FL2C methods.

First, the minimal and maximal evolutions of behaviours of output data are very close between the Abaqus and HPP-FL2C methods, which again confirms the precision of the proposed HPP method. We can note the significant effect of input perturbation on the x-axis displacement for node E. In fact, an output variation of ±90 percent is observed for node E against ±5 percent for node A. This study shows that moderate input perturbations can generate large variations in the output. The same significant evolution of behaviour is observed for the contact loads. Finally, in terms of computational time, this study was performed in approximately twelve hours using Abaqus compared with one hour using the HPP-FL2C method with Matlab, representing

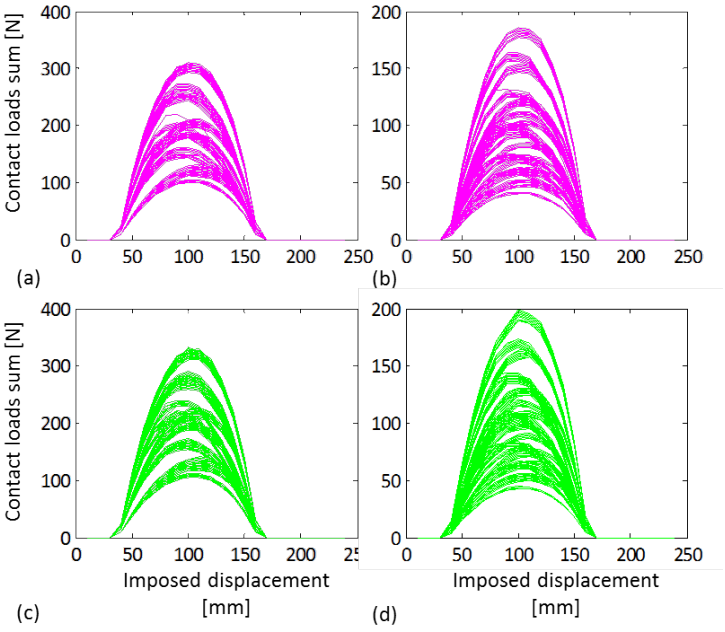


Figure 4.14 – Comparison of DOE results obtained with Abaqus and HPP-FL2C for the sum of contact loads. (a;b) Abaqus; (c;d) HPP-FL2C; (a;c) sum of normal contact loads; (b;d) sum of tangential contact loads.

a computational gain factor of twelve.

6 Conclusion

This chapter has presented a numerical strategy to reanalyze a modified static frictional contact problem. This one relies on the coupling of the FL2C method useful to the solving of the contact problem and the HPP method used for the reanalysis of coupling contact projection matrix. Indeed, in the context of multiple samplings, the input parameters are perturbed and affect the finite element matrices and so the static modes (which are the key elements of the contact projection matrix). Thus, we have proposed to reanalyse the modified static modes with a homotopy development and a new projection step. The different steps of the HPP-FL2C method have been developed.

Different tests have been performed to evaluate both the precision and the performance of the proposed HPP-FL2C method. We have highlighted that HPP-FL2C is a convenient strategy when parametric study such as DOE is considered. Indeed, with a first order of truncation, it is possible to obtain a level of precision compatible with advanced direct simulations. Moreover, an important gain of computational time can be obtained whichever category of variable parameter is involved,

namely interface, material or topology. We have shown that moderate input perturbations can generate large variations on the output contact data and both local and global modification of behaviours. Now, considering HPP-FL2C method, it is now possible to investigate the reanalysis of the equilibrium position of frictional induced vibration problems. The next step, studied in the next chapter, is the reanalysis of complex eigensolutions used in stability analysis.

Chapter 5

A global strategy for the stability analysis of friction induced vibration problem with parameter variations

Contents

1 Introduction 102

2 Stability analysis for friction-induced vibrations problems 103

2.1 Nominal description 103

2.2 Modified configuration and perturbation integration 105

3 Reanalysis of modified stability analysis 107

3.1 Main steps of the CHOC strategy 107

3.2 Reanalysis of the equilibrium position 109

3.3 Reanalysis of modified eigenmodes 110

3.4 Calculation of the modified complex eigendata 112

4 Application to simplified brake system stability analysis 113

4.1 Numerical model description 113

4.2 Nominal coalescence graph 114

4.3 Perturbed coalescence graph 118

4.4 Effects of input parameter modifications 121

5 Conclusion 122

1 Introduction

Considering the previous results about the reanalysis of a modified static equilibrium position (Chapter 4), we propose to investigate in this chapter the reanalysis of a friction induced vibration problems in a context of multiple samplings. Thus, a frequency stability analysis is here considered and performed thanks to a Complex Eigenvalue Analysis, in which system of equations are linearized around a stationary state determined from a nonlinear static contact analysis. Recently, to reduce the computational time of multiple samplings analyses, alternative methods are focussed on surrogate models, such as Kriging [Nobari et al., 2015b, Nechak et al., 2015]. This strategy allows to build mathematical functions alternative to classical numerical simulations from only a set of specific samples, calculated with a reference method. To avoid this last step, which can be time consuming too, we propose to reanalyse the modified solutions according to a nominal solution (performed with the reference method) and perturbations.

Thus, a complete strategy, named CHOC, is proposed to perform Multiple CEA analyses, by coupling both **C**ontrol approach, **HO**motopy and **C**omponent mode synthesis techniques. Indeed, Fuzzy logic control approach is used to manage the sliding contact problem. Homotopy perturbation and projection techniques allow to reanalyse efficiently perturbed projection matrices due to model parameter variations whereas component mode synthesis solves the modified undamped coupled eigenproblem. This solution strategy allows the complex eigenvalues to be approximated with a reduced computational time. Thus, Section 2 summarizes the main equations of a nominal stability problem in a finite element context. The contributions of input parameters perturbations on different data, such as stiffness matrices, contact conditions, coupling matrices, are highlighted. Section 3 presents the CHOC strategy and details the main ingredients, namely:

— the reanalysis of modified modal basis, static modes and contact projection basis,
— the solving of reduced modified contact problem,
— the calculation of modified modal basis of undamped coupled system,
— the calculation of modified complex eigensolutions.

To verify the efficiency and the robustness of the CHOC strategy, a numerical application is presented in Section 4. Each main step will be validated individually and the effects on input variability on an unstable mode are highlighted. Conclusions and remarks of this work are provided in Section 5.

2 Stability analysis for friction-induced vibrations problems

2.1 Nominal description

This section presents equations governing the instability of the steady sliding status. A local basis $(\vec{\mathbf{n}}, \vec{\mathbf{t}}, \vec{\mathbf{b}})$ is considered on the contact zone, with $\vec{\mathbf{n}}$ being the outward normal, $\vec{\mathbf{t}}$ is the sliding direction such as $\vec{\mathbf{t}} = \dfrac{\vec{v_g}}{\|\vec{v_g}\|}$ with $\vec{v_g}$ is the sliding velocity and $\vec{\mathbf{b}} = \vec{\mathbf{n}} \wedge \vec{\mathbf{t}}$. A perturbed dynamic solution is considered in the vicinity of this steady sliding equilibrium, so that the contact point remains in sliding status.

The mechanical dynamic equation in finite element context is presented as follow:

$$\begin{aligned}\mathbf{M}^{(0)}\ddot{\mathbf{U}}^{(0)} + \mathbf{C}^{(0)}\dot{\mathbf{U}}^{(0)} + \mathbf{K}^{(0)}\mathbf{U}^{(0)} = \mathbf{F}_{ext}^{(0)} + \mathbf{P}_n^{T(0)}\mathbf{F}_n^{(0)}(\mathbf{U}^{(0)}) + \dots \\ \mathbf{P}_t^{T(0)}\mathbf{F}_t^{(0)}(\mathbf{U}^{(0)}) + \mathbf{P}_b^{T(0)}\mathbf{F}_b^{(0)}(\mathbf{U}^{(0)})\end{aligned} \tag{5.1}$$

where the upper script "(0)" defines the nominal or initial configuration and $\mathbf{M}^{(0)}$, $\mathbf{K}^{(0)}$, $\mathbf{C}^{(0)}$, $\mathbf{U}^{(0)}$, $\mathbf{F}_{ext}^{(0)}$, $\mathbf{F}_n^{(0)}(\mathbf{U}^{(0)})$, $\mathbf{F}_t^{(0)}(\mathbf{U}^{(0)})$, $\mathbf{F}_b^{(0)}(\mathbf{U}^{(0)})$, $\mathbf{P}_n^{T(0)}$, $\mathbf{P}_t^{T(0)}$ and $\mathbf{P}_b^{T(0)}$ respectively represent the nominal mass matrix, the nominal stiffness matrix, the nominal damping matrix, the nominal displacement vector, the nominal external load vector, the nominal normal and tangential contact loads and their associated localization matrices.

The displacements $\mathbf{U}^{(0)}$ are broken down into a nodal displacement of the system at a steady sliding equilibrium $\mathbf{U}^{s(0)}$ and a perturbed state $\mathbf{U}^{*(0)}$, such as:

$$\mathbf{U}^{(0)} = \mathbf{U}^{s(0)} + \mathbf{U}^{*(0)} \tag{5.2}$$

By integrating the decomposition of displacements (Eq. 5.2) into Eq. 5.1, the mechanical dynamic equation is:

$$\begin{aligned}\mathbf{M}^{(0)}\ddot{\mathbf{U}}^{*(0)} + \mathbf{C}^{(0)}\dot{\mathbf{U}}^{*(0)} + \mathbf{K}^{(0)}(\mathbf{U}^{s(0)} + \mathbf{U}^{*(0)}) = \mathbf{F}_{ext}^{(0)} + \dots \\ \mathbf{P}_n^{T(0)}(\mathbf{F}_n^{s(0)} + \mathbf{F}_n^{*(0)}) + \mathbf{P}_t^{T(0)}(\mathbf{F}_t^{s(0)} + \mathbf{F}_t^{*(0)}) + \mathbf{P}_b^{T(0)}(\mathbf{F}_b^{s(0)} + \mathbf{F}_b^{*(0)})\end{aligned} \tag{5.3}$$

where $\mathbf{F}_n^{*(0)}$, $\mathbf{F}_t^{*(0)}$ and $\mathbf{F}_b^{*(0)}$ are normal and tangential contact loads associated to a perturbed state $\mathbf{U}^{*(0)}$.

The static equilibrium displacement $\mathbf{U}^{s(0)}$ is calculated by considering the following equation:

$$\mathbf{K}^{(0)}\mathbf{U}^{s(0)} = \mathbf{F}_{ext}^{(0)} + \mathbf{P}_n^{T(0)}\mathbf{F}_n^{s(0)}(\mathbf{U}^{(0)}) + \mathbf{P}_t^{T(0)}\mathbf{F}_t^{s(0)}(\mathbf{U}^{(0)}) + \mathbf{P}_b^{T(0)}\mathbf{F}_b^{s(0)}(\mathbf{U}^{(0)}) \tag{5.4}$$

where $\mathbf{F}_n^{s(0)}$, $\mathbf{F}_t^{s(0)}$ and $\mathbf{F}_b^{s(0)}$ are respectively the static normal and tangential contact loads.

Eq. 5.4 can be simplified by introducing the static equilibrium Eq. 5.3 as:

$$\mathbf{M}^{(0)}\ddot{\mathbf{U}}^{*(0)} + \mathbf{C}^{(0)}\dot{\mathbf{U}}^{*(0)} + \mathbf{K}^{(0)}\mathbf{U}^{*(0)} = \mathbf{P}_n^{T(0)}\mathbf{F}_n^{*(0)} + \mathbf{P}_t^{T(0)}\mathbf{F}_t^{*(0)} + \mathbf{P}_b^{T(0)}\mathbf{F}_b^{*(0)} \tag{5.5}$$

The system being in sliding state, the tangential load $\mathbf{F}_t^{*(0)}$ is given by:

$$\mathbf{F}_t^{*(0)} = \mu\mathbf{F}_n^{*(0)} \tag{5.6}$$

where μ is the friction coefficient.

The binormal load $\mathbf{F}_b^{*(0)}$ is expressed as a function of the velocity $\dot{U}^{*(0)}$:

$$\mathbf{F}_b^{*(0)} = \mu\mathbf{D}\mathbf{P}_b^{(0)}\dot{\mathbf{U}}^{*(0)} \tag{5.7}$$

where $\mathbf{D}$ is dependent of the sliding velocity for each node in contact and comparable to a supplementary damping contribution.

The normal contact conditions is recalled by Eq. 5.8:

$$\mathbf{P}_n^{(0)}\mathbf{U}^{*(0)} = 0 \tag{5.8}$$

This relation is equivalent to Eq. 5.9 by considering a projection matrix $\mathbf{T}_n^{(0)}$ which contains the normal connection between the slave and master nodes of the contact interface.

$$\mathbf{U}^{*(0)} = \mathbf{T}_\mathbf{N}^{(0)}\mathbf{U}_w^{*(0)} \tag{5.9}$$

where $\mathbf{U}_w^{*(0)}$ is a restriction of $\mathbf{U}^{*(0)}$

Introducing Eq. 5.6 and Eq. 5.7 in Eq. 5.5 and after some algebra, we obtain the following equation:

$$\mathbf{M}^{(0)}\mathbf{T}_\mathbf{N}^{(0)}\ddot{\mathbf{U}}^{*(0)} + (\mathbf{C}^{(0)} - \mu\mathbf{P}_b^{T(0)}\mathbf{D}\mathbf{P}_b^{(0)})\mathbf{T}_\mathbf{N}^{(0)}\dot{\mathbf{U}}^{*(0)} + \mathbf{K}^{(0)}\mathbf{T}_\mathbf{N}^{(0)}\mathbf{U}^{*(0)} = \left(\mathbf{P}_n^{T(0)} + \mu\mathbf{P}_t^{T(0)}\right)\mathbf{F}_n^{*(0)} \tag{5.10}$$

Next, we introduce a second projection basis $\mathbf{T}_\mu^{(0)}$ which allows to vanish the second right side of equation 5.10. This one depends on $\mathbf{T}_\mathbf{N}^{(0)}$, $\mathbf{P}_n^{(0)}$, $\mathbf{P}_t^{(0)}$ and μ of contact data. Premultiplying this equation with $\mathbf{T}_\mu^{T(0)}$, we obtain the equation that governs the smooth dynamic evolution of the system :

$$\tilde{\mathbf{M}}^{(0)}\ddot{\mathbf{U}}_w^{*(0)} + \tilde{\mathbf{C}}^{(0)}\dot{\mathbf{U}}_w^{*(0)} + \tilde{\mathbf{K}}^{(0)}\mathbf{U}_w^{*(0)} = 0 \tag{5.11}$$

where $\tilde{\mathbf{M}}^{(0)} = \mathbf{T}_{\mu}^{T(0)}\mathbf{M}^{(0)}\mathbf{T}_{\mathbf{N}}^{(0)}$, $\tilde{\mathbf{K}}^{(0)} = \mathbf{T}_{\mu}^{T(0)}\mathbf{K}^{(0)}\mathbf{T}_{\mathbf{N}}^{(0)}$, $\tilde{\mathbf{C}}^{(0)} = \mathbf{T}_{\mu}^{T(0)}(\mathbf{C} - \mu\mathbf{P}_b^{T(0)}\mathbf{D}\mathbf{P}_b^{(0)})\mathbf{T}_{\mathbf{N}}^{(0)}$ and $\mathbf{T}_{\mu}^{(0)} = \mathbf{T}_{\mathbf{N}}^{(0)}(\mathbf{P}_n^{T(0)} + \mu\mathbf{P}_t^{T(0)})$

The linear analysis of the dynamic stability of the system, defined by Eq. 5.11, leads classically to the generalized eigenproblem:

$$(s^{2(0)}\tilde{\mathbf{M}}^{(0)} + s^{(0)}\tilde{\mathbf{C}}^{(0)} + \tilde{\mathbf{K}}^{(0)})\Psi^{(0)} = 0 \tag{5.12}$$

where $\Psi^{(0)}$ is the full right eigenvector corresponding to the eigenvalue $s^{(0)}$.

To determine eigenvalues and eigenvectors, a 2n-dimensional right eigenproblems is generally defined:

$$\mathbf{A}^{(0)}\mathbf{u}^{(0)} = s^{(0)}\mathbf{B}^{(0)}\mathbf{u}^{(0)} \tag{5.13}$$

where

$$\mathbf{A}^{(0)} = \begin{bmatrix} -\tilde{\mathbf{K}}^{(0)} & 0 \\ 0 & \tilde{\mathbf{M}}^{(0)} \end{bmatrix}, \mathbf{B}^{(0)} = \begin{bmatrix} \tilde{\mathbf{C}}^{(0)} & \tilde{\mathbf{M}}^{(0)} \\ \tilde{\mathbf{M}}^{(0)} & 0 \end{bmatrix}, \mathbf{u}^{(0)} = \begin{bmatrix} \Psi^{(0)} \\ s^{(0)}\Psi^{(0)} \end{bmatrix} \tag{5.14}$$

In practice, the solving of Eq. 5.13 is performed using a QZ algorithm by previously considering a projection on the modal basis of the undamped coupled system, defined as follows:

$$\left(\left[\mathbf{T}_{\mathbf{N}}^{T(0)}\mathbf{K}^{(0)}\mathbf{T}_{\mathbf{N}}^{(0)}\right] - \lambda_c^{(0)}\left[\mathbf{T}_{\mathbf{N}}^{T(0)}\mathbf{M}^{(0)}\mathbf{T}_{\mathbf{N}}^{(0)}\right]\right)\Phi^{(0)} = 0 \tag{5.15}$$

Considering the complex eigensolutions, the stability of the mechanical system will be performed in the Lyapunov's sense. If the complex eigenvalue have a positive real part, the mode will be defined as unstable whereas it is considered stable if the eigenvalue have a negative real part. The divergence rate is defined as the division of the real part by the imaginary part of the complex eigenvalue.

2.2 Modified configuration and perturbation integration

A perturbation on parameters definition of finite element model such as material, geometric or interface properties is now considered. As the studied problem is enough complex and dependent on multiple calculation steps (non linear static contact problem, calculation of coupling matrices, calculation of modal basis of coupled system and calculation of complex eigendata), a small modification of input parameters may cause multiple and possibly significant effects on output parameters such as divergence rate and unstable frequencies. Fig. 5.1 illustrates the effect of an

input parameter perturbation $\Delta\mathbf{p}$ on the main output mechanical data for the stability problem.

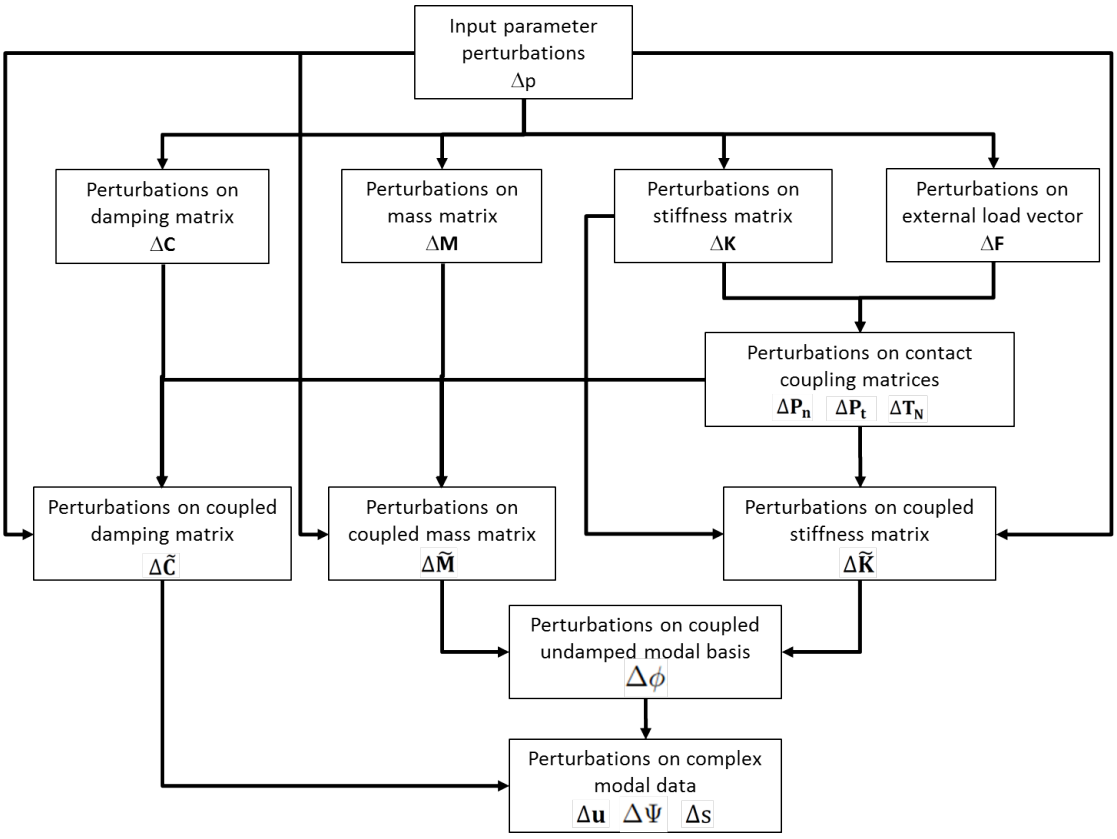


Figure 5.1 – Effect of input variability on output mechanical data for the stability problem

Indeed, an input parameter perturbation $\Delta\mathbf{p}$ generates a perturbation on the finite element mass $\Delta\mathbf{M}$, damping $\Delta\mathbf{C}$ and stiffness $\Delta\mathbf{K}$ matrices and on the loading vector $\Delta\mathbf{F}$. Next, considering a perturbation on stiffness matrix $\Delta\mathbf{K}$ and loading vector $\Delta\mathbf{F}$, the solutions of the static non linear contact problem are modified and the equilibrium position, which is a strong assumption of the stability problem, is changed too. Thus, a perturbation on normal $\Delta\mathbf{P}_n$ and tangential $\Delta\mathbf{P}_t$ and $\Delta\mathbf{P}_b$ contact localization matrices is observed. The modification of normal contact conditions generates a perturbation of normal projection matrix $\Delta\mathbf{T_N}$, which is used to create the coupled finite element matrices. The observed perturbations on these matrices, noted $\Delta\tilde{\mathbf{M}}$, $\Delta\tilde{\mathbf{C}}$ and $\Delta\tilde{\mathbf{K}}$, clearly modify the results of linear and complex eigenvalue problems and supply some perturbations on eigendata $\Delta\phi$, $\Delta\Psi$ and Δs. Finally, we highlighted that perturbations, which can be introduced in Eq. 5.13 governing the stability problem, are dependent of multiple perturbations at different levels. To be efficient and predictive, the proposed reanalysis strategy, developed in the next section, must take into account this specific context of perturbation.

3 Reanalysis of modified stability analysis

3.1 Main steps of the CHOC strategy

The aim of the CHOC strategy is to propose an alternative way to perform stability analysis in a context of multiple samplings. The proposed strategy must supply stability results with reducing the computational time without losing precision. Classically, surrogate models, such as moving least square or kriging methods, can be performed to investigate variations of parameters. These methods allow to build mathematical functions alternative to classical numerical simulations from only a set of specific samples of a DOE. The general idea is to approximate a higher dimension system by another one but with much lower dimension. For this kind of analysis, the main problem is to identify the necessary number of samples to build surrogate models with accuracy as a function of number of variable parameters. Moreover, the degree of validity of mathematical model clearly depends on the choice of samplings. Thus, the most time consuming part is associated to the evaluation of different samplings by a classical way rather than the evaluation of mathematical model as a function of parameters variations. To avoid these problems, we propose to reanalyse modified solutions associated to each sampling according to a nominal solution and perturbations.

Fig. 5.2 summarizes the main steps and equations for performing a stability analysis, respectively with Abaqus reference and with CHOC strategy both for the nominal and perturbed cases. For reference method, the non linear static problem is solved by using a Newton Raphson algorithm to determine the equilibrium position. After building contact coupling matrix, a complex eigenvalue problem is solved considering a projection on the modes associated to the undamped coupled problem. For the two eigenvalues problems, QZ and Lanczos solvers are respectively chosen. For the nominal case with CHOC strategy, we propose first to replace Newton Raphson algorithm by a fuzzy logic control approach and more precisely the FL2C method [Massa et al., 2015a]. The main advantage is to build a reduced contact problem by considering a projection matrix composed of eigenmodes and static modes for each component of the studied system. Second, Lanczos algorithm used for the linear eigenvalue problem is replaced by a CMS method where the modified attachment modes are calculated as a linear combination of static modes of each component and contact localization matrix. For the perturbed case with CHOC strategy, we propose to reanalyse modified eigenmodes and static modes for each component by considering HPP method [Massa et al., 2015b, Massa et al., 2011b].

CHOC strategy relies on offline and online steps. The offline step is dedicated to the calculation of nominal data by considering the nominal values of model parameter:

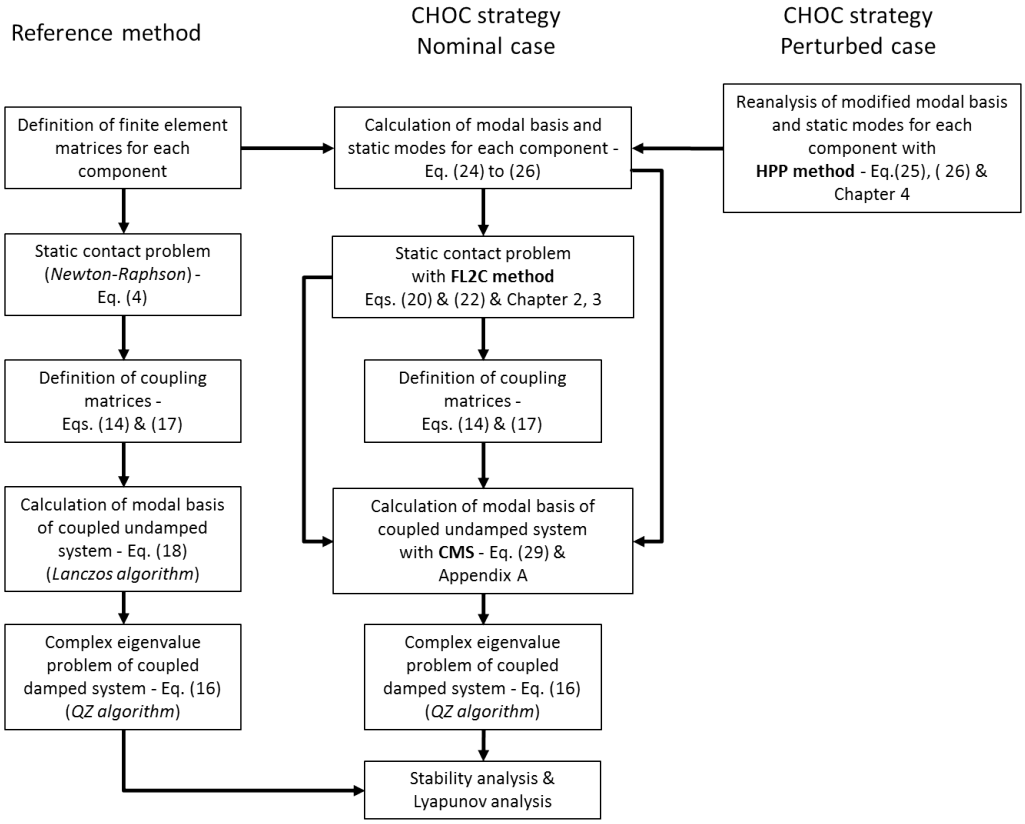


Figure 5.2 – Flowchart of the reference method and CHOC strategy

— The calculation of nominal modal basis and nominal static modes for each component in contact to build the nominal projection matrix,
— The design of Fuzzy Logic Controllers,

The online step, which is performed for each perturbation, relies on:

— The reanalysis of modified modal basis and modified static modes as a function of introduced perturbations with HPP method to build modified projection matrix,
— The solving of reduced modified contact problem with FL2C method,
— The calculation of modified eigenmodes of the modified undamped eigenproblem of the coupled system with a CMS method,
— The calculation of modified complex eigensolutions

The reanalysis of the equilibrium position and eigendata are detailed in the two next subsections.

3.2 Reanalysis of the equilibrium position

The stability problem relies first on a non linear static analysis in Eq. 5.4 by considering the finite element matrices of each component of the studied system. To solve the frictional contact problem, a Newton-Raphson iterative procedure is currently used. The solving of this step can be time consuming as soon as perturbations on finite element matrices are considered. Indeed, mathematically, several linear systems, whose sizes are directly dependent of the finite element mesh, must be solved. Moreover, the tangent matrix, built to take into account the contact conditions, must be updated and factorized for each new perturbation.

To decrease the computational time in the context of multiple samplings (due to multiple perturbations), we propose to replace the classical Newton algorithm by Fuzzy Logic Controllers to solve the contact problem and consider the FL2C (Fuzzy Logic Controller for Contact) method, proposed by Massa et al. [Massa et al., 2015a]. The FL2C method is an iterative method which decomposes the nonlinear contact problem into a series of linear problems where the contact data are calculated iteratively.

Considering a perturbation of the nominal values of the finite element model, the static equilibrium, Eq. 5.4 can be rewritten for each iteration k as follows :

$$\begin{aligned}\mathbf{K}^{(m)}\mathbf{U}^{s,(m,k)} = \mathbf{F}_{ext}^{(m)} + \mathbf{P}_n^{T(m,k)}\mathbf{F}_n^{s,(m,k)}(\mathbf{U}^{s,(m,k)}) + \dots \\ \mathbf{P}_t^{T(m,k)}\mathbf{F}_t^{s,(m,k)}(\mathbf{U}^{s,(m,k)}) + \mathbf{P}_b^{T(m,k)}\mathbf{F}_b^{s,(m,k)}(\mathbf{U}^{s,(m,k)})\end{aligned} \tag{5.16}$$

The upper script "(m)" defines the modified configuration of vectors and matrices of the modified problem. Each contact load is calculated according to a increment of contact load. In the case of the normal contact load, one obtain:

$$\mathbf{F}_n^{s,(m,k+1)} = \mathbf{F}_n^{s,(m,k)} + \Delta\mathbf{F}_n^{s,(m,k+1)} \tag{5.17}$$

$$\Delta\mathbf{F}_n^{s,(m,k+1)} = \gamma\Delta\mathbf{F}_n^{s,(m,k)} \tag{5.18}$$

where γ is the normal coefficient associated with the increment of normal load and determined with a FLC. The same way is performed to calculate the tangential loads due to a sticking state. The main steps of the FL2C method are presented in chapter 2 and 3.

This method avoids any coupling of the component matrices and then allow to perform projection technique in a way to reduce the size of the problem. To reduce the size of system to be solved, a projection matrix $\mathbf{T}_s$, which contains the specific static modes for each component of the studied system, can be built.

Eq. 5.16 can be rewritten as follows:

$$\begin{aligned}\left[\mathbf{T}_s^T\mathbf{K}^{(m)}\mathbf{T}_s\right]\mathbf{q}^{s,(m,k)} = \mathbf{T}_s^T\Big(\mathbf{F}_{ext}^{(m)} + \mathbf{P}_n^{T(m,k)}\mathbf{F}_n^{s,(m,k)}(\mathbf{U}^{s,(m,k)}) + \dots \\ \mathbf{P}_t^{T(m,k)}\mathbf{F}_t^{s,(m,k)}(\mathbf{U}^{s,(m,k)}) + \mathbf{P}_b^{T(m,k)}\mathbf{F}_b^{s,(m,k)}(\mathbf{U}^{s,(m,k)})\Big)\end{aligned} \tag{5.19}$$

$$\mathbf{U}^{s,(m,k)} = \mathbf{T}_s\mathbf{q}^{s,(m,k)} \tag{5.20}$$

where $\mathbf{q}^{s,(m,k)}$ represents the modified reduced coordinates vector.

$$\begin{aligned}&\mathbf{T}_s = \left[\left\{\Gamma_1^{(m)}\dots\Gamma_p^{(m)}\dots\Gamma_{n_{sta}}^{(m)}\right\}_z\right] \\ &p = 1\dots n_{sta}, z = 1\dots n_{comp}\end{aligned} \tag{5.21}$$

where $\left\{\Gamma_p^{(m)}\right\}_z$ represents the n_{sta} static modes of the n_{comp} components in contact, calculated considering the following equations:

$$\left\{\mathbf{K}^{(m)}\right\}_z\left\{\Gamma_p^{(m)}\right\}_z = \mathbf{F_I} \quad \text{for} \quad z = 1\dots n_{comp} \tag{5.22}$$

where $\left\{\mathbf{K}^{(m)}\right\}_z$ are the modified stiffness matrices, $\left\{\Gamma_p^{(m)}\right\}_z$ and $\mathbf{F_I}$ the modified displacement vector and the unitary load vectors.

Moreover, to reduce the computational time, Eq. **??** and Eq. 5.22 are not calculated for each perturbation but are rather reanalysed by using the HPP method, proposed by Massa et al. [Massa et al., 2011b, Massa et al., 2015b], as a function of introduced perturbations. Thus, if the perturbation is localized into a specific component of the studied system, only the associated data of this component are reanalyzed, that allows to reduce one more time the computational time.

The main steps of the HPP method are presented in chapter 4 for static modes and in the next subsection for the eigenmodes.

3.3 Reanalysis of modified eigenmodes

The modified eigenmodes $\boldsymbol{\phi}_j^{(m)}$ are obtained thanks to the modified eigenvalue problem, and associated normalization which are reiterated as follows:

$$\mathbf{K}^{(m)}\boldsymbol{\phi}_j^{(m)} = \boldsymbol{\lambda}_j^{(m)}\mathbf{M}^{(m)}\boldsymbol{\phi}_j^{(m)} \quad \text{with} \quad j = 1\dots n_{mod} \tag{5.23}$$

$$\boldsymbol{\phi}_j^{(m)^T}\mathbf{M}^{(m)}\boldsymbol{\phi}_j^{(m)} = 1 \tag{5.24}$$

Considering the Homotopy Perturbation Method, Eqs 5.23 and 5.24 can be rewritten as:

$$\begin{aligned}\left(\mathbf{K}^{(0)}+\epsilon\Delta\mathbf{K}\right)\left(\boldsymbol{\phi}_j^{(0)}+\epsilon^1\boldsymbol{\phi}_j^{(1)}+\ldots+\epsilon^{n_1}\boldsymbol{\phi}_j^{(n_1)}\right)=\ldots\\ \left(\boldsymbol{\lambda}_j^{(0)}+\epsilon^1\boldsymbol{\lambda}_j^{(1)}+\ldots+\epsilon^{n_1}\boldsymbol{\lambda}_j^{(n_1)}\right)\left(\mathbf{M}^{(0)}+\epsilon\Delta\mathbf{M}\right)\left(\boldsymbol{\phi}_j^{(0)}+\epsilon^1\boldsymbol{\phi}_j^{(1)}+\ldots+\epsilon^{n_1}\boldsymbol{\phi}_j^{(n_1)}\right)\end{aligned} \tag{5.25}$$

$$\left(\boldsymbol{\phi}_j^{(0)}+\epsilon^1\boldsymbol{\phi}_j^{(1)}+\ldots+\epsilon^{n_1}\boldsymbol{\phi}_j^{(n_1)}\right)^T\left(\mathbf{M}^{(0)}+\epsilon\Delta\mathbf{M}\right)\left(\boldsymbol{\phi}_j^{(0)}+\epsilon^1\boldsymbol{\phi}_j^{(1)}+\ldots+\epsilon^{n_1}\boldsymbol{\phi}_j^{(n_1)}\right)=1 \tag{5.26}$$

As previously for static modes, identifying the different order terms of parameter ϵ again, one first obtains the nominal eigenvalue problem which is solved using the Lanczos method:

$$\mathbf{K}^{(0)}\boldsymbol{\phi}_j^{(0)} \;=\; \boldsymbol{\lambda}_j^{(0)}\mathbf{M}^{(0)}\boldsymbol{\phi}_j^{(0)} \tag{5.27}$$

Secondly the high-order terms, $\boldsymbol{\lambda}_j^{(i)}$ and $\boldsymbol{\phi}_j^{(i)}(i=1\ldots n_1)$ are determined using implicit Wang methods. The i^{th} high-order eigenvector perturbations $\boldsymbol{\phi}_j^{(i)}$ is expressed as a linear combination of initial eigenvectors and a static correction, as written in Eq 5.28:

$$\boldsymbol{\phi}_j^{(i)}=\sum_{z=1}^{n_{mod}}c_{jz}\boldsymbol{\phi}_z^{(0)}+\boldsymbol{\Psi}_j^{(i)} \tag{5.28}$$

where $\boldsymbol{\Psi}_j^{(i)}$ is the pseudo static solution associated with the truncation order:

$$\boldsymbol{\Psi}_j^{(i)}=\mathbf{K}^{(0)}\mathbf{F}_j^{(i)}-\sum_{z=1}^{n_{mod}}\frac{\boldsymbol{\phi}_z^{(0)^T}\mathbf{F}_j^{(i)}}{\boldsymbol{\lambda}_z^{(0)}}\boldsymbol{\phi}_j^{(0)} \tag{5.29}$$

where coefficients c_{jz} and $F_j^{(i)}$ are calculated using Eqs 5.30 and 5.31:

$$\begin{aligned}c_{jz}&=\frac{\boldsymbol{\phi}_z^{(0)^T}\mathbf{F}_j^{(i)}}{\boldsymbol{\lambda}_z^{(0)}-\boldsymbol{\lambda}_j^{(0)}} \qquad \text{for} \quad j\neq z\\ c_{jz}&=\mathbf{H}_j^{(i)} \qquad\qquad\qquad \text{for} \quad j=z\end{aligned} \tag{5.30}$$

$$\begin{aligned}\mathbf{F}_j^{(i)}&=-\left(\Delta\mathbf{K}\boldsymbol{\phi}_j^{(i-1)}-\sum_{z=0}^{i-1}\boldsymbol{\lambda}_i^{(z)}\Delta\mathbf{M}\boldsymbol{\phi}_j^{(i-z-1)}-\sum_{z=1}^{i-1}\boldsymbol{\lambda}_j^{(z)}\mathbf{M}^{(0)}\boldsymbol{\phi}_j^{(i-z)}-\mathbf{M}^{(0)}\boldsymbol{\phi}_j^{(0)}\boldsymbol{\lambda}_j^{(i)}\right)\\ \mathbf{H}_j^{(i)}&=-0.5\left(\sum_{z=0}^{i-1}\boldsymbol{\phi}_j^{(z)^T}\Delta\mathbf{M}\boldsymbol{\phi}_j^{(i-z-1)}+\sum_{z=1}^{i-1}\boldsymbol{\phi}_j^{(z)^T}\mathbf{M}^{(0)}\boldsymbol{\phi}_j^{(i-z)}\right)\end{aligned} \tag{5.31}$$

Wang's method needs the same factorization of the symmetric matrix $\mathbf{K}^{(0)}$ as for static modes and thus does not leads to an excessive additional computational time.

As previously, the projection matrix $\mathbf{T}_{\phi}^{(m)}$ is orthonormalized and a reduced modified problem is defined for the modal case as follows:

$$\left[\mathbf{T}_{\phi}^{(m)^T}\mathbf{K}^{(m)}\mathbf{T}_{\phi}^{(m)}\right]\boldsymbol{\phi}_{jR}^{(m)} = \left[\mathbf{T}_{\phi}^{(m)^T}\mathbf{M}^{(m)}\mathbf{T}_{\phi}^{(m)}\right]\boldsymbol{\phi}_{jR}^{(m)}\boldsymbol{\lambda}_{j}^{(m)} \tag{5.32}$$

$$\boldsymbol{\phi}_{j}^{(m)} = \mathbf{T}_{\phi}^{(m)}\boldsymbol{\phi}_{jR}^{(m)} \tag{5.33}$$

$$\mathbf{T}_{\phi}^{(m)} = \left[\boldsymbol{\phi}_{1}^{(0)} \dots \boldsymbol{\phi}_{n_{mod}}^{(0)}\boldsymbol{\phi}_{1}^{(1)} \dots \boldsymbol{\phi}_{n_{mod}}^{(1)} \dots \boldsymbol{\phi}_{1}^{(i)} \dots \boldsymbol{\phi}_{n_{mod}}^{(i)} \dots \boldsymbol{\phi}_{1}^{(n_1)} \dots \boldsymbol{\phi}_{n_{mod}}^{(n_1)}\right] \tag{5.34}$$

3.4 Calculation of the modified complex eigendata

The modified static analysis allows to build the modified coupling matrices integrating the modified normal and tangential contribution. As a consequence, modified coupled finite element matrices are so generated. The complex eigenvalues $s^{(m)}$ are given by the modified complex eigenvalue problem defined by Eq. 5.35.

$$\mathbf{A}^{(m)}\mathbf{u}^{(m)} = s^{(m)}\mathbf{B}^{(m)}\mathbf{u}^{(m)} \tag{5.35}$$

To solve this problem, a QZ solver and a projection on modified eigenmodes of the modified undamped eigenvalue problem (with the use of only the coupling due to the modified normal conditions) are considered. The associated modified eigenmodes $\Phi_{w}^{(m)}$ are defined in Eq. 5.36:

$$\left(\left[\mathbf{T}_{\mathbf{N}}^{T(m)}\mathbf{K}^{(m)}\mathbf{T}_{\mathbf{N}}^{(m)}\right] - \lambda_{c}^{(m)}\left[\mathbf{T}_{\mathbf{N}}^{T(m)}\mathbf{M}^{(m)}\mathbf{T}_{\mathbf{N}}^{(m)}\right]\right)\Phi^{(m)} = 0 \tag{5.36}$$

This step is time consuming too because the modified eigenvalue problem must be calculated for each perturbation introduced in modified coupled finite element matrices $\mathbf{T}^{(m)}$.

In the CHOC strategy, the modified eigenmodes $\Phi^{(m)}$are evaluated considering a CMS method and more particularly the works of Mac Neal [MacNeal, 1971]. The calculation times associated to this step will be reduced because all the data necessary to the CMS method are already available after the reanalysis of $\left\{\Phi_{j}^{(m)}\right\}_{z}$ and $\left\{\Gamma_{p}^{(m)}\right\}_{z}$. The modified attachment modes $\Gamma^{(m)}$ of the CMS method are calculated as a linear combination of modified static modes of each component and modified localization matrices $\mathbf{P}_{n}^{(m)}$, such as:

$$\Gamma^{(m)} = \Gamma_{p}^{(m)}\mathbf{P}_{n}^{T(m)} \tag{5.37}$$

The main steps of the Mac-Neal CMS method are recalled in A.

4 Application to simplified brake system stability analysis

First, this section is dedicated to the validation of the main steps of the CHOC strategy (calculation of contact loads, reanalysis of modal bases, reanalysis of static modes, calculation of eigenvectors by CMS method). Second, CHOC strategy is used for sensitivity analysis which involves multiple CEA. Results obtained with Abaqus software are considered as references.

4.1 Numerical model description

The finite element model of the simplified brake system, which is here reduced to a disk and two pads, is presented in Fig. 5.3. Each pad is constituted by a backplate and a lining. The inner surface of the disc is assumed clamped and the translational movements of the upper surface of each pad in the tangential directions are blocked. A pressure of 2.5 $10^6 N/m^2$ is applied on the upper surface of each pad.

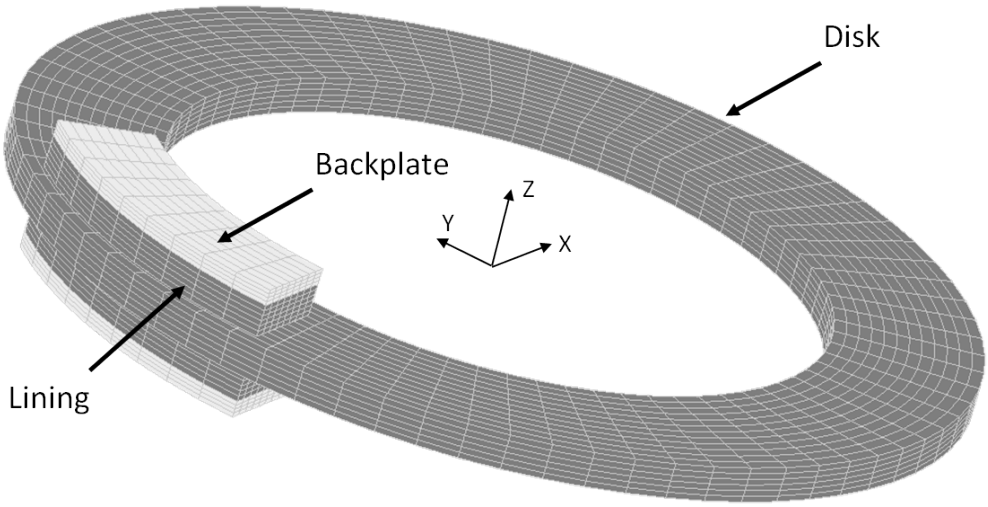


Figure 5.3 – Description of the finite element model

The numerical model has 6552 nodes for the disc and 990 nodes per pad, which corresponds to a total number of 25596 degrees of freedom. 90 contact nodes are defined at the interface between each pad and the disc. The geometry characteristics for disc and pads are given in Table 5.1 while the material properties are summarized Table 5.2. An orthotropic modelisation is chosen for the lining of each pad.

Table 5.1 – Nominal geometrical characteristics

	Disc	Pad
Inner radius (m)	0.1	0.11
Outer radius (m)	0.145	0.140
Thickness (m)	0.011	0.005 (Backplate)
		0.01 (Lining)
Pad angle (radian)		$\pi/8$

Table 5.2 – Nominal material properties

	Disc	Backplate	Lining
Density (kg/m^3)	7200	7300	2600
Young's moduli (GPa)	130	170	6.5 (Ex)
			3.5 (Ez)

4.2 Nominal coalescence graph

The aim of this section is to compare the nominal coalescence graph calculated with the CHOC strategy and Abaqus considering a friction coefficient varying from 0 to 0.6 at the contact interface. Before presenting these results, we propose to make a focus on the calculation of contact data with the FL2C method, on the integration of a projection matrix for contact problem and on the determination of eigenmodes of the nominal coupled undamped eigenproblem with CMS method.

First, bases of the projection matrix are calculated classically using a Lanczos solver for the nominal eigensolutions and LU decomposition for the nominal static modes. In the present case, we consider 100 eigenmodes for the disc, 80 eigenmodes and 270 static modes for each pad. The number of eigenmodes have been chosen to ensure a frequency study up to 10kHz and a good precision with the CMS method. Moreover, all the nodes at contact interface have been taken into account for the calculation of static modes. No selection has been performed as in recent works proposed by Fazio et al. [Fazio et al., 2015]. So, the projection matrix corresponds to a reduction of the size of the problem to 800 generalized coordinates compared to 25596 dofs. Second, contact data are calculated with the FL2C method.

For the next applications, the error criterion is defined as the ratio betwen the absolute value

of the difference of reference and proposal results and the reference one. Fig. 5.4 presents the mean and maximal errors for normal contact loads using FL2C method, with and without projection matrix, compared to the reference solutions.

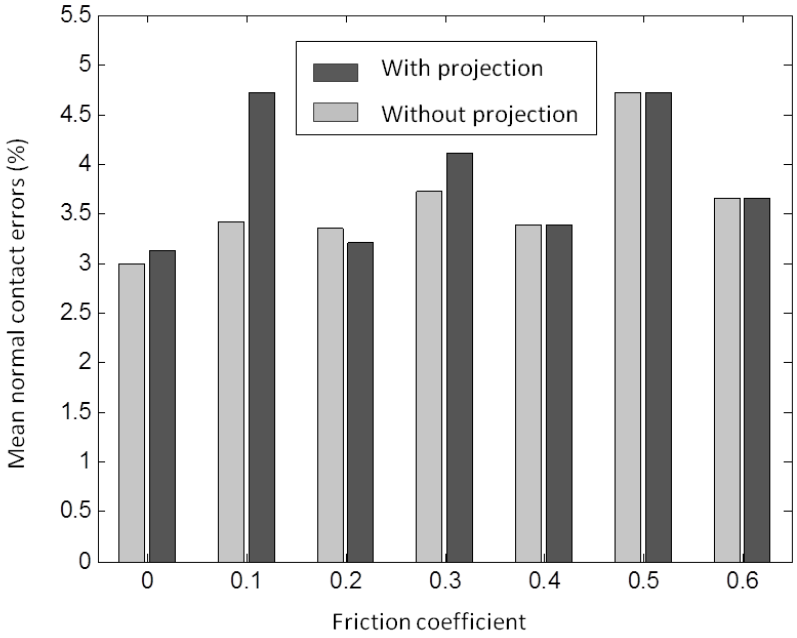


Figure 5.4 – Errors of mean normal contact loads between Abaqus and FL2C method with or without projection matrix

The obtained results are very interesting because the errors for normal contact loads between the FL2C method and Abaqus are inferior to 5 percent (Fig. 5.4) whatever is the value of the friction coefficient. Moreover, Fig. 5.4 highlights that the integration of the projection matrix does not globally deteriorate the results because the level of errors is globally the same. A small increase of the error in the projection case can be observed with friction coefficients fixed to 0.1 and 0.3. Fig. 5.5 highlights the localization of maximal errors in term of contact loads. The maximal errors are associated to black areas whereas minimal errors are defined to white areas. It can be shown that these main differences are detected at the bottom of the pad and at the right top corner and can reach 20 percent for the smallest amplitudes of contact loads. However, this error does not clearly modify the distribution of normal contact loads and so the equilibrium position used in stability analysis. The other contact data (normal and tangential vectors, position of slave nodes on master area) useful to build the contact localization matrices are calculated with a comparable precision.

The next step is dedicated to the calculation of the nominal eigenmodes of the associated

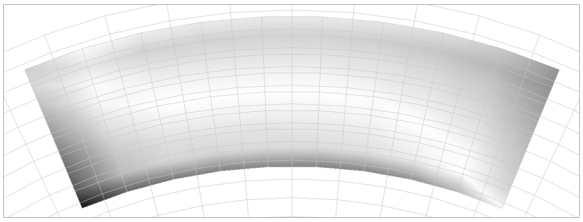


Figure 5.5 – Distribution of contact loads errors on pads between FL2C method and Abaqus for $\mu = 0.1$

coupled undamped coupled eigenproblem in Eq. 5.15. In the present case, we consider the nominal spectral and modal bases of each component in contact, the contact localization matrix for normal case and the static modes to build the nominal attachment modes of the CMS method in Eq. 5.37. A comparison of modal basis calculated with the CMS method and Abaqus is proposed in Fig. 5.6 using a Modal Assurance Criterion (MAC).

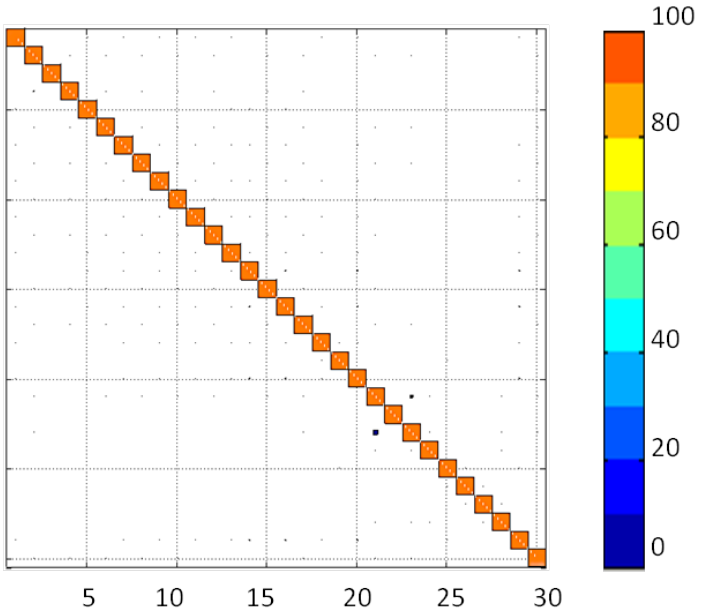


Figure 5.6 – MAC matrix of the first 30 eigenmodes between Lanczos algorithm and CMS method

For all of mode shapes, the MAC is near 100 percent, which shows the efficiency of CMS method to build these eigenmodes according the nominal data. Considering now all these intermediary data, it is possible to calculate the coalescence graph and compare the results to the reference. A focus about the frequency range [5kHz-8kHz], where two coalescence modes are detected, is proposed in Fig. 5.7.

The obtained results are very satisfying. We oberve a good correlation between the results

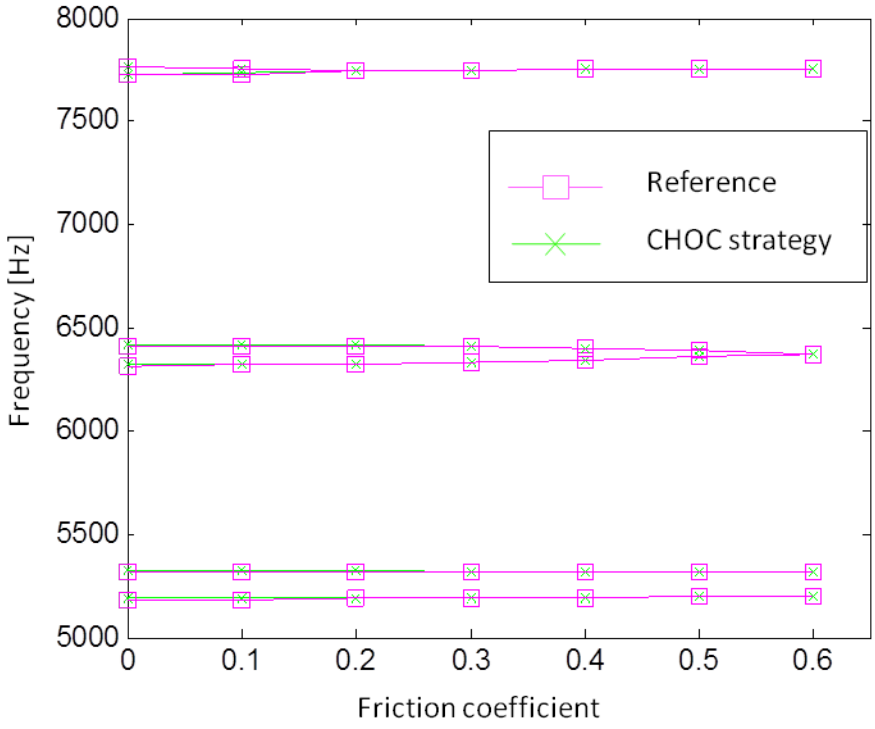


Figure 5.7 – Coalescence graph for nominal data

obtained with the CHOC strategy and Abaqus both for stable and unstable frequencies. Indeed, we detect with precision two mode coupling. The first one appears for a friction coefficient close to 0.6 and at a frequency of 6374 Hz by the two methods. This coupled mode is due to the coupling of the 14^{th} mode of the disk, calculated at 7946 Hz and corresponding to seven nodal diameter, and the 4^{th} mode (bending around X-axis) of pads at 5260Hz. The second one is observed for a friction coefficient near to 0.2 for the two methods and for a frequency of 7753 Hz with the CHOC strategy and 7757Hz with Abaqus.

Considering the same computational framework, this simulation has been performed in 180s with the proposed approach against 600s for Abaqus, representing a gain factor equal to 3. For the CHOC strategy, the main time consuming steps are dedicated to:

— the calculation of modal bases of disk and pads, 20s,
— the calculation of static modes of disk and pads, 10s,
— he calculation of contact data by FL2C method, 8s,
— the calculation of nominal eigenvectors of undamped coupled problem, 4s,
— the calculation of eigenvectors of dissipative coupled problem, 7s

Moreover, it is important to note that a large part of computational time of FL2C method

is associated to the calculation and the management of FE matrices, orthonormalization of the projection matrix and storage of data. In the future, the computational time of these different tasks could be undoubtedly reduced again.

This section has allowed to validate several steps of the proposed strategy namely the use of the FL2C method to solve the reduced contact problem and the CMS method to calculate the nominal eigenmodes of the undamped coupled eigenproblem. In the next section, we propose to evaluate the efficiency of the CHOC strategy when some parameter perturbations of the nominal problem are introduced.

4.3 Perturbed coalescence graph

The aim of this section is to take into account some perturbations of the order of 10% on model parameters and validate the reanalysis step concerning the contact projection matrix. Second, the perturbed coalescence graph calculated with the CHOC strategy and Abaqus are compared.

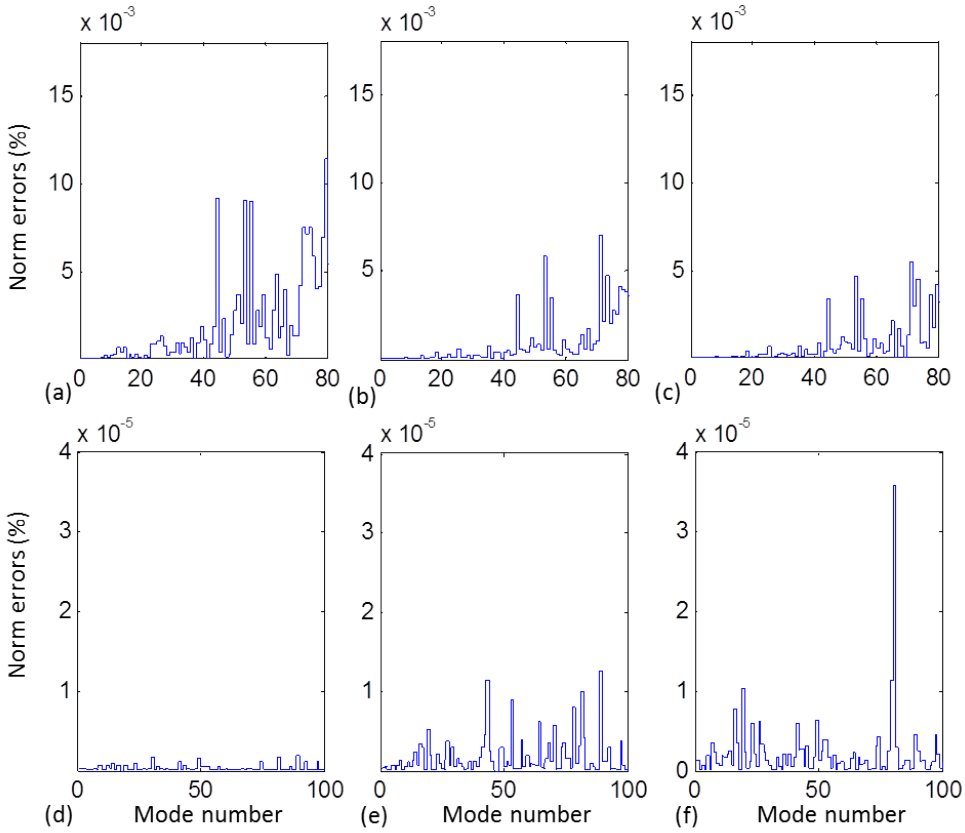


Figure 5.8 – Norm errors between reference and reanalysed eigenmodes. (a;b;c) pads (d;e;f) disc; (a;d) order 1; (b;e) order 2; (c;f) order 3.

Let us consider perturbations on the Young's moduli of different components and focus on

the following set of parameters, namely 117 GPa for the Young's modulus of disk, 187 GPa for the backplate, 6.175 GPa and 3.85 GPa for the lining with respect to X and Z-axis.

The first evaluation concerns the reanalysis of the modal basis. Fig. 5.8 presents the norm errors between reference and reanalysed modes as a function of the order of truncature (first, second or third order).

The obtained results highlight the efficiency of the HPP method even if a low order of truncature is considered. Indeed, the use of a first-order allows to have a maximum error which does not exceed respectively 1.10^{-6}% and 1.10^{-3}% for disc and pads modal bases. An increase to a superior order of truncature do not improve the approximation and can slightly deteriorate the results for the disk. This behavior has been often observed for this kind of problem [Massa et al., 2011b]. Thus, a first order will be considered for the next steps.

The same study is performed for the static modes and the results in terms of norm errors are presented in Fig. 5.9 for the three orders of truncature.

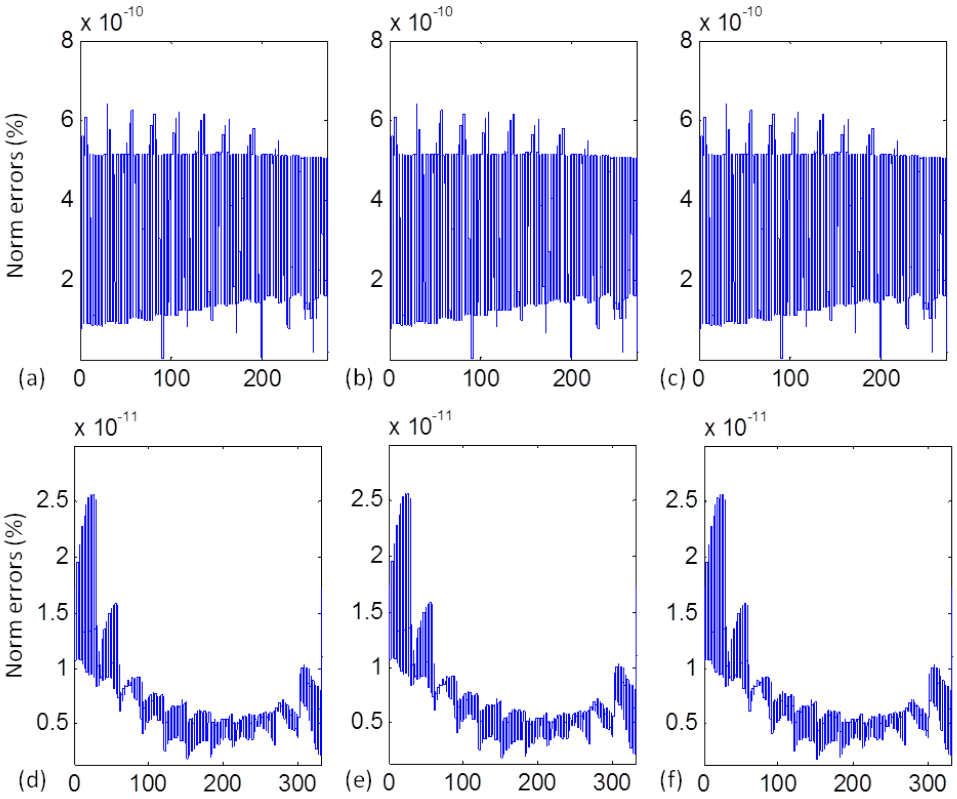


Figure 5.9 – Norm errors between reference and reanalysed static modes. (a;b;c) pads (d;e;f) disc; (a;d) order 1; (b;e) order 2; (c;f) order 3.

As previously, the obtained results are very precise even if the first order is chosen. A maximal error of 1.10^{-11}% and 1.10^{-10}% are respectively observed for the static modes of disc and pads.

Next, the reanalyzed modified eigenmodes and static modes are integrated in the contact projection matrix to build the reduced modified contact problem, which is solved with the FL2C method. The CMS method is used again to determine the modified eigenmodes of the modified coupled undamped eigenproblem. Finally, the perturbed coalescence graph is proposed Fig. 5.10.

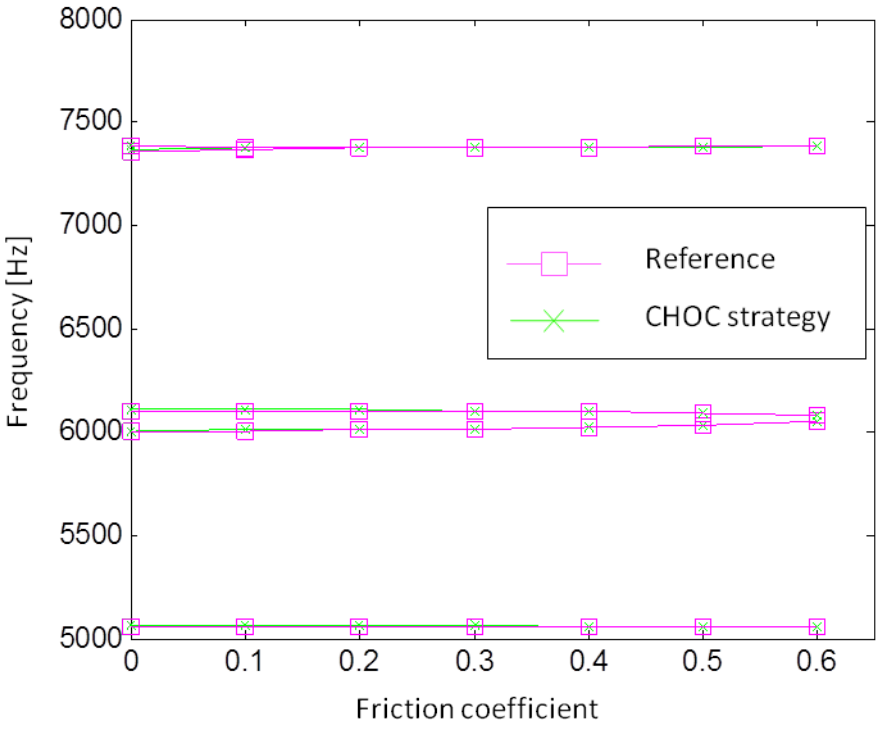


Figure 5.10 – Coalescence graph of the modified model

We observe a good agreement between the results obtained by the CHOC strategy and the reference. The first mode coupling, already detected for the nonimal configuration near to 6kHz, is not present for this set of parameter.As expected, this situation shows that a perturbation of input parameters can modify the spectrum of unstable modes. The second mode coupling around 7500 Hz is always detected but now for a friction coefficient close to 0.1. Moreover, we observe a shift of frequencies towards the nominal configuration. The gap between the reference and reanalyzed associated unstable frequency is really low, namely 2 Hz with 7374 Hz for the CHOC strategy and 7372 Hz for Abaqus. For this perturbed case, the simulation has been performed in 120s with the CHOC strategy against 10 mn for Abaqus. The reduction of computational time for the proposed method is due to the reanalysis of the projection matrix, used in the contact problem.

In this section, the CHOC strategy has been validated for a specific set of perturbation. We

have shown that a first order of truncature is sufficient to supply a good approximation of the contact projection basis. The FL2C method is enough robust to calculate with efficiency the contact data. Finally, the CMS method based on the modified data included in the contact projection matrix allows to precisely calculate the modified eigenmodes of modified undamped coupled eigenproblem. The CHOC strategy will be considered in the next section to study the effects of multiple input perturbations on complex eigensolutions.

4.4 Effects of input parameter modifications

In order to estimate the effect of input model parameters on the complex eigenvalues of the brake system, a parametric analysis is performed and a focus on the second unstable mode, detected near to 7 kHz in the previous section, is so proposed. Table 5.3 summarizes the inferior and superior bounds of variation of studied parameters, namely the Young's moduli and densities of each component and the friction coefficient. Excepted the friction coefficient, which varies between 0 and 0.6, an arbitrary variation of ±10% is considered for all others parameters.

Table 5.3 – Inferior and superior bounds of variation of input parameters

	Minimum value	Maximum value
Friction coefficient	0.0	0.6
Disc Young's modulus (GPa)	117	143
Backplate Young's modulus (GPa)	153	187
Lining (Ex) Young's modulus (GPa)	5.85	7.15
Lining (Ez) Young's modulus (GPa)	3.15	3.85
Disc density (kg/m^3)	6480	7920
Backplate density (kg/m^3)	6570	8030
Lining density (kg/m^3)	2340	2860
Disc damping (s^{-1})	18	22
Pad damping (s^{-1})	18	22

The evolution of complex eigenvalue as a function of each input parameter are evaluated with the CHOC strategy. For each material parameter, five values are considered. The friction coefficient range is divided in seven values with a nominal value classically fixed at 0.5. Fig. 5.11 traduces the extreme variation of frequencies and damping rates whereas the circle defines the

nominal configuration. All results have been adimensionalized according to the nominal value in order to compare more objectively the effects of each parameter.

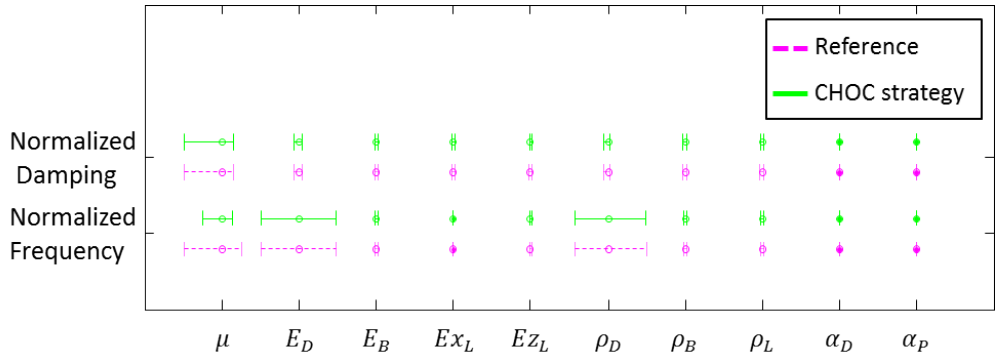


Figure 5.11 – Evolution of unstable frequency around 7500 Hz as a function of ten variable model parameters

First of all, Fig. 5.11 highlights that the results obtained with the CHOC strategy are very close to those obtained with Abaqus both for the frequency and the growth rate. Only a difference is observed for the determination of frequency range of friction coefficient. Second, considering the same level of perturbation for each material parameters, it can be seen that the disk parameters have a more significant effect on the frequency and the growth rate than parameters associated to the pad. So, it is very important to well quantify the possible variation associated to the disk component from an experimental campaign. Next, we observe, as in many references, that the friction coefficient have an significant effect both on frequency and growth rate [Nechak et al., 2015].

Concerning the computational time, all the parametric analyses have been performed in 15mn with the CHOC strategy against 1 hour for Abaqus. Thus, we have shown that, in this current context (namely a parametric analysis with ten variable parameters and a numerical model with more of 25000 dofs), the computational time can be divided by a factor four without losing precision of results. These first numerical calculations highlight the interest of the CHOC strategy in a design step where advanced calculations are performed.

5 Conclusion

This chapter has presented the CHOC numerical strategy to reanalyze a modified stability problem. After highlighting the effect of input perturbation on the different mechanical output data useful to calculate the perturbed complex eigendata, a new strategy has been proposed to revisit the global scheme of solving. Indeed, thanks to the finite element matrices for each

component in contact, the first step is to calculate the modal basis and static modes associated to the contact zone. The last ones allow to build a projection matrix to reduce the size of the contact problem. Considering then a reduced contact problem, the solving is realized by Fuzzy Logic Control (FL2C method) to define the equilibrium position of the stability problem. Next, the obtained coupling matrices allow to define the complex eigendata of the coupled dissipative problem which are calculated by a QZ solver. A second reduced problem where the projection matrix is defined through the modal basis of the undamped coupled system is also built. Another originality of the proposal is the calculation of modal basis vectors of the undamped coupled system considering the component synthesis method in which modal basis and static modes, previously calculated in the contact step, are re-exploited.

Different tests have been performed to evaluate the performance of each step of the proposed CHOC strategy. A numerical application dedicated to squeal problem shows that the proposal is a convenient strategy as soon as a parametric study is considered. This study has confirmed the observations of chapter 4 about the order of truncation of homotopy developments. Indeed, a first order development is sufficient to reanalyse with accuracy the studied data. Moreover, with the simplified model, we have highlighted that the disk parameters have a most significant effect on the frequency and the growth rate than parameters associated to the pad. So, it is very important to well quantify the possible variation associated to the disk component from an experimental campaign. Next, we have observed that the friction coefficient have a significant effect both on frequency and growth rate. Considering these developments about the reanalysis of studied solutions, we propose to integrate them in advanced methods namely a non-deterministic analysis where the variations are modelled by fuzzy sets theory.

Chapter 6

Uncertain friction induced vibration study: coupling of fuzzy logic, fuzzy sets and interval theories

Contents

1 Introduction 125

2 Uncertainty management 125

2.1 Fuzzy sets theory 125

2.2 Interval discretization 126

3 Proposed strategy for calculating fuzzy membership function 127

3.1 Uncertainty propagation by optimization 127

3.2 Integration of reanalysis techniques 129

4 Numerical Applications for friction induced vibration problem with fuzzy data 131

4.1 System description 131

4.2 Deterministic results 132

4.3 Definition of fuzzy input parameters 133

4.4 Validation of fuzzy contact loads 133

4.5 Validation of fuzzy equilibrium position 135

4.6 Validation of fuzzy complex frequencies 135

4.7 Effects of fuzzy input data on instability 136

5 Conclusion 137

1 Introduction

This last chapter is dedicated to friction induced vibrations problems with uncertainty. This topic has recently been investigated with a probabilistic modelisation, alternative to MCS. Indeed, considering a polynomial chaos approach, Nechak et al. [Nechak et al., 2011, Nechak et al., 2013] took the influence of uncertain friction coefficient into account on a dry friction system to predict stable and instable behaviours. In the same way, Sarrouy et al. [Sarrouy et al., 2013b] determined both uncertain eigenvalues and stochastic limit cycles of a self-excited non-linear system. They have also computed stochastic complex eigenvalues of a simplified brake system with uncertain friction coefficient [Sarrouy et al., 2013a]. On the contrary to the previous authors, we propose here to model the uncertainty by fuzzy numbers as Gauger et al. [Gauger et al., 2006] and investigate the uncertainty propagation step for calculating fuzzy contact data, fuzzy frequencies and fuzzy growth rates.

In this chapter, a comprehensive strategy is proposed to calculate fuzzy output data. An optimization strategy is considered to explore the design space. Moreover, our objective is to exploit the reanalysis methods, previously developed in the previous chapters, to reduce the computational time associated to this kind of approach. Thus, Section 2 describes fuzzy sets modelling and interval discretization. Section 3 is dedicated to uncertainty propagation problem, which is rewritten as an optimization problem to reduce the number of deterministic simulations in comparison to the discrete Zadeh's Extension Principle implementation. The integration of reanalysis techniques, described in chapter 5, is proposed. Section 4 highlights the main obtained results to show the potential of the proposed method. Conclusions are provided in Section 5.

2 Uncertainty management

2.1 Fuzzy sets theory

The fuzzy set theory was introduced by Zadeh [Zadeh, 1965] as an extension of the classic set theory. A membership degree, varying between 0 and 1, is associated with the different values of the non-deterministic parameters. Thus, a fuzzy number is defined using a membership function in Fig 6.1 that can take different forms according to the kind of imperfection considered. Triangular or trapezoidal membership functions are a common choice when no specific information is available about imperfections. To solve problems described by fuzzy formalism, Zadeh proposes to use the Extension Principle, which extends general operations for real numbers to the corresponding operations for fuzzy numbers. Zadeh's Extension Principle is outlined below:

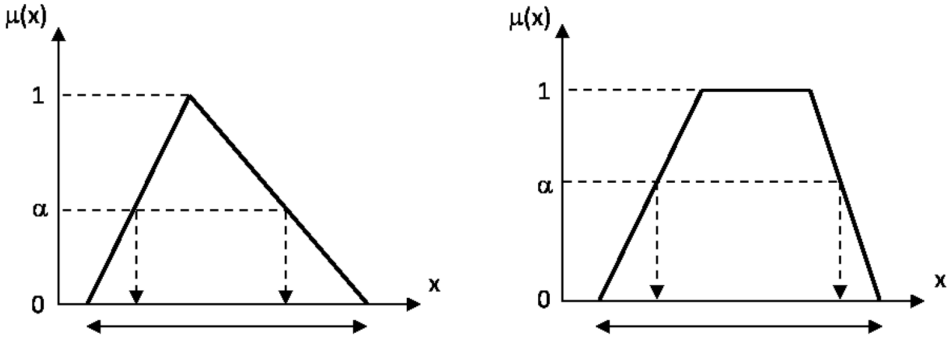


Figure 6.1 – Triangular and trapezoidal membership functions

Given a function φ that maps from $X = X_1 \times X_2 \times \ldots \times X_N$ to universe Y, such that $y = \varphi(\mathrm{x}_1, \mathrm{x}_2, \ldots, \mathrm{x}_n)$ where $y \in Y$ and $\mathrm{x}_i \in X_i, \forall i$ and considering fuzzy subsets $A_1, A_2, \ldots, A_n$ defined for reference sets $X_1, X_2, \ldots, X_n$, the Extension Principle defines a fuzzy subset B of Y using data from fuzzy subsets $A_1, A_2, \ldots, A_n$ of X. A fuzzy characterization of the membership function in Y is written as follows:

$$\begin{aligned} &\text{If} \quad \varphi^{-1}(\mathrm{y}) \neq \oslash, \mu_B(\mathrm{y}) = \sup\{\min(\mu_A(\mathrm{x}_1), \mu_A(\mathrm{x}_2), \ldots, \mu_A(\mathrm{x}_n))\}_{\{\mathrm{x} \in X, \mathrm{y} = \varphi(\mathrm{x})\}} \\ &\text{If} \quad \varphi^{-1}(\mathrm{y}) = \oslash, \mu_B(\mathrm{y}) = 0 \end{aligned} \tag{6.1}$$

2.2 Interval discretization

Zadeh's Extension Principle has already been implemented to propagate uncertainties in mechanical engineering applications and is called the Transformation Method [Moens and Hanss, 2011]. In practice, this approach initially requires a discretization of input membership functions following the level of confidence in Fig 6.2 rather than the support. This strategy defines a set of intervals $\left[\mathrm{x}_i^{\inf}; \mathrm{x}_i^{\sup}\right]^{\alpha}$ for which a level of confidence is also associated and thus transforms the fuzzy problem in Eq 6.2 into several interval problems in Eq 6.3.

$$[\tilde{\mathrm{y}}_1, \ldots, \tilde{\mathrm{y}}_m] = \mathrm{f}(\tilde{\mathrm{x}}_1, \ldots, \tilde{\mathrm{x}}_n) \tag{6.2}$$

where $\tilde{\mathrm{x}}_1, \ldots, \tilde{\mathrm{x}}_n$ and $\tilde{\mathrm{y}}_1, \ldots, \tilde{\mathrm{y}}_m$ are respectively the input and output fuzzy numbers and $\tilde{\mathrm{f}}$ the function representative of the fuzzy problem to solve.

$$\left[[\mathrm{y}_1^{\inf}; \mathrm{y}_1^{\sup}]^{\alpha}, \ldots, [\mathrm{y}_m^{\inf}; \mathrm{y}_m^{\sup}]^{\alpha}\right] = \mathrm{f}\left([\mathrm{x}_1^{\inf}; \mathrm{x}_1^{\sup}]^{\alpha}, \ldots, [\mathrm{x}_n^{\inf}; \mathrm{x}_n^{\sup}]^{\alpha}\right) \tag{6.3}$$

In this paper, this approach is considered to calculate the membership function of fuzzy frequencies and growth rates. Next, a calculation of deterministic solutions corresponding to all

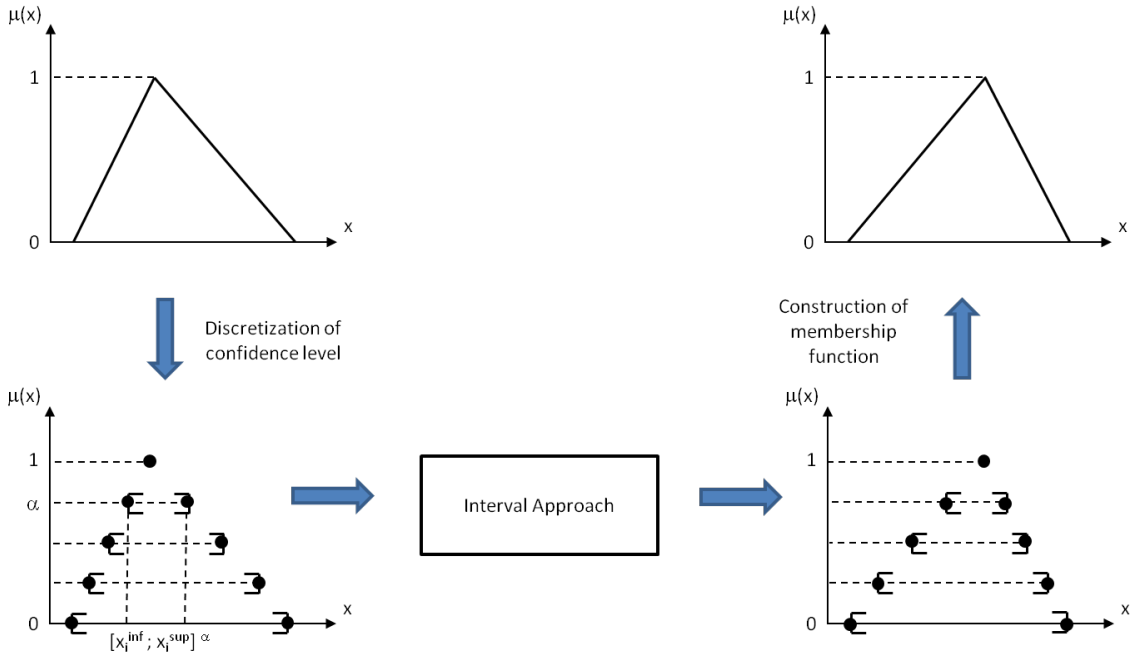


Figure 6.2 – Definition of the interval approach

combinations of fuzzy input parameter values is performed to determine all possible evolutions for output data. Finally, an evaluation of the degree of confidence for all solutions is considered to build the membership functions of output data.

Since the implementation of the Extension Principle is time consuming to propagate the uncertainty with precision in a finite element context, several methods have already been proposed in the literature and are known as the fuzzy finite element method. These are based either on specific combinatorial samplings [Moens and Hanss, 2011], on interval arithmetic [Massa et al., 2008a], on series development [Massa et al., 2004] or on optimization problems [Massa et al., 2011a]. All these methods have a common goal, which is to precisely determine all modifications of behaviours of studied solutions in a time frame compatible with a mechanical design step.

3 Proposed strategy for calculating fuzzy membership function

3.1 Uncertainty propagation by optimization

To reduce the conservatism of the output solutions, we propose to build the output intervals by considering an optimization technique rather than interval arithmetic which can seriously overes-

timate the output set [Moens and Hanss, 2011, Massa et al., 2008a] because of multi-occurrence problems. The interval problem, defined for each α-cut level, is transformed as a min-max optimization problem in Eq 6.4 for each output data y_i, defined as follows:

$$\left[y_1^{\inf}; y_1^{\sup}\right]^{\alpha} = \begin{bmatrix} \operatorname{argmin}\left(f\left(\left[x_1^{\inf}; x_1^{\sup}\right]^{\alpha}, \ldots, \left[x_n^{\inf}; x_n^{\sup}\right]^{\alpha}\right)\right); \ldots \\ \operatorname{argmin}\left(-f\left(\left[x_1^{\inf}; x_1^{\sup}\right]^{\alpha}, \ldots, \left[x_n^{\inf}; x_n^{\sup}\right]^{\alpha}\right)\right) \end{bmatrix}^{\alpha} \tag{6.4}$$

where f is the function representative of the deterministic problem to solve.

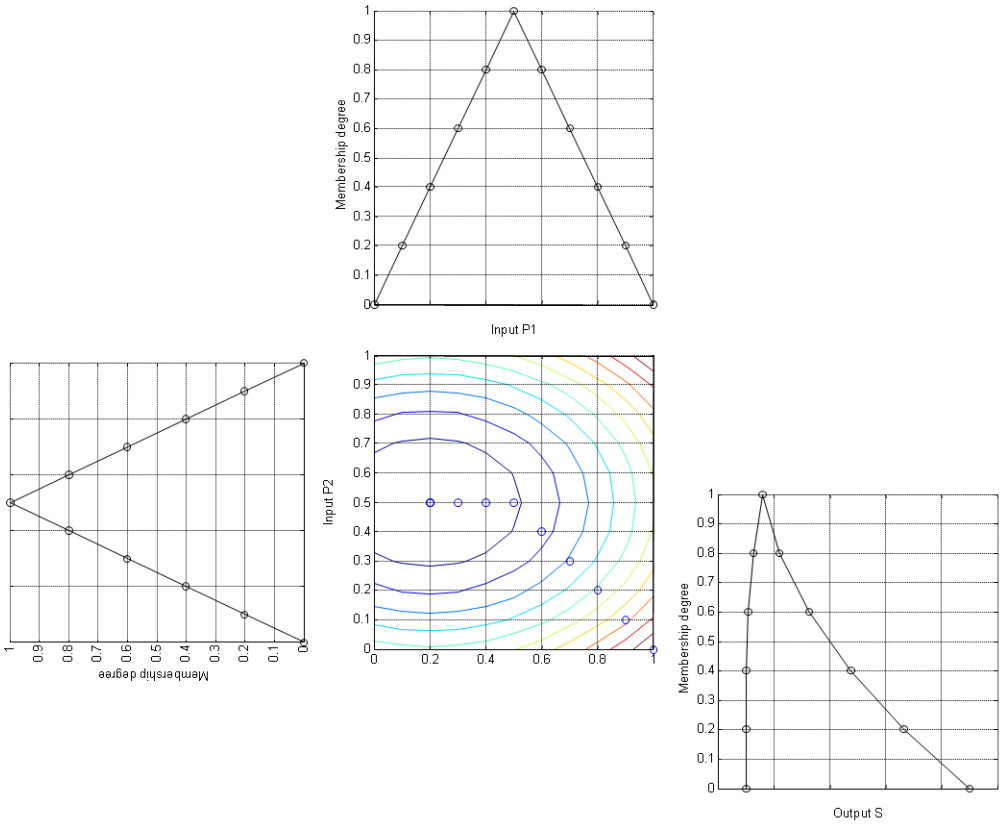


Figure 6.3 – Propagation of uncertainty for fuzzy data

The choice of optimization technique is mainly guided by the functional dependence of the solutions, the kind of studied uncertain parameters and the mathematical problem to solve (linear system for static, eigenvalue problem for modal, time or frequency dependence for dynamic analysis). For certain parameters, simple rules can be defined because the solutions' functional dependence is monotonic. For example, eigenvalues tend to increase as Young's modulus increases and decrease as density increases. However, for other parameters, the functional dependence is not always monotonic, particularly with large variations. Moreover, functional dependence can be different for each component of the solution vector.

In the present case, the functional dependence of the solutions are not always monotonic and we propose to consider a local gradient algorithm adapted to the management of the different α-cut levels in Fig 6.3.

Firstly, for each α-cut level, a search of parameter combinations leading to extreme solutions is performed. The sensitivity of the output data is evaluated between each level to determine how the response function is evolving. The output quantities and their first sensitivities for each fuzzy parameter are determined for the crisp values ($\alpha = 1$). The signs of the first-order sensitivities indicate the functional dependence of the response function and define the combinations of discrete fuzzy parameter values, which could supply the minimum and maximum variations for the following α-cut level. The signs of the derivatives are compared with those obtained at the previous α-cut level. If the sensitivities have the same signs, the response function is considered to be locally monotonic, and the determined combinations provide the minimum and maximum variations of the modal quantities for the current α-cut level. If the sensitivities have different signs, the response function cannot be considered monotonic, giving rise to an extremum between these two α-cut levels. The combination nearest the extremum is chosen and the search is stopped for this variation. Finally, the fuzzy output data are then built α-cut by α-cut.

To reduce the computational time associated with uncertainty propagation, we propose now to substitute the classical solver for stability problem (which can be solved several times in the optimization scheme) with a reanalysis technique. The proposed strategy is described in the next section.

3.2 Integration of reanalysis techniques

The aim of this section is to summarize the main steps and equations used in the proposed strategy to propagate uncertainty into output data (fuzzy frequencies and growth rates in the present case). To facilitate the comprehension, a flowchart is proposed in Fig 6.4. The membership function of output data is built α-cut level by α-cut level.

For the crisp values ($\alpha = 1$), the modal bases of each component in contact and the stability data are calculated in a classical way thanks to Eq.5.13 & Eq.5.15.

Next, for the following α-cut level ($\alpha \in [0, 1]$), an optimization problem, described by Eq 6.4, is solved to detect the minimal and maximal evolutions (of the output data). During the iterative scheme based on gradients analysis, each calculation is reanalysed according to projection techniques to reduce the computational time. The reanalysis of frequencies and growth rates rely on:

- The definition of perturbed mass, damping and stiffness matrices,

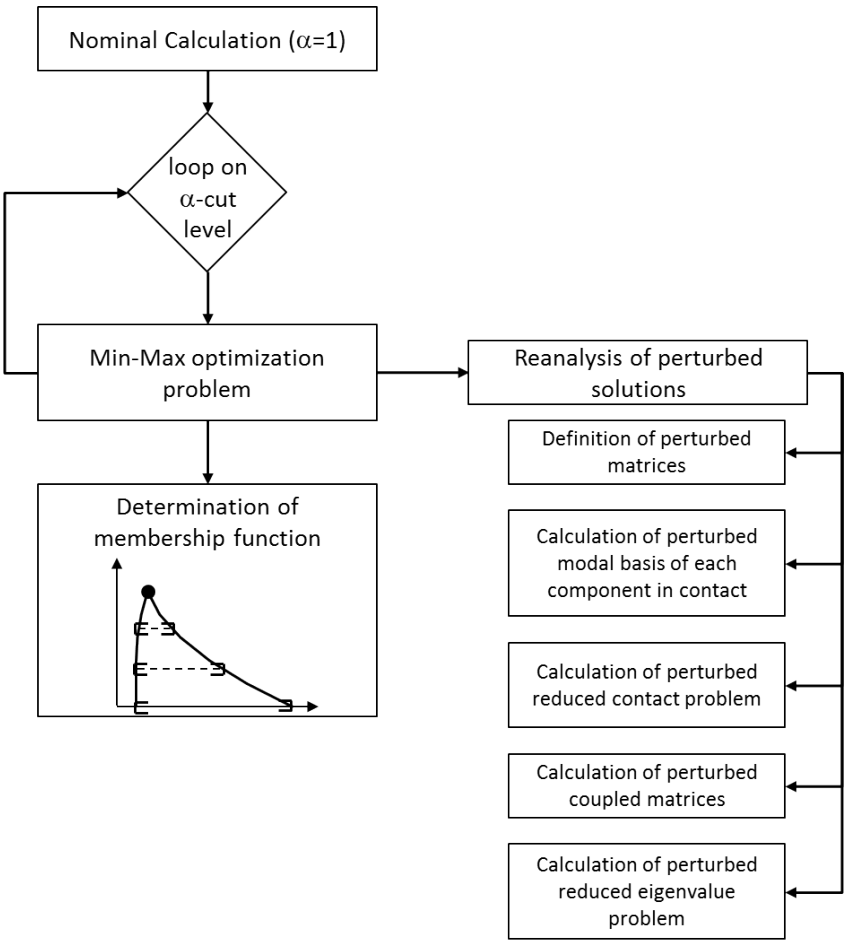


Figure 6.4 – Flowchart of the proposed uncertainty propagation strategy

- The calculation of perturbed modal basis of each component in contact,
- The calculation of perturbed reduced contact problem,
- The calculation of perturbed coupled matrices,
- The calculation of perturbed reduced complex eigenvalue problem.

In the next section, this proposed strategy is used to study the effects of fuzzy input data on the frequencies and growth rates of a friction induced vibration system.

To control the computational time due to multiple samplings during optimization, we propose to review the global strategy used to solve a stability problem. Traditionally, the stability problem, described in section 5.2, relies on two calculations, namely a nonlinear static analysis and a complex modal analysis. In this section, we propose two alternative methods:

- Reanalysis of a perturbed static problem using a Fuzzy Logic control approach that allows a reduced contact problem to be defined (see chapters 2 and 3),
- Reanalysis of a perturbed eigenvalue problem by considering homotopy perturbation and

projection techniques (see chapters 4 and 5).

4 Numerical Applications for friction induced vibration problem with fuzzy data

4.1 System description

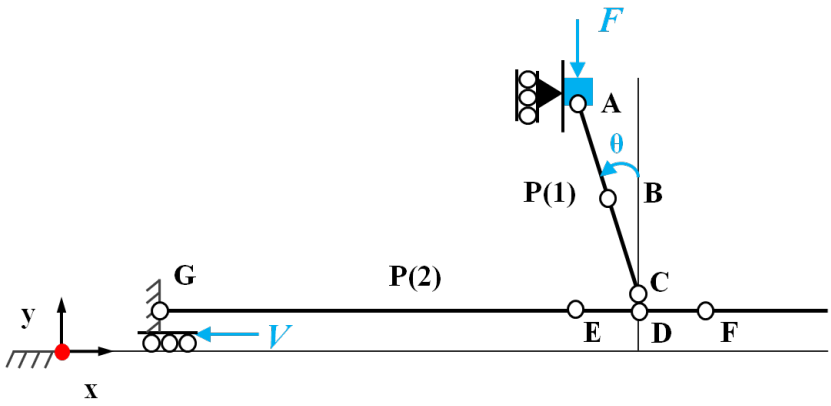


Figure 6.5 – Description of the beam-on-beam system

Table 6.1 – Beam properties

	P(1)	P(2)
Length [m]	0.05	0.15
Width [m]	0.01	0.015
Thickness [m]	0.0015	0.003
Density [kg/m^3]	7900	7900
Young modulus [GPa]	185	185
Number of elements	300	900

A beam-on-beam system in Fig 6.5, which can be qualified as phenomenological, is considered here. This model [Meziane et al., 2010] successively generates sticking and sliding conditions and examines the appearance of instabilities by considering a coupling mode mechanism as encountered in squeal simulations. Contact incidence angle θ and contact distance $d = [GD]$ are respectively imposed as 5°and $0.08m$ to induce instability. Beam P(1) is fixed at point A in

translation in the x-direction and in rotation in the z-direction. A concentrated mass of 3 kg is added at point A. In the first step, a load of $F = 9N$ is applied in the y-direction at point A to push beam P(1) into contact with beam P(2) at node D. Then, in the second step, velocity $V = 0.002m/s$ in the x-direction is imposed at point G of beam P(2). Beam properties are shown in Table 6.1. For deterministic simulation, the friction coefficient is fixed as 0.4.

4.2 Deterministic results

Fig 6.6 presents the evolution of growth rates as a function of frequencies. Three instabilities are detected at 406Hz, 2811Hz and 7774Hz and the associated growth rates are respectively equal to 0.36, 0.19 and 0.09.

Although frequency stability computations supply important information about the behaviour of a nonlinear system, the validity range is unknown and clearly depends on the stationary state. The static equilibrium position is directly related to the description of the contact surface [Heussaff et al., 2012] and to the definition of mechanical input parameters used in the nominal model. The next section discusses the uncertainty propagation of input parameters and the contribution of uncertainty to improve the predictivity of frequency simulations.

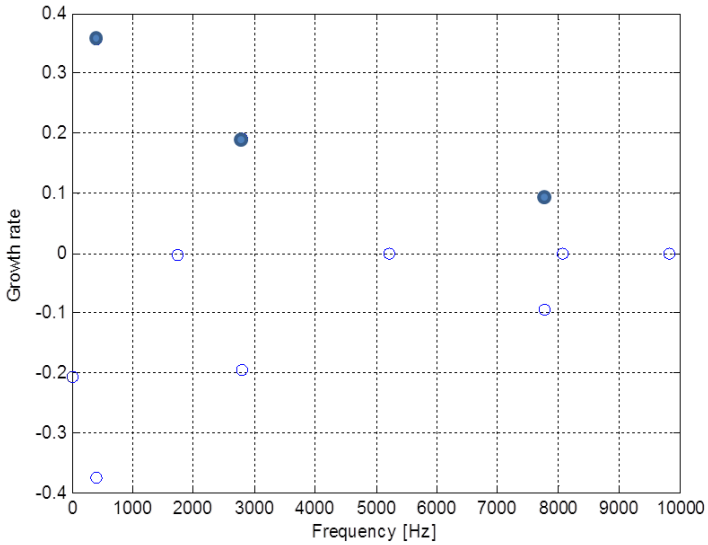


Figure 6.6 – Frequency and growth rate of the studied system

4.3 Definition of fuzzy input parameters

In this study, the section of each beam described by the width (noted B) and thickness (noted H) parameters, the Young's modules (noted E) and the friction coefficient (noted μ) are considered fuzzy. The seven fuzzy parameters are described in Fig 6.7. Variations of $\pm 20\%$, $\pm 10\%$ and $\pm 25\%$ are respectively imposed for geometric data B and H, material data E and the friction coefficient. For the Fuzzy Logic Controllers, the crisp values of gap parameters are respectively established as $-1\mu m$ for NL, $-1nm$ for NS, $0m$ for N, $1nm$ for PS and $1\mu m$ for PL. The crisp values of normal load coefficient γ are defined as 0 for NZ, 0.3 for S, 0.5 for M, 0.79 for L and 1 for NO, whereas those of the β coefficients for tangent contribution are 0 for NZ, 0.3 for S, 0.5 for M, 0.9 for L and 1 for NO.

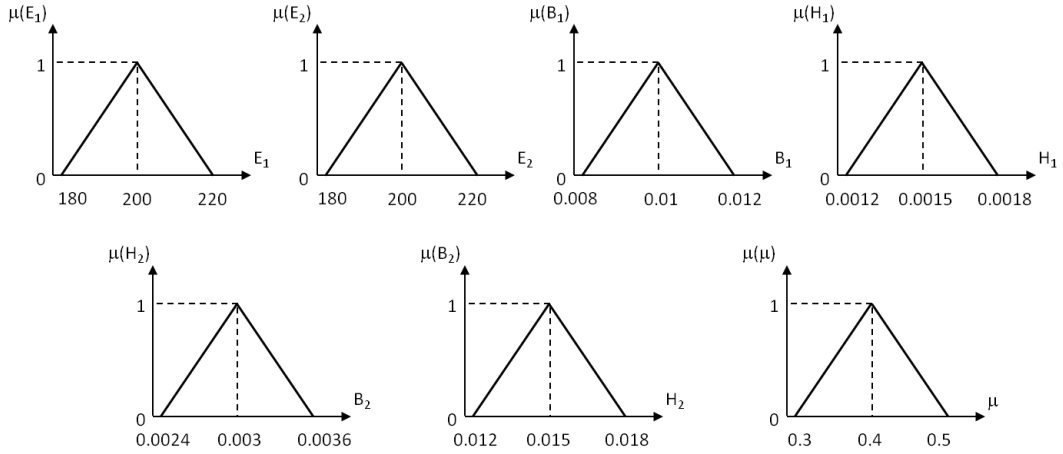


Figure 6.7 – Definition of fuzzy input parameters

The next three first subsections are respectively dedicated to the calculation and validation of fuzzy contact loads, fuzzy equilibrium position and fuzzy complex frequencies. A comparison of results, respectively determined with the proposed strategy and an implementation of the Extension Principle, is presented. The last subsection shows how the fuzzy data can be used to detect the most severe instabilities.

4.4 Validation of fuzzy contact loads

At the beginning of the simulation, node C is in contact with node D. Figs 6.8 & 6.9 present the membership functions of the normal and tangential contact loads and dynamical friction coefficient, respectively calculated after the two static steps. The fuzzy contact loads, calculated using the two methods, were almost the same for each static step. The maximal observed error is inferior to 0.01%. For all calculations, the maximum gap for the slave node was in the order

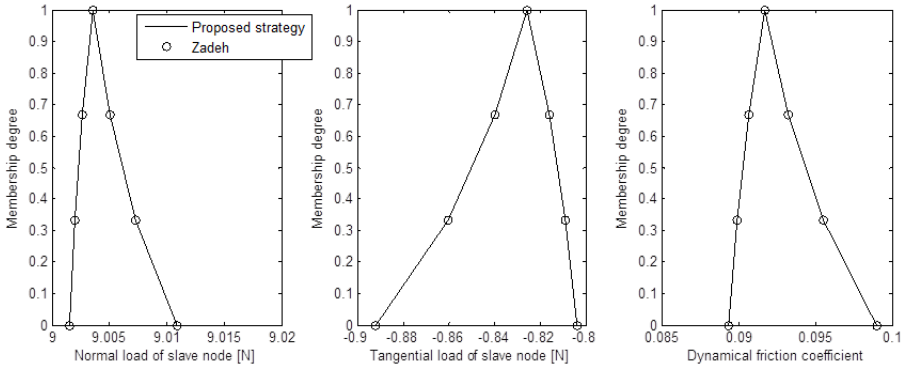


Figure 6.8 – Membership functions of normal and tangential contact loads and dynamical friction coefficient after the first step

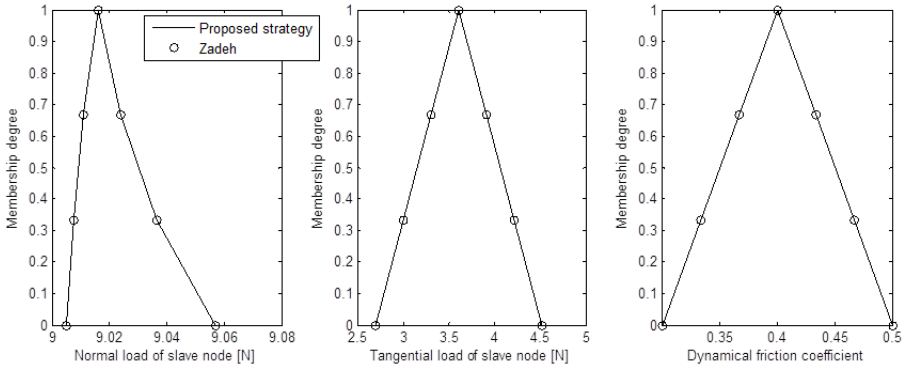


Figure 6.9 – Membership functions of normal and tangential contact loads and dynamical friction coefficient after the second step

of $1.10^{-8}m$, which guarantees good convergence of the proposed algorithm based on Fuzzy Logic Controllers. The fuzzy dynamical friction coefficient, calculated as the ratio between the tangential load and normal load at the slave node, is the same for both methods and indicates that the contact state has sticking status for the first static step and sliding status for the second static step. For the two steps, the input uncertainties have a very low effect on the output response in terms of normal load (range of variation inferior to 1%). For the tangential load, we observe a more extensive range of the variation equal to 10% for the first static step and nearly 100% for the second static step.

Finally, the minimal errors, inferior to 0.01%, between the proposed strategy and the implementation of Zadeh's Extension Principle justify the use of projection matrices composed of reanalyzed perturbed modal bases.

4.5 Validation of fuzzy equilibrium position

This section focuses on the equilibrium position of the slave node calculated after the second step. This is a key element for the calculation of stability analysis. Fig 6.10 presents the membership functions of the x-axis and y-axis positions of node C. The results obtained by the FL2C method are compatible with those obtained by Zadeh's Extension Principle. The maximal gap, observed for the calculation of x-axis and y-axis positions, is inferior to $1.10^{-5}m$.

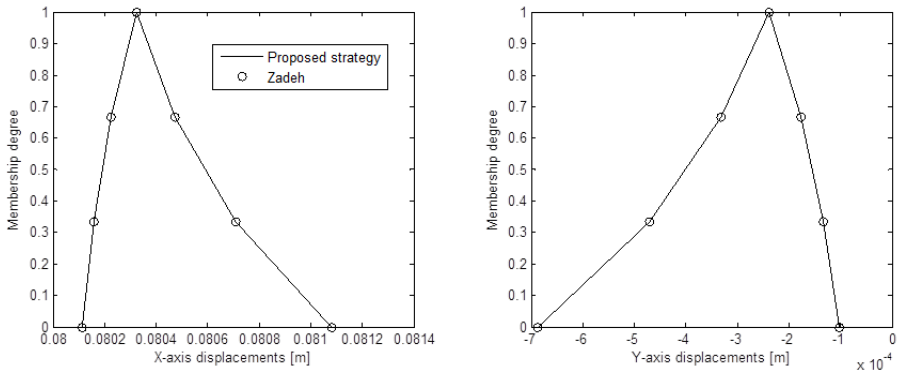


Figure 6.10 – Membership functions of x-axis and y-axis positions of node C for the second step

The input uncertainties globally have no effect on the x-axis position of Node C as previously seen for the normal load whereas the range of variation for the y-axis position is more significant as shown in Fig 6.10. Now, it is important to quantify the effects of these uncertainties, detected for the sliding equilibrium positions, on the complex frequencies.

4.6 Validation of fuzzy complex frequencies

This section is dedicated to the calculation of fuzzy complex frequencies. Considering the previously calculated equilibrium positions, we study the effects of input uncertainty on unstable frequencies and the growth rate coefficient. The membership functions of the latter group are respectively proposed in Figs 6.11 & 6.12. Only the data associated with unstable modes are presented here. The results obtained by the FL2C method are always compatible with those obtained by Zadeh's Extension Principle. The maximal detected error is inferior to 0.1% for all the frequencies. In terms of computational time, the proposed strategy is very efficient too. The uncertainty propagation by optimization drastically reduces the numbers of deterministic calculations. For this example, considering only three levels of α-cuts, Zadeh's Extension Principle requires 7^7 calculations (nearly one million calculations). For the proposed strategy, the membership functions can be built with fewer than 500 calculations. Moreover, the integration

of reanalyses in the control approach globally decreases computational time by a factor of five for each deterministic evaluation of the stability problem.

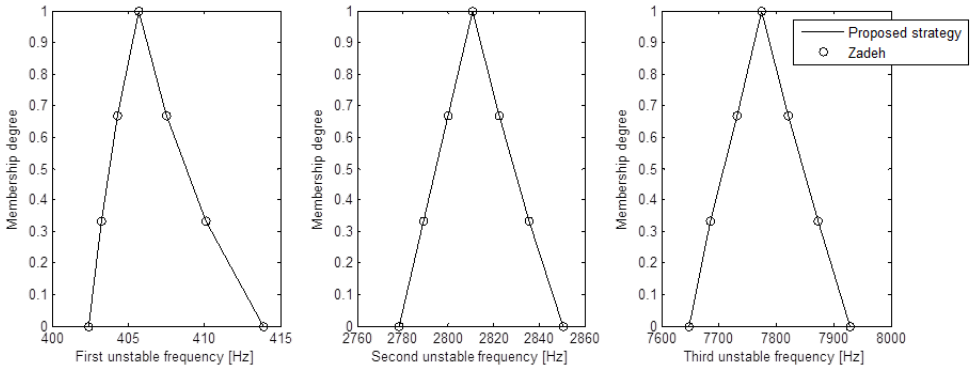


Figure 6.11 – Membership functions of unstable frequencies

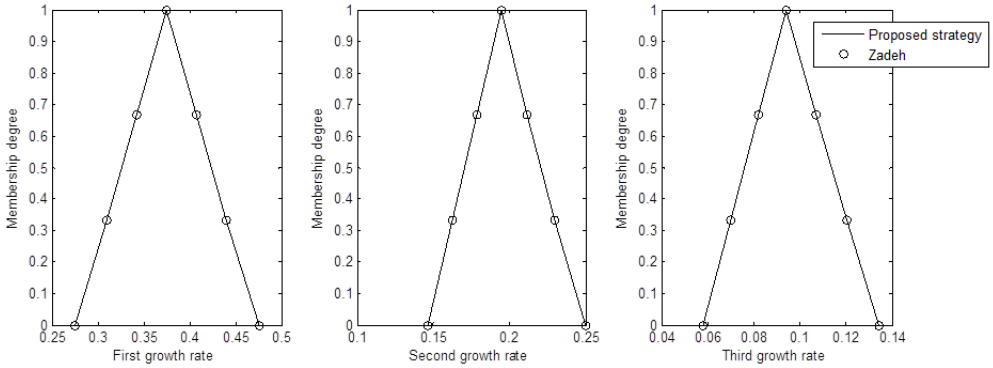


Figure 6.12 – Membership functions of the growth rate coefficient

4.7 Effects of fuzzy input data on instability

In a context of a probabilistic description of uncertainty, Tison et al [Tison et al., 2014] propose a methodology to improve the lack of predictivity of the complex eigenvalue analysis for squeal detection. The methodology is based on robustness and occurrence concepts. It is shown than an unstable mode which presents a large occurrence of appearance and a weak sensitivity to the variability of input parameters is the best candidate for dynamic instability. The underlying idea is that the robustness (i.e stable values) of an unstable mode increases the degree of confidence that the dynamic instability will appear in a real situation.

When statistics on uncertain parameters cannot be available, for example friction coefficient, this strategy can be applied considering fuzzy description and only robustness. This is the subject

of the analysis presented in this subsection.

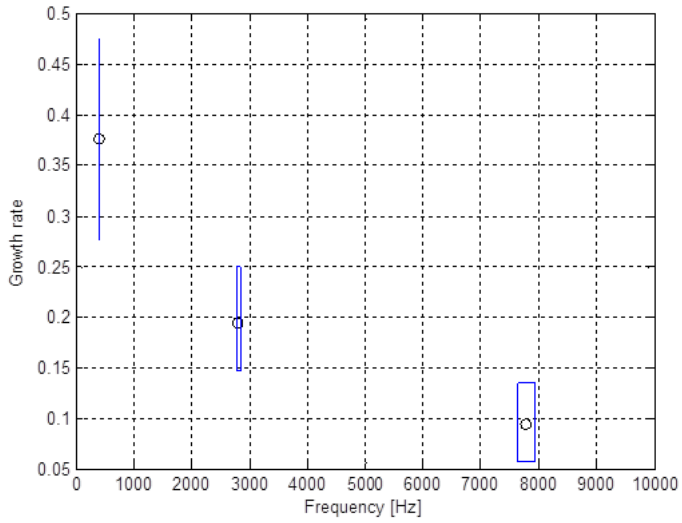


Figure 6.13 – Membership function support of frequency and growth rate

From the results obtained on the 2 beams rubbing system presented above, one can notice that uncertainty introduced in the model mainly affects the third unstable frequency for which the range of variation of the support is of 1768Hz, whereas the ranges of variation are 72Hz and 451Hz for the first two frequencies. The three coalescences are observed for different growth rate coefficient intervals, namely namely $[0.27; 0.48]$, $[0.15; 0.24]$ and $[0.05; 0.14]$. Fig 6.13 summarizes these evolutions by considering the supports of the fuzzy frequencies and growth rates. The higher growth rate coefficient values are observed for the first unstable frequency, whereas the second presents the smaller growth rate coefficient range of variation.

From Fig 6.13 it can be seen that the second unstable mode verifies the robustness assumption, namely a small range of variation of frequency and growth rate. These numerical results match with experimental ones presented by Meziane et al. (see particularly figure, indexed 7b, in reference [Meziane et al., 2010] where the second frequency around 2700 Hz is the most severely unstable frequency.

5 Conclusion

This chapter presents a complete strategy to calculate fuzzy frequencies and fuzzy growth rates for a friction-induced vibration problem. First, the number of simulations to propagate uncertainty has been controlled by exploiting the results of functional dependence analysis and

rewriting the uncertainty propagation problem as an optimization problem. Second, the computational cost of each deterministic evaluation has been maintained by using alternative reanalysis methods. A control-based approach including fuzzy logic controllers is proposed here to determine the perturbed equilibrium position whereas a homotopy perturbation method coupled with projection is considered to calculate frequencies and modal bases.

The academic numerical application has first highlighted the efficiency of the proposal to build the membership function of the studied solutions such as fuzzy contact data, fuzzy frequencies and fuzzy growth rates. Second, the effects of fuzzy input variations on instabilities have been highlighted. Next, a robustness analysis, based on supports of membership functions, is then used to identify the unstable modes which present the maximal confidence of appearance.

Nevertheless, to improve these developments and quantify a level of predictivity of this approach, it will be necessary to investigate now more realistic brake squeal numerical model, as presented in chapter 5. This last remark will be taken up in the perspective section.

Conclusion and perspectives

This report, entitled "Reduced model and uncertainty propagation for frictional contact and friction induced vibrations problems", focused on the study of frictional contact and stability problems in a context of multiple samplings, that is to say when the numerical simulations are performed several times for different values of input parameters. In design step, direct applications are DOE, sensitivity analyses, optimization problems or non-deterministic analyses. Nowadays, these advanced methods are primordial to define reliable and robust designs but are still time consuming although the development of computational resources is obvious. Thus, to generalize the use of these advanced methods, it is necessary to investigate alternative numerical methods, which directly take into account in their formulation some perturbations or uncertainties on input model parameters, as a function of the studied problem. The aim is to calculate the modified or uncertain mechanical solutions with reduced computational time without losing precision.

These last years, several efficient methods have been proposed for linear applications (static, modal, buckling, thermal) both to approximate perturbed solutions and to propagate uncertainty. In the present case, the main scientific lock is due to the dependence of output mechanical solutions to the contact non-linearity, which already represents a major challenge in the deterministic case. Indeed, although this phenomenon has been studied for many years, the non-differentiability of contact laws, the integration of regularization techniques, the discretization of the contact interface and the iterative solving scheme are the main drawbacks to the development of universal algorithms.

In this work, we have first proposed to investigate a new way, based on the integration of automation controllers, to calculate the frictional contact data and to define reduced modified contact problems as a function of the introduced perturbations. An associated modified projection matrix is built considering global and interface local data of each structure in contact. A focus on the reanalysis of the modified reduced contact problem and modified projection matrix is proposed by integrating homotopy developments. Second, these works have been extended to the case of the modified stability analysis for friction induced vibrations problems, where the modified equilibrium position is obtained according to the results of a modified static sliding

contact problem. A reanalysis of modified complex eigensolutions have been investigated too. Finally, the proposed strategy to reanalyse modified complex eigensolutions have been integrated in uncertainty propagation scheme considering fuzzy formalism.

In summary, the main developments, detailed in this report, are associated to:

- The integration of control approach in frictional contact problem
- The reanalysis of modified reduced static frictional contact problem
- The reanalysis of modified stability problem
- The uncertainty propagation for fuzzy friction-induced vibrations problems

The main theoretical and numerical results as well as identified perspectives are summarized in the next subsections.

Control approach in frictional contact problem

The integration of control approach for solving contact problem has been exposed for the frictionless case in the chapter 2 and the frictional case in the chapter 3. The assessment of these studies shows that a Fuzzy Logic Controller must be integrated for each gap (normal and sticking case) to be reduced in order to make a link between the observed gaps and the associated contact loads. The design of the controllers has been proposed and the rules bases have been defined by considering the human expertise of the mechanical problem. So, at each iteration of the proposed iterative scheme, an increment of contact loads is calculated by the controllers to control the contact gaps and regulate the contact loads. Next, the controllers have been integrated inside a contact loop, where the determination of contact pairs and contact states (no contact, sticking, sliding) is performed. Considering this approach, the non linear problem is decomposed into a set of linear problems, where the contact loads are considered as external loads. Moreover, we have shown that it is possible to reduce the size of each linear problem by considering a projection matrix. In the present case, the eigenmodes or static modes (locally defined at the contact interface) of each structure in contact are considered. This numerical method has been successfully performed to several test cases (described in chapters 2 to 6). We have highlighted that the reduction of computational time is possible without losing precision.

Nevertheless, to estimate the real capability of the proposed new way to manage contact problems, more developments will be necessary. First, it will be interesting to test other numerical models with more and more degrees of freedom to evaluate the efficiency of reduction technique and more contact pairs to validate the strategy of contact management. Recently, Kudawoo [Kudawoo, 2013] has shown that it is possible to simultaneously manage contact parameters

(contact pairs, geometric description, status) in a single contact loop for continuous contact algorithm. In our proposal, the organization of the different steps in the contact loop is not fixed and must clearly be investigated again. A first analysis about the integration of controllers (in series or in parallel) has already been performed in chapter 3. Moreover, we have highlighted in chapter 2 that although the convergence of the controller is not always fast, the associated computational time is reduced. An optimization of the fuzzy laws could be first performed to reduce the number of iterations as proposed by Bingul et al [Bingul and Karahan, 2011]. Indeed, a global optimization can be performed to improve the choice of transition value of fuzzy laws for each controller. Second, as the efficiency of the FLC approach is clearly dependent to the human expertise during the step of definition of the rule basis, it will be interesting to investigate the other automation control approaches, which rely on strong mathematical base, such as static feedback control, as proposed by Gonzales et al [Gonzalez et al., 2014]. A comparison of these two kinds of controllers could be interesting. Considering the current results for static contact problem, an integration of the control approach in an implicit transient dynamic scheme could be performed in a short time.

Finally, these works have highlighted the interest of studying a contact problem considering a new way based on automation control approaches and define the basis of future multidisciplinary works.

Reanalysis of modified reduced static frictional contact problem

This work is dedicated to the reanalysis of modified static frictional contact problem. The term "modified" makes here reference to the evolution of values of input model parameters, which evolve from nominal values to a modified values due to perturbations. Each perturbation necessarily implies a modification of the finite element matrices and a new solving of mathematical equations which govern the mechanical problem. As soon as multiple perturbations must be studied, the associated computational time can be very important due to the calculation of systems of linear equations. In the case of frictional contact problem, each perturbation gives rise to a modification of the projection matrix, used to reduce the size of the contact problem and so the definition of modified static modes. To reduce the computational time, we have proposed to integrate a reanalysis technique for calculating the modified static modes and so the modified projection matrix. The reanalysis technique relies on the decomposition of modified finite element matrices in a nominal and perturbed part and a homotopy development of each studied mechanical solution.

The identification of high order perturbed solutions for each modified systems of linear equations allows to calculate the modified data with a reduced computational cost. Different investigations have shown that a good approximation of modified data can be successfully performed with only a first order of truncation of development series.

The numerical method has been tested for several test cases (described in chapters 4 to 6) with an interesting compromise between precision and computational time. However, it will be interesting to investigate again the choice of the reanalysis technique. Currently, the calculation of the high order perturbed solutions must be evaluated for each different perturbation, which is the most time consuming step. The definition of an unique projection matrix for each modified problem could be an efficient way. A recent work, developed by Giacoma et al [Giacoma et al., 2015], has considered the same idea by coupling PGD method to take into account perturbations in contact problem and LATIN method to manage the non-linearity. Another solution will be to build the high order perturbed solutions with derivatives data as in Massa et al [Massa et al., 2011b]. Finally, as already mentioned in the previous section, the proposed reanalysis method can certainly be extended for contact problems in the dynamic case by considering the same theoretical framework.

Reanalysis of modified stability problem

After studying the modified static frictional contact problem, we have proposed to investigate the modified stability problem in the case of friction-induced vibration. Indeed, the stability problem relies first on a static contact problem to calculate the equilibrium position with a sliding state of contact nodes and second on a complex eigenvalue problem of the dissipative coupled problem to calculate the unstable frequencies and damping rate. In the present case, a new complexity has been observed because a modification introduced on input model parameters implies some perturbations at different levels of the calculation. These perturbations affect both the finite element matrices, the equilibrium position, coupling contact matrices and the complex eigensolutions problem. A small perturbation on input data can generate a large perturbation on output data. Thus, the modified equilibrium position is determined with FL2C method described is chapter 3 that's allows to build the modified coupling contact matrices with a reduced computational time. Next, a Component Modal Synthesis method has been introduced to solve the modified complex eigenvalue problem. Indeed, the objective is here to avoid the calculation of a modified eigenvalue problem for each perturbation. This step is not time consuming because all ingredients (modal bases for each component in contact and modified attachment modes) necessary to perform the CMS method are already calculated during the reanalysis of modified static

contact problem. Indeed, the modified attachment modes are calculated as a linear combination of the modified static modes. Finally, the modified complex eigensolutions are determined using a QZ classical algorithm. This solution strategy has been successfully applied to several test cases (described in chapters 5 and 6).

However, the calculation of the modified complex eigensolutions has been partially covered in this work and some improvements could be realised. Indeed, these quantities are calculated considering a projection space only defined with the modified eigenmodes of the modified undamped coupled eigenvalue problem. To improve this prediction, it will be interesting to couple for example the proposed reanalysis technique and the residue iteration scheme [Bobillot and Balmès, 2002] or to define a direct reanalysis of complex eigensolutions with homotopy techniques as proposed by Massa et al [Massa et al., 2015a]. In a short time, these works could be applied for a more realistic model of a brake system to perform a numerical and experimental correlation as recently proposed by Renault et al [Renault et al., 2014]. Moreover, some additional developments concerning reanalysis techniques will be necessary to take into account some topological perturbations as identified on pad surface in Tison et al [Tison et al., 2014].

Uncertainty propagation for fuzzy friction-induced vibrations problems

The last topic discussed on this report concerns the propagation of uncertainty for frictional static and friction-induced vibrations problems. In the present case, the fuzzy sets theory is considered to model the variability and each variable parameter is defined by a membership function. To propagate the uncertainty while reducing the conservatism of the output solutions, we have proposed to decompose each input membership function in a set of intervals and calculate the extreme evolution of each interval by performing a min-max optimization problem. The choice of optimization technique has been guided by the functional dependence of the studied solutions, which are not highly non-linear in the present case although the problem to be solved is non-linear. Thus, a local gradient algorithm adapted to the management of the different α-cut levels has been considered rather than a global algorithm, such as DOE or metaheuristic, where more calculations would be necessary. Moreover, to control the computational time, each evaluation of the mechanical output solutions is performed by the reanalysis technique, previously presented. The numerical method has been tested on an academic model, which can be qualified as phenomenological, because it represents friction induced vibration problematics detailed in chapter 6. We have first shown that it is possible to propagate uncertainty with precision and for

reduced calculation time. Second, we have discussed on the appropriateness between the support of fuzzy eigensolutions and the confidence of appearance of the unstable mode.

This last study, which is based on a robustness analysis, must be detailed on future analyses and compare to results based on the occurrence of appearance, as performed by Tison et al [Tison et al., 2014]. The development of a robustness criterion could be an interesting indicator for the track of unstable modes in optimization during the design step. However, the current results can be introduced in a short time in robust fuzzy optimization as proposed by Massa et al [Massa et al., 2011a]. Another work will be to model the uncertainty by a probabilistic way as proposed by Nechak et al [Nechak et al., 2013] and quantify the possibility of integration of proposed reanalysis in a stochastic formalism. Finally, a comparison of non-deterministic numerical data (fuzzy, interval or probabilistic) with experimental results is essential to quantify how the uncertain data can improve the predictivity of simulations. A discussion about the positioning of transient simulations towards non-deterministic simulations will deserve to be performed.

In conclusion of this report, the current works have highlighted the interest of investigating new ways based on multidisciplinary cooperation with automation, computer science and mathematics domains. As already said in the conclusion of different topics, the next challenge is to apply the different proposals on industrial numerical models and integrate them in optimization strategy to produce innovative designs. Nevertheless, this work is not an easy task considering the size of finite element models (generally superior to 1 million of degrees of freedom) and the size of data to manage and store.

Appendix A

Mac-Neal Component Modal Synthesis method

The MacNeal method is a hybrid Component Modal Synthesis method which uses a combination of free vibration modes and residual flexibility [MacNeal, 1971].

Considering a structure decomposed in two substructures, respectively defined by the spectral matrices Λ_a and Λ_b and the modal bases Φ_a and Φ_b. Let us define Λ and Φ two block matrices containing respectively the spectral matrices and modal bases of each substructure and $\mathbf{P}$ a localization matrix relative to the couplings between the two structures, the CMS method allows to calculate the i^{th} eigenvector $\tilde{\Phi}_i$ of the complete structure as follows:.

$$\tilde{\Phi}_i = \Phi\varphi^{(i)} - \mathbf{Q}\mathbf{F_L} \quad \text{where} \quad i = 1 \dots n_{mod} \tag{A.1}$$

with $\mathbf{Q}$ the residual flexibility matrix and $\mathbf{F_L}$ the linking forces.

The matrix φ is calculated through an eigenvalue problem (Eq. A.2) integrating the contribution of spectral matrices and modal bases of each substructure, the coupling matrix and some residues:

$$\begin{bmatrix} \Lambda_a & 0 & (\mathbf{P}\Phi_a)^T \\ 0 & \Lambda_b & (\mathbf{P}\Phi_b)^T \\ \mathbf{P}\Phi_a & \mathbf{P}\Phi_b & -\mathbf{G}_{La} - \mathbf{G}_{Lb} - 2\mathbf{K}_L^{-1} \end{bmatrix} \begin{pmatrix} \varphi_a \\ \varphi_b \\ \mathbf{F}_L \end{pmatrix} = \begin{bmatrix} \mathbf{I}_a & 0 & 0 \\ 0 & \mathbf{I}_b & 0 \\ 0 & 0 & 0 \end{bmatrix} \begin{pmatrix} \varphi_a \\ \varphi_b \\ \mathbf{F}_L \end{pmatrix} \alpha \tag{A.2}$$

where $\mathbf{G}_{La}$ and $\mathbf{G}_{Lb}$ are the residual flexibility matrices restrained to the interface degrees of freedom and $\mathbf{K}_L$ is the connection stiffness matrix, α are the eigenvalues of coupled system.

Data are expressed as follows:

$$\varphi = \begin{bmatrix} \varphi_a & \varphi_b \end{bmatrix}^T \quad \text{and} \quad \Phi = \begin{bmatrix} \Phi_a & 0 \\ 0 & \Phi_b \end{bmatrix} \tag{A.3}$$

The residual flexibility matrices, noted $\mathbf{G}_{La}$ or $\mathbf{G}_{Lb}$ as a function of the studied substructure, are determined as follows:

$$\mathbf{G_L} = \mathbf{P}\left(\mathbf{\Gamma} - \mathbf{Q}\right) \tag{A.4}$$

$$\mathbf{Q} = \Phi \Lambda^{-1} \Phi^T \mathbf{P}^T \tag{A.5}$$

where $\mathbf{\Gamma}$ represents the attachment modes calculated in the proposed strategy with Eq. 5.37.

Bibliography

[Abbas, 2013] Abbas, M. (2013). Discrete formulation of the contact-friction. *Code Aster documentation*.

[Abichou et al., 2002] Abichou, H., Zahrouni, H., and Potier-Ferry, M. (2002). Asymptotic numerical method for problems coupling several nonlinearities. *Computer Methods in Applied Mechanics and Engineering*, 191(51-52):5795 – 5810.

[AbuBakar and Ouyang, 2006] AbuBakar, A. R. and Ouyang, H. (2006). Complex eigenvalue analysis and dynamic transient analysis in predicting disc brake squeal. *International Journal of Vehicle Noise and Vibration*, 2(2):143–155.

[AbuBakar and Ouyang, 2008] AbuBakar, A. R. and Ouyang, H. (2008). Wear prediction of friction material and brake squeal using the finite element method. *Wear*, 264(11-12):1069 – 1076.

[Aggoune et al., 2004] Aggoune, W., Zahrouni, H., and Potier-Ferry, M. (2004). High-order prediction-correction algorithms for unilateral contact problems. *Journal of Computational and Applied Mathematics*, 168(1-2):1 – 9.

[Akay, 2002] Akay, A. (2002). Acoustics of friction. *Acoustical Society of America Journal*, 111:1525–1548.

[Akay et al., 2009] Akay, A., Giannini, O., Massi, F., and Sestieri, A. (2009). Disc brake squeal characterization through simplified test rigs. *Mechanical Systems and Signal Processing*, 23(8):2590 – 2607.

[Alart and Curnier, 1991] Alart, P. and Curnier, A. (1991). A mixed formulation for frictional contact problems prone to newton like solution methods. *Computer Methods in Applied Mechanics and Engineering*, 92(3):353 – 375.

[Alvin et al., 1998] Alvin, K., Oberkampf, W., Diegert, K., and Rutherford, B. (1998). Uncertainty quantification in computational structural dynamics: A new paradigmfor model validation. In *Proceedings of the 16th International Modal Analysis Conference (IMAC), Santa Barbara, California*, pages 1191–1198.

[Arya et al., 2006] Arya, L., Titare, L., and Kothari, D. (2006). Determination of probabilistic risk of voltage collapse using radial basis function (rbf) network. *Electric Power Systems Research*, 76(6-7):426 – 434.

[Asensio et al., 2007] Asensio, C., Pavón, I., Ruiz, M., Pagan, R., and Recuero, M. (2007). Estimation of directivity and sound power levels emitted by aircrafts during taxiing, for outdoor noise prediction purpose. *Applied Acoustics*, 68(10):1263 – 1279.

[Babuska et al., 2007] Babuska, I., Nobile, F., and Tempone, R. (2007). A Stochastic Collocation Method for Elliptic Partial Differential Equations with Random Input Data. *SIAM Journal on Numerical Analysis*, 45(3):1005–1034.

[Babuska et al., 2004] Babuska, I., Tempone, R., and Zouraris, G. E. (2004). Galerkin Finite Element Approximations of Stochastic Elliptic Partial Differential Equations. *SIAM Journal on Numerical Analysis*, 42(2):800–825.

[Balajewicz et al., 2015] Balajewicz, M., Amsallem, D., and Farhat, C. (2015). Projection-based model reduction for contact problems. *Int. J. Numer. Meth. Engng*, pages 1 – 14.

[Balmès, 1996a] Balmès, E. (1996a). Optimal ritz vectors for component mode synthesis using the singular value decomposition. *AIAA journal*, 34(6):1256–1260.

[Balmès, 1996b] Balmès, E. (1996b). Parametric families of reduced finite element models: Theory and applications. *Mechanical Systems and Signal Processing*, 10(4):381 – 394.

[Bandemer and Gebhardt, 2000] Bandemer, H. and Gebhardt, A. (2000). Bayesian fuzzy kriging. *Fuzzy Sets and Systems*, 112(3):405 – 418.

[Baxter, 1992] Baxter, B. J. C. (1992). *The interpolation theory of radial basis functions.* PhD thesis, Cambridge University.

[Ben-Haim and Elishakoff, 1990] Ben-Haim, Y. and Elishakoff, I. (1990). *Convex models of uncertainty in applied mechanics.* Studies in Applied Mechanics 25. Elsevier, Amsterdam.

[Benfratello and Muscolino, 1998] Benfratello, S. and Muscolino, G. (1998). A perturbation approach for the response of dynamically modified structural systems. *Computers & Structures*, 68(1-3):101 – 112.

[Bi et al., 2013] Bi, S., Deng, Z., and Chen, Z. (2013). Stochastic validation of structural FE-models based on hierarchical cluster analysis and advanced Monte Carlo simulation. *Finite Elements in Analysis and Design*, 67:22 – 33.

[Bingul and Karahan, 2011] Bingul, Z. and Karahan, O. (2011). A fuzzy logic controller tuned with pso for 2 dof robot trajectory control. *Expert Systems with Applications*, 38(1):1017 – 1031.

[Blatman and Sudret, 2008] Blatman, G. and Sudret, B. (2008). Sparse polynomial chaos expansions and adaptive stochastic finite elements using a regression approach. *Comptes Rendus Mécanique*, 336(6):518 – 523.

[Blau and McLaughlin, 2003] Blau, P. and McLaughlin, J. (2003). Effects of water films and sliding speed on the frictional behavior of truck disc brake materials. *Tribology International*, 36(10):709 – 715.

[Bobillot and Balmès, 2002] Bobillot, A. and Balmès, E. (2002). Iterative techniques for eigenvalue solutions of damped structures coupled with fluids. *43rd AIAA/ASME/ASCE/AHS/ASC Structures, Structural Dynamics, and Materials Conference*, 3(2002-1391):1425 – 1433.

[Bouazzouni et al., 1997] Bouazzouni, A., Lallement, G., and Cogan, S. (1997). Selected a ritz basis for the reanalysis of the frequency response functions of modified structures. *Journal of Sound and Vibration*, 199(2):309 – 322.

[Bouchon-Meunier, 1994] Bouchon-Meunier, B. (1994). *La logique floue,*. Presses Universitaires de France, Paris.

[Boyaval et al., 2009] Boyaval, S., Bris, C. L., Maday, Y., Nguyen, N. C., and Patera, A. T. (2009). A reduced basis approach for variational problems with stochastic parameters: Application to heat conduction with variable robin coefficient. *Computer Methods in Applied Mechanics and Engineering*, 198(41-44):3187 – 3206.

[Bussetta et al., 2012] Bussetta, P., Marceau, D., and Ponthot, J.-P. (2012). The adapted augmented lagrangian method: a new method for the resolution of the mechanical frictional contact problem. *Computational Mechanics*, 49(2):259–275.

[Butlin and Woodhouse, 2011] Butlin, T. and Woodhouse, J. (2011). A systematic experimental study of squeal initiation. *Journal of Sound and Vibration*, 330(21):5077 – 5095.

[Butlin and Woodhouse, 2013] Butlin, T. and Woodhouse, J. (2013). Friction-induced vibration: Model development and comparison with large-scale experimental tests. *Journal of Sound and Vibration*, 332(21):5302 – 5321.

[Cambier et al., 2002] Cambier, S., Guihot, P., and Coffignal, G. (2002). Computational methods for accounting of structural uncertainties, applications to dynamic behavior prediction of piping systems. *Structural Safety*, 24(1):29 – 50.

[Cao et al., 2013] Cao, J., Du, F., and Ding, S. (2013). Global sensitivity analysis for dynamic systems with stochastic input processes. *Reliability Engineering & System Safety*, 118:106 – 117.

[Capiez-Lernout and Soize, 2004] Capiez-Lernout, E. and Soize, C. (2004). Nonparametric modeling of random uncertainties for dynamic response of mistuned bladed disks. *Journal of Engineering for Gas Turbines and Power*, 126(3):610–618.

[Cazier, 2012] Cazier, O. (2012). *Instabilités dynamiques de systèmes frottants en présence de variabilités paramétriques - Application au phénomène de crissement.* Thèses, Laboratoire d'Automatique, de Mécanique et d'Informatique Industrielles et Humaines.

[Chakraborty and Dey, 1998] Chakraborty, S. and Dey, S. (1998). A stochastic finite element dynamic analysis of structures with uncertain parameters. *International Journal of Mechanical Sciences*, 40(11):1071 – 1087.

[Chaudhary and Bathe, 1986] Chaudhary, A. B. and Bathe, K.-J. (1986). A solution method for static and dynamic analysis of three-dimensional contact problems with friction. *Computers & Structures*, 24(6):855 – 873.

[Chebli and Soize, 2004] Chebli, H. and Soize, C. (2004). Experimental validation of a nonparametric probabilistic model of nonhomogeneous uncertainties for dynamical systems. *The Journal of the Acoustical Society of America*, 115(2):697–705.

[Chen et al., 2014] Chen, N., Yu, D., and Xia, B. (2014). Hybrid uncertain analysis for the prediction of exterior acoustic field with interval and random parameters. *Computers & Structures*, 141:9 – 18.

[Chen et al., 2006] Chen, S. H., Wu, X. M., and Yang, Z. J. (2006). Eigensolution reanalysis of modified structures using epsilon-algorithm. *International Journal for Numerical Methods in Engineering*, 66(13):2115–2130.

[Chentouf et al., 2011] Chentouf, S., Bouhaddi, N., and Laitem, C. (2011). Robustness analysis by a probabilistic approach for propagation of uncertainties in a component mode synthesis context. *Mechanical Systems and Signal Processing*, 25(7):2426 – 2443.

[Chinesta et al., 2010] Chinesta, F., Amine, A., and Elías, C. (2010). Recent advances and new challenges in the use of the proper generalized decomposition for solving multidimensional models. *Archives of Computational Methods in Engineering*, 17(4):327–350.

[Chinesta et al., 2011] Chinesta, F., Ladeveze, P., and Cueto, E. (2011). A short review on model order reduction based on proper generalized decomposition. *Archives of Computational Methods in Engineering*, 18(4):395–404.

[Chowdhury and Adhikari, 2012] Chowdhury, R. and Adhikari, S. (2012). Fuzzy parametric uncertainty analysis of linear dynamical systems: A surrogate modeling approach. *Mechanical Systems and Signal Processing*, 32:5 – 17.

[Cocu et al., 1996] Cocu, M., Pratt, E., and Raous, M. (1996). Formulation and approximation of quasistatic frictional contact. *International Journal of Engineering Science*, 34(7):783 – 798.

[Corus et al., 2006] Corus, M., Balmès, E., and Nicolas, O. (2006). Using model reduction and data expansion techniques to improve SDM. *Mechanical Systems and Signal Processing*, 20(5):1067 – 1089.

[Crestaux et al., 2009] Crestaux, T., Maître, O. L., and Martinez, J.-M. (2009). Polynominal chaos expansion for sensitivity analysis. *Reliability Engineering & System Safety*, 94(7):1161 – 1172.

[Culla and Massi, 2009] Culla, A. and Massi, F. (2009). Uncertainty model for contact instability prediction. *The Journal of the Acoustical Society of America*, 126(3):1111–1119.

[Curnier and Alart, 1988] Curnier, A. and Alart, P. (1988). A generalized Newton method for contact problems with friction. *J. de Mécanique Théorique et Appliquée, special issue entitled "Numerical Methods in Mechanics of Contact involving Friction"*, pages 67–82.

[Damil et al., 1999] Damil, N., Potier-Ferry, M., Najah, A., Chari, R., and Lahmam, H. (1999). An iterative method based upon padé approximants. *Communications in Numerical Methods in Engineering*, 15(10):701–708.

[David et al., 2012] David, A., J, Z. M., and Charbel, F. (2012). Nonlinear model order reduction based on local reduced-order bases. *International Journal for Numerical Methods in Engineering*, 92(10):891–916.

[Degrauwe et al., 2009] Degrauwe, D., Roeck, G. D., and Lombaert, G. (2009). Uncertainty quantification in the damage assessment of a cable-stayed bridge by means of fuzzy numbers. *Computers & Structures*, 87(17-18):1077 – 1084.

[Dilintas et al., 1988] Dilintas, G., Laurent-Gengoux, P., and Trystram, D. (1988). A Conjugate projected gradient method with preconditioning for unilateral contact problems. *Computers & Structures*, 29(4):675 – 680.

[Ditlevsen and Madsen, 1996] Ditlevsen, O. and Madsen, H. (1996). *Sensitivity Analysis*. John Wiley & Sons, Chichester.

[Donders et al., 2005] Donders, S., Vandepitte, D., de Peer, J. V., and Desmet, W. (2005). Assessment of uncertainty on structural dynamic responses with the short transformation method. *Journal of Sound and Vibration*, 288(3):523 – 549.

[Duigou et al., 2003] Duigou, L., Daya, E. M., and Potier-Ferry, M. (2003). Iterative algorithms for non-linear eigenvalue problems. application to vibrations of viscoelastic shells. *Computer Methods in Applied Mechanics and Engineering*, 192(11-12):1323 – 1335.

[Duvaut and Lions, 1976] Duvaut, G. and Lions, J. (1976). *Inequalities in mechanics and physics*. Springer-Verlag.

[El-Tayeb and Liew, 2008] El-Tayeb, N. and Liew, K. (2008). Effect of water spray on friction and wear behaviour of noncommercial and commercial brake pad materials. *Journal of Materials Processing Technology*, 208(1-3):135 – 144.

[El-Tayeb and Liew, 2009] El-Tayeb, N. and Liew, K. (2009). On the dry and wet sliding performance of potentially new frictional brake pad materials for automotive industry. *Wear*, 266(1-2):275 – 287.

[Esgandari and Olatunbosun, 2015] Esgandari, M. and Olatunbosun, O. (2015). Implicit-explicit co-simulation of brake noise. *Finite Elements in Analysis and Design*, 99:16 – 23.

[Falsone and Ferro, 2005] Falsone, G. and Ferro, G. (2005). A method for the dynamical analysis of FE discretized uncertain structures in the frequency domain. *Computer Methods in Applied Mechanics and Engineering*, 194(42-44):4544 – 4564.

[Fan et al., 2011] Fan, N., Chen, G., and Qian, L. (2011). Analysis of squeaking on ceamic hip endoprosthesis using the complex eigenvalue method. *Wear*, 271(9-10):2305 – 2312.

[Fazio et al., 2015] Fazio, O., Nacivet, S., and Sinou, J.-J. (2015). Reduction strategy for a brake system with local frictional non-linearities - application for the prediction of unstable vibration modes. *Applied Acoustics*, 91:12 – 24.

[Feng, 1998] Feng, Z. (1998). Some text examples of 2d and 3d contact problems involving coulomb friction and large slip. *Mathematical and Computer Modelling*, 28(4-8):469 – 477.

[Feng, 1991] Feng, Z.-Q. (1991). *Contribution à la modélisation des problèmes non linéaires: contact, plasticité et endomagement*. PhD thesis, Unversité de technologie de Compiegne, France.

[Fieldhouse et al., 2010] Fieldhouse, J. D., Bryant, D., and Talbot, C. J. (2010). Investigation of brake squeal and the influence of the abutment faces. In *Proceedings of 6th European Conference on Braking, JEF 2010*, European Conference on Braking, pages 255–262. Groupement Regional Nord/Pas-de-Calais pour la Recherche dans les Transports, Universite de Lille 1, France.

[Fisher, 1935] Fisher, R. A. (1935). The design of experiments. *Oliver and Boyd, Edinburgh*.

[Forrester et al., 2008] Forrester, A., Sobester, A., and Keane, A. (2008). *Engineering design via surrogate modelling: a practical guide*. Wiley.

[Fritz et al., 2007] Fritz, G., Sinou, J.-J., Duffal, J.-M., and Jézéquel, L. (2007). Investigation of the relationship between damping and mode-coupling patterns in case of brake squeal. *Journal of Sound and Vibration*, 307(3-5):591 – 609.

[Ganapathysubramanian and Zabaras, 2007] Ganapathysubramanian, B. and Zabaras, N. (2007). Sparse grid collocation schemes for stochastic natural convection problems. *Journal of Computational Physics*, 225(1):652 – 685.

[Gauger et al., 2006] Gauger, U., Hanss, M., and Gaul, L. (2006). On the inclusion of uncertain parameters in brake squeal analysis. *IMAC-XXIV: Conference & Exposition on Structural Dynamics, St. Louis, MO, January*.

[Gauger et al., 2008] Gauger, U., Turrin, S., Hanss, M., and Gaul, L. (2008). A new uncertainty analysis for the transformation method. *Fuzzy Sets and Systems*, 159(11):1273 – 1291. Theme: Fuzzy Interval Analysis.

[Gayton et al., 2003] Gayton, N., Bourinet, J., and Lemaire, M. (2003). CQ2RS: a new statistical approach to the response surface method for reliability analysis. *Structural Safety*, 25(1):99 – 121.

[Ghanem and Spanos, 1991] Ghanem, R. G. and Spanos, P. D. (1991). *Stochastic finite elements: a spectral approach*. Springer-Verlag, New York.

[Giacoma et al., 2015] Giacoma, A., Dureisseix, D., Gravouil, A., and Rochette, M. (2015). Toward an optimal a priori reduced basis strategy for frictional contact problems with latin solver. *Computer Methods in Applied Mechanics and Engineering*, 283:1357–1381.

[Gingold and Monaghan, 1977] Gingold, R. A. and Monaghan, J. J. (1977). Smoothed Particle Hydrodynamics-Theory and application to nonspherical stars. *Monthly Notices of the Royal Astronomical Society*, 181:375–389.

[Goldberg, 1989] Goldberg, D. E. (1989). *Genetic Algorithms in Search, Optimization and Machine Learning*. Addison-Wesley Longman Publishing Co., Inc., Boston, MA, USA, 1st edition.

[Gonzalez et al., 2014] Gonzalez, A., Lauber, J., Guerra, T., Massa, F., and Tison, T. (2014). Large time simulation reduction for solving the mechanical contact problem: A fuzzy control approach. *World Congress*, 19(1):2558–2563.

[Goulet, 2004] Goulet, P. (2004). *Modélisation du comportement thermo-électro-mécanique des interfaces de contact d'une cuve de Hall-Héroult*. PhD thesis, Université Laval,(Québec).

[Guangxiong et al., 2002] Guangxiong, C., Zhongrong, Z., Kapsa, P., and Vincent, L. (2002). Effect of surface topography on formation of squeal under reciprocating sliding. *Wear*, 253(3-4):411 – 423.

[Guedri et al., 2006] Guedri, M., Bouhaddi, N., and Majed, R. (2006). Reduction of the stochastic finite element models using a robust dynamic condensation method. *Journal of Sound and Vibration*, 297(1-2):123 – 145.

[Haag et al., 2010] Haag, T., Herrmann, J., and Hanss, M. (2010). Identification procedure for epistemic uncertainties using inverse fuzzy arithmetic. *Mechanical Systems and Signal Processing*, 24(7):2021 – 2034. Special Issue: {ISMA} 2010.

[Handa and Andersson, 1981] Handa, K. and Andersson, K. (1981). Application of finite element methods in the statistical analysis of structures. *In T. Moan and M. Shinozuka (Eds) Proc. of the 3rd International Conference on Structure Safety and Reliability*, pages 409 – 420.

[Hanss, 2002] Hanss, M. (2002). The transformation method for the simulation and analysis of systems with uncertain parameters. *Fuzzy Sets and Systems*, 130(3):277 – 289.

[Hanss, 2003] Hanss, M. (2003). Simulation and analysis of fuzzy-parameterized models with the extended transformation method. *JProceedings of the 22th International Conference of the North American Fuzzy Information Processing Society, NAFIPS, Chicago, USA*.

[Hanss and Turrin, 2010] Hanss, M. and Turrin, S. (2010). A fuzzy-based approach to comprehensive modeling and analysis of systems with epistemic uncertainties. *Structural Safety*, 32(6):433 – 441. Modeling and Analysis of Rare and Imprecise Information.

[Hayajneh et al., 2006] Hayajneh, M. T., Radaideh, S. M., and Smadi, I. A. (2006). Fuzzy logic controller for overhead cranes. *Engineering Computations*, 23(1):84–98.

[Haykin, 1999] Haykin, S. (1999). *Neural Networks: A Comprehensive Foundation*. Prentice Hall, Upper Saddle River, NJ.

[He, 1999] He, J.-H. (1999). Homotopy perturbation technique. *Computer Methods in Applied Mechanics and Engineering*, 178(3-4):257 – 262.

[Helton and Davis, 2003] Helton, J. and Davis, F. (2003). Latin hypercube sampling and the propagation of uncertainty in analyses of complex systems. *Reliability Engineering & System Safety*, 81(1):23 – 69.

[Hetzler and Willner, 2012] Hetzler, H. and Willner, K. (2012). On the influence of contact tribology on brake squeal. *Tribology International*, 46(1):237 – 246.

[Heussaff et al., 2012] Heussaff, A., Dubar, L., Tison, T., Watremez, M., and Nunes, R. (2012). A methodology for the modelling of the variability of brake lining surfaces. *Wear*, 289:145 – 159.

[Hinrichs et al., 2011] Hinrichs, R., Vasconcellos, M., Osterle, W., and Prietzel, C. (2011). A TEM snapshot of magnetite formation in brakes: The role of the disc's cast iron graphite lamellae in third body formation. *Wear*, 270(5-6):365 – 370.

[Hoffmann and Gaul, 2003] Hoffmann, N. and Gaul, L. (2003). Effects of damping on mode-coupling instability in friction induced oscillations. *ZAMM - Journal of Applied Mathematics and Mechanics / Zeitschrift für Angewandte Mathematik und Mechanik*, 83(8):524–534.

[Hong et al., 2011] Hong, S.-K., Epureanu, B. I., Castanier, M. P., and Gorsich, D. J. (2011). Parametric reduced-order models for predicting the vibration response of complex structures with component damage and uncertainties. *Journal of Sound and Vibration*, 330(6):1091 – 1110.

[Hughes et al., 2005] Hughes, T. J. R., Cottrell, J. A., and Bazilevs, Y. (2005). Isogeometric analysis: Cad, finite elements, nurbs, exact geometry and mesh refinement. *Computer Methods in Applied Mechanics and Engineering*, 194(39-41):4135–4195.

[Ibrahim, 1994a] Ibrahim, R. A. (1994a). Friction-induced vibration, chatter, squeal, and chaos-part i: Mechanics of contact and friction. *ASME Applied Mechanics Reviews*, 47(7):209 – 226.

[Ibrahim, 1994b] Ibrahim, R. A. (1994b). Friction-induced vibration, chatter, squeal, and chaos-part ii: Dynamics and modeling. *ASME Applied Mechanics Reviews*, 47(7):227 – 253.

[Jaynes, 1957] Jaynes, E. T. (1957). Information theory and statistical mechanics. ii. *Phys. Rev.*, 108:171–190.

[Johnson et al., 2003] Johnson, E., Proppe, C., Jr., B. S., Bergman, L., Székely, G., and Schueller, G. (2003). Parallel processing in computational stochastic dynamics. *Probabilistic Engineering Mechanics*, 18(1):37 – 60.

[Johnson et al., 1997] Johnson, E. A., Bergman, L., and Spencer, B. (1997). Parallel implementation of monte carlo simulation - comparative studies from stochastic structural dynamics. *Probabilistic Engineering Mechanics*, 12(4):208–212.

[Jones et al., 1998] Jones, D. R., Matthias, S., and Welch, W. J. (1998). Efficient global optimization of expensive black-box functions. *Journal of Global Optimization*, 13(4):455–492.

[Júnior et al., 2008] Júnior, M. T., Gerges, S. N., and Jordan, R. (2008). Analysis of brake squeal noise using the finite element method: A parametric study. *Applied Acoustics*, 69(2):147 – 162.

[Kaymaz, 2005] Kaymaz, I. (2005). Application of kriging method to structural reliability problems. *Structural Safety*, 27(2):133 – 151.

[Kelesoglu, 2007] Kelesoglu, O. (2007). Fuzzy multiobjective optimization of truss-structures using genetic algorithm. *Advances in Engineering Software*, 38(10):717 – 721.

[Kennedy and Eberhart, 1995] Kennedy, J. and Eberhart, R. (1995). Particle swarm optimization. In *Neural Networks, 1995. Proceedings., IEEE International Conference on*, volume 4, pages 1942–1948 vol.4.

[Khabbaz et al., 2009] Khabbaz, R. S., Manshadi, B. D., Abedian, A., and Mahmudi, R. (2009). A simplified fuzzy logic approach for materials selection in mechanical engineering design. *Materials & Design*, 30(3):687–697.

[Kinkaid et al., 2003] Kinkaid, N., O'Reilly, O., and Papadopoulos, P. (2003). Automotive disc brake squeal. *Journal of Sound and Vibration*, 267(1):105 – 166.

[Kirsch and Bogomolni, 2004] Kirsch, U. and Bogomolni, M. (2004). Procedures for approximate eigenproblem reanalysis of structures. *International Journal for Numerical Methods in Engineering*, 60(12):1969–1986.

[Kirsch and Bogomolni, 2007] Kirsch, U. and Bogomolni, M. (2007). Nonlinear and dynamic structural analysis using combined approximations. *Computers & Structures*, 85(10):566 – 578.

[Kirsch et al., 2006] Kirsch, U., Bogomolni, M., and Sheinman, I. (2006). Nonlinear dynamic reanalysis of structures by combined approximations. *Computer Methods in Applied Mechanics and Engineering*, 195(33-36):4420 – 4432.

[Kiureghian et al., 1987] Kiureghian, A. D., Lin, H., , and Hwang, S. (1987). Second-order reliability approximations. *Journal of Engineering Mechanics*, 113(8):1208–1225.

[Klarbring, 1986] Klarbring, A. (1986). A mathematical programming approach to three-dimensional contact problems with friction. *Computer Methods in Applied Mechanics and Engineering*, 58(2):175 – 200.

[Klarbring and Bjoourkman, 1992] Klarbring, A. and Bjoourkman, G. (1992). Solution of large displacement contact problems with friction using newton's method for generalized equations. *International Journal for Numerical Methods in Engineering*, 34(1):249–269.

[Kleijnen, 2010] Kleijnen, J. (2010). Design and analysis of computational experiments: Overview. In Bartz-Beielstein, T., Chiarandini, M., Paquete, L., and Preuss, M., editors, *Experimental Methods for the Analysis of Optimization Algorithms*, pages 51–72. Springer Berlin Heidelberg.

[Kohn-Rich and Flashner, 2003] Kohn-Rich, S. and Flashner, H. (2003). Robust fuzzy logic control of mechanical systems. *Fuzzy Sets and Systems*, 133(1):77 – 108.

[Kolluri et al., 2011] Kolluri, D., Boidin, X., Desplanques, Y., Degallaix, G., Ghosh, A., Kumar, M., and Bijwe, J. (2011). Effect of natural graphite particle size in friction materials on thermal localisation phenomenon during stop-braking. *Wear*, 268(11-12):1472 – 1482.

[Kudawoo, 2013] Kudawoo, A. D. (2013). *Problèmes industriels de grande dimension en mécanique numérique du contact: performance, fiabilité et robustesse.* Theses, Université d'Aix Marseille.

[Ladevèze, 1999] Ladevèze, P. (1999). *Nonlinear computational structural mechanics: new approaches and non-incremental methods of calculation.* Springer Verlag.

[Ladevèze and Chamoin, 2011] Ladevèze, P. and Chamoin, L. (2011). On the verification of model reduction methods based on the proper generalized decomposition. *Computer Methods in Applied Mechanics and Engineering*, 200(23-24):2032 – 2047.

[Ladevèze et al., 2010] Ladevèze, P., Passieux, J., and Néron, D. (2010). The {LATIN} multiscale computational method and the proper generalized decomposition. *Computer Methods in Applied Mechanics and Engineering*, 199(21-22):1287 – 1296.

[Lallemand et al., 1999] Lallemand, B., Cherki, A., Tison, T., and Level, P. (1999). Fuzzy modal finite element analysis of structures with imprecise material properties. *Journal of Sound and Vibration*, 220(2):353 – 365.

[Laursen, 2003] Laursen, T. A. (2003). *Computational Contact and Impact Mechanics.* Springer-Verlag Berlin Heidelberg.

[Lemaire, 2005] Lemaire, M. (2005). *Fiabilité des structures-Couplage mécano-fiabiliste statique.* Hermès - Lavoisier.

[Lew et al., 2006] Lew, T., Spencer, A., Scarpa, F., Worden, K., Rutherford, A., and Hemez, F. (2006). Identification of response surface models using genetic programming. *Mechanical Systems and Signal Processing*, 20(8):1819 – 1831.

[Li et al., 2015] Li, F., Sun, G., Huang, X., Rong, J., and Li, Q. (2015). Multiobjective robust optimization for crashworthiness design of foam filled thin-walled structures with random and interval uncertainties. *Engineering Structures*, 88:111 – 124.

[Li et al., 2014] Li, G., Lu, Z., Lu, Z., and Xu, J. (2014). Regional sensitivity analysis of aleatory and epistemic uncertainties on failure probability. *Mechanical Systems and Signal Processing*, 46(2):209 – 226.

[Liao, 1996] Liao, T. (1996). A fuzzy multicriteria decision-making method for material selection. *Journal of Manufacturing Systems*, 15(1):1–12.

[Lieu et al., 2006] Lieu, T., Farhat, C., and Lesoinne, M. (2006). Reduced-order fluid/structure modeling of a complete aircraft configuration. *Computer Methods in Applied Mechanics and Engineering*, 195(41-43):5730 – 5742.

[Linck, 2005] Linck, V. (2005). *Modélisation numérique temporelle d'un contact frottant. Mise en évidence d'instabilités locales de contact - Conséquences tribologiques.* PhD thesis, Thèse de Doctorat en Génie Mécanique, Institut National des Sciences Appliquées de Lyon.

[Liu et al., 2007] Liu, P., Zheng, H., Cai, C., Wang, Y., Lu, C., Ang, K., and Liu, G. (2007). Analysis of disc brake squeal using the complex eigenvalue method. *Applied Acoustics*, 68(6):603 – 615.

[Liu et al., 1986] Liu, W. K., Belytschko, T., and Mani, A. (1986). Probabilistic finite elements for nonlinear structural dynamics. *Computer Methods in Applied Mechanics and Engineering*, 56(1):61 – 81.

[Loeven et al., 2007] Loeven, G., Witteveen, J., and Bijl, H. (2007). Probabilistic collocation: an efficient non-intrusive approach for arbitrarily distributed parametric uncertainties. *Proceedings of the 45th AIAA Aerospace Sciences Meeting and Exhibit, AIAA paper*, 317.

[Louf and Champaney, 2013] Louf, F. and Champaney, L. (2013). Fast validation of stochastic structural models using a pgd reduction scheme. *Finite Elements in Analysis and Design*, 70-71:44 – 56.

[Lyu et al., 2015] Lyu, Y., Bergseth, E., Olofsson, U., Lindgren, A., and Hojer, M. (2015). On the relationships among wheel-rail surface topography, interface noise and tribological transitions. *Wear*, 338-339:36 – 46.

[Mabrouk et al., 2013] Mabrouk, A. E., Cheriet, A., and Feliachi, M. (2013). Fuzzy logic control of electrodynamic levitation devices coupled to dynamic finite volume method analysis. *Applied Mathematical Modelling*, 37(8):5951 – 5961.

[MacNeal, 1971] MacNeal, R. H. (1971). A hybrid method of component mode synthesis. *Computers & Structures*, 1(4):581 – 601. Special Issue on Structural Dynamics.

[Maday and Ronquist, 2002] Maday, Y. and Ronquist, E. (2002). A reduced-basis element method. *Journal of Scientific Computing*, 17(1-4):447–459.

[Magnier et al., 2014] Magnier, V., Brunel, J., and Dufrénoy, P. (2014). Impact of contact stiffness heterogeneities on friction-induced vibration. *International Journal of Solids and Structures*, 51(9):1662 – 1669.

[Maître et al., 2004] Maître, O. L., Knio, O., Najm, H., and Ghanem, R. (2004). Uncertainty propagation using wiener-haar expansions. *Journal of Computational Physics*, 197(1):28 – 57.

[Mamdani and Assilian, 1975] Mamdani, E. and Assilian, S. (1975). An experiment in linguistic synthesis with a fuzzy logic controller. *International Journal of Man-Machine Studies*, 7(1):1 – 13.

[Mamdani, 1974] Mamdani, E. H. (1974). Application of fuzzy algorithms for control of simple dynamic plant. *Proceedings of The Institution of Electrical Engineers*, 121:1585 – 1588.

[Marceau, 2001] Marceau, D. (2001). *Modélisation du contact tridimensionnel avec frottement en grande transformation et son application à l'étude des dispositifs d'ancrage multitorons*. PhD thesis, Université Laval(Québec,Canada).

[Massa et al., 2015a] Massa, F., Do, H. Q., Tison, T., and Cazier, O. (2015a). Uncertain friction induced vibration study: coupling of fuzzy logic, fuzzy sets and interval theories. *ASCE-ASME Journal of Risk and Uncertainty in Engineering Systems, Part B: Mechanical Engineering*.

[Massa et al., 2009a] Massa, F., Lallemand, B., and Tison, T. (2009a). Fuzzy multiobjective optimization of mechanical structures. *Computer Methods in Applied Mechanics and Engineering*, 198(5-8):631 – 643.

[Massa et al., 2015b] Massa, F., Lallemand, B., and Tison, T. (2015b). Multi-level homotopy perturbation and projection techniques for the reanalysis of quadratic eigenvalue problems: The application of stability analysis. *Mechanical Systems and Signal Processing*, 52-53:88 – 104.

[Massa et al., 2004] Massa, F., Lallemand, B., Tison, T., and Level, P. (2004). Fuzzy eigensolutions of mechanical structures. *Engineering Computations*, 21(1):66–77.

[Massa et al., 2011a] Massa, F., Leroux, A., Lallemand, B., Tison, T., Buffe, F., and Mary, S. (2011a). Fuzzy vibration analysis and optimization of engineering structures: Application to Demeter satellite. In Belyaev, A. K. and Langley, R. S., editors, *IUTAM Symposium on the Vibration Analysis of Structures with Uncertainties*, volume 27 of *IUTAM Bookseries*, pages 57–69. Springer Netherlands.

[Massa et al., 2008a] Massa, F., Mourier-Ruffin, K., Lallemand, B., and Tison, T. (2008a). Structural analysis by interval approach. *European Journal of Computational Mechanics*, 17(5 - 7):869 – 880.

[Massa et al., 2008b] Massa, F., Ruffin, K., Tison, T., and Lallemand, B. (2008b). A complete method for efficient fuzzy modal analysis. *Journal of Sound and Vibration*, 309(1-2):63 – 85.

[Massa et al., 2006] Massa, F., Tison, T., and Lallemand, B. (2006). A fuzzy procedure for the static design of imprecise structures. *Computer Methods in Applied Mechanics and Engineering*, 195(9 -12):925 – 941.

[Massa et al., 2009b] Massa, F., Tison, T., and Lallemand, B. (2009b). Fuzzy analysis: Prediction of experimental behaviours. *Journal of Sound and Vibration*, 322(1-2):135 – 154.

[Massa et al., 2011b] Massa, F., Tison, T., Lallemand, B., and Cazier, O. (2011b). Structural modal reanalysis methods using homotopy perturbation and projection techniques. *Computer Methods in Applied Mechanics and Engineering*, 200(45-46):2971 – 2982.

[Massi et al., 2007] Massi, F., Baillet, L., Giannini, O., and Sestieri, A. (2007). Brake squeal: Linear and nonlinear numerical approaches. *Mechanical Systems and Signal Processing*, 21(6):2374 – 2393.

[Massi et al., 2006] Massi, F., Giannini, O., and Baillet, L. (2006). Brake squeal as dynamic instability: An experimental investigation. *Journal of the Acoustical Society of America*, 120(3):1388–1398.

[Masson et al., 2006] Masson, G., Brik, B. A., Cogan, S., and Bouhaddi, N. (2006). Component mode synthesis (cms) based on an enriched ritz approach for efficient structural optimization. *Journal of Sound and Vibration*, 296(4-5):845 – 860.

[McWilliam, 2001] McWilliam, S. (2001). Anti-optimisation of uncertain structures using interval analysis. *Computers & Structures*, 79(4):421 – 430.

[Mehta, 1991] Mehta, L. (1991). *Random Matrices*. Academic Press.

[Melchers, 1999] Melchers, R. E. (1999). *Structural Reliability Analysis and Prediction*. John Wiley & Sons.

[Metropolis and Ulam, 1949] Metropolis, N. and Ulam, S. (1949). The monte carlo method. *Journal of the American Statistical Association*, 44(247):pp. 335–341.

[Meziane, 2007] Meziane, A. (2007). *Apport des analyses numériques temporelles et fréquentielle dans l'étude des instabilités de contact -Validation expérimentale*. PhD thesis, Thèse de Doctorat en Génie Mécanique, Institut National des Sciences Appliquées de Lyon.

[Meziane et al., 2010] Meziane, A., Baillet, L., and Laulagnet, B. (2010). Experimental and numerical investigation of friction-induced vibration of a beam-on-beam in contact with friction. *Applied Acoustics*, 71(9):843 – 853.

[Meziane et al., 2007] Meziane, A., DÉrrico, S., Baillet, L., and Laulagnet, B. (2007). Instabilities generated by friction in a pad-disc system during the braking process. *Tribology International*, 40(7):1127 – 1136.

[Millman et al., 2005] Millman, D. R., King, P. I., and Beran, P. S. (2005). Airfoil pitch-and-plunge bifurcation behavior with fourier chaos expansions. *Journal of Aircraft*, 42(2):376 – 384.

[Moens and Hanss, 2011] Moens, D. and Hanss, M. (2011). Non-probabilistic finite element analysis for parametric uncertainty treatment in applied mechanics: Recent advances. *Finite Elements in Analysis and Design*, 47(1):4 – 16.

[Moens and Vandepitte, 2005] Moens, D. and Vandepitte, D. (2005). A survey of non-probabilistic uncertainty treatment in finite element analysis. *Computer Methods in Applied Mechanics and Engineering*, 194(12-16):1527 – 1555.

[Moller et al., 2008] Moller, B., Liebscher, M., Schweizerhof, K., Mattern, S., and Blankenhorn, G. (2008). Structural collapse simulation under consideration of uncertainty - improvement of numerical efficiency. *Computers & Structures*, 86(19-20):1875 – 1884.

[Montenegro et al., 2015] Montenegro, P., Neves, S., cada, R. C., Tanabe, M., and Sogabe, M. (2015). Wheel-rail contact formulation for analyzing the lateral train-structure dynamic interaction. *Computers & Structures*, 152:200 – 214.

[Moore, 1966] Moore, R. E. (1966). *Interval analysis*, volume 4. Prentice-Hall Englewood Cliffs.

[Mouatassim, 1989] Mouatassim, M. E. (1989). *Modélisation en grandes transformations des solides massifs par éléments finis*. PhD thesis, Unversité de technologie de Compiegne, France.

[Myers et al., 2009] Myers, R., Montgomery, D., and Anderson-Cook, C. (2009). *Response Surface Methodology: Process and Product Optimization Using Designed Experiments*. Wiley Series in Probability and Statistics. Wiley.

[Nechak et al., 2011] Nechak, L., Berger, S., and Aubry, E. (2011). A polynomial chaos approach to the robust analysis of the dynamic behaviour of friction systems. *European Journal of Mechanics - A/Solids*, 30(4):594 – 607.

[Nechak et al., 2012] Nechak, L., Berger, S., and Aubry, E. (2012). Prediction of Random Self Friction-induced Vibrations in Uncertain Dry Friction Systems Using a Multi-Element Generalized Polynomial Chaos Approach. *Journal of Vibration and Acoustics*, 134(4):1–14.

[Nechak et al., 2013] Nechak, L., Berger, S., and Aubry, E. (2013). Non-intrusive generalized polynomial chaos for the robust stability analysis of uncertain nonlinear dynamic frction systems. *Journal of Sound and Vibration*, 332(5):1204 – 1215.

[Nechak et al., 2015] Nechak, L., Gillot, F., Besset, S., and Sinou, J.-J. (2015). Sensitivity analysis and kriging based models for robust stability analysis of brake systems. *Mechanics Research Communications*, 69:136 – 145.

[Nieuwenhof and Coyette, 2002] Nieuwenhof, B. V. D. and Coyette, J.-P. (2002). A perturbation stochastic finite element method for the time-harmonic analysis of structures with random mechanical properties. *Proceedings of the 5th World Congress on Computational Mechanics, Vienna, Austria*.

[Nobari et al., 2015a] Nobari, A., Ouyang, H., and Bannister, P. (2015a). Statistics of complex eigenvalues in friction-induced vibration. *Journal of Sound and Vibration*, 338:169 – 183.

[Nobari et al., 2015b] Nobari, A., Ouyang, H., and Bannister, P. (2015b). Uncertainty quantification of squeal instability via surrogate modelling. *Mechanical Systems and Signal Processing*, 60-61:887 – 908.

[Nouy, 2010] Nouy, A. (2010). A priori model reduction through proper generalized decomposition for solving time-dependent partial differential equations. *Computer Methods in Applied Mechanics and Engineering*, 199(23-24):1603 – 1626.

[Oberkampf et al., 1999] Oberkampf, W., S.Deland, Rutherford, B., K.V.Diegert, and Alvin, K. (1999). A new methodology for the estimation of total uncertainty in computational simulation. In *Proceedings of the 40th AIAA/ ASME/ ASCE/ AHS/ ASC Structures, Structural Dynamics and Materials Conference, AIAA-99-1612*, pages 3061–3083.

[Oberst and Lai, 2011] Oberst, S. and Lai, J. (2011). Statistical analysis of brake squeal noise. *Journal of Sound and Vibration*, 330(12):2978 – 2994.

[Oden and Martins, 1985] Oden, J. and Martins, J. (1985). Models and computational methods for dynamic fricton phenomena. *Computer Methods in Applied Mechanics and Engineering*, 52(1-3):527 – 634.

[Ouenzerfi et al., 2015] Ouenzerfi, G., Massi, F., Renault, E., and Berthier, Y. (2015). Squeaking friction phenomena in ceramic hip endoprosthesis: Modeling and experimental validation. *Mechanical Systems and Signal Processing*, 58-59:87 – 100.

[Ouyang et al., 2005] Ouyang, H., Nack, W., Yuan, Y., and Chen, F. (2005). Numerical analysis of automotive disc brake squeal: a review. *International Journal of Vehicle Noise and Vibration*, 1(3):207 – 231.

[Papadrakakis and Kotsopulos, 1999] Papadrakakis, M. and Kotsopulos, A. (1999). Parallel solution methods for stochastic finite element analysis using monte carlo simulation. *Computer Methods in Applied Mechanics and Engineering*, 168(1-4):305 – 320.

[Park, 2008] Park, K. (2008). *Component-based Vibration Modeling Methods for Fast Reanalyses and Design of Complex Structures*. PhD thesis, PhD Thesis, University of Michigan.

[Perić and Owen, 1992] Perić, D. and Owen, D. (1992). Computational model for 3-d contact problems with friction based on the penalty method. *International journal for numerical methods in engineering*, 35(6):1289–1309.

[Ponthot, 1997] Ponthot, J.-P. (1997). *Traitement unifié de la mécanique des milieux continus solides en grandes transformations par la méthode des éléments finis*. PhD thesis, Unversité de Liège, Faculté des sciences appliquées, Belgique.

[Pradlwarter et al., 2002] Pradlwarter, H., Schueller, G., and Szekely, G. (2002). Random eigenvalue problems for large systems. *Computers & Structures*, 80(27-30):2415 – 2424.

[Puso and Laursen, 2004a] Puso, M. A. and Laursen, T. A. (2004a). A mortar segment-to-segment contact method for large deformation solid mechanics. *Computer Methods in Applied Mechanics and Engineering*, 193(6-8):601 – 629.

[Puso and Laursen, 2004b] Puso, M. A. and Laursen, T. A. (2004b). A mortar segment-to-segment frictional contact method for large deformations. *Computer Methods in Applied Mechanics and Engineering*, 193(45-47):4891 – 4913.

[Qiu and Elishakoff, 1998] Qiu, Z. and Elishakoff, I. (1998). Antioptimization of structures with large uncertain-but-non-random parameters via interval analysis. *Computer Methods in Applied Mechanics and Engineering*, 152(3-4):361 – 372.

[Ragot, 2007] Ragot, P. (2007). *Contribution à la conception robuste en dynamique des systèmes: Application à un systÃ¨me frottant présentant des instabilités de type Sprag-Slip*. Thèses, Ecole Nationale Supérieure d'Ingénieurs Sud Alsace, UHA.

[Ramalho, 2015] Ramalho, A. (2015). Wear modelling in rail-wheel contact. *Wear*, 330-331:524 – 532.

[Ramík, 2007] Ramík, J. (2007). Optimal solutions in optimization problem with objective function depending on fuzzy parameters. *Fuzzy Sets Syst.*, 158(17):1873–1881.

[Rao et al., 2010] Rao, M. R., Pownuk, A., Vandewalle, S., and Moens, D. (2010). Transient response of structures with uncertain structural parameters. *Structural Safety*, 32(6):449 – 460.

[Renaud et al., 2012] Renaud, F., Chevallier, G., Dion, J.-L., and TaudiÃ¨re, G. (2012). Motion capture of a pad measured with accelerometers during squeal noise in a real brake system. *Mechanical Systems and Signal Processing*, 33:155 – 166.

[Renault et al., 2014] Renault, A., Massa, F., Lallemand, B., and Tison, T. (2014). Variability effects on automotive brake squeal prediction. *Colloque francophone sur l'Analyse Vibratoire Expérimental, France*.

[Renouf and Alart, 2005] Renouf, M. and Alart, P. (2005). Conjugate gradient type algorithms for frictional multi-contact problems: applications to granular materials. *Computer in Applied Mechanics and Engineering*, 194(18-20):2019 – 2041.

[Rong et al., 2003] Rong, F., Chen, S. H., and Chen, Y. D. (2003). Structural modal reanalysis for topological modifications with extended kirsch method. *Computer Methods in Applied Mechanics and Engineering*, 192(5-6):697 – 707.

[Ruffin-Mourier, 2008] Ruffin-Mourier, K. (2008). *Réponse dynamique de structures mécaniques à paramètres imprécis*. PhD thesis, Thèse de Doctorat en Génie Mécanique, Université de Valenciennes et du Hainaut-Cambrésis.

[Ryckelynck, 2005] Ryckelynck, D. (2005). A priori hyperreduction method: an adaptive approach. *Journal of Computational Physics*, 202(1):346 – 366.

[Sacks et al., 1989] Sacks, J., Welch, W. J., Mitchell, T. J., and Wynn, H. P. (1989). Design and analysis of computer experiments. *Statist. Sci.*, 4(4):409–423.

[Sakata et al., 2003] Sakata, S., Ashida, F., and Zako, M. (2003). Structural optimization using kriging approximation. *Computer Methods in Applied Mechanics and Engineering*, 192(7-8):923 – 939.

[Saltelli et al., 2000] Saltelli, A., Chan, K., and Scott, E. M. (2000). *Structural reliability methods*. John Wiley & Sons, Ltd.

[Sarrouy et al., 2013a] Sarrouy, E., Dessombz, O., and Sinou, J.-J. (2013a). Piecewise polynomial chaos expansion with an application to brake squeal of a linear brake system. *Journal of Sound and Vibration*, 332(3):577 – 594.

[Sarrouy et al., 2013b] Sarrouy, E., Dessombz, O., and Sinou, J.-J. (2013b). Stochastic study of a non-linear self-excited system with friction. *European Journal of Mechanics - A/Solids*, 40:1 – 10.

[Saxcé and Feng, 1998] Saxcé, G. D. and Feng, Z. (1998). The bipotential method: A constructive approach to design the complete contact law with friction and improved numerical algorithms. *Mathematical and Computer Modelling*, 28(4-8):225 – 245.

[Schueller, 1997] Schueller, G. (1997). A state-of-the-art report on computational stochastic mechanics. *IASSAR report on Computational Stochastic Mechanics, Probabilistic Engineering Mechanics*, 12(4):197 – 321.

[Schueller, 2001] Schueller, G. (2001). Computational stochastic mechanics - recent advances. *Computers & Structures*, 79(22-25):2225 – 2234.

[Shah et al., 2015] Shah, H., Hosder, S., Koziel, S., Tesfahunegn, Y. A., and Leifsson, L. (2015). Multi-fidelity robust aerodynamic design optimization under mixed uncertainty. *Aerospace Science and Technology*, 45:17 – 29.

[Shin et al., 2002] Shin, K., Brennan, M., Oh, J.-E., and Harris, C. (2002). Analysis of disc brake noise using a two-degree-of-freedom model. *Journal of Sound and Vibration*, 254(5):837 – 848.

[Shin et al., 2002] Shin, K., Oh, J.-E., and Brennan, M. (2002). Nonlinear analysis of friction induced vibrations of a two-degree-of-freedom model for disc brake squeal noise. *JSME International Journal Series C*, 45:426–432.

[Shinozuka, 1972] Shinozuka, M. (1972). Monte carlo solution of structural dynamics. *Computers & Structures*, 2(5-6):855–874.

[Shinozuka and Yamazaki, 1988] Shinozuka, M. and Yamazaki, F. (1988). Stochastic finite element analysis: an introduction. *Stochastic Structural Dynamics, Progress in Theory and Applications*, pages 241–291.

[Sinou et al., 2004] Sinou, J., Thouverez, F., and Jézéquel, L. (2004). Methods to reduce non-linear mechanical systems for instability computation. *Archives of Computational Methods in Engineering*, 11(3):257–344.

[Sinou, 2010] Sinou, J.-J. (2010). Transient non-linear dynamic analysis of automotive disc brake squeal - on the need to consider both stability and non-linear analysis. *Mechanics Research Communications*, 37(1):96 – 105.

[Sinou et al., 2006a] Sinou, J.-J., Dereure, O., Mazet, G.-B., Thouverez, F., and Jezequel, L. (2006a). Friction-induced vibration for an aircraft brake system-part 1: Experimental approach and stability analysis. *International Journal of Mechanical Sciences*, 48(5):536 – 554.

[Sinou et al., 2006b] Sinou, J.-J., Thouverez, F., Jezequel, L., Dereure, O., and Mazet, G.-B. (2006b). Friction induced vibration for an aircraft brake system-part 2: Non-linear dynamics. *International Journal of Mechanical Sciences*, 48(5):555 – 567.

[Sliva et al., 2010] Sliva, G., Brezillon, A., Cadou, J., and Duigou, L. (2010). A study of the eigenvalue sensitivity by homotopy and perturbation methods. *Journal of Computational and Applied Mathematics*, 234(7):2297 – 2302.

[Soderberg and Andersson, 2009] Soderberg, A. and Andersson, S. (2009). Simulation of wear and contact pressure distribution at the pad-to-rotor interface in a disc brake using general purpose finite element analysis software. *Wear*, 267(12):2243 – 2251.

[Soize, 2000] Soize, C. (2000). A nonparametric model of random uncertainties for reduced matrix models in structural dynamics. *Probabilistic Engineering Mechanics*, 15(3):277 – 294.

[Soize, 2005a] Soize, C. (2005a). A comprehensive overview of a non-parametric probabilistic approach of model uncertainties for predictive models in structural dynamics. *Journal of Sound and Vibration*, 288(3):623 – 652.

[Soize, 2005b] Soize, C. (2005b). Random matrix theory for modeling uncertainties in computational mechanics. *Computer Methods in Applied Mechanics and Engineering*, 194(12-16):1333 – 1366.

[Soize, 2010] Soize, C. (2010). Generalized probabilistic approach of uncertainties in computational dynamics using random matrices and polynomial chaos decompositions. *International Journal for Numerical Methods in Engineering*, 81(8):939–970.

[Soobbarayen et al., 2013] Soobbarayen, K., Besset, S., and Sinou, J.-J. (2013). Noise and vibration for a self-excited mechanical system with friction. *Applied Acoustics*, 74(10):1191 – 1204.

[Soobbarayen et al., 2014] Soobbarayen, K., Sinou, J.-J., and Besset, S. (2014). Numerical study of friction-induced instability and acoustic radiation - effect of ramp loading on the squeal propensity for a simplified brake model. *Journal of Sound and Vibration*, 333(21):5475 – 5493.

[Spalart et al., 2010] Spalart, P. R., Shur, M. L., Strelets, M. K., and Travin, A. K. (2010). Towards noise prediction for rudimentary landing gear. *Procedia Engineering*, 6:283 – 292.

[Sudret, 2007] Sudret, B. (2007). Uncertainty propagation and sensitivity analysis in mechanical models– contributions to structural reliability and stochastic spectral methods. *Habilitation à Diriger des Recherches, Université Blaise Pascal - Clermont II.*

[Taguchi et al., 2005] Taguchi, G., Chowdhury, S., and Wu, Y. (2005). *Taguchi's Quality Engineering Handbook*. Wiley.

[Tanyildizi, 2009] Tanyildizi, H. (2009). Fuzzy logic model for prediction of mechanical properties of lightweight concrete exposed to high temperature. *Materials & Design*, 30(6):2205–2210.

[Tison et al., 2014] Tison, T., Heussaff, A., Massa, F., Turpin, I., and Nunes, R. (2014). Improvement in the predictivity of squeal simulations: Uncertainty and robustness. *Journal of Sound and Vibration*, 333(15):3394 – 3412.

[Tran et al., 2010] Tran, Q. H., Ouisse, M., and Bouhaddi, N. (2010). A robust component mode synthesis method for stochastic damped vibroacoustics. *Mechanical Systems and Signal Processing*, 24(1):164 – 181.

[Vermot Des Roches, 2011] Vermot Des Roches, G. (2011). *Frequency and time simulation of squeal instabilities. Application to the design of industrial automotive brakes.* Thèses, Ecole Centrale Paris.

[Wan and Karniadakis, 2005] Wan, X. and Karniadakis, G. E. (2005). An adaptive multi-element generalized polynomial chaos method for stochastic differential equations. *Journal of Computational Physics*, 209(2):617 – 642.

[Wang et al., 2013] Wang, P., Lu, Z., and Tang, Z. (2013). An application of the kriging method in global sensitivity analysis with parameter uncertainty. *Applied Mathematical Modelling*, 37(9):6543 – 6555.

[Wei et al., 2004] Wei, C., Ruichen, J., and Agus, S. (2004). Analytical variance-based global sensitivity analysis in simulation-based design under uncertainty. *Journal of Mechanical Design*, 127(5):875 – 886.

[Wiener, 1938] Wiener, N. (1938). The homogeneous chaos. *American Journal of Mathematics*, 60(4):pp. 897–936.

[Wriggers, 2006] Wriggers, P. (2006). *Computational Contact Mechanics*. Springer Berlin Heidelberg.

[Xiu and Hesthaven, 2005] Xiu, D. and Hesthaven, J. S. (2005). High-order collocation methods for differential equations with random inputs. *SIAM Journal on Scientific Computing*, 27(3):1118–1139.

[Xiu and Karniadakis, 2002] Xiu, D. and Karniadakis, G. E. (2002). Modeling uncertainty in steady state diffusion problems via generalized polynomial chaos. *Computer Methods in Applied Mechanics and Engineering*, 191(43):4927 – 4948.

[Yang et al., 2005] Yang, B., Laursen, T. A., and Meng, X. (2005). Two dimensional mortar contact methods for large deformation frictional sliding. *International Journal for Numerical Methods in Engineering*, 62(9):1183–1225.

[Yang et al., 2001] Yang, X., Chen, S., and Wu, B. (2001). Eigenvalue reanalysis of structures using perturbations and padé approximants. *Mechanical Systems and Signal Processing*, 15(2):257 – 263.

[Yapici et al., 2009] Yapici, F., Ozcifci, A., Akbulut, T., and Bayir, R. (2009). Determination of modulus of rupture and modulus of elasticity on flakeboard with fuzzy logic classifier. *Materials & Design*, 30(6):2269 – 2273.

[Yastrebov, 2013] Yastrebov, V. A. (2013). *Numerical Methods in Contact Mechanics*. ISTE/Wiley.

[Yvonnet et al., 2007] Yvonnet, J., Zahrouni, H., and Potier-Ferry, M. (2007). A model reduction method for the post-buckling analysis of cellular microstructures. *Computer Methods in Applied Mechanics and Engineering*, 197(1-4):265 – 280.

[Zadeh, 1965] Zadeh, L. (1965). Fuzzy sets. *Information and Control*, 8(3):338–353.

[Zadeh, 1975a] Zadeh, L. (1975a). The concept of a linguistic variable and its application to approximate reasoning-1. *Information Sciences*, 8(3):199–249.

[Zadeh, 1975b] Zadeh, L. (1975b). The concept of a linguistic variable and its application to approximate reasoning-2. *Information Sciences*, 8(4):301–357.

[Zadeh, 1975c] Zadeh, L. (1975c). The concept of a linguistic variable and its application to approximate reasoning-3. *Information Sciences*, 9(1):43–80.

[Zadeh, 1978] Zadeh, L. (1978). Fuzzy sets as a basis for theory of possibility. *Fuzzy Sets and Systems*, 1:3–28.

[Zhang and Pandey, 2014] Zhang, X. and Pandey, M. D. (2014). An effective approximation for variance-based global sensitivity analysis. *Reliability Engineering & System Safety*, 121:164 – 174.

[Zienkiewicz and Taylor, 1994] Zienkiewicz, O. and Taylor, R. (1994). *The finite element method*. McGraw-hill London,fourth edition.

[Zienkiewicz and Taylor, 2002] Zienkiewicz, O. C. and Taylor, R. L. (2002). The finite element method. fifth edition. *Bautechnik*, 79(2):122–123.